University of Alberta

The resistance mechanisms located at the DISC level and the mitochondria level regulate the sensitivity of cancer cells to TRAIL-induced apoptosis

by

Peng Wang 

A thesis submitted to the Faculty of Graduate Studies and Research in partial fulfillment

of the requirements for the degree of

Doctor of Philosophy

In

Medical Sciences-Laboratory Medicine and Pathology

Edmonton, Alberta

Fall 2008

Your file Votre référence
ISBN: 978-0-494-46444-1
Our file Notre référence
ISBN: 978-0-494-46444-1

Abstract

The TNF-related apoptosis-inducing ligand (TRAIL) has emerged as a potential therapeutic agent against cancer because it is capable of selectively killing tumor cells over normal cells. Unfortunately, the majority of human cancers are resistant to TRAIL treatment. Here, we show that TRAIL-resistance mechanisms focus at two major levels, the DISC level and mitochondria level, in which the death receptor-initiated extrinsic apoptosis pathway and the mitochondria-associated intrinsic apoptosis pathway, respectively, were blocked separately. At the DISC level, TRAIL-resistance either comes from the loss of crucial apoptosis-inducing molecules, including FADD and caspase-8, or from the over-expression of anti-apoptotic factors, including RIP and c-FLIP. At the mitochondria level, TRAIL-resistance either comes from the over-expression of anti-apoptotic factors, including Bcl-2 and Bcl-xL, or the down-regulation of pro-apoptotic factors, including Bax and Bak. Importantly, by using quantitative MS analysis, we found that Bax, not only functions as a pro-apoptotic factor, but also pursues its crucial apoptosis-inducing function by affecting the expression or the stability of other proteins. Together, these findings advance our understanding of the TRAIL signaling network at the molecular level, indicate the crucial TRAIL-induced apoptosis regulators, and address several facets of TRAIL-resistance mechanisms, thus providing the basis to overcome TRAIL resistance by interference with the TRAIL-induced apoptosis pathway, and assist the development of TRAIL-based tumor therapy in the future

Acknowledgements

There are many people that have contributed to my graduate study, and I wish to express my gratitude to them. First, I would like to thank my supervisor, Dr. Raymond Lai and my co-supervisor, Dr. Liang Li. Thanks for giving me the opportunity to work with you and for your helpful suggestions and enthusiasm throughout the course of my study. They dedicated their precious time to guide me and help me revising the manuscripts, the abstracts for conferences, and this thesis.

I would like to thank my previous supervisor, Dr. Charlie Hao for his guiding me into the TRAIL research area and helpful instruction for my project. I would like to thank the member of my supervisory committee, Dr. Michele Barry for her helpful advice throughout my program. Thank you to the Thesis Examining Committee for their time and contribution to the examination process.

Thanks to the Department of Laboratory Medicine and Pathology. In particular, I would like to thank Jennifer Mcphee, Dr, Jason Acker, and Dr. Fiona Bamforth. Thanks to Alberta Cancer Board for providing me with stipend funding during the course of my graduate work.

I would like to express special thanks to Fang Wu and Andy Lo who in addition to teaching me the Mass Spectrometry techniques and helping me with Data analysis, have also been wonderful friends. I would like to extend appreciation to my fellow in the Lab, Dr. Jin H. Song and Doyoun K. Song for their training me with molecular biology techniques. And finally, thanks to my parents and my wife for their long time support, encouragement, and understanding of my academic endeavors.

Table of Contents

List of Figures

Chapter 3

Chapter 4

List of Abbreviations

ACN.....Acetoniltrile

Act D.....actinomycin D

Apaf1.....apoptotic protease-activating factor 1

Apaf-1.....Apoptosis protease activating factor-1

Bak.....Bcl-2 antagonist/killer

Bax.....Bcl-2 associated x protein

Bcl-2.....B-cell lymphoma 2

Bcl-X_L.....Long form of Bcl-X

Bcl-X_S.....Short form of Bcl-X

Bid.....Bcl-2 inhibitory BH3 domain-containing protein

bp.....base pair

BSA.....Bovine serum albumin

CAD.....Collision-activated dissociation

CARD.....Caspase-recruitment domain

caspase.....cysteinyl aspartic acid protease

cDNA.....complementary DNA

CDDP.....cisplatin

c-$FLIP_L$.....cellular FADD-like, IL-1β-converting enzyme inhibitory protein long form

c-$FLIP_S$.....cellular FADD-like, IL-1β-converting enzyme inhibitory protein short form

CID.....Collision-induced dissociation

CPT.....camptothecin

CRD.....Cystein-rich domain

C-terminal.....carboxy terminal

CTL.....Cytotoxic T-lyphocyte

Cys.....cysteine (amino acid)

Cyto c.....cytochrome *c*

DR.....death receptor

DcR.....decoy receptor

DD.....death domain

DED.....death effector domain

DFF.....DNA fragmentation factor

DHB.....2,5-Dihydroxybenzoic acid

DMSO.....Dimethyl sulfoxide

DISC.....death inducing signaling complex

DOX.....doxorubicin

DTT.....Dithiothreitol

ECL.....Enhanced chemiluminescence

EDTA.....ethylenediamine tetraacetic acid

EGTA.....ethylene glycol tetraacetic acid

ERK1/2.....extracellular signal-regulated kinase

ER.....Endoplasmic reticulum

ESI.....Electrospray ionization

FACScan.....fluorescence-activated cell sorting scan

FADD.....Fas-associated death domain

FBS.....fetal bovine serum

fmk.....fluoromethyl ketone

5-FU.....5-fluorouracil

Gly.....glycine (amino acid)

HDAC.....inhibitor of histone deacetylase

HRP.....horse radish peroxidase

HSP.....Heat shock protein

HUVECs.....human umbilical vein endothelial cells

IAP.....inhibitor of apoptosis proteins

ICAD.....Inhibitor of caspase-activated DNase

ICE.....Interleukin-1β-converting enzyme

IFN.....Interferon

IgG.....Immunoglobulin G

IFN-γ.....interferon gamma

IT.....Ion Trap

kDa.....kiloDalton

LC.....Liquid chromatography

LOH .....loss of heterozygosity

mAbs.....monoclonal antibodies

MALDI.....Matrix-assisted laser desorption and ionization

MBP-1.....C-myc promoter-binding protein

MCA.....Methylcholanthrene

MIF.....Macrophage migration inhibitory factor

mRNA.....messenger ribonucleic acid

MS..... Mass Spectrometry

m/z.....Mass-to-charge ratio

NF-κB .....nuclear factor kappa B

NK cells .....natural killer cells

NSCLC.....non-small lung carcinoma

N-terminal .....amino-terminal

OPG.....osteoprotegerin

p-Akt .....phosphorylated Akt

PARP.....poly (ADP-ribose) polymerase

PBLs.....peripheral blood lymphocytes

PBS .....phosphate buffered saline

PI.....propidium iodide

PI3K.....phosphoinositide 3-kinase

PKB.....protein kinase B otherwise known as Akt

PKC.....protein kinase C

PLAD.....Pre-ligand assembly domain

PMF.....peptide mass fingerpinting

PMSF .....phenylmethylsulfonyl fluoride

ppm.....Parts per million

PRKDC.....DNA-dependent protein kinase catalytic subunit

PTM.....Post-translation modification

p value.....probability (of incorrectly rejecting the null hypothesis)

RHIM.....RIP homotypic interaction motif

RP.....Reverse phase

RIP .....receptor interacting protein

RISC.....RNA-induced silencing complex

RNAi .....RNA interference

SD .....standard deviation of the mean

SDS .....sodium dodecyl sulphate

siRNA .....small interfering RNA

SEM .....standard error of the mean

Ser .....serine (amino acid)

SILAC.....Stable isotope labeling by amino acid in cell culture

Smac/DIABLO .....second mitochondria-derived activator of caspase/direct inhibitor of apoptosis binding protein [IAP] with low pI

S/N.....Signal-to-noise ratio

tBid.....truncated Bid

TBST.....Tris buffered saline with Tween-20

TFA.....Trifluoroacetic acid

Thr.....threonine (amino acid)

TNFα .....Tumor Necrosis Factor alpha

TNFR .....TNF receptor

TOF.....Time-of-flight

TRADD.....TNFR1 associated death domain

TRAIL.....TNF-related apoptosis-inducing ligand

TRAIL-R.....TRAIL receptor

TRAP1.....TNFR-associated protein 1

Tris-HCl .....tris[hydroxymethyl]-aminomethane hydrochloride

TSA.....Trichostatin A

VDAC.....Voltage-dependent anion-selective channel protein

XIAP .....X-linked inhibitor of apoptosis proteins

z.....carbobenzyloxy-

Chapter 1: General Introduction

1.0 Thesis Overview

Tumor necrosis factor-related apoptosis-inducing ligand (TRAIL) has been well characterized as a reagent which can selectively induce apoptotic cell death of cancer cells instead of normal cells [1] and recombinant forms of human TRAIL and its agonist antibodies have therefore entered phase I-II clinical trials in treating human cancers [6, 7]. However, it has been shown that the majority of human cancer cells are resistant to TRAIL [8, 9] and preclinical studies examining the biological basis for TRAIL resistance have lagged behind the clinical trials. Thus, clarifying the molecular mechanism(s) by which human cancer cells become resistant to TRAIL may allow the development of correlated novel strategies that can overcome TRAIL resistance in human cancer cells[10].

TRAIL [11], also known as Apo2 ligand (Apo2L) [12], was originally cloned because of its sequence homology to TNF-α and Fas ligand (FasL/CD95L), which was identified as a member of the TNF death ligand family [1]. TRAIL is a type II membrane protein with a short intracellular amino-terminal tail and a long extracellular carboxy-terminal receptor-binding domain. TRAIL is expressed on the cell surface of natural killer and activated T cells and plays a role in immune surveillance against tumor development and metastasis in mice [13-15]. These studies suggest that TRAIL is a natural cancer killer *in vivo*. Recombinant TRAIL kills many human cancer cells in culture [16, 17] and inhibits tumor growth in animals [16, 18]. These studies have raised the possibility that TRAIL could be used as a cancer therapeutic agent [19]. Several studies of various cancer cell lines have shown that TRAIL is capable of inducing apoptosis in select cancer cells. However, these studies have also demonstrated that most of the cancer cell lines are resistant to TRAIL-induced apoptosis. The molecular mechanisms that generate resistance to TRAIL

remain largely unknown. Existing published evidence suggests that TRAIL interacts with the death receptors, DR4 and DR5, leading to assembly of the death inducing signal complex (DISC). Caspase-8 is activated in the DISC, releasing active subunits which can directly activate downstream caspase-3 to induce apoptosis. This is known as the extrinsic apoptotic cell death pathway. At the same time, activated forms of caspase-8 can transform Bid to truncated Bid which will activate BAX and BAK to damage the mitochondrial membrane potential (MMP). After MMP damage, some apoptotic factors, such as cytochrome c [20] and Smac [21], will be released. These apoptotic factors can activate downstream caspase-9 and caspase-3 to induce apoptosis. This is the mitochondria-associated intrinsic pathway.

Results provided in this study demonstrate that the TRAIL resistance primarily comes from two levels; DISC level and mitochondria level. In the DISC level, there are two major resistance mechanisms involved: (1) loss of crucial apoptotic signal transducers, such as FADD and caspase-8; and (2) over-expression of anti-apoptotic factors, such as cFLIP and RIP.

In the mitochondria level, there are also two major resistance mechanisms involved: (1) loss or down-regulation of crucial apoptotic factors, such as Bax and Bak; (2) over-expression of anti-apoptotic factors, such as Bcl-2 and Bcl-xL. By down-regulating the anti-apoptotic factors, we are able to transform various TRAIL-resistant cancer cells to TRAIL-sensitive cells. These data provide further input to the clinical treating strategy of mediating TRAIL treatment.

1.1 TRAIL and its Receptors

As a type II membrane protein of 281 amino acids, TRAIL has an extracellular carboxy-terminal domain (amino acids 114-281) and an intracellular amino-terminal tail [11, 12]. The extracellular domain of TRAIL forms a bell-shaped structure of the receptor-binding site [22] and can be proteolytically cleaved to yield a vesicle-associated, soluble, biologically active form (19-20 kDa) [23, 24]. The generation of this soluble recombinant TRAIL is dependent on the functional activity of cysteine proteases. Among the TNF family of proteins, TRAIL shares the highest homology and signaling characteristics with Fas ligand. The crystal structure shows that the C-terminal extracellular region of TRAIL exhibits a homotrimeric subunit structure (Fig 1.1) [22]. With this structure, TRAIL can interact with five receptors to serve as an extracellular signal. The five receptors are: DR4 (TRAIL-R1) [25] and DR5 (TRAIL-R2/TRICK2/KILLER) [26], DcR1 (TRAIL-R3/TRID) [26], DcR2 (TRAIL-R4/TRUNDD/LIT) [26, 27], and a soluble receptor for TRAIL, osteoprotegrin (OPG) [28, 29]. As a result, the binding of TRAIL leads to its receptor trimerization and initiates the downstream signals (Fig 1.2).

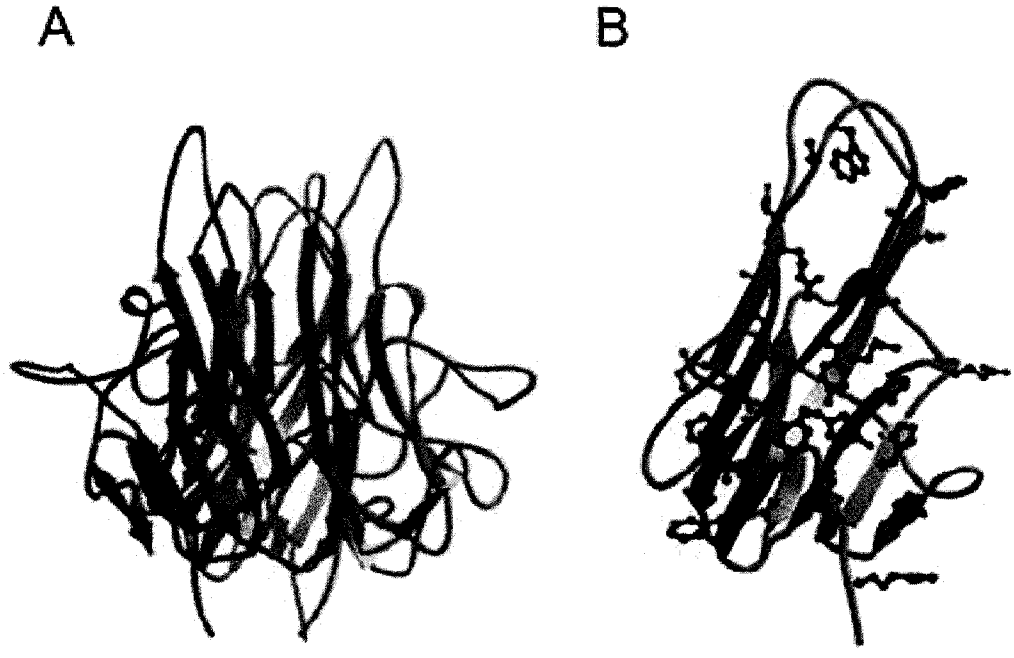

Figure 1.1 Crystal Structures of TRAIL. (A) Side view of TRAIL trimer. (B) Side view of TRAIL monomer. Adapted from [4].

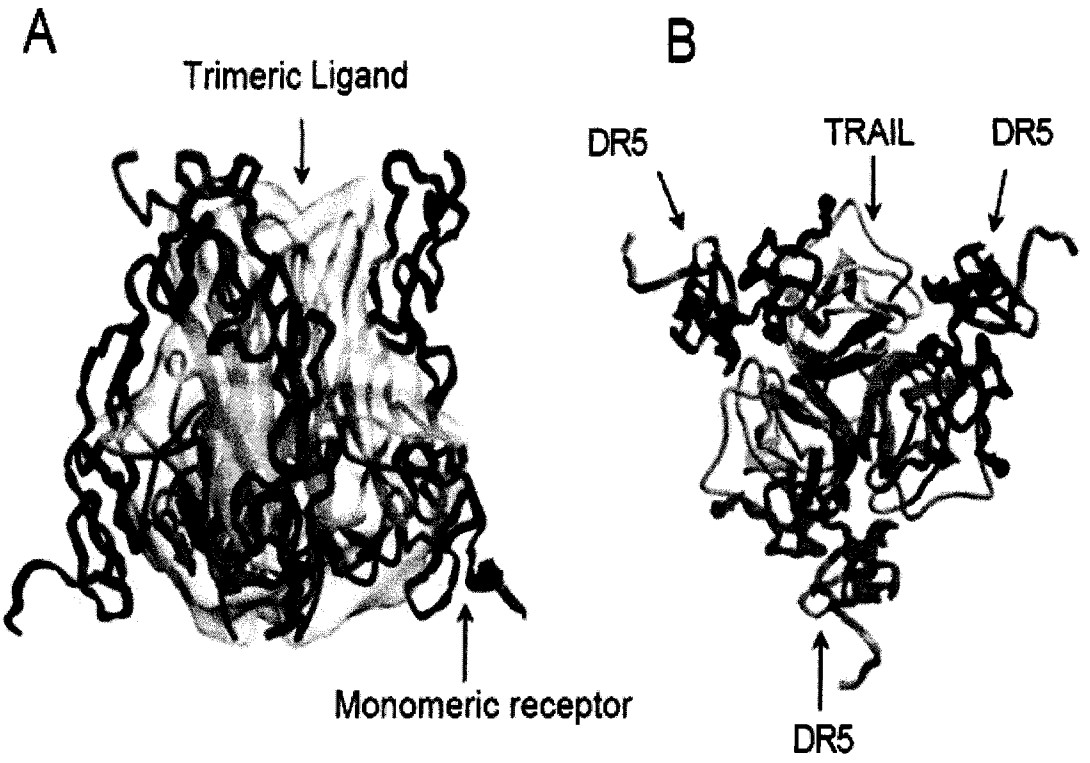

Figure 1.2 Crystal Structures of TRAIL/DR5 complex. (A) Side view of TRAIL/DR5 complex: The TRAIL trimer is encased in a clear shell, and the interdigitated DR5 monomers are indicated by red, green, and blue. (B) Top view of the TRAIL/DR5 complex: the TRAIL monomers are indicated by yellow, pink, and turquoise colors. Adapted from [4].

The four membrane-anchored receptors, DR4 [25], DR5 [26], DcR1, and DcR2 contain two cysteine-rich domains by which they can bind to TRAIL. DR4 and DR5 are implicated in pro-apoptotic signaling through their cytoplasmic death domains (DDs). Over-expression of these two death receptors has been found to induce apoptosis independent of ligand binding due to oligomerization of the DDs, whereas deletion of the death domains on both receptors blocks the TRAIL death signal [25, 30]. On the other hand, DcR1 [26] and DcR2 [26, 27] are unable to transduce a death signal upon binding to TRAIL since they lack a functional death domain motif and their over-expression is believed to inhibit TRAIL-induced apoptosis (Fig 1.3 A) [30]. DcR2 contains a truncated death domain motif and DcR1 is a glycophosphatidylinositol (GPI) -anchored protein that lacks a cytoplasmic tail [26, 27, 30] (Fig 1.3A). High levels of mRNA for DcR1 and DcR2 have been found in normal cells, including spleen, heart, lung, kidney, liver, bone marrow, and placenta [26, 30, 31]. In contrast, low levels of both decoy receptors have been detected in transformed cell lines and their over-expression in sensitive cell lines confers resistance to TRAIL-induced apoptosis [26, 27, 30]. Hence, some reports hypothesize that DcR1 and DcR2 compete with DR4 and DR5 for the binding of TRAIL and thereby protect normal cells from TRAIL-induced apoptosis (Fig 1.3A).

This ligand-binding dependent model of inhibition of apoptosis is dependent on the high binding affinity of DcRs to TRAIL. However, it was reported that the binding affinity of DcR1 and DcR2 is 10 to 100 fold lower than the binding affinity of DR4 and DR5 to TRAIL. Consequently, some alternative regulatory models have been raised for the explanations of DcRs-mediated inhibition of TRAIL-induced apoptosis. DcR2 has been reported to be capable of activating NF-kB [27] and the subsequent up-regulation of

some anti-apoptotic genes by DcR2 might inhibit apoptotic signals (Fig 1.3B). Alternatively, DcR2 is also proposed as a regulatory rather than decoy receptor which inhibits apoptosis by the formation of ligand-independent complexes with DR5 [32]. It is reported that DcR2 interacts with DR5 with the pre-ligand assembly domain (PLAD) and the ligand-independent association of DcR2 with DR5 is crucial for the inhibitory effect of DcR2 on DR5-induced apoptosis (Fig 1.3C)

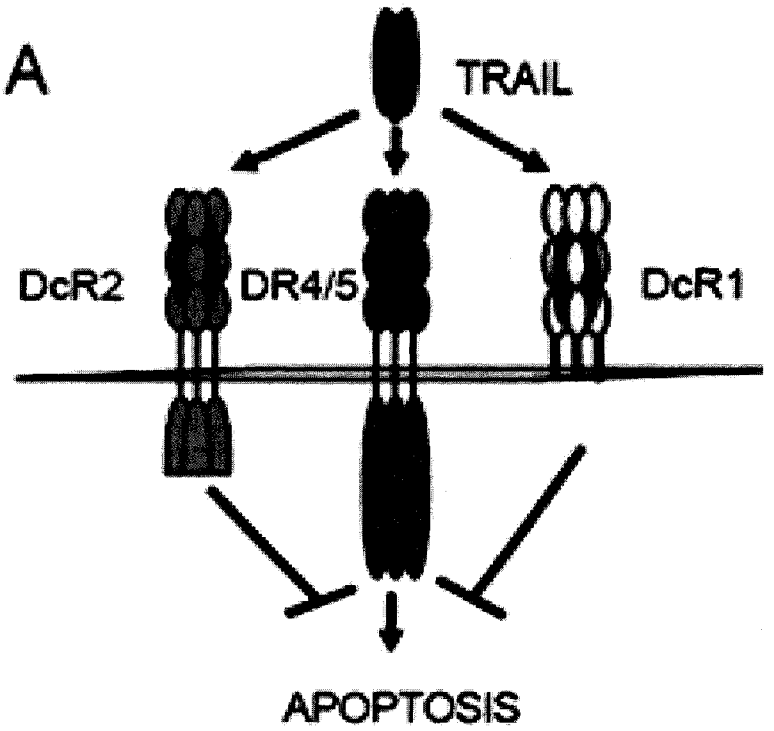

Figure 1.3 (A) DcR2 contains a truncated death domain motif and DcR1 is a glycophosphatidylinositol (GPI) -anchored protein that lacks a cytoplasmic tail. Because of the lack of death domains, DcR1 and DcR2 can not transduce the apoptotic signals to downstream caspases and may competitively bind with TRAIL to inhibit DR4/DR5-initiated apoptosis. Adapted from [4].

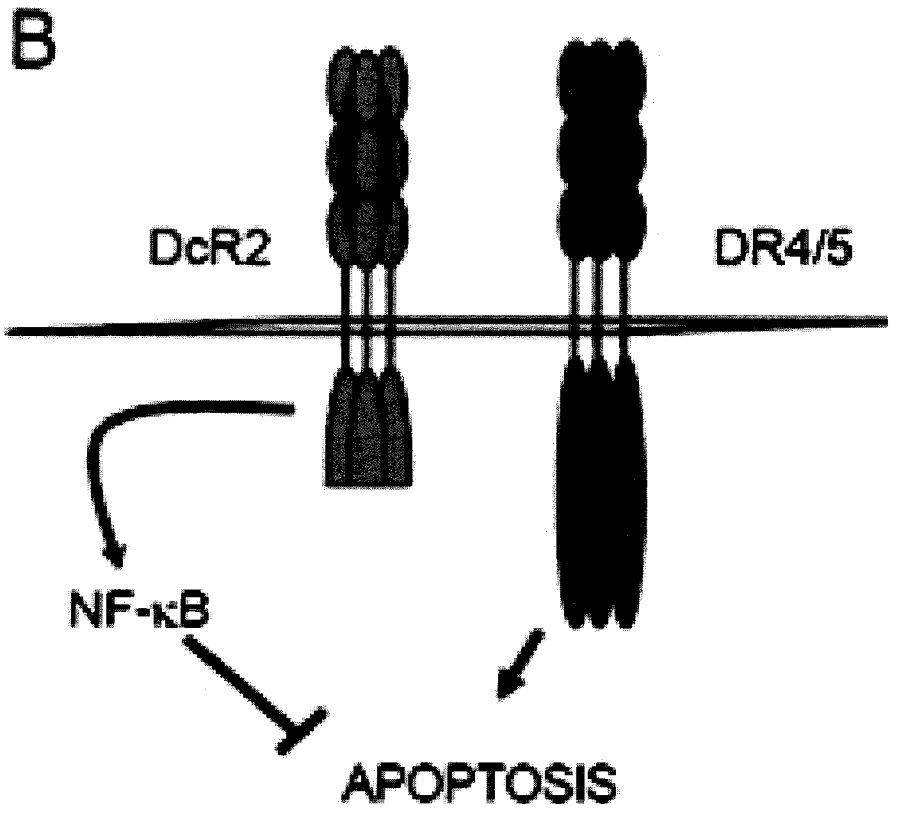

Figure 1.3 (B) DcR2 can activate Nf-kB pathway which up-regulates some anti-apoptotic genes ,including DcR1, to inhibit apoptosis. Adapted from [4].

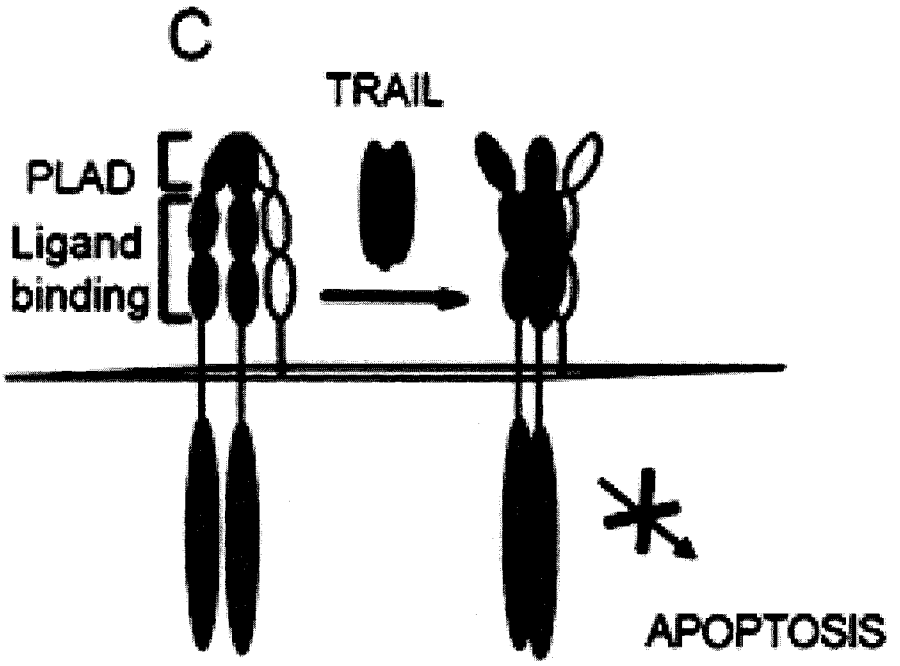

Figure 1.3 (C) Through its PLAD, DcR2 can bind with DR4/DR5 which will block the subsequent TRAIL signaling. Adapted from [4].

A soluble receptor for TRAIL, osteoprotegrin (OPG) [28, 29] has also been identified. It can bind to another TNF-like cytokine, TRANCE, and has a more prominent role in regulating bone resorption and bone mass by preventing osteoclast differentiation [28], rather than in mediating TRAIL-induced apoptosis because of its low affinity for TRAIL at 37°C [33, 34].

1.2 TRAIL: Gene and Protein

The TRAIL gene is located on chromosome 3 at position 3q26. Expression of TRAIL mRNA has been found in most human tissues, such as spleen, lung, and prostate, but not in brain, liver, and testes [11, 35]. Expression of the TRAIL protein has been detected on immune cells, such as natural killer cells [14], activated monocytes [36], and dendritic cells [37]. TRAIL forms homotrimers that bind three receptor molecules, resulting in a receptor/ligand (3:3) hexagonal complex that can initiate a signaling cascade [38, 39]. Optimal biological activity of TRAIL is dependent on the stability of the trimeric ligand and on the final tertiary configuration of the ligand complex [40]. Both the recombinant soluble form, as well as the cell-associated form, of TRAIL contains an unpaired cysteine residue (Cys230) in their receptor-binding domain. The presence of Cys230 is critical for maintaining activity of the ligand as it can either bind another Cys to form a disulfide bridge or chelate one Zn^{2+} ion per TRAIL trimer unit [40]. If the Cys forms a disulfide bond, there is reduced affinity of TRAIL for DR5 and the resulting TRAIL was found to be slightly active [40]. Alternately, when a Zn^{2+} ion was bound to a TRAIL trimeric unit, the resulting ligand retained its biological activity, suggesting a role for Zn^{2+} in stabilizing the ligand configuration for receptor binding [40].

Because of this specific interaction, the amount of Zn^{2+} is important in determining the final selectivity and cytotoxicity in recombinant soluble TRAIL used in research and clinically [41].

Toxicity of different versions of recombinant TRAIL to hepatocytes varies depending on the preparation of the ligand [42-45]. Hepatocyte toxicity [42, 43] was reported for TRAIL prepared in the absence of zinc ions. It has been suggested that zinc depletion reduces solubility of the recombinant product and causes aggregation [41]. In contrast, recombinant soluble, non-tagged versions of TRAIL produced in the presence of Zn^{2+} had no adverse cytotoxic effects on human and non-human primate hepatocytes [43, 44] and keratinocytes [45]. In addition, certain forms of aggregated, poly-histidine tagged, and antibody crosslinked TRAIL can trigger apoptosis and cytotoxicity in normal cell types, such as astrocytes [18, 44], keratinocytes [45], hepatocytes [42] and neurons [44].

Previous studies in our laboratory also found that non-tagged recombinant human TRAIL proteins are saturated with zinc ions and are present as homotrimers [46], whereas the tagged hepatotoxic TRAIL [42] is zinc ion poor, leading to the formation of heterodimers [43]. The heterodimers tend to aggregate and thus surpass the high threshold for TRAIL-induced signals in normal human cells [47].

1.3 TRAIL-induced apoptosis

Two well recognized signalling pathways control the initiation of apoptosis: the DISC-initiated extrinsic pathway through the death receptors [1] and the mitochondria-associated intrinsic pathway through mitochondria [48]. Both extrinsic and intrinsic pathways are involved in TRAIL-induced apoptosis. The extrinsic pathway is initiated by

the binding of TRAIL to its cognate death receptors DR4 [25, 27, 30, 49] and DR5 [26, 50-52]. Upon binding to TRAIL, DR4 and DR5 recruit the intracellular adaptor protein, FADD, [49, 51] through DDs forming the DISC. FADD contains a carboxy-terminal DD and an amino-terminal death effector domain (DED) [53, 54]. Procaspase-8 is recruited to DISC through homophilic interactions between DED domains on FADD and caspase-8 [55, 56].

Procaspase-8 has two DED prodomains and one caspase domain [55, 57]. In the DISC, close proximity of procaspase-8 to other procaspase-8 molecules leads to dimer formation followed by autocatalytic activation [58, 59] to form activated caspase subunits in a two-step mechanism [57]. In the first step, precursor or procaspase forms are cleaved at Asp374 into p43 (N-terminal) and p12 fragments (C-terminal) [57]. The p12 fragment undergoes further processing to generate an active p10 protease subunit [57]. The p43 fragment is also cleaved into a smaller p26 fragment containing two DED domains and an active enzyme p18 fragment containing the QACQG-active site [57, 60]. Both active subunits of caspase-8, p10 and p18, are released into the cytosol where they can activate downstream effector caspases [55, 60], such as caspase-3. The caspase-8 orthologue, caspase-10, can also be recruited and cleaved in the DISC to initiate apoptosis [61-64]. However, many cancer cells do not express caspase-10 [61] and reconstitution of caspase-8-deficient Jurkat cells by stable transfection with DR4 in combination with caspase-10 failed to sensitize these cells to death receptor-induced apoptosis [63]. Therefore, caspase-8 is the most crucial initiator of death receptor-mediated apoptosis in the DISC-initiated extrinsic apoptosis pathway [1].

Caspase-9, another crucial initiator, is involved in the mitochondria-associated intrinsic apoptosis pathway. Upon TRAIL treatment, activated casapse-8 subunits cleave the Bid to truncated Bid (tBid). tBid induces mitochondrial membrane permeabilization, leading to the release of Smac/DIABLO and cytochrome c from mitochondria to the cytosol [21, 65]. Smac releases the XIAP-dependent inhibition of caspase-3 and indirectly activates caspase-3 [66]. Cytochrome c assembles with dATP and Apaf-1 which recruits caspase-9 with its N-terminal caspase recruitment domain (CARD), leading to the formation of the apoptosome. Within the apoptosome, caspase-9 can be activated by cleavage and rearrangements of surface loops providing a surface compatible with catalytic organization of the active site [67, 68].

In contrast to caspase-8 or caspase-9, caspase-3 exists within the cytosol as an inactive dimer [59]. It is activated from its p32 precursor through cleavage by activated caspase-8 or caspase-9, into p20, p17 and p10 fragments [69]. Once activated, caspase-3 can induce and execute programmed cell death through the cleavage and activation of substrates that inhibit cell survival, such as DNA fragmentation factor (DFF) [70]. Substrates cleaved by 'effector' caspases include: poly (ADP-ribose) polymerase (PARP), DFF as well as lamins, actin, cytokeratins and Bcl-2 and Bcl-xL. Cleavage of these substrates results in the morphological and biochemical changes associated with apoptosis [71] (Fig 1.4).

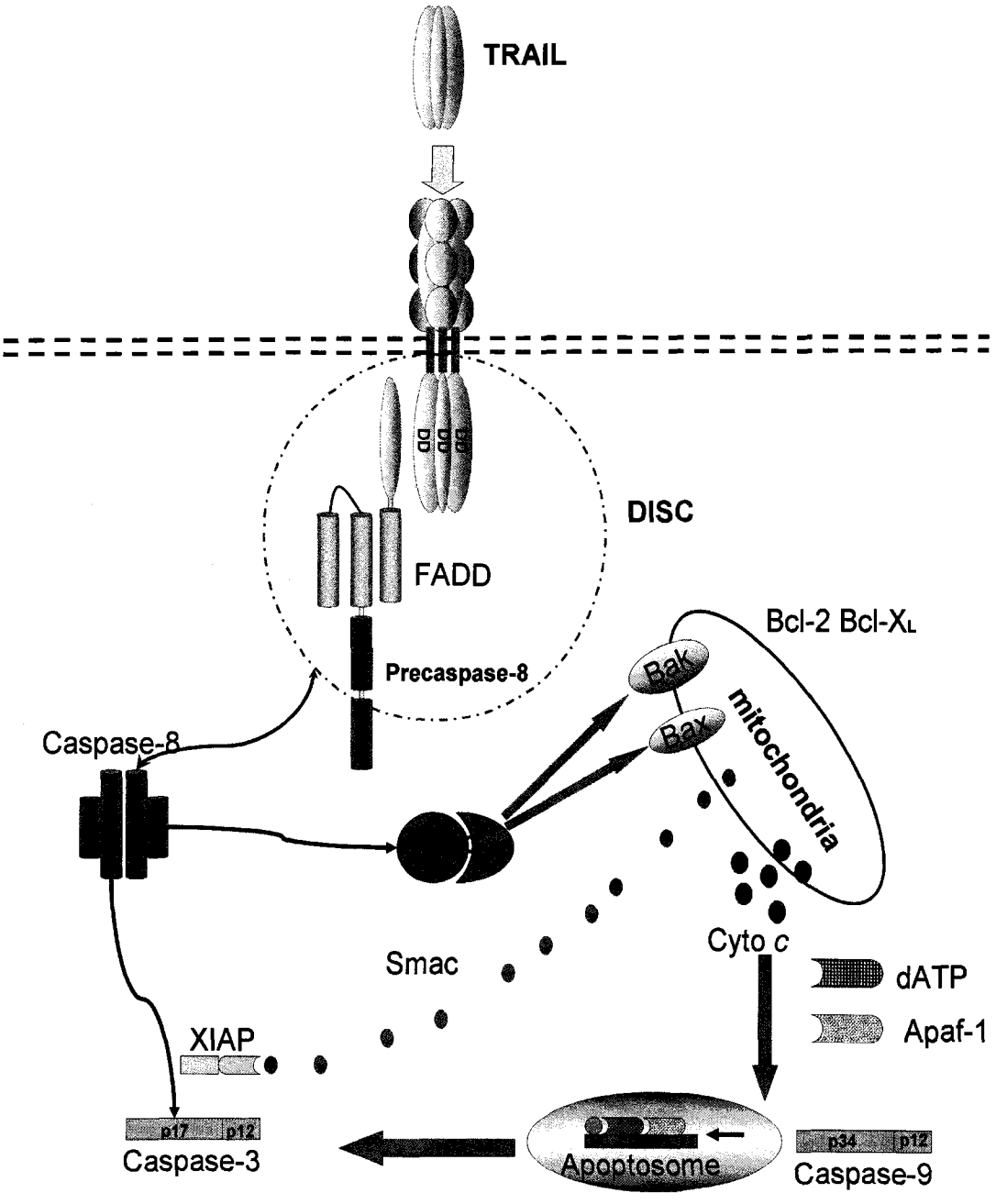

Figure 1.4 TRAIL-induced apoptosis signal pathway. Upon TRAIL binding, DR4/5 initiates DISC formation and caspase cascade activation. By transferring Bid to tBid, an activated form of caspase-8 also induces apoptosis through the mitochondria-associated intrinsic pathway.

1.4 Apoptosis

Apoptosis allows multicellular organisms to remove old or damaged cells in a process that is distinct from other forms of cell death, especially necrosis [72, 73]. Necrosis is a kind of pathological or accidental cell death and is instigated upon acute injury to a cell. Necrosis results in irreversible swelling of a cell's cytoplasm and organelles followed by the eventual lysis and release of its contents to its surroundings [74]. Moreover, necrosis is accompanied by the release of special enzymes, stored by lysosomes, which are capable of digesting cell components or the entire cell itself [75]. Necrosis typically occurs when cells are exposed to traumatic conditions, such as hypoxia, ischemia, hyperthermia, complement attack from the innate immune system, or metabolic toxins, as well as direct cell trauma The injuries received by the cell may compromise the lysosome membrane, or may initiate a chain reaction which causes the release of enzymes (Fig 1.5).

Unlike necrosis, apoptosis is morphologically characterized by chromatin condensation and fragmentation, cell shrinkage and membrane blebbing (Fig 1.5) [73, 76, 77]. First, since the protein structures that comprise the cytoskeleton (actin, cytokeratins) are digested by caspases, cells become round. Second, chromatin undergoes initial condensation. Chromatin undergoes further condensation into compact patches against the nuclear envelope. At this stage, the nuclear membrane still appears complete; however, the nuclear pore protein and lamin underneath the nuclear envelope have already begun to be degraded by caspases. This stage is usually called pyknosis and is considered a hallmark of apoptosis. Third, the nuclear envelope becomes intact and the DNA is fragmented, a process called karyorrhexis. Because of the degradation of DNA,

the nucleus breaks into several discrete chromatin bodies or nucleosomal units. The plasma membrane begins to bleb and changes in the plasma membrane composition during apoptosis provide signals for phagocytes to absorb the apoptotic cell without provoking a generalized inflammatory response [76, 77]. Finally, the cells are phagocyted or broken apart into several apoptotic bodies. Through this process, cellular contents are not released into the surrounding tissue which prevents initiating an inflammatory reaction [75].

As an important physiological event, apoptosis is required for normal cell development and controlling pathological processes [73, 75]. As a tightly regulated process, any abrogation of normal apoptosis can lead to a number of pathological situations [74]. For example, accumulation of uncontrolled cells, due to insufficient apoptosis, can lead to cancer, whereas cell loss due to excess apoptosis can result in a stroke, neurodegeneration, or heart failure [74]. In multi-cellular organisms, apoptosis is a highly regulated and programmed form of cell suicide that is involved in embryogenesis, tissue homeostasis and in the development of various disorders, such as autoimmunity, cancer, and neurodegenerative diseases [74, 78].

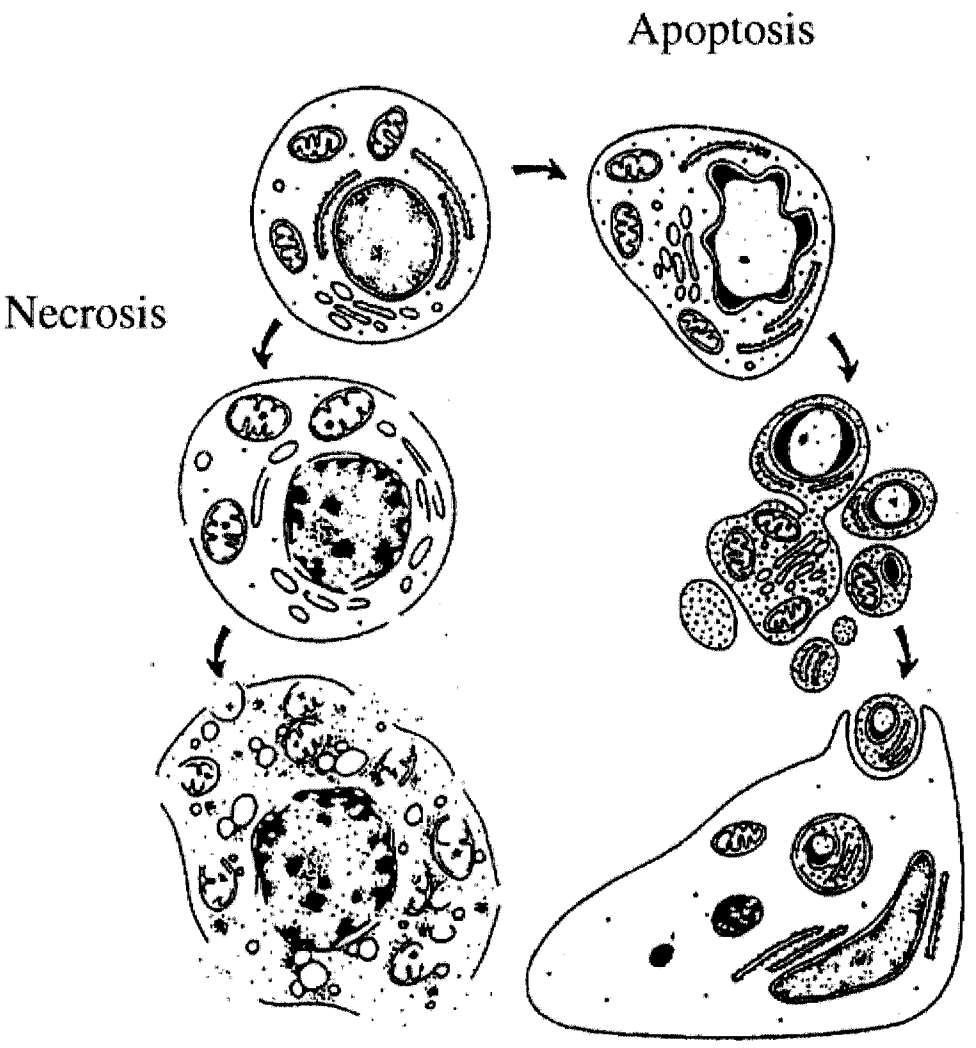

Figure 1.5 Necrosis and apoptosis. Necrosis typically occurs under pathological conditions, characterizes by the release of lysosome enzymes which digest the cell components and even entire cell itself. In contrast, apoptosis is a highly controlled program cell death.

1.5 Regulators of TRAIL-induced apoptosis pathway

1.5.1 FADD

As an adaptor molecule, FADD contains both DD and DED motifs. Its essential role in death signal transduction was first identified in FasL-induced apoptosis. Through its interactions with activated Fas at the DD and caspase-8 at the DED, FADD transmits the cell death signal from Fas to caspase-8 [56]. Previous evidence showed that defects in FADD can lead to complete TRAIL resistance. *In vivo* data showed that $FADD^{-/-}$ embryonic fibroblasts stably transfected with mouse or human TRAIL death receptors were completely resistant to TRAIL-induced apoptosis, but $FADD^{+/-}$ fibroblasts stably transfected with mouse TRAIL death receptors were sensitive to TRAIL-induced apoptosis [79]. These data suggest that FADD plays an essential role in TRAIL-induced apoptosis. With its DD and DED domains, FADD is able to form FADD-FADD, FADD-DRs, and FADD-procasapse-8 interactions. Since the interactions of FADD-FADD or FADD-DRs were not seen by Co-IP from cells expressing the FADD DD [80, 81], the affinity of FADD-DRs or FADD-FADD interactions must be relatively low in isolation. This explains why FADD does not spontaneously activate cell death in the absence of the ligand stimulation. Moreover, FADD was reported to be necessary for the recruitment of caspase-8 or casapse-10 to the DISC [63]. Based on the above reports, the assembly of DISC requires a membrane-localized, activated receptor which interacts with FADD, and then a FADD homodimer may form at or between activated DRs to create the structural context necessary for the recruitments of downstream caspases.

1.5.2 Caspases

It is now clear that the execution of apoptosis in eukaryotic cells is carried out by a family of cysteinyl aspartate proteinases known as caspases [82, 83]. Since the first recognized member of this family, caspase-1, was found to be required for the activation of IL-1β [84], fourteen caspases have been identified in total [3, 71]. All of them contain a conserved pentapeptide, QACXG (X can be R, Q, or D), which includes the active-site cysteine [3]. Based on their biological activities, they can be subdivided into three groups: 'initiator' caspases (caspases -2, -8, -9, or -10), 'effector caspases' (caspase-3, -6, -7), and mediators of inflammation (caspase-1, -4, -5, -11, -12, -13, 14). In this study, the focus was on the caspases that function in apoptosis.

These caspases are normally present as an inactive proenzyme (zymogen or procaspase), comprised of an N-terminal prodomain, a large subunit, and a small subunit (Fig 1.6). In the event of apoptotic stimuli, recruitment of these caspases through clustering of adaptor molecules results in their accumulation. This leads to the activation of the procaspases by proteolytic cleavage at the Asp-X sites between the prodomain and the large subunit domain, as well as the large and the small subunit domains. Functionally, the different prodomains of procaspases are crucial in determining their different roles in the apoptotic caspase cascade system. The initiator caspases have a relatively longer prodomain (~ 200 amino acids) that contains a specific protein-protein interaction domain. These prodomains of initiator caspases contain either a CARD (as in caspase-2 and -9) or two DEDs (as in caspase-8 and -10) which enable them to be recruited to the DISC, resulting in autocatalytic activation. On the other hand, the effector casspases have a relatively short prodomains, usually less than 20 amino acids.

Once the initiator caspases are activated, they can directly or indirectly activate the downstream effector caspases, mainly caspase-3. Once these effector caspases are activated, they can go on to cleave substrates, including caspase-activated DNase/DNA fragment 45 (ICAD/DFF45), poly (ADP-ribose) polymerase (PARP), nuclear lamins, PAK2, and cytoskeletal proteins, such as gelsolin and fodrin, Bcl-2, and Bcl-xL. Cleavage of these substrates results in apoptosis.

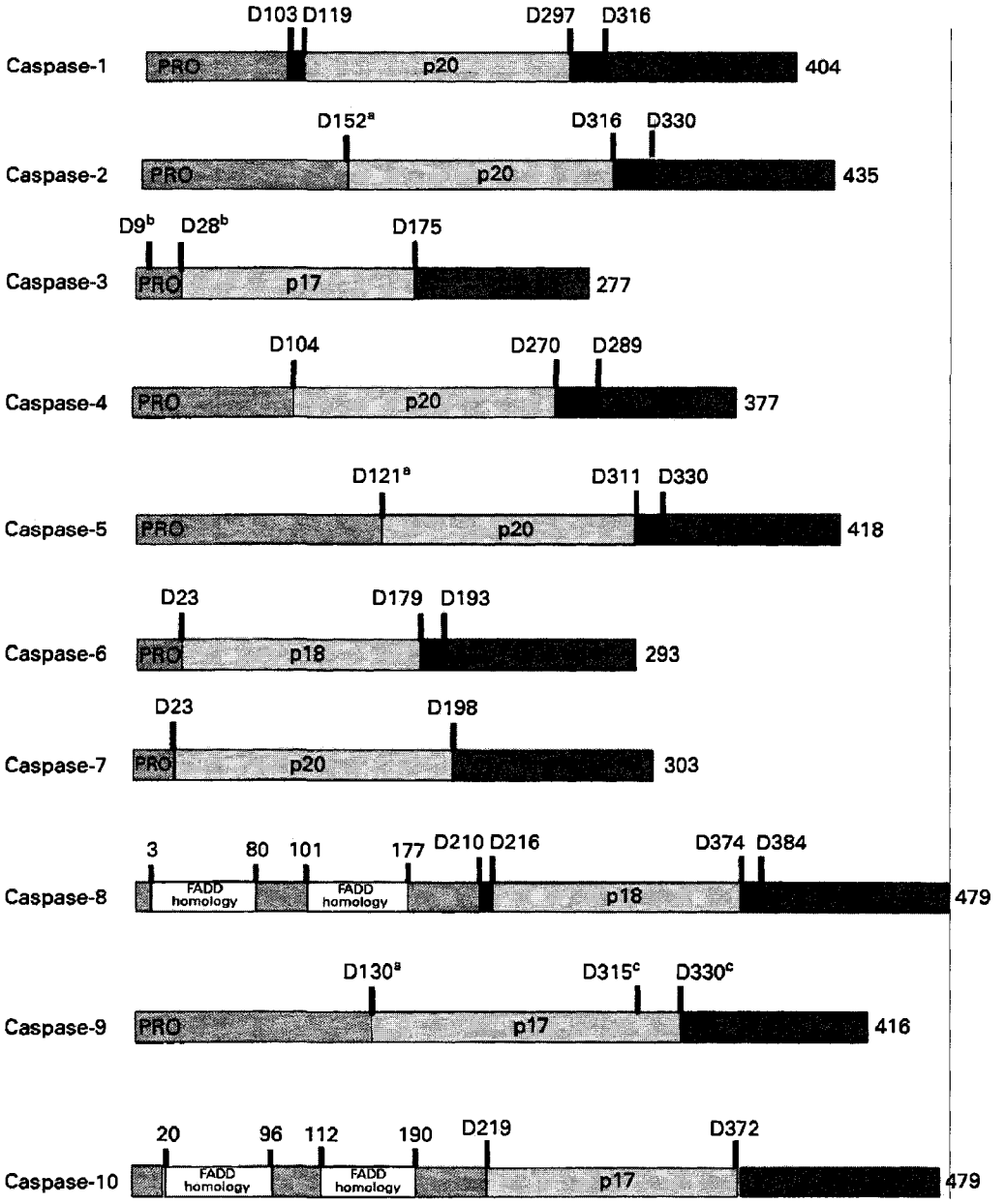

Figure 1.6 Domains and cleavage sites of caspases. The caspases are usually cleaved at specific Asp residues, indicated by Dn (n is the number of the amino acids in the protein). [a]exact cleavage site is not known. [b]either D9 or D28 may be the cleavage site of caspase-3. Adapted from [3].

1.5.3 c-FLIP

Cellular FADD-like, IL-1β-converting enzyme-inhibitory protein (c-FLIP), is a caspase homologue with a DED, and is recruited to the Fas-DISC by FADD [85] where it modulates caspase-8 recruitment and activation [61]. The gene encoding c-FLIP consists of 13 exons and is found between the genes encoding caspase-8 and caspase-10 on chromosome 2 [86, 87]. The c-FLIP gene is alternatively spliced into four mRNA variants but only two forms of the protein have been detected [85, 88, 89]. The short form of c-FLIP (c-FLIP$_S$) contains two DEDs and twenty unique C-terminal amino acids [85]. In contrast, the long form of c-FLIP (55 kDa) contains two DEDs and a caspase-8-like domain that lacks catalytic activity because of the replacement of the active site cysteine with tyrosine [85]. Both c-FLIP$_L$ and c-FLIP$_S$ are recruited to the Fas- and TRAIL-DISC where c-FLIP$_L$ undergoes caspase-8-mediated first step cleavage to generate a 43 kDa isoform [88, 90]. In the DISC, c-FLIP$_L$ and c-FLIP$_S$ inhibit caspase-8 second step cleavage [90]. Knockdown of c-FLIP$_L$ in lung cancer cells [91] and inhibition of c-FLIP$_S$ expression in glioblastoma cells [92] sensitizes the cells to TRAIL, further establishing c-FLIP$_L$ and c-FLIP$_S$ as caspase-8 inhibitors. On the other hand, studies of T lymphocytes have shown that c-FLIP$_L$ interacts with RIP [93] and TNFR-associated factor 2 (TRAF2) [94] for the activation of NF-κB and ERK1/2. Both c-FLIP$_L$ and c-FLIP$_S$ have been detected in many different tissues and while the short form is predominantly found in lymphatic tissue [85, 86], high levels of c-FLIP$_L$ protein are detected in tumors [17]. c-FLIP is known to be an important anti-apoptotic protein modulating TRAIL-DISC resistance in some cancer cell lines [95-97]. High levels of expression of c-FLIP were also reported to correlate strongly with TRAIL resistance and malignant potential in

colonic adenocarcinomas [97], melanoma [95], and hepatocellular carcinoma [96]. Moreover, c-FLIP is constitutively expressed in a variety of normal cells, but highly expressed in human cancers and thus implicated in tumorigenesis [85]. An elevated expression of c-FLIP results in the escape of tumors from TRAIL-mediated immune surveillance [98, 99]. Taken together, c-FLIP is a crucial tumorigenesis and surveillance mediator.

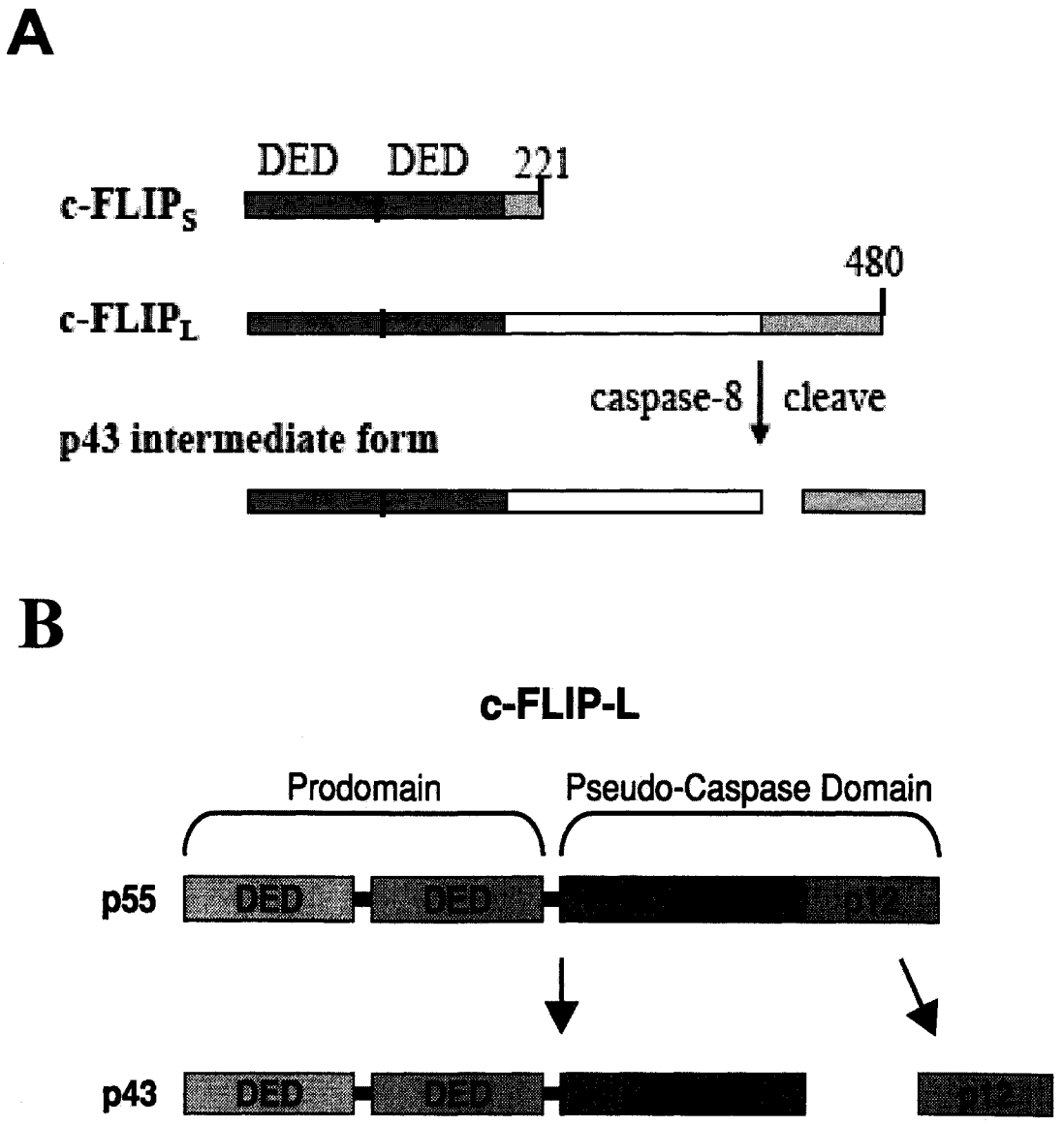

Figure 1.7 c-FLIP structure. (A) c-FLIP$_S$ contains two DED domains. c-FLIP$_L$ contains two DED domains and a caspase-like domain. (B). Structure of c-FLIP$_L$ and cleavage mechanism. Cleavage sites and the size of cleavage products are indicated. Adapted from Vitamins and Hormones, Volume 67, 192 (2004)).

1.5.4 RIP

RIP or RIP1 [100, 101] belongs to a family of related kinases that includes seven members [102-104]. These kinases share similar amino-terminal kinase domains (KD), but possess distinct carboxy-termini (Fig 1.8). RIP is classified as a serine/threonine kinase and possesses a carboxy-terminal death domain (DD), allowing recruitment to large protein complexes initiating different signaling pathways [100, 101]. RIP also bears a RIP homotypic interaction motif (RHIM) in its intermediate domain (ID) which is also present in the C-terminus of RIP3. This RHIM enables the interaction between RIP and RIP3 [105]. The RIP-DD complex has been shown to be important for binding to various death receptors, including Fas, TNF-R1, DR4, and DR5, and to DD-containing adaptor proteins, including TNF-receptor-associated death domain (TRADD) and FADD.

In the TRAIL signaling pathway, RIP is recruited to the DISC by DR4 and DR5 via its DD and couples the DISC to the NF-κB pathway [106, 107], and mediates NF-κB activation by recruiting the IKK complex to the DISC [108]. The IKK complex is composed of two kinases, IKKα and IKKβ, and a regulatory subunit, IKKγ. RIP interacts via its ID with IKKγ and thus recruits IKKα and IKKβ to the DISC where IKKα and IKKβ kinases are activated. The IKK complex phosphorylates IκB, allowing its degradation and releasing its inhibition of NF-κB. With its ID, RIP also recruits other kinases, such as MEKK1 and MEKK3. The function of the RIP kinase domain (KD) is less well characterized, although one report suggests that RIP KD may stimulate TNF, FasL, and TRAIL-induced necrotic cell death [109]. An active KD also was reported to enable RIP to autophosphorylate [100, 110]. RIP has been detected in the TRAIL-DISC in human HeLa cell line, suggesting that endogenous RIP may play a role in TRAIL

signaling in human cancer cells [106]. However, RIP has also been reported not to be recruited directly to DRs initiating DISC, but recruited to a secondary signaling complex which lacks DR4/DR5 but retains FADD and caspase-8 [107, 111] upon TRAIL stimulation. In this model, the caspase-8 activation is essential for the dissociation of FADD from DR4/DR5. When caspase-8 activity is blocked by z-VAD-fmk, DRs-DISC is stabilized and the formation of the secondary complex is impeded. Altogether, RIP acts on the crossroads decision of cells to live or die in response to various stress signals.

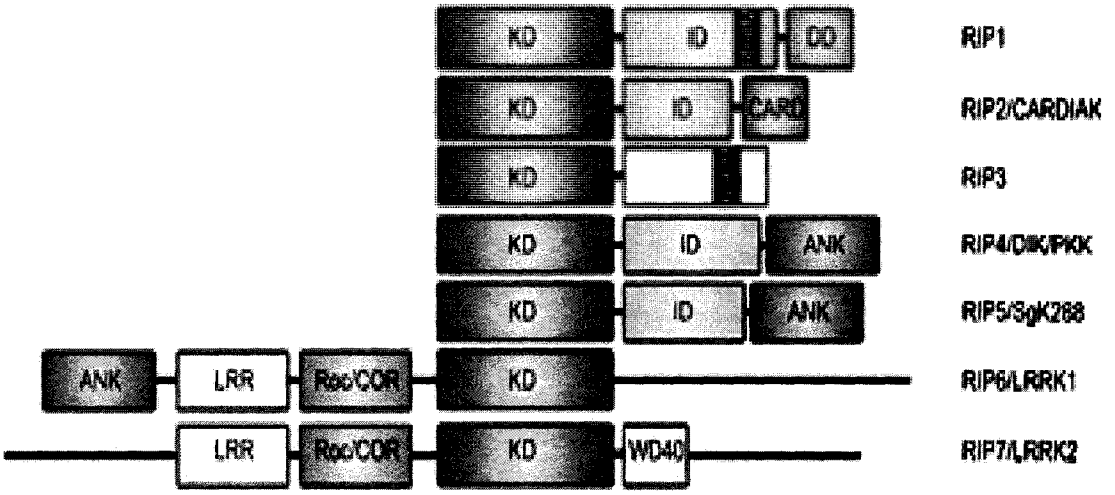

Figure 1.8 Domain organization of the RIP kinases. All seven members shared a homologous KD. RIP shares ID with RIP2, RIP4, and RIP5. With this ID, RIP also can interact with RIP3. RIP has a C-terminal DD. Adapted from [5].

1.5.5 Bcl-2 family

There are three groups of Bcl family proteins, including: (1) BH3 only proteins, Bid and Bim; (2) pro-apoptotic proteins, Bax and Bak, which contain three BH domains from BH1-3; and (3) pro-survival, Bcl-xL and Bcl-2, which contain four BH domains (1-4) (Fig 1.7).

1.5.5.1 Bid

The cross-talk between the DISC-initiated extrinsic apoptosis pathway and the mitochondria-associated intrinsic apoptosis pathway is mediated by a member of the BH3 domain only subgroup of the Bcl-2 family, Bid. The BH3 domain is exposed in all BH3-only proteins, except Bid [112]. As the exception, Bid appears to exist as an inactive cytosolic protein containing conserved sequence within the BH3 amphipathic α-helical domain, which is essential for the heterodimerization with other Bcl-2 family members [113]. Upon caspase-8 activation, Bid (p22) undergoes a proteolytic cleavage responsible for generating truncated p15 Bid (tBid) and BH3 exposure during apoptosis. tBid can directly bind and induce the oligomerization of Bax/Bak, leading to the damage of mitochondrial membrane potentials, followed by the release of apoptotic factors, such as cytochrome c and Smac/DIABLO [114].

Although the exact model of tBid-triggering Bax conformation change is still obscure, it is now generally accepted that tBid-Bax interaction could disrupt the Bax D33-K64 bond, thereby initiating the Bax conformational change. Once Bax is activated, Bid affinity to the activated Bax drastically decreases. This illustrates the "hit-and –run" model of Bid-induced activation [115, 116]. This kind of transient association is also

observed between tBid and Bak [117]. Taken together, tBid can transiently interact with Bax/Bak to cause their conformation change to induce Bax/Bak oligermerization.

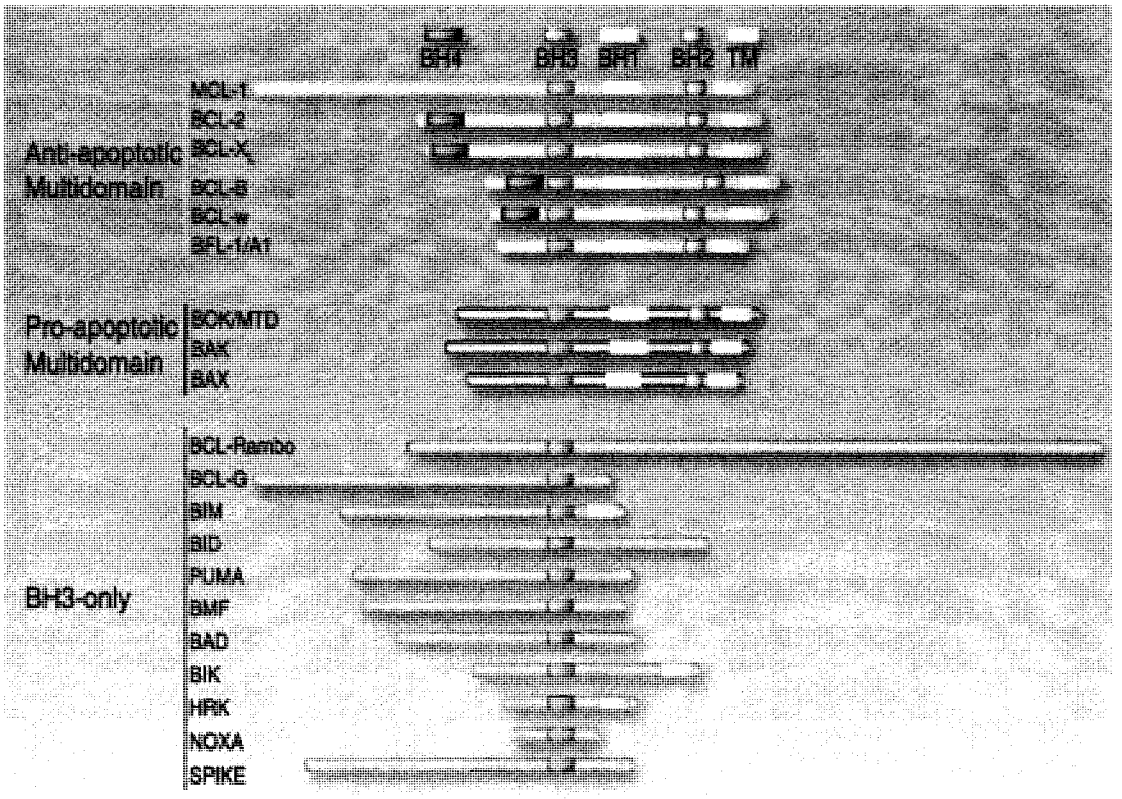

Figure 1.9 Three groups of the Bcl-2 family of proteins. Most members have a C-terminal transmembrane domain (TM). The first group, anti-apoptotic Bcl-2 family members, conserve all four Bcl-2 homolgy (BH) domains. The second group, the pro-apoptotic family members, conserve multidomains, including BH1-BH3. Members of the third group have only a BH3 domain. Adapted from [2].

1.5.5.2 Bax and Bak

Cells that are doubly deficient of both Bax and Bak fail to release cytochrome c and are resistant to all apoptotic stimuli, including ultraviolet radiation, growth factor deprivation, and ER stress [118].Lack of the proapoptotic genes of Bax or Bak can render cancer cells resistant to apoptosis induced by TRAIL or chemotherapy. In one study, Bak-deficient Jurkat cells were more resistant than wild-type Jurkat cells to apoptosis induced by TRAIL, UV, staurosporin, VP-16, bleomycin, or cisplatin. Restoring the Bak gene restored cytochrome c release and the sensitivity of the Bak-deficient cells to VP-16 [119]. These data indicate that Bax and Bak are required molecules for the mitochondria-associated intrinsic apoptosis pathway.

Bax is mostly cytosolic with a minor fraction lightly bound to the outer mitochondrial membrane (OMM) [120], whereas natively, Bak resides on the OMM. It has been reported that the COOH-terminal tail of Bax is required for its insertion into OMM. Upon apoptotic stimulation, cytosolic Bax undergoes a conformational change to insert into the OMM by releasing its COOH-terminal tail and to expose an NH_2-terminal epitope. Dependent on the exposed NH_2-terminal epitope, OMM-integrated monomers subsequently oligomerize to form pores [121]. Multiple Bax binding partners, including Bcl-2 and tBid, have been reported to regulate Bax translocation, insertion, and oligermerization [122]. Moreover, Bax-lipid interactions also influence Bax conformation and its ability to permeabilize the OMM [123].

Differing from Bax, Bak is integrated into the OMM before the induction of apoptosis. How Bak is activated during the mitochondria-associated apoptosis process is still unclear. One model proposes that Bak monomer interacts with two anti-apoptotic

proteins, Mcl-1 and Bcl-xL, which inhibit the oligomerization and activation of Bak in healthy cells [114]. Another model proposes that the intra-membranous oligomerization of Bak is inhibited by voltage-dependent anion channel 2 (VDAC2) which binds and stabilizes Bak in mitochondria [124]. Upon apoptotic signal stimulation, tBid or other BH3-only proteins can replace and dissociate the Bak from its binding partner to allow the conformational changes necessary for Bak activation.

1.5.5.3 Bcl-2 and Bcl-xL

Over-expression of Bcl-xL or Bcl-2 in some types of cells blocks TRAIL-mediated apoptosis, suggesting the dependence of TRAIL-induced apoptosis on the mitochondrial pathway [125]. The Bcl-xL expression level in three pancreatic adenocarcinoma cell lines has also been reported to be inversely correlated with their sensitivity to TRAIL-induced apoptosis [126]. In the animal model, Bcl-xL has also been reported to be essential for normal embryogenesis since Bcl-xL$^{-/-}$ mice displayed severe defects in erythropoiesis and neuronal development. Moreover, Bcl-2$^{-/-}$ mice displayed polycystic kidney disease and defects in their immune system. Clinically, the over-expression of Bcl-2 was also demonstrated to correlate with cancer recurrence, progression, and poor prognosis in various cancer patients [127-129]. These reports indicate the important anti-apoptotic role of Bcl-xL or Bcl-2 in the mitochondria-associated apoptosis pathway.

Besides the previously discussed models, in which tBid can directly bind and induce the oligermerizatin of Bax/Bak leading to mitochondrial membrane potential (MMP) changes [114, 123], research data about Bcl-xL and Bcl-2 suggest an alternative indirect activation model by which Bax/Bak is activated during apoptosis. In this model,

Bcl-xL and Bcl-2 selectively bind and inhibit Bax or Bak in certain cell types. BH3-only proteins mediate apoptosis by binding these anti-apoptotic proteins and thereby neutralize their inhibitory effects on Bax/Bak (Fig 1.8). In turn, Bax and Bak are then dissociated from these anti-apoptotic molecules to undergo conformational changes. During the process of TRAIL-induced apoptosis, activation of the initiator caspase-8 can transmit death signals, either through direct activation of the effector caspase-3, or by a mitochondrial pathway involving cleavage of the pro-apoptotic Bcl-2 family member, Bid [130]. In this mitochondrial pathway, the ratio of expression of the pro-apoptotic Bax protein and the anti-apoptotic Bcl-2 or Bcl-xL proteins ultimately determines cell death or survival [131, 132].

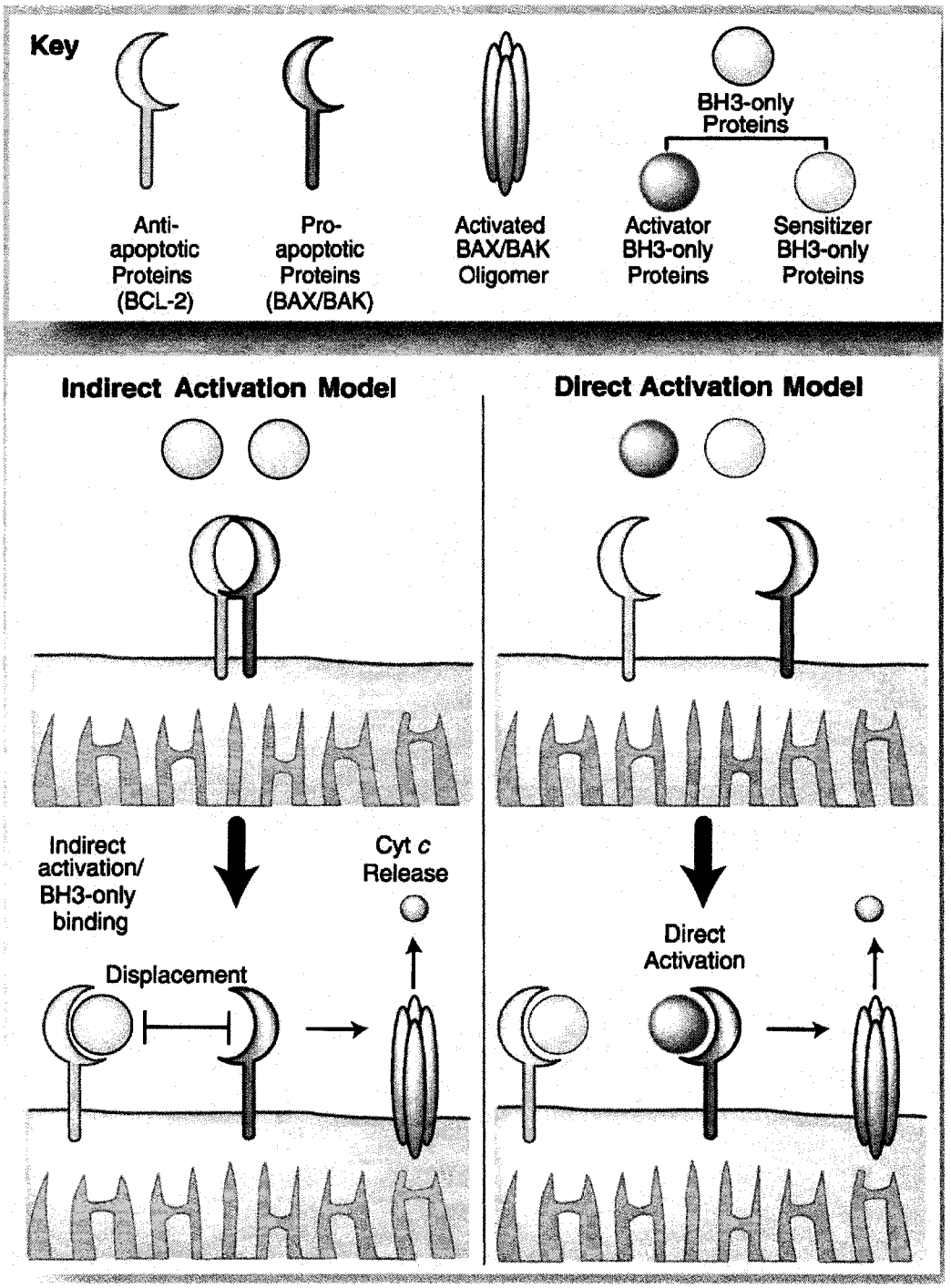

Figure 1.10 Two models for the activation of Bax/Bak by the BH3-only proteins. Indirect model and direct model. Adapted from [2].

1.6 TRAIL in cancer therapy

1.6.1 TRAIL-regulated immune surveilliance and its therapeutic roles against cancers

Expression of TRAIL mRNA has been detected in a variety of tissues [11]. Moreover, expression of the TRAIL protein ligand on the cell surface has been reported in NK cells [13-15] and contributes to NK cell-mediated inhibition of tumor development and metastasis in mice [13]. Studies *in vitro* have shown that recombinant TRAIL induces the selective death of various cancer cells, such as non-small cell lung carcinoma (NSCLC), colorectal cancer cells, pancreatic cancer cells, glioma cells, and leukemia cells, while sparing most normal cells [17, 46, 133, 134]. Pre-clinical experiments in mice and non-human primates have also shown that systemic administration of recombinant human TRAIL inhibits tumor growth with low level toxicity to normal tissues [16, 18]. These studies have placed TRAIL in the limelight of chemotherapy development [19, 135].

Several studies in vivo have proposed an important role for TRAIL in mediating auto-immunity since TRAIL-/- mice were more prone to disease development and have an increased susceptibility to collagen-induced arthritis and streptozotocin-induced diabetes [136, 137]. For cancer research, a study using TRAIL *in vivo* has also shown that TRAIL-deficient mice are more susceptible to tumor development [133]. In that study, wild type and TRAIL-deficient mice were inoculated with the chemical carcinogen, methylcholanthrene (MCA), in doses ranging from 5 to 400 μg. In previous research, it has been shown that MCA induction of fibrosarcomas is dose-dependent and is primarily controlled by NK cells [138], T cells [139], and the effector molecules, perforin and

interferon-γ (IFN-γ) [140]. Although injection of high doses of MCA induced fibrosarcomas in both WT and TRAIL-deficient mice, there was an earlier onset of fibrosarcomas in the TRAIL-deficient mice. As the dose of MCA was reduced, a difference in tumor onset and the susceptibility of WT and TRAIL-deficient mice to tumor development was observed. Notably, 100 μg of MCA induced fibrosarcomas in 70% of TRAIL-deficient mice, but in only 20% of WT mice, and tumor onset was earlier in TRAIL-deficient mice. Moreover, TRAIL-dependent anti-tumorigenicity has been shown in IFN-γ-stimulated monocytes, peripheral T cells, NK cells, and dendritic cells [37, 141-143]. These data indicate a clear suppression function of TRAIL against primary tumor development *in vivo*. Another *in vivo* study carried out in our laboratory showed that intraperitoneal injections of TRAIL inhibited intraperitoneal and subcutaneous tumor growth without inducing apoptosis in human hepatocytes carried on chimeric mice. Those data suggested that the recombinant soluble human TRAIL has a profound apoptotic effect on tumor cells but is nontoxic to human hepatocytes.

1.6.2 TRAIL based cancer therapeutics in the clinical trial

In the 1990s, anti-Fas Abs were tested in preclinical models *in vivo*. However, agonistic antimurine Fas mAbs were found to be extremely toxic, rapidly inducing hepatocyte apoptosis [144]. Moreover, FasL/Fas interactions have been reported to be important in the regulation of T-cell homeostasis [145]. Therefore, it is impossible to move nonspecific Fas-based therapeutics in the clinical trial. In contrast to FasL, recombinant TRAIL has been shown to selectively induce tumor cell apoptosis but have no toxicity to human hepatocytes [46]. TRAIL-deficient mice do not show global

perturbation in T-cell development and homeostasis [146], and constitutive expression of TRAIL receptors has been observed in a wide variety of tumor types. Thus, several approaches that engage or mimic the TRAIL pathway on cancer cells were explored. One chain of research has used trimeric TRAIL as the therapeutic agents, but significant toxicity to liver cells was observed. Subsequently, by using recombinant non-tagged TRAIL, the hepatotoxicity could be avoided, reopening the door to clinical applications of TRAIL [43, 46].

At the 2006 Annual Meeting of the American Society of Clinical Oncology, early results of a study using recombinant TRAIL showing that one patient with a chondrosarcoma demonstrated a partial response without major dose-limiting toxicity, were presented. Another chain of research focuses on the development of mAbs against human TRAIL receptors (DR4 and DR5). In a phase I trial of an anti-DR5 mAb (HGS-ETR2), one patient with chemotherapy-refractory Hogkin's disease experienced a clinical response. In another study, a combination trial of carboplatin and paclitaxel with anti-DR4 mAB (HGS-ETR1) was reported with at least four clinical responses. Moreover, data from another phase I clinical trial of HGS-ETR1 showed that HGS-ETR1 can be safely administrated to patients with advanced malignancy up to high doses without causing hepatic or hematological toxicity [147]. These reports suggest that we have passed the period of anxiety over possible life-threatening toxicity with clinical TRAIL-based therapies. However, it is desirable to increase our understanding of the biological mechanisms underlying TRAIL-resistance for the development of an appropriate treatment strategy and patient selection to enrich a responsive population.

1.7. Hypothesis and Objectives

This thesis work is focused on investigating the underlying mechanisms by which cancer cells become resistant to TRAIL-induced apoptosis. TRAIL has long been a promising candidate for novel cancer therapy since it can selectively trigger apoptotic cell death in cancer cells but spare normal cells [46]. However, there are many cancer cells that are resistant to different extents to TRAIL-induced apoptosis and the underlining mechanism(s) is(are) still largely unknown. Our previous work showed that TRAIL-induced apoptosis proceeds through two pathways: the DISC-initiated extrinsic pathway and the mitochondria-associated intrinsic pathway [148]. To investigate the potential therapeutic role of TRAIL for various cancers, we need first to clarify the two pathways followed by further exploration of the crucial apoptosis regulators involved in these pathways.

Thus, the broad objective of my thesis work was to characterize the process of TRAIL-induced apoptosis at the molecular level, with a focus on the resistance mechanisms of cancer cells to TRAIL treatment. In this study, we hypothesized that TRAIL resistant mechanism(s) are focused on two levels: the DISC level or the mitochondria level for the loss of crucial apoptotic factors or over-expression of anti-apoptotic factors. To examine this proposition, three key processes regulating cancer cell sensitivity to TRAIL-induced apoptosis were proposed and probed as follows.

1) TRAIL induces apoptosis through the DISC-initiated extrinsic pathway and the mitochondria-associated intrinsic pathway. FADD and caspase-8 are the crucial apoptotic

factors at the DISC level, and Bcl-2 and Bcl-xL are crucial anti-apoptotic factors at the mitochondria level.

2) RIP and cFLIP are crucial anti-apoptotic factors in the DISC level.

3) Knock out the Bax, the crucial apoptotic factor in the mitochondria level, four groups of apoptosis-related proteins are differentially expressed by which these cancer cells further lose their apoptotic potentials.

1.8. References

1. Ashkenazi, A., *Targeting death and decoy receptors of the tumour-necrosis factor superfamily.* Nat Rev Cancer, 2002. **2**(6): p. 420-30.
2. Danial, N.N., *BCL-2 family proteins: critical checkpoints of apoptotic cell death.* Clin Cancer Res, 2007. **13**(24): p. 7254-63.
3. Cohen, G.M., *Caspases: the executioners of apoptosis.* Biochem J, 1997. **326 (Pt 1)**: p. 1-16.
4. Kimberley, F.C. and G.R. Screaton, *Following a TRAIL: update on a ligand and its five receptors.* Cell Res, 2004. **14**(5): p. 359-72.
5. Festjens, N., et al., *RIP1, a kinase on the crossroads of a cell's decision to live or die.* Cell Death Differ, 2007. **14**(3): p. 400-10.
6. Ashkenazi, A., *Targeting death receptor mediated apoptosis in cancer.* 96th Annual meeting of the American Association for Cancer Research, Anaheim, CA, April 16-20, 2005.
7. Fox, N.L., *Antibodies against TRAIL receptor-2 protein.* 4th International Confress on Targeted Therapies in Cancer, Washington, DC, 2005.
8. Hao, C., et al., *Induction and intracellular regulation of tumor necrosis factor-related apoptosis-inducing ligand (TRAIL) mediated apotosis in human malignant glioma cells.* Cancer Res, 2001. **61**(3): p. 1162-70.
9. Song, J.H., et al., *TRAIL triggers apoptosis in malignant glioma cells through extrinsic and intrinsic pathways.* Brain Pathol, 2003. **13**(4): p. 539-553.
10. Adams, J., *The proteasome: a suitable antineoplastic target.* Nat Rev Cancer, 2004. **4**(5): p. 349-60.
11. Wiley, S.R., et al., *Identification and characterization of a new member of the TNF family that induces apoptosis.* Immunity, 1995. **3**(6): p. 673-82.
12. Pitti, R.M., et al., *Induction of apoptosis by Apo-2 ligand, a new member of the tumor necrosis factor cytokine family.* J Biol Chem, 1996. **271**(22): p. 12687-90.
13. Takeda, K., et al., *Involvement of tumor necrosis factor-related apoptosis-inducing ligand in surveillance of tumor metastasis by liver natural killer cells.* Nat Med, 2001. **7**(1): p. 94-100.
14. Smyth, M.J., et al., *Tumor necrosis factor-related apoptosis-inducing ligand (TRAIL) contributes to interferon gamma-dependent natural killer cell protection from tumor metastasis.* J Exp Med, 2001. **193**(6): p. 661-70.
15. Takeda, K., et al., *Critical role for tumor necrosis factor-related apoptosis-inducing ligand in immune surveillance against tumor development.* J Exp Med, 2002. **195**(2): p. 161-9.
16. Ashkenazi, A., et al., *Safety and antitumor activity of recombinant soluble Apo2 ligand.* J Clin Invest, 1999. **104**(2): p. 155-62.
17. Leverkus, M., et al., *Regulation of tumor necrosis factor-related apoptosis-inducing ligand sensitivity in primary and transformed human keratinocytes.* Cancer Res, 2000. **60**(3): p. 553-9.
18. Walczak, H., et al., *Tumoricidal activity of tumor necrosis factor-related apoptosis-inducing ligand in vivo.* Nat Med, 1999. **5**(2): p. 157-63.
19. Smyth, M.J., et al., *Nature's TRAIL--on a path to cancer immunotherapy.* Immunity, 2003. **18**(1): p. 1-6.

20. Luo, X., et al., *Bid, a Bcl2 interacting protein, mediates cytochrome c release from mitochondria in response to activation of cell surface death receptors.* Cell, 1998. **94**(4): p. 481-90.
21. Du, C., et al., *Smac, a mitochondrial protein that promotes cytochrome c-dependent caspase activation by eliminating IAP inhibition.* Cell, 2000. **102**(1): p. 33-42.
22. Cha, S.S., et al., *2.8 A resolution crystal structure of human TRAIL, a cytokine with selective antitumor activity.* Immunity, 1999. **11**(2): p. 253-61.
23. Mariani, S.M. and P.H. Krammer, *Differential regulation of TRAIL and CD95 ligand in transformed cells of the T and B lymphocyte lineage.* Eur J Immunol, 1998. **28**(3): p. 973-82.
24. Wajant, H., et al., *Differential activation of TRAIL-R1 and -2 by soluble and membrane TRAIL allows selective surface antigen-directed activation of TRAIL-R2 by a soluble TRAIL derivative.* Oncogene, 2001. **20**(30): p. 4101-6.
25. Pan, G., et al., *The receptor for the cytotoxic ligand TRAIL.* Science, 1997. **276**(5309): p. 111-3.
26. Sheridan, J.P., et al., *Control of TRAIL-induced apoptosis by a family of signaling and decoy receptors.* Science, 1997. **277**(5327): p. 818-21.
27. Degli-Esposti, M.A., et al., *The novel receptor TRAIL-R4 induces NF-kappaB and protects against TRAIL-mediated apoptosis, yet retains an incomplete death domain.* Immunity, 1997. **7**(6): p. 813-20.
28. Simonet, W.S., et al., *Osteoprotegerin: a novel secreted protein involved in the regulation of bone density.* Cell, 1997. **89**(2): p. 309-19.
29. Emery, J.G., et al., *Osteoprotegerin is a receptor for the cytotoxic ligand TRAIL.* J Biol Chem, 1998. **273**(23): p. 14363-7.
30. Pan, G., et al., *An antagonist decoy receptor and a death domain-containing receptor for TRAIL.* Science, 1997. **277**(5327): p. 815-8.
31. MacFarlane, M., et al., *Identification and molecular cloning of two novel receptors for the cytotoxic ligand TRAIL.* J Biol Chem, 1997. **272**(41): p. 25417-20.
32. Clancy, L., et al., *Preligand assembly domain-mediated ligand-independent association between TRAIL receptor 4 (TR4) and TR2 regulates TRAIL-induced apoptosis.* Proc Natl Acad Sci U S A, 2005. **102**(50): p. 18099-104.
33. Truneh, A., et al., *Temperature-sensitive differential affinity of TRAIL for its receptors. DR5 is the highest affinity receptor.* J Biol Chem, 2000. **275**(30): p. 23319-25.
34. Holen, I., et al., *Osteoprotegerin (OPG) is a survival factor for human prostate cancer cells.* Cancer Res, 2002. **62**(6): p. 1619-23.
35. Gochuico, B.R., et al., *TRAIL expression in vascular smooth muscle.* Am J Physiol Lung Cell Mol Physiol, 2000. **278**(5): p. L1045-50.
36. Griffith, T.S., et al., *Monocyte-mediated tumoricidal activity via the tumor necrosis factor-related cytokine, TRAIL.* J Exp Med, 1999. **189**(8): p. 1343-54.
37. Fanger, N.A., et al., *Human dendritic cells mediate cellular apoptosis via tumor necrosis factor-related apoptosis-inducing ligand (TRAIL).* J Exp Med, 1999. **190**(8): p. 1155-64.

38. Hymowitz, S.G., et al., *Triggering cell death: the crystal structure of Apo2L/TRAIL in a complex with death receptor 5.* Mol Cell, 1999. **4**(4): p. 563-71.
39. Mongkolsapaya, J., et al., *Structure of the TRAIL-DR5 complex reveals mechanisms conferring specificity in apoptotic initiation.* Nat Struct Biol, 1999. **6**(11): p. 1048-53.
40. Bodmer, J.L., et al., *Cysteine 230 is essential for the structure and activity of the cytotoxic ligand TRAIL.* J Biol Chem, 2000. **275**(27): p. 20632-7.
41. Almasan, A. and A. Ashkenazi, *Apo2L/TRAIL: apoptosis signaling, biology, and potential for cancer therapy.* Cytokine Growth Factor Rev, 2003. **14**(3-4): p. 337-48.
42. Jo, M., et al., *Apoptosis induced in normal human hepatocytes by tumor necrosis factor-related apoptosis-inducing ligand.* Nat Med, 2000. **6**(5): p. 564-7.
43. Lawrence, D., et al., *Differential hepatocyte toxicity of recombinant Apo2L/TRAIL versions.* Nat Med, 2001. 7(4): p. 383-5.
44. Nitsch, R., et al., *Human brain-cell death induced by tumour-necrosis-factor-related apoptosis-inducing ligand (TRAIL).* Lancet, 2000. **356**(9232): p. 827-8.
45. Qin, J., et al., *Avoiding premature apoptosis of normal epidermal cells.* Nat Med, 2001. 7(4): p. 385-6.
46. Hao, C., et al., *TRAIL inhibits tumor growth but is nontoxic to human hepatocytes in chimeric mice.* Cancer Res, 2004. **64**(23): p. 8502-6.
47. LeBlanc, H.N. and A. Ashkenazi, *Apo2L/TRAIL and its death and decoy receptors.* Cell Death Differ, 2003. **10**(1): p. 66-75.
48. Green, D.R. and J.C. Reed, *Mitochondria and apoptosis.* Science, 1998. **281**(5381): p. 1309-12.
49. Schneider, P., et al., *Characterization of two receptors for TRAIL.* FEBS Lett, 1997. **416**(3): p. 329-34.
50. Chaudhary, P.M., et al., *Death receptor 5, a new member of the TNFR family, and DR4 induce FADD-dependent apoptosis and activate the NF-kappaB pathway.* Immunity, 1997. 7(6): p. 821-30.
51. Walczak, H., et al., *TRAIL-R2: a novel apoptosis-mediating receptor for TRAIL.* Embo J, 1997. **16**(17): p. 5386-97.
52. Wu, G.S., et al., *KILLER/DR5 is a DNA damage-inducible p53-regulated death receptor gene.* Nat Genet, 1997. **17**(2): p. 141-3.
53. Chinnaiyan, A.M., et al., *FADD, a novel death domain-containing protein, interacts with the death domain of Fas and initiates apoptosis.* Cell, 1995. **81**(4): p. 505-12.
54. Boldin, M.P., et al., *A novel protein that interacts with the death domain of Fas/APO1 contains a sequence motif related to the death domain.* J Biol Chem, 1995. **270**(14): p. 7795-8.
55. Muzio, M., et al., *FLICE, a novel FADD-homologous ICE/CED-3-like protease, is recruited to the CD95 (Fas/APO-1) death--inducing signaling complex.* Cell, 1996. **85**(6): p. 817-27.
56. Kischkel, F.C., et al., *Cytotoxicity-dependent APO-1 (Fas/CD95)-associated proteins form a death-inducing signaling complex (DISC) with the receptor.* Embo J, 1995. **14**(22): p. 5579-88.

57. Medema, J.P., et al., *FLICE is activated by association with the CD95 death-inducing signaling complex (DISC).* Embo J, 1997. **16**(10): p. 2794-804.
58. Muzio, M., et al., *An induced proximity model for caspase-8 activation.* J Biol Chem, 1998. **273**(5): p. 2926-30.
59. Boatright, K.M., et al., *A unified model for apical caspase activation.* Mol Cell, 2003. **11**(2): p. 529-41.
60. Boldin, M.P., et al., *Involvement of MACH, a novel MORT1/FADD-interacting protease, in Fas/APO-1- and TNF receptor-induced cell death.* Cell, 1996. **85**(6): p. 803-15.
61. Xiao, C., et al., *Tumor necrosis factor-related apoptosis-inducing ligand-induced death-inducing signaling complex and its modulation by c-FLIP and PED/PEA-15 in glioma cells.* J Biol Chem, 2002. **277**(28): p. 25020-5.
62. Kischkel, F.C., et al., *Death receptor recruitment of endogenous caspase-10 and apoptosis initiation in the absence of caspase-8.* J Biol Chem, 2001. **276**(49): p. 46639-46.
63. Sprick, M.R., et al., *Caspase-10 is recruited to and activated at the native TRAIL and CD95 death-inducing signalling complexes in a FADD-dependent manner but can not functionally substitute caspase-8.* Embo J, 2002. **21**(17): p. 4520-30.
64. Wang, J., et al., *Caspase-10 is an initiator caspase in death receptor signaling.* Proc Natl Acad Sci U S A, 2001. **98**(24): p. 13884-8.
65. Verhagen, A.M., et al., *Identification of DIABLO, a mammalian protein that promotes apoptosis by binding to and antagonizing IAP proteins.* Cell, 2000. **102**(1): p. 43-53.
66. Li, L., et al., *A small molecule Smac mimic potentiates TRAIL- and TNFalpha-mediated cell death.* Science, 2004. **305**(5689): p. 1471-4.
67. Renatus, M., et al., *Dimer formation drives the activation of the cell death protease caspase 9.* Proc Natl Acad Sci U S A, 2001. **98**(25): p. 14250-5.
68. Srinivasula, S.M., et al., *A conserved XIAP-interaction motif in caspase-9 and Smac/DIABLO regulates caspase activity and apoptosis.* Nature, 2001. **410**(6824): p. 112-6.
69. Samali, A., et al., *Presence of a pre-apoptotic complex of pro-caspase-3, Hsp60 and Hsp10 in the mitochondrial fraction of jurkat cells.* Embo J, 1999. **18**(8): p. 2040-8.
70. Liu, X., et al., *DFF, a heterodimeric protein that functions downstream of caspase-3 to trigger DNA fragmentation during apoptosis.* Cell, 1997. **89**(2): p. 175-84.
71. Bratton, S.B. and G.M. Cohen, *Apoptotic death sensor: an organelle's alter ego?* Trends Pharmacol Sci, 2001. **22**(6): p. 306-15.
72. Kerr, J.F., et al., *Anatomical methods in cell death.* Methods Cell Biol, 1995. **46**: p. 1-27.
73. Kerr, J.F., A.H. Wyllie, and A.R. Currie, *Apoptosis: a basic biological phenomenon with wide-ranging implications in tissue kinetics.* Br J Cancer, 1972. **26**(4): p. 239-57.
74. Fadeel, B., S. Orrenius, and B. Zhivotovsky, *Apoptosis in human disease: a new skin for the old ceremony?* Biochem Biophys Res Commun, 1999. **266**(3): p. 699-717.

75. Wyllie, A.H., J.F. Kerr, and A.R. Currie, *Cell death: the significance of apoptosis.* Int Rev Cytol, 1980. **68**: p. 251-306.
76. Arends, M.J. and A.H. Wyllie, *Apoptosis: mechanisms and roles in pathology.* Int Rev Exp Pathol, 1991. **32**: p. 223-54.
77. Takahashi, A. and W.C. Earnshaw, *ICE-related proteases in apoptosis.* Curr Opin Genet Dev, 1996. **6**(1): p. 50-5.
78. Igney, F.H. and P.H. Krammer, *Death and anti-death: tumour resistance to apoptosis.* Nat Rev Cancer, 2002. **2**(4): p. 277-88.
79. Kuang, A.A., et al., *FADD is required for DR4- and DR5-mediated apoptosis: lack of trail-induced apoptosis in FADD-deficient mouse embryonic fibroblasts.* J Biol Chem, 2000. **275**(33): p. 25065-8.
80. Zhang, J. and A. Winoto, *A mouse Fas-associated protein with homology to the human Mort1/FADD protein is essential for Fas-induced apoptosis.* Mol Cell Biol, 1996. **16**(6): p. 2756-63.
81. Sandu, C., et al., *FADD self-association is required for stable interaction with an activated death receptor.* Cell Death Differ, 2006. **13**(12): p. 2052-61.
82. Nicholson, D.W. and N.A. Thornberry, *Caspases: killer proteases.* Trends Biochem Sci, 1997. **22**(8): p. 299-306.
83. Salvesen, G.S. and V.M. Dixit, *Caspases: intracellular signaling by proteolysis.* Cell, 1997. **91**(4): p. 443-6.
84. Howard, A.D., et al., *Probing the role of interleukin-1 beta convertase in interleukin-1 beta secretion.* Agents Actions Suppl, 1991. **35**: p. 77-83.
85. Irmler, M., et al., *Inhibition of death receptor signals by cellular FLIP.* Nature, 1997. **388**(6638): p. 190-5.
86. Rasper, D.M., et al., *Cell death attenuation by 'Usurpin', a mammalian DED-caspase homologue that precludes caspase-8 recruitment and activation by the CD-95 (Fas, APO-1) receptor complex.* Cell Death Differ, 1998. **5**(4): p. 271-88.
87. Kischkel, F.C., et al., *Assignment of CASP8 to human chromosome band 2q33-->q34 and Casp8 to the murine syntenic region on chromosome 1B-proximal C by in situ hybridization.* Cytogenet Cell Genet, 1998. **82**(1-2): p. 95-6.
88. Scaffidi, C., et al., *The role of c-FLIP in modulation of CD95-induced apoptosis.* J Biol Chem, 1999. **274**(3): p. 1541-8.
89. Shu, H.B., D.R. Halpin, and D.V. Goeddel, *Casper is a FADD- and caspase-related inducer of apoptosis.* Immunity, 1997. **6**(6): p. 751-63.
90. Krueger, A., et al., *FLICE-inhibitory proteins: regulators of death receptor-mediated apoptosis.* Mol Cell Biol, 2001. **21**(24): p. 8247-54.
91. Sharp, D.A., D.A. Lawrence, and A. Ashkenazi, *Selective Knockdown of the Long Variant of Cellular FLICE Inhibitory Protein Augments Death Receptor-mediated Caspase-8 Activation and Apoptosis.* J Biol Chem, 2005. **280**(19): p. 19401-9.
92. Panner, A., et al., *mTOR controls FLIPS translation and TRAIL sensitivity in glioblastoma multiforme cells.* Mol Cell Biol, 2005. **25**(20): p. 8809-23.
93. Dohrman, A., et al., *Cellular FLIP (long form) regulates CD8+ T cell activation through caspase-8-dependent NF-kappa B activation.* J Immunol, 2005. **174**(9): p. 5270-8.

94. Kataoka, T. and J. Tschopp, *N-terminal fragment of c-FLIP(L) processed by caspase 8 specifically interacts with TRAF2 and induces activation of the NF-kappaB signaling pathway.* Mol Cell Biol, 2004. **24**(7): p. 2627-36.
95. Bullani, R.R., et al., *Selective expression of FLIP in malignant melanocytic skin lesions.* J Invest Dermatol, 2001. **117**(2): p. 360-4.
96. Okano, H., et al., *Cellular FLICE/caspase-8-inhibitory protein as a principal regulator of cell death and survival in human hepatocellular carcinoma.* Lab Invest, 2003. **83**(7): p. 1033-43.
97. Ryu, B.K., et al., *Increased expression of cFLIP(L) in colonic adenocarcinoma.* J Pathol, 2001. **194**(1): p. 15-9.
98. Djerbi, M., et al., *The inhibitor of death receptor signaling, FLICE-inhibitory protein defines a new class of tumor progression factors.* J Exp Med, 1999. **190**(7): p. 1025-32.
99. Medema, J.P., et al., *Immune escape of tumors in vivo by expression of cellular FLICE-inhibitory protein.* J Exp Med, 1999. **190**(7): p. 1033-8.
100. Hsu, H., et al., *TNF-dependent recruitment of the protein kinase RIP to the TNF receptor-1 signaling complex.* Immunity, 1996. **4**(4): p. 387-96.
101. Stanger, B.Z., et al., *RIP: a novel protein containing a death domain that interacts with Fas/APO-1 (CD95) in yeast and causes cell death.* Cell, 1995. **81**(4): p. 513-23.
102. McCarthy, J.V., J. Ni, and V.M. Dixit, *RIP2 is a novel NF-kappaB-activating and cell death-inducing kinase.* J Biol Chem, 1998. **273**(27): p. 16968-75.
103. Sun, X., et al., *RIP3, a novel apoptosis-inducing kinase.* J Biol Chem, 1999. **274**(24): p. 16871-5.
104. Meylan, E., et al., *RIP4 (DIK/PKK), a novel member of the RIP kinase family, activates NF-kappa B and is processed during apoptosis.* EMBO Rep, 2002. **3**(12): p. 1201-8.
105. Meylan, E. and J. Tschopp, *The RIP kinases: crucial integrators of cellular stress.* Trends Biochem Sci, 2005. **30**(3): p. 151-9.
106. Harper, N., et al., *Modulation of tumor necrosis factor apoptosis-inducing ligand-induced NF-kappa B activation by inhibition of apical caspases.* J Biol Chem, 2001. **276**(37): p. 34743-52.
107. Lin, Y., et al., *The death domain kinase RIP is essential for TRAIL (Apo2L)-induced activation of IkappaB kinase and c-Jun N-terminal kinase.* Mol Cell Biol, 2000. **20**(18): p. 6638-45.
108. Karin, M. and A. Lin, *NF-kappaB at the crossroads of life and death.* Nat Immunol, 2002. **3**(3): p. 221-7.
109. Holler, N., et al., *Fas triggers an alternative, caspase-8-independent cell death pathway using the kinase RIP as effector molecule.* Nat Immunol, 2000. **1**(6): p. 489-95.
110. Ting, A.T., F.X. Pimentel-Muinos, and B. Seed, *RIP mediates tumor necrosis factor receptor 1 activation of NF-kappaB but not Fas/APO-1-initiated apoptosis.* Embo J, 1996. **15**(22): p. 6189-96.
111. Varfolomeev, E., et al., *Molecular determinants of kinase pathway activation by Apo2 ligand/tumor necrosis factor-related apoptosis-inducing ligand.* J Biol Chem, 2005. **280**(49): p. 40599-608.

112. Walensky, L.D., et al., *Activation of apoptosis in vivo by a hydrocarbon-stapled BH3 helix.* Science, 2004. **305**(5689): p. 1466-70.
113. Wang, K., et al., *BID: a novel BH3 domain-only death agonist.* Genes Dev, 1996. **10**(22): p. 2859-69.
114. Kim, H., et al., *Hierarchical regulation of mitochondrion-dependent apoptosis by BCL-2 subfamilies.* Nat Cell Biol, 2006. **8**(12): p. 1348-58.
115. Chen, S., et al., *Mcl-1 down-regulation potentiates ABT-737 lethality by cooperatively inducing Bak activation and Bax translocation.* Cancer Res, 2007. **67**(2): p. 782-91.
116. Suzuki, M., R.J. Youle, and N. Tjandra, *Structure of Bax: coregulation of dimer formation and intracellular localization.* Cell, 2000. **103**(4): p. 645-54.
117. Dlugosz, P.J., et al., *Bcl-2 changes conformation to inhibit Bax oligomerization.* Embo J, 2006. **25**(11): p. 2287-96.
118. Wei, M.C., et al., *Proapoptotic BAX and BAK: a requisite gateway to mitochondrial dysfunction and death.* Science, 2001. **292**(5517): p. 727-30.
119. Wang, G.Q., et al., *A role for mitochondrial Bak in apoptotic response to anticancer drugs.* J Biol Chem, 2001. **276**(36): p. 34307-17.
120. Hsu, Y.T., K.G. Wolter, and R.J. Youle, *Cytosol-to-membrane redistribution of Bax and Bcl-X(L) during apoptosis.* Proc Natl Acad Sci U S A, 1997. **94**(8): p. 3668-72.
121. Annis, M.G., et al., *Bax forms multispanning monomers that oligomerize to permeabilize membranes during apoptosis.* Embo J, 2005. **24**(12): p. 2096-103.
122. Lucken-Ardjomande, S. and J.C. Martinou, *Newcomers in the process of mitochondrial permeabilization.* J Cell Sci, 2005. **118**(Pt 3): p. 473-83.
123. Kuwana, T., et al., *Bid, Bax, and lipids cooperate to form supramolecular openings in the outer mitochondrial membrane.* Cell, 2002. **111**(3): p. 331-42.
124. Cheng, E.H., et al., *VDAC2 inhibits BAK activation and mitochondrial apoptosis.* Science, 2003. **301**(5632): p. 513-7.
125. Thomas, W.D., et al., *TNF-related apoptosis-inducing ligand-induced apoptosis of melanoma is associated with changes in mitochondrial membrane potential and perinuclear clustering of mitochondria.* J Immunol, 2000. **165**(10): p. 5612-20.
126. Hinz, S., et al., *Bcl-XL protects pancreatic adenocarcinoma cells against CD95- and TRAIL-receptor-mediated apoptosis.* Oncogene, 2000. **19**(48): p. 5477-86.
127. Gallo, O., et al., *bcl-2 protein expression correlates with recurrence and survival in early stage head and neck cancer treated by radiotherapy.* Clin Cancer Res, 1996. **2**(2): p. 261-7.
128. King, E.D., et al., *Incidence of apoptosis, cell proliferation and bcl-2 expression in transitional cell carcinoma of the bladder: association with tumor progression.* J Urol, 1996. **155**(1): p. 316-20.
129. Bilim, V., et al., *Prognostic value of Bcl-2 and p53 expression in urinary tract transitional cell cancer.* J Natl Cancer Inst, 1996. **88**(10): p. 686-8.
130. Daniel, P.T., et al., *The kiss of death: promises and failures of death receptors and ligands in cancer therapy.* Leukemia, 2001. **15**(7): p. 1022-32.
131. Kluck, R.M., et al., *The release of cytochrome c from mitochondria: a primary site for Bcl-2 regulation of apoptosis.* Science, 1997. **275**(5303): p. 1132-6.

132. Liu, X., et al., *Induction of apoptotic program in cell-free extracts: requirement for dATP and cytochrome c.* Cell, 1996. **86**(1): p. 147-57.
133. Cretney, E., et al., *Increased susceptibility to tumor initiation and metastasis in TNF-related apoptosis-inducing ligand-deficient mice.* J Immunol, 2002. **168**(3): p. 1356-61.
134. Wang, P., et al., *Role of death receptor and mitochondrial pathways in conventional chemotherapy drug induction of apoptosis.* Cell Signal, 2006. **18**(9): p. 1528-35.
135. Hao, C., et al., *Modulation of TRAIL signaling complex.* Vitam Horm, 2004. **67**: p. 81-99.
136. Lamhamedi-Cherradi, S.E., et al., *Defective thymocyte apoptosis and accelerated autoimmune diseases in TRAIL-/- mice.* Nat Immunol, 2003. **4**(3): p. 255-60.
137. Sedger, L.M., et al., *Characterization of the in vivo function of TNF-alpha-related apoptosis-inducing ligand, TRAIL/Apo2L, using TRAIL/Apo2L gene-deficient mice.* Eur J Immunol, 2002. **32**(8): p. 2246-54.
138. Davis, J.E., M.J. Smyth, and J.A. Trapani, *Granzyme A and B-deficient killer lymphocytes are defective in eliciting DNA fragmentation but retain potent in vivo anti-tumor capacity.* Eur J Immunol, 2001. **31**(1): p. 39-47.
139. Smyth, M.J., et al., *Differential tumor surveillance by natural killer (NK) and NKT cells.* J Exp Med, 2000. **191**(4): p. 661-8.
140. Street, S.E., E. Cretney, and M.J. Smyth, *Perforin and interferon-gamma activities independently control tumor initiation, growth, and metastasis.* Blood, 2001. **97**(1): p. 192-7.
141. Kayagaki, N., et al., *Involvement of TNF-related apoptosis-inducing ligand in human CD4+ T cell-mediated cytotoxicity.* J Immunol, 1999. **162**(5): p. 2639-47.
142. Thomas, W.D. and P. Hersey, *TNF-related apoptosis-inducing ligand (TRAIL) induces apoptosis in Fas ligand-resistant melanoma cells and mediates CD4 T cell killing of target cells.* J Immunol, 1998. **161**(5): p. 2195-200.
143. Sedger, L.M., et al., *IFN-gamma mediates a novel antiviral activity through dynamic modulation of TRAIL and TRAIL receptor expression.* J Immunol, 1999. **163**(2): p. 920-6.
144. Ogasawara, J., et al., *Lethal effect of the anti-Fas antibody in mice.* Nature, 1993. **364**(6440): p. 806-9.
145. Nagata, S. and T. Suda, *Fas and Fas ligand: lpr and gld mutations.* Immunol Today, 1995. **16**(1): p. 39-43.
146. Cretney, E., et al., *Normal thymocyte negative selection in TRAIL-deficient mice.* J Exp Med, 2003. **198**(3): p. 491-6.
147. Tolcher, A.W., et al., *Phase I pharmacokinetic and biologic correlative study of mapatumumab, a fully human monoclonal antibody with agonist activity to tumor necrosis factor-related apoptosis-inducing ligand receptor-1.* J Clin Oncol, 2007. **25**(11): p. 1390-5.
148. Song, J.H., et al., *TRAIL triggers apoptosis in human malignant glioma cells through extrinsic and intrinsic pathways.* Brain Pathol, 2003. **13**(4): p. 539-53.

Chapter 2: TRAIL- and conventional chemotherapy drug-induced apoptosis pathways

A portion of this chapter is published as: Wang, Peng, et al., Role of death receptor and mitochondrial pathways in conventional chemotherapy drug induction of apoptosis. Cell Signal, 2006. 18(9): p. 1528-35. (Appendix 1)Bcl-2 and Bcl-xL part experiments were done by Jing Zhang.

2.0 Introduction

Natural killer cell or T-cell-mediated immune surveillance for tumor development suppression seems to utilize death receptor-mediated apoptosis [1, 2]. Targeting the death receptor-mediated apoptotic pathway is believed to be a novel therapeutic method for cancers. In this aspect, the anti-cancer ability of tumor necrosis factor-related apoptosis-inducing ligand (TRAIL), a transmembrane protein belonging to the TNF receptor family, has been extensively studied [3-5] because of its selective cytotoxicity through the death receptor pathway in transformed tumor cells but not in normal cells [5, 6]. TRAIL depends upon death receptors clustering on the plasma membrane, then recruiting the intracellular adaptor molecule, FADD, and the apoptosis initiator, procaspase-8. When caspase-8 is cleaved, the active fragment of caspase-8 is released into the cytosol where an executioner of apoptosis, caspase-3, is activated [7, 8]. There is overwhelming evidence that cross-talk between these two apoptotic pathways is much more effective for the execution of apoptosis in many cancer cells [9]. The idea of amplifying apoptotic signaling in cancers has been proven by TRAIL and chemotherapy combination treatment that efficiently killed chemotherapy-resistant cancer cells in culture and inhibited tumor growth in animal models [10, 11]. Therefore, it is important to understand precisely the molecular mechanisms underlying apoptotic signaling induced by TRAIL and chemotherapeutic drugs. The synergistic effect of chemotherapeutic drugs and TRAIL often causes controversy in understanding the intracellular signaling pathway induced by these anticancer agents. Contradicting results have been reported regarding involvement of caspase-8 in chemotherapy-induced apoptosis [12-15]. In general, conventional chemotherapy drug induction of apoptosis is mediated through caspase

activation following DNA damage-mediated activation of p53 [16]. This process involves pro-apoptotic molecules, such as Bax and Bak. These pro-apoptotic molecules ultimately modulate mitochondrial membrane potential (MMP) and promote the release of cytochrome c into the cytosol, where cytochrome c binds to Apaf1 to recruit dATP and procaspase-9 to form an apoptosome [17]. Caspase-9 is cleaved and concurrently cleaves caspase-3, thereby executing apoptosis [18]. Antiapoptotic Bcl-2 family molecules, such as Bcl-2 and Bcl-xL, inhibit death signaling by modulating this process [19].

The involvement of the death receptor and its downstream signal transduction pathway in the conventional chemotherapy drug-induced apoptosis route is not completely understood. Here we dissected apoptotic signaling pathways induced by chemotherapy drugs in the absence or presence of death receptor components, such as FADD and caspase-8. Jurkat T leukemia cell lines, including wild type, caspase-8-deficient and FADD-deficient cells, were used for this study in order to show the occurrence of chemotherapy drug-induced apoptosis independent of the death receptor pathway. We consistently showed that the conventional chemotherapy drug profoundly affects the mitochondrial membrane potential, which is regulated by the Bcl-2 family proteins.

2.1. Materials and methods

2.1.1. Materials and antibodies

The recombinant nontagged, native sequence soluble form of human TRAIL (amino acids 114–281) was obtained from PeproTech, Inc. (Rocky Hill, NJ). Recombinant human soluble FLAG-tagged TRAIL (Alexis, San Diego, CA) and anti-

FLAG monoclonal antibody M2 (Sigma-Aldrich, St. Louis, MO) were used for the co-immunoprecipitation assay. The tetrapeptide caspase inhibitor, z-VAD-fmk, z-IETD-fmk, z-LEHD-fmk (R&D Systems, Minneapolis, MN), was prepared as a 20 mM stock in DMSO. Cisplatin and etoposide (VP16) (Sigma-Aldrich) were prepared freshly from a 50 mg/mL stock in DMSO. Mouse monoclonal antibodies, anti-FADD (1:500) and anti-cytochrome c (1:500), were purchased from BD Biosciences (San Diego, CA). Mouse monoclonal anti-DFF45 (1:1000), rabbit polyclonal anticaspase-3 (1:5000) and anti-ERK1/2 (1:1000) antibodies were purchased from StressGen Biotechnologies (Victoria, British Columbia, Canada). Monoclonal antibody c-FLIP (NF6) (1:500) was obtained from Alexis. Rabbit polyclonal caspase-9 antibody (1:1000) was from Cell Signaling (Beverley, MA). HRP-conjugated goat anti-mouse (1:5000) and goat anti-rabbit antibodies (1:5000) were purchased from Jackson IR Labs (West Grove, PA). All of the other chemicals used were of analytical grade and purchased from Sigma-Aldrich, unless otherwise indicated.

2.1.2. Cell cultures, cell viability and apoptosis assay

The human parental Jurkat cells, FADD-deficient (FADD-/-) and caspase-8-deficient (Casp-8-/-) clones (gifts from J. Blenis; Boston, MA) were cultured in RPMI1640 medium (Invitrogen) supplemented with 10% fetal bovine serum and 1% 10 000 unit penicillin antibiotics (Invitrogen). For the cell viability assay, the suspended cells were collected by centrifugation (300 *g* for 5 min) and the pellet was resuspended in culture medium. The monolayered cells ($1x10^6$cells/10 mL) were treated with TRAIL, Fas CH-11 mAb, cisplatin, or VP16. After incubation, cells were washed with PBS once

and then resuspended in 5 mL PBS. 50 μL were placed in each well of 96-well plates. Cell death was determined by an acid phosphatase assay.

Acid Phosphatase Assay

Cell viability was assessed by the acid phosphatase assay as described previously [20-22]. This assay assesses cell viability by measuring cellular lysosomal acid phosphatase activity [23]. The substrate for the reaction is p-nitrophenylphosphate (pNPP) which, after ester hydrolysis by the enzyme, releases p-nitrophenol in addition to an inorganic phosphate [23]. The reaction is stopped by the addition of NaOH, which reacts with the p-nitrophenol product by removing the phenolic proton to produce p-nitrophenolate, a yellow colored product that absorbs at 405 nm and therefore can be quantitated spectrophotometrically [23]. A linear relationship was obtained between cell viability and acid phosphatase activity over a range of 10^3-10^5 cells (R^2= 0.996). The optimum plating density of cells was determined to be 1.0 x 10^4 cells/well for maximum sensitivity of the assay.

In brief, 50 μL buffer containing 0.2 M sodium acetate (pH 5.5), 0.2 % (v/v) Triton X-100 and 20 mM *p*-nitrophenyl phosphate (Sigma 104 phosphatase substrate) were added to each well. The plates were placed in a water-jacketed incubator at 37 °C for 2 h. The reaction was stopped by the addition of 10 μL 1 M NaOH to each well and the color development measured at 405 nm, using a microplate reader (Bio-Rad).

2.1.3. Western blot analysis

Cells in culture were harvested and lysed in 20 mM Tris-HCl (pH 7.4) containing

150 mM NaCl, 2 mM EDTA, 10 % glycerol, 1 % Triton X-100, 1 mM phenylmethylsulfonyl fluoride, and protease inhibitor cocktail (Sigma). The lysed cells were centrifuged at 18 000 *g* for 15 min. Protein concentrations of the cell extracts were determined by the Bradford protein assay by following the manufacturer's protocol (Bio-Rad). Equal amounts of protein from cell lysates (100 μg) were separated by SDS-polyacrylamide gel electrophoresis using Bio-Rad's Mini-PROTEAN 3 system with 15% or 12% separating gels and 3.5% stacking gels for 1.5 hours at 150 V. One of the lanes in each gel was reserved for a molecular weight marker (Bio-Rad). The separated proteins were transferred to immunoblot membranes using Mini Trans-Blot Cell (Bio-Rad) at 30 V for 990 min. After blocking unoccupied regions of the membrane in TBST+5% non-fat milk, the membranes were blotted overnight with various primary antibodies. Following three successive washes (5, 5, 10 min), the membranes were incubated for one hour with horseradish peroxidase (HRP)-conjugated goat anti-mouse or goat anti-rabbit secondary antibodies. After incubation with the secondary antibody, the membranes were subjected to three successive washes (10, 10, 15 min) and developed by ECL on Kodak BioMax MR Film. Films were scanned and saved in TIFF format. The relative difference in protein expression was determined by visual inspection. The Mini-PROTEAN 3 system was run with two gels at the same time. The same sequences and amounts of samples were loaded on the two gels. After transfer to the membrane, caspase-8 and -9 were detected using each membrane first, then stripping antibodies and reusing the membrane for subsequent caspase-3 and DFF45 detection. Loading control ERK1/2 analysis was detected for each gel.

2.1.4. Measurements of mitochondrial membrane potential

The mitochondrial membrane potential (MMP) of intact cells was measured by flow cytometry with the lipophilic cationic probe, 5,5′,6,6′-tetrachloro-1,1′,3,3′ tetraethylbenzimidazolcarbocyanine iodide (JC-1; Mīt-E-PsiTM Apoptosis & Mitochondria Permeability Detection Kit, Biomol International, Plymouth Meeting, PA). This JC-1 Assay Kit uses a cationic dye (5,5′,6,6′-tetrachloro-1,1′,3,3′ tetraethylbenzimidazolylcarbocyanine iodide) to measure the loss of mitochondrial membrane potential. In healthy cells, the intact mithochondrial membrane potential allows this lipophilic dye to enter the mitochondrial matrix to form J-aggregates, which fluoresce red. In apoptotic cells, the mitochondrial membrane potential collapses and the accumulation of JC-1 within the mitochondria is lost. In these cells JC-1 remains in the cytoplasm in a green fluorescent monomeric form. Apoptotic cells will show a loss of red fluorescence and gain green fluorescence compared with healthy cells. The aggregated red form has absorption/emission maxima of 585/590 nm. The green monomeric form has absorption/emission maxima of 510/527 nm. In this research, we found that it is difficult to accurately monitor the MMP changes by measuring the gain of green fluorescence. So, we measure the MMP changes from cells after different treatments by monitoring the loss of red fluorescence by flow cytometry.

After cells were treated with the indicated agents, JC-1 was added directly to the cell culture medium (1 μM final concentration) including cells ($0.5x10^6$/mL) and incubated for 15 min at 37 °C. The medium was then replaced with PBS and the cells were quantitated for J-aggregate green fluorescence intensity by using a Becton and Dickinson FACScanTM (Mountain View, CA). Data analysis was processed by using

Cell QuestTM software (Becton and Dickinson).

2.1.5. Subcellular fractionation

Cytochrome c release from the mitochondria was determined in the cytosolic fraction. Cells were treated with TRAIL or chemotherapeutic agents. Cells were harvested and the cell pellet was suspended in 5 volumes of isotonic buffer (10 mM HEPES-KOH [pH 7.5], 210 mM mannitol, 70 mM sucrose, 1 mM Na-EDTA, and 1 mM Na-EGTA) supplemented with 1 mM phenylmethylsulfonyl fluoride (PMSF) and protease inhibitor mixture. The cells were incubated on ice for 15 minutes and passed through a 22 gauge needle 15 times. After centrifugation twice at 700 g for 10 min at 4°C, the supernatant was collected and centrifuged at 13 000 g for 10 min at 4°C. The resulting mitochondrial pellets were suspended in lysis buffer (50 mM Tris-HCl [pH 7.4], 150 mM NaCl, 2 mM EDTA, 10% glycerol, 1% Triton-X 100, 1 mM PMSF, and 0.2% protease inhibitor cocktail). The supernatants from the 13 000 g centrifugation were further centrifuged at 100 000g for one hour at 4°C, and the resulting supernatants were designated as the S-100 cytosolic fractions [24].

2.1.6. Transient gene transfection

Bcl-2 expressing pUSEamp plasmid was obtained from Upstate (Lake Placia, NY). Bcl-xL expressing pcDNA3 was a kind gift from Dr. Jorge Filmus (Sunnybrook and Women's College Health Sciences Centre, University of Toronto). Cells (500 000) grown on 6-well plates were transfected with either *Bcl-2*/pUSEamp or Bcl-xL/pcDNA-3 using the LipofectAMINE^{TM} method following the manufacturer's protocol (Invitrogen). After

transfection for 24 h, the cells were subjected to cell death assay and Western blot analysis for cleavage of caspases and DFF45.

2.1.7. Bak shRNA constructs and transfection

For a vector-based RNAi, a short hairpin double-stranded RNA (shRNA) was cloned into the BamHI-XhoI site of pRNAT-U6.1/neo-cGFP vector (GenScript Corporation, Piscataway, NJ). The shRNA specific sequence against Bak was: 5'-*GATCCC*ACCGCCATCAGCAGGAACA**TTGATATCCG**TGTTCCTGCTGATGGCG GT*CTCGAG*-3'. The underlined and bold letters denote the hairpin loop, terminal signal and target sites of the restriction enzymes, BamHI and XhoI, respectively. Wild-type Jurkat cells were transfected with the control vector pRNAT-U6.1/neo-cGFP or the expression vectors for Bak shRNA using the Lipofectamine2000 transfection reagent (Invitrogen) according to the protocol recommended by the manufacturer [25].

2.2 Results

2.2.1. TRAIL and Cisplatin induce apoptotic cell death of Jurkat T leukemia cells by activation of caspases

Jurkat T leukemia cells are a well-known model system for apoptosis since they are vulnerable to diverse stimuli, such as death ligands (including FasL and TRAIL) and conventional chemotherapeutic drugs (including cisplatin, etoposide, and camptothecin). Here we clarify the molecular mechanisms underlying apoptosis induced by chemotherapeutic drugs and death ligands using several Jurkat clones, including wild

type, caspase-8 deficient, and FADD-deficient clones. To dissect apoptotic signal pathways induced by chemotherapeutic drugs, Jurkat cells were treated with cisplatin in a dose-dependent and a time-dependent manner. Treatment of Jurkat cells with cisplatin led to time- and dose-dependent induction of cell death, as determined by acid phosphatase assay. Doses of 10-50 μg/mL cisplatin were sufficient to induce significant cytotoxicity (Fig. 2.1A). Cell death was detectable 16 h after treatment with 20 μg/mL cisplatin (Fig. 2.1B). We examined caspase activation by Western blotting to demonstrate that cisplatin-induced cell death occurs through apoptosis. Cisplatin treatment for 16 h induced cleavage of caspase-9, -3, -8, and DFF45 (Fig. 2.1C). Higher doses increased caspase cleavage, which was consistent with the degree of cell death shown in Fig. 2.1A. When cells were treated with 20 μg/mL cisplatin, cleaved forms of caspase-9, -3, -8, and DFF45 were detected after 6 h of treatment (Fig. 2.1C).

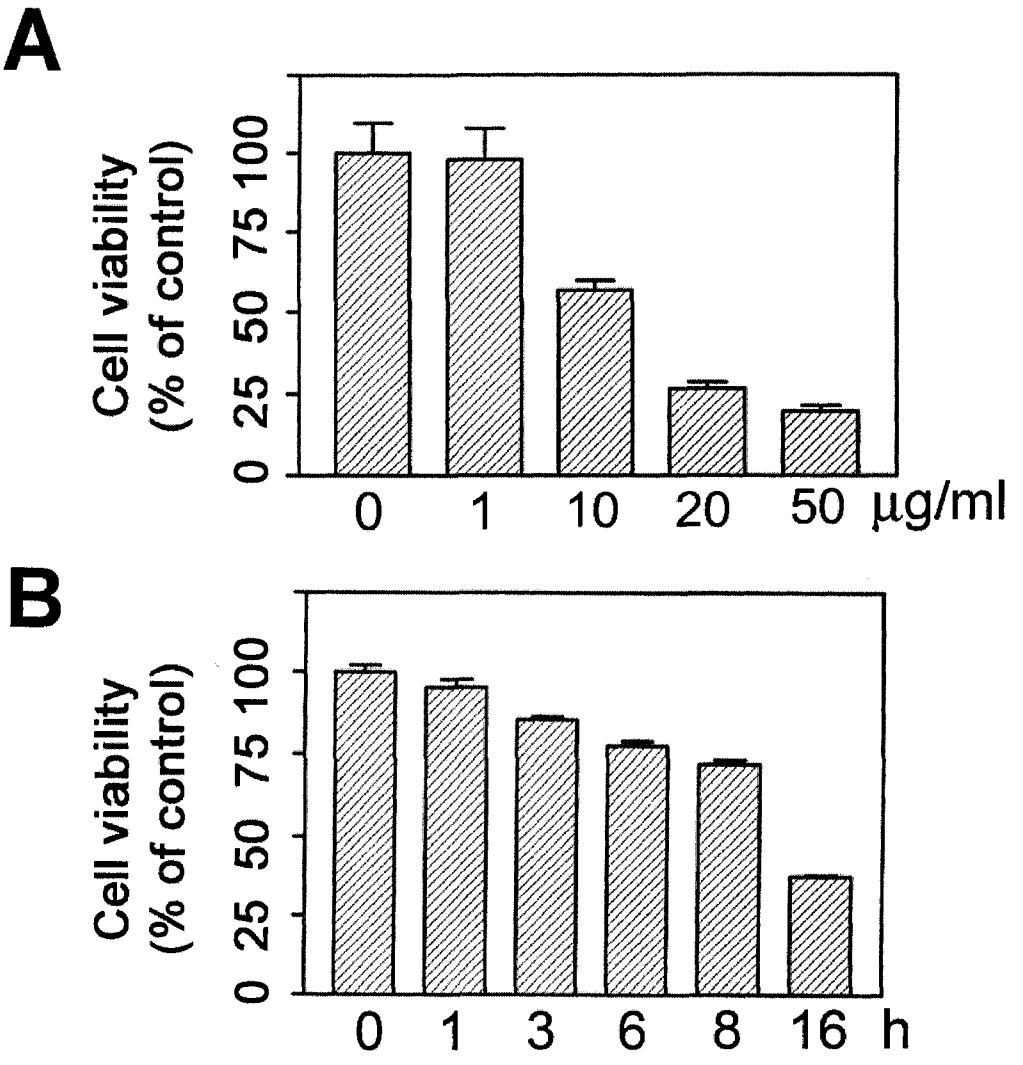

Figure 2.1 Cisplatin induction of caspases and DFF45 cleavage and cell death. Jurkat T leukemia cells were treated with cisplatin for 24 h in a dose-dependent fashion in a range of 1-50 μg/mL (**A**), or the cells were also treated with 20 μg/ml of cisplatin for the different times as indicated (**B**). After treatments, cell viability was determined by acid phosphatase assay. Percentage of cell viability was calculated by comparisin with the untreated control value (0 h).

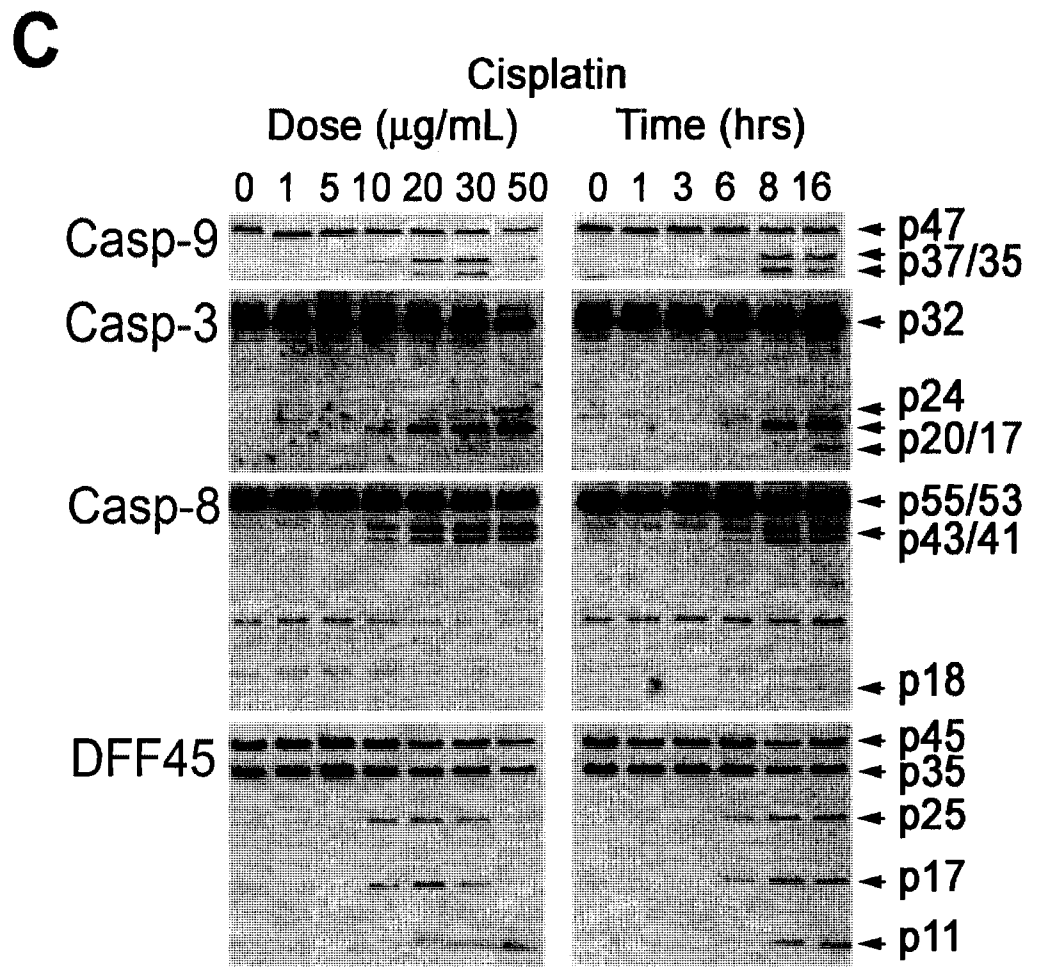

Figure 2.1 For the Western blot, cells were harvested and whole cell lysates from equal amounts of protein (50 μg) were separated by SDS-PAGE and immunoblotted (c) Western blot analysis detected 47 kDa procaspase-9 without cisplatin treatment (0 h), whereas 37 and 35 kDa apoptosis-related cleavage fragments were increased by cisplatin treatment in a dose- and time-dependent manner. Antibody against caspase-8 detected the inactive forms (55 and 53 kDa), cleaved intermediates (43 and 41 kDa), and active subunit (18 kDa). Anti-caspase-3 antibody detected both the inactive (32 kDa) and active forms (20 and 17 kDa). An antibody against DFF45 detected both the inactive (45 and 35 kDa) and active form (25, 17 and 11 kDa).

In the next set of experiments, TRAIL-induced apoptosis was tested in Jurkat cells. Doses of 100-300 ng/mL TRAIL were clearly cytotoxic to Jurkat cells (Fig. 2.2 A). Western blotting showed activation of caspase-8, -9, -3 and DFF45 (Fig. 2.2B). Thus, both cisplatin and TRAIL have an ability to induce apoptosis by activation of caspases. Although caspases are cleaved by treatment with these anticancer agents, time-dependent analysis by Western blotting failed to show which caspase is responsible for induction of apoptosis. In order to discern essential caspases in the apoptosis pathways induced by either cisplatin or TRAIL, specific caspases inhibitors (z-IETD-fmk for caspase-8 inhibitor and z-LEHD-fmk for caspase-9) were used for pre-treatment of 2 h, and then cells were either treated with cisplatin or TRAIL for 16 h. Pretreatment of cells with caspase-9 inhibitor z-LEHD-fmk blocked cisplatin-induced apoptotic death, but caspase-8 inhibitor z-IETD-fmk failed to block cell death, suggesting caspase-8 activation may not be required for cisplatin-induced apoptosis (Fig. 2.3A). However, pretreatment of Jurkat cells with caspase-8 inhibitor z-IETD-fmk or caspase-9 inhibitor z-LEHD-fmk prevented TRAIL-induced apoptotic death, indicating the activation of caspase-8 and -9 is necessary for TRAIL-induced apoptosis (Fig. 2.3B) in Jurkat T leukemia cells.

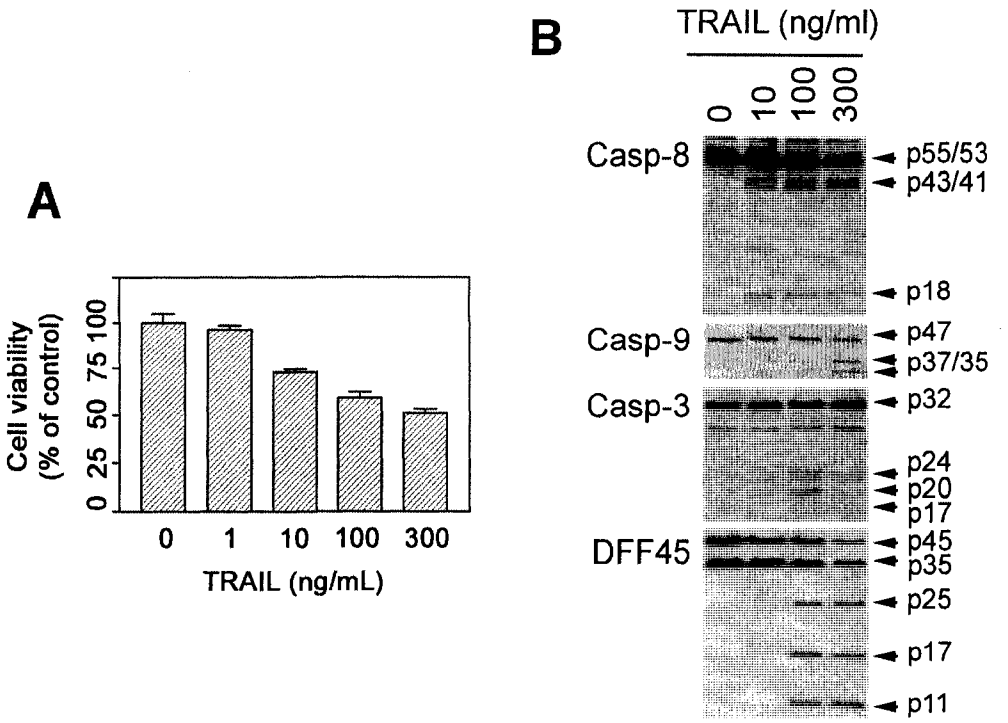

Figure 2.2 TRAIL induction of caspase activation and cell death. Jurkat T leukemia cells were treated with TRAIL in a dose-dependent fashion in a range of 1-300 ng/L (**A**) for 16 h. After treatments, cell viability was determined by acid phosphatase assay and was calculated by comparing with untreated control value (0 h). A representative experiment is shown as bar graph +/- SD (n=6). For the Western blot, whole cell lysates from equal amounts of protein (50 μg) were separated by SDS-PAGE and immunoblotted with antibodies against caspase-8, -9 and -3, and DFF45. Western blotting detects cleaved fragments of caspase-8, -9, -3, and DFF45 after treatment of TRAIL in a range of 10-300 ng/mL.

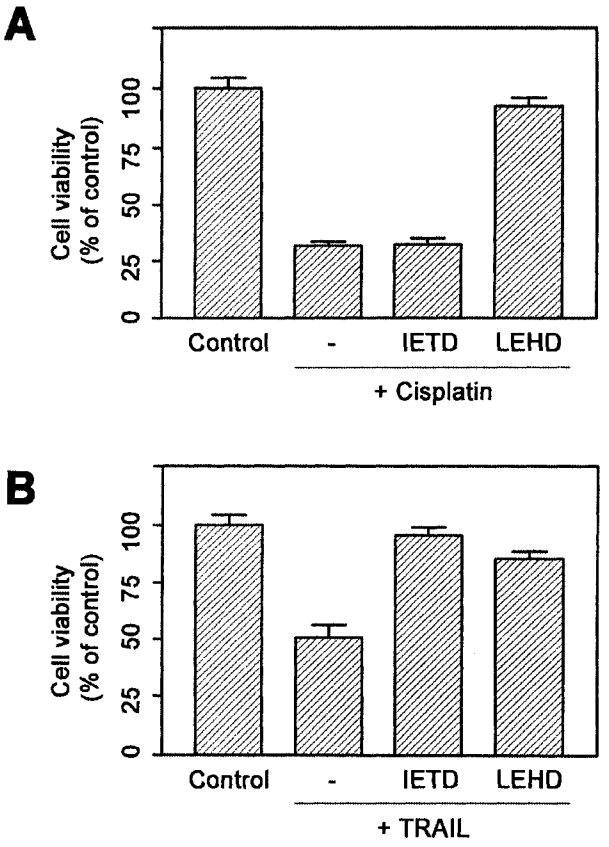

Figure 2.3 Differential involvement of caspse-8 and caspase-9 in apoptosis induced by cisplatin and TRAIL. Jurkat T-leukemia cells were treated without or with either caspase-8 specific inhibitor z-IETD-fmk (50 μM) or caspase-9 specific inhibitor z-LEHD-fmk (50 μM) for 2 h and then followed by 20 μg/mL cisplatin or 300 ng/mL TRAIL for 16 h. Cell viability was determined by acid phosphatase assay. Changes in the cell viability after treatments were calculated by comparison with the untreated control value (100 %). A representative experiment is shown as a bar graph +/- SD (n=6).

2.2.2. FADD and caspase-8 are not required for cisplatin-induced apoptosis

Because inhibition of caspase-8 activation by pretreatment with z-IETD-fmk failed to block cisplaitn-induced apoptosis, it was speculated cisplatin-induced apoptosis is independent of the death receptor pathway. To further substantiate the interpretation that cisplatin-induced apoptosis is independent of death receptor signaling pathways involving FADD and caspase-8, we examined chemotherapeutic drug-induced apoptosis using FADD-deficient (FADD-/-) and caspase-8-deficient (Casp-8-/-) Jurkat clones. As expected, lack of either FADD or caspase-8 abrogated apoptosis induced by TRAIL as well as Fas agonistic mAb CH11 (Fig. 2.4A). In contrast, both cisplatin and etoposide (VP16) clearly induced apoptosis in FADD-/- cells. These data are consistent with the results that Casp-8-/- cells were extremely sensitive to cisplatin and VP16, whereas Casp-8-/- cells were resistant to TRAIL and Fas CH-11 (Fig. 2.4A). In addition, no significant differences in the kinetics of apoptotic death induction by cisplatin were detectable when comparing FADD-/- cells, Casp-8-/- cells and wild-type Jurkat cells. As expected, treatment of FADD-/- cells with TRAIL or Fas CH-11 failed to activate caspase-8, -9, -3 and DFF45. Treatment of Casp-8-/- cells with TRAIL or Fas CH-11 also failed to activate caspase-8, -9, -3 and DFF45.

These results confirmed that expression of FADD and caspase-8 is essential for death receptor-mediated apoptosis. In contrast to death ligands, both FADD-/- cells and Casp-8-/- cells underwent apoptosis after treatment of cisplatin and VP16, as evident in the detection of cleavage products of caspase-9, -3 and DFF45 by Western blotting. Further, no significant differences in the degree of caspase-9, -3 and DFF45 cleavage were found between different clones treated with chemotherapeutic drugs (Fig. 2.4B).

Taken together, our data indicate that chemotherapeutic drugs can trigger apoptosis by mechanisms independent of the death receptor pathways.

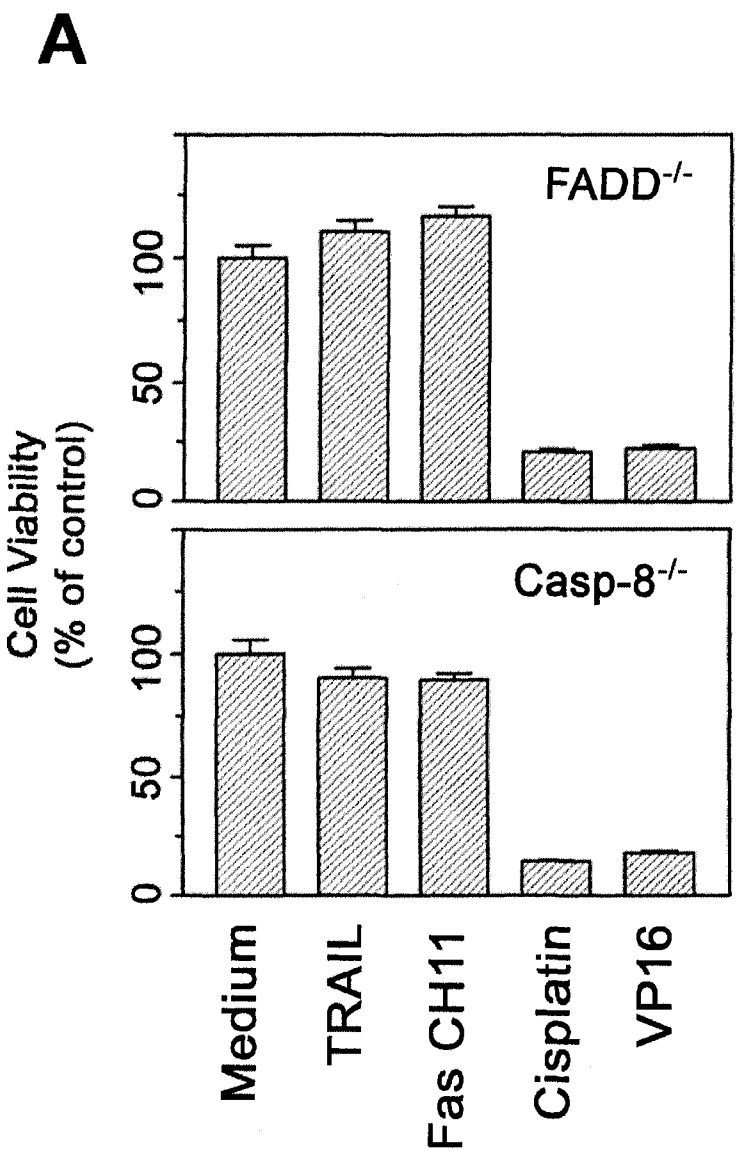

Figure 2.4 Cisplatin, but not TRAIL, induction of apoptosis in caspase-8- and FADD-deficient Jurkat clones. Jurkat cells deficient in caspase-8 and FADD expression were treated with TRAIL, Fas monoclonal antibody CH11, cisplatin or etoposide (VP16). After 16 h treatment, cell viability was determined by acid phosphatase assay (A). Caspase-8- or FADD-deficient cells were insensitive to TRAIL and Fas CH11, but sensitive to chemotherapeutic drugs, such as cisplatin and etoposide, respectively. A representative experiment is shown as a bar graph +/- SD (n=6). The Western blot was performed after 6 h treatment.

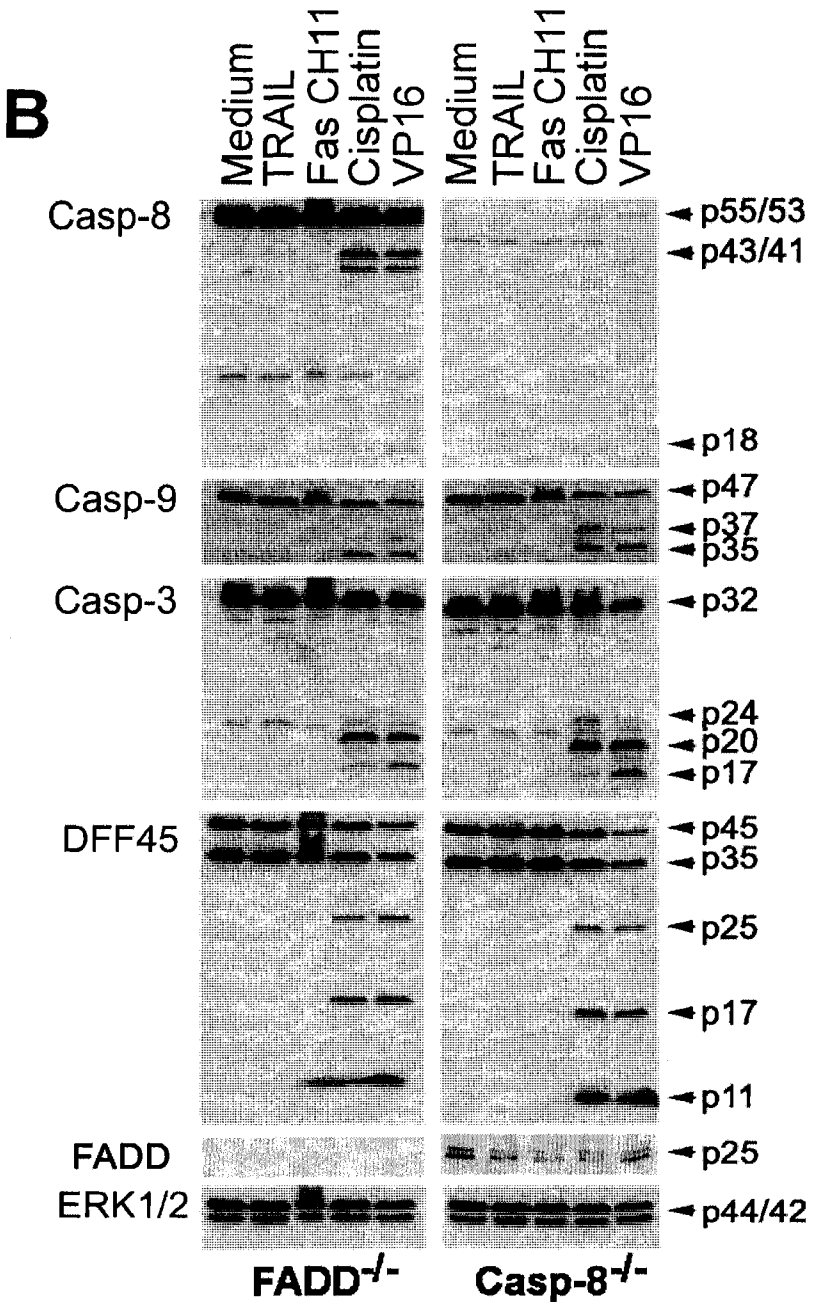

Figure 2.4 (B) The detection of caspase-8, -9, -3, DFF45 cleavage and FADD expression. Equal protein loading was confirmed by ERK1/2 detection. Caspase cascade was initiated by treatment with cisplatin or VP16 of Jurkat cells deficient in either caspase-8 or FADD expression. Hence, neither TRAIL nor Fas CH11 shows cleavage of any caspases.

2.2.3. Mitochondria play a key role in cisplatin and TRAIL-induced apoptosis

Our results showed that pretreatment with caspase-9 inhibitor z-LEHD-fmk blocked cisplatin-induced apoptosis and TRAIL-induced apoptosis (Fig. 2.3), suggesting the mitochondrial pathway is critical in executing apoptotic death. To further elucidate the role of mitochondria in the execution of apoptosis in response to cisplatin and TRAIL, we first examined changes in mitochondrial membrane potential (MMP). Wild-type Jurkat cells were exposed to either cisplatin or TRAIL and the frequency of cells exhibiting loss of MMP was determined by assessing MMP-sensitive dye, JC-1, treatment. In TRAIL-treated wild type Jurkat cells, changes in MMP were seen at 3 h and increased over time (Fig. 2.5A). However, TRAIL-activated caspase-8 was seen at 2 h after treatment. Thus, our data imply active caspase-8 engages the mitochondrial pathway, as previously reported [7]. In cisplatin-treated cells, changes in MMP increased in a time-dependent fashion and were detectable within 3 h of treatments (Fig. 2.5A), which is earlier than any caspase activation seen in Fig. 1. In addition, increased MMP changes were determined in FADD-/- cells and Casp-8-/- cells after treatment with cisplatin (Fig. 2.5A). As expected, TRAIL failed to increase the MMP changes in both cell lines (Fig. 2.5B). In contrast to TRAIL, neither absence of FADD nor caspase-8 abrogated cisplatin-induced MMP changes. Thus, these results support the independence of cisplatin-induced apoptosis from a death receptor pathway. In addition, pan caspase peptide inhibitor z-VAD-fmk was used to evaluate whether caspases are involved in MMP changes during cisplatin-induced apoptosis. As expected, pretreatment of wild-type Jurkat cells with z-VAD-fmk almost completely prevented TRAIL-induced MMP changes, confirming

caspase-8 activation-initiated TRAIL-induced apoptosis (Fig. 2.5C). In contrast, addition of z-VAD-fmk failed to block MMP changes induced by cisplatin. In parallel experiments, the cytosolic extracts from cisplatin-treated cells were found to accumulate mitochondrial release of cytochrome c well before they contained significant levels of activated caspase-9 and -3 (Fig. 2.5D).

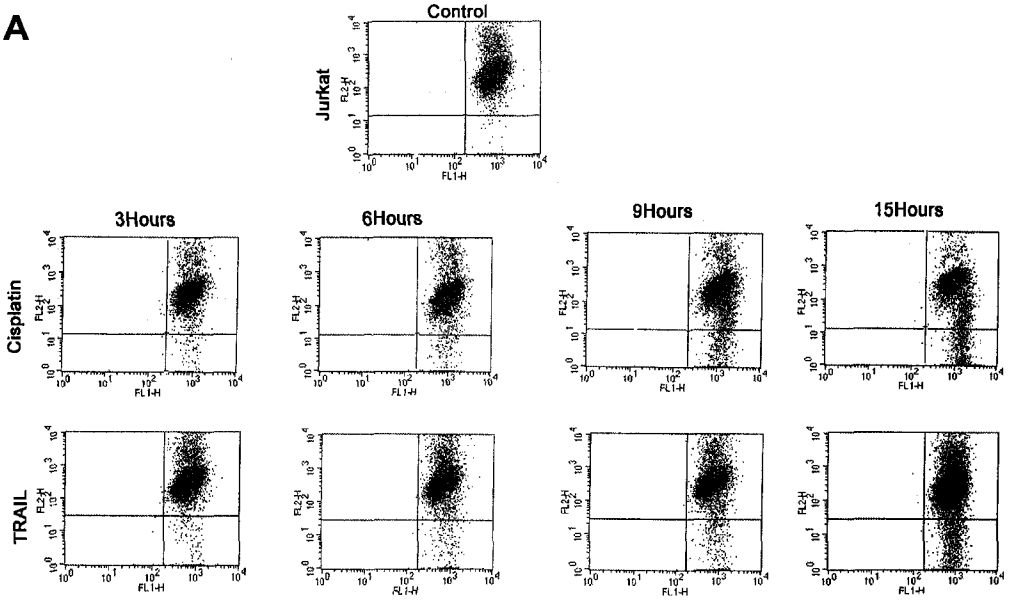

Figure 2.5. Requirement of MMP changes in apoptosis triggered by TRAIL or cisplatin. Cells were treated with TRAIL or cisplatin for the different times indicated and stained with JC-1 (A).

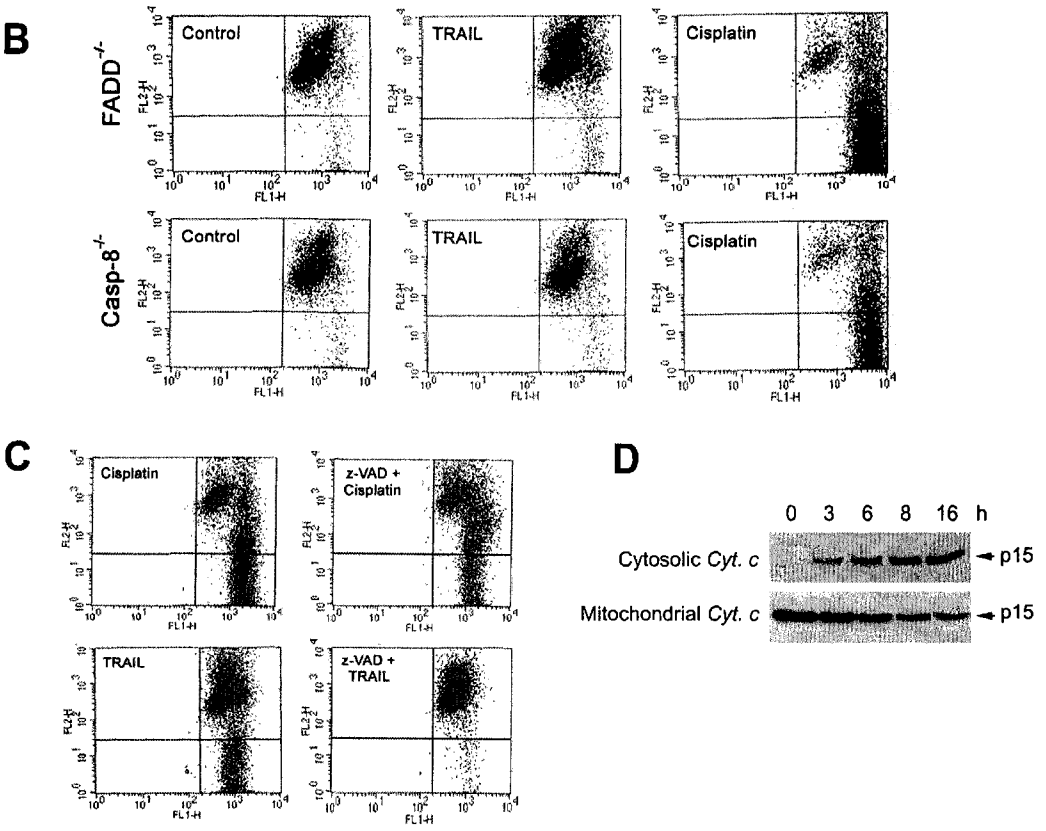

Figure 2.5. Flow cytometry analysis showed cisplatin and TRAIL were both able to increase changes in MMP in wild type Jurkat cells. TRAIL failed to show MMP changes in cells deficient with either caspase-8 or FADD expression (B). While cisplatin still increased MMP changes without differences, compared with wild type cells (B and C). Changes in MMP by TRAIL, but not cisplatin, are inhibited in presence of z-VAD-fmk (50 μM, pretreated for 2 h). Changes in MMP were determined after 16 h treatment and a representative experiment is shown. Cisplatin treatment (20 μg/mL) induced cytosolic release of cytochrome c from mitochondria in a time-dependent manner (D). Subcellular fractions for cytosol and mitochondria were subjected to Western blotting with anti-cytochrome c.

2.2.4. Over-expression of Bcl-2 and Bcl-xL is protective

Throughout the study, we observed that caspase-8 was cleaved by cisplatin treatment. Contrasting to the result that TRAIL-induced caspase-8 cleavage was completely inhibited in FADD-/- cells, FADD deficiency failed to suppress caspase-8 cleavage in cisplatin-treated cells. This suggests caspase-8 activation is a downstream event of caspase-9 in cisplatin-induced apoptosis and that the caspase-8 cleavage takes place in the cytosol, which differs from caspase-8 cleavage in the DISC in TRAIL-treated cells. To test this, we over-expressed anti-apoptotic genes Bcl-2 and Bcl-xL, which can inhibit the loss of MMP and cytochrome c from the mitochondrial inter-membrane space and eventually protect cells from apoptosis. We first compared the cisplatin- and TRAIL-induced apoptosis in Jurkat cells stably transfected with either Bcl-2 or Bcl-xL. Over-expression levels of Bcl-2 and Bcl-xL protein were verified by Western blotting (Fig. 2.6A). Over-expression of Bcl-2 or Bcl-xL in Jurkat cells significantly diminished apoptotic death induced by cisplatin and TRAIL (Fig. 2.6B). These results were consistent with reduction of MMP changes in over-expressed Jurkat cells with either Bcl-2 or Bcl-xL (Fig. 2.6C). Western blot analysis for caspase activation demonstrated that over-expression of Bcl-2 or Bcl-xL diminished TRAIL-induced activation of caspase-3 (Fig. 2.6D). In cisplatin-treated cells, over-expression of Bcl-2 or Bcl-xL diminished the cleavage of caspase-3 (Fig. 2.6D). Therefore, these results indicate that over-expression of Bcl-2 or Bcl-xL is protective in both TRAIL- and cisplatin-induced apoptosis signal pathways.

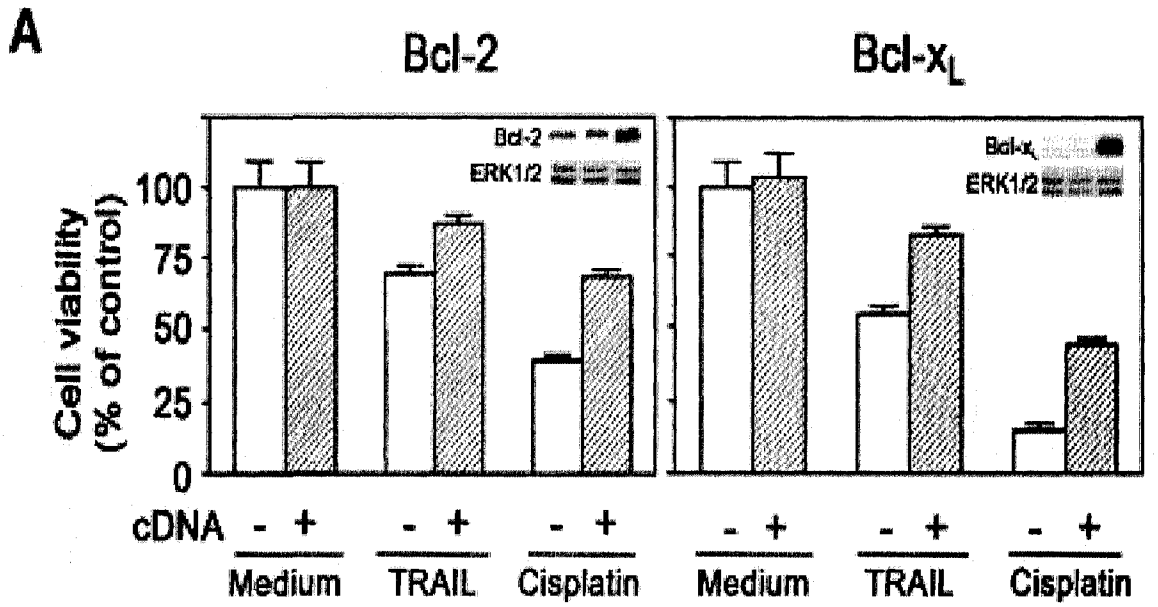

Figure 2.6. Less susceptibility of Bcl-2 or Bcl-xL-over-expressing cells to apoptosis induced by TRAIL or cisplatin. Transient transfection of Bcl-2 or Bcl-xL cDNA increased expression of Bcl-2 or Bcl-xL levels at least ten-fold, as shown by western blotting (A). ERK1/2 was used as an equal loading control. Cell viability was performed and a representative experiment is shown as bar graph +/- SD (n=6) (A)

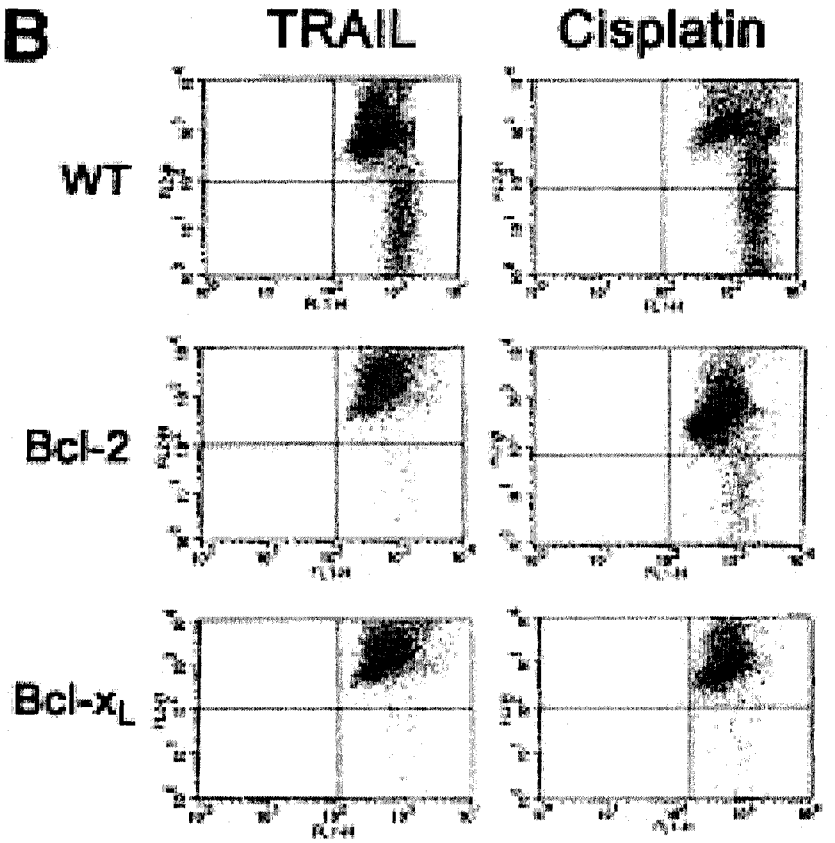

Figure 2.6 Changes in MMP mediated by TRAIL or cisplatin are inhibited when cells over-expressed Bcl-2 or Bcl-xL (B). Western blot analysis with antibodies against caspase-3 and DFF45 detects caspase-3 and DFF45 cleavage after treatment of TRAIL or cisplatin in wild-type Jurkat cells.

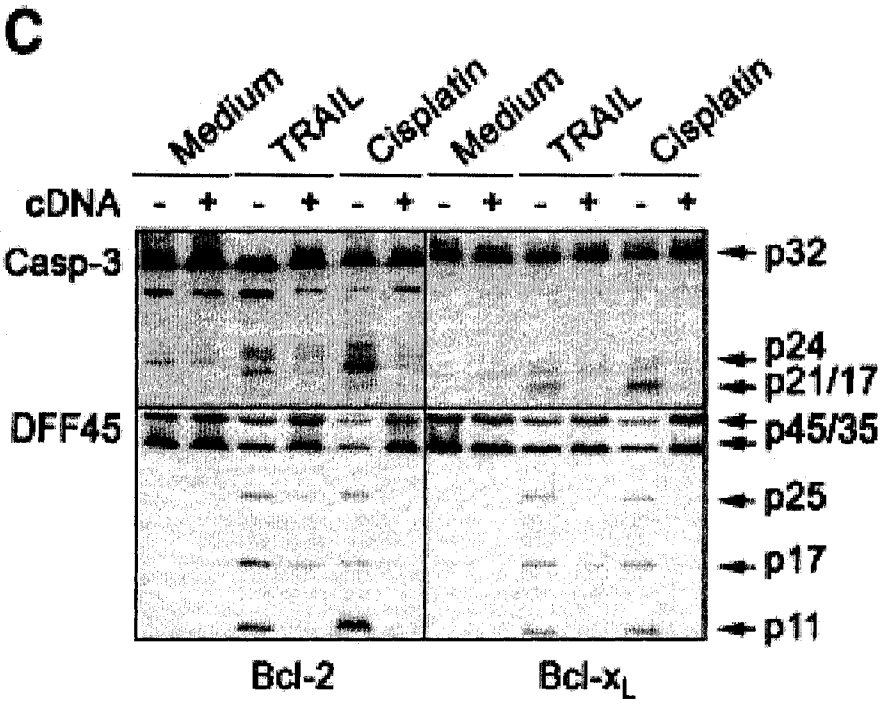

Figure 2.6 (C). Compared to wild-type cells, less cleavage of caspase-3 and DFF45 was detected in Bcl-2- or Bcl-xL-over-expressing cells. A representative experiment is shown after 6 h of treatment.

2.2.5. Knockdown of Bak is inhibitive.

Besides the two anti-apoptotic factors, Bcl-2 and Bcl-xL, two other Bcl-2 family members, Bax and Bak, play a crucial apoptotic role in both cisplatin- and TRAIL-induced apoptosis pathways. In our research system, since the Jurkat clone is Bax deficient, it was appropriate to explore the apoptotic role of Bak. After time course Bak shRNA vector transfection, Bak was knocked down to different levels (Figure 2.7A). Corresponding to the Bak expression level, cisplatin- and TRAIL-induced MMP damage were down-regulated (Figure 2.7B). These data indicate that Bak plays a crucial apoptotic role at the mitochondrial level in both the cisplatin- and TRAIL-induced apoptosis pathways.

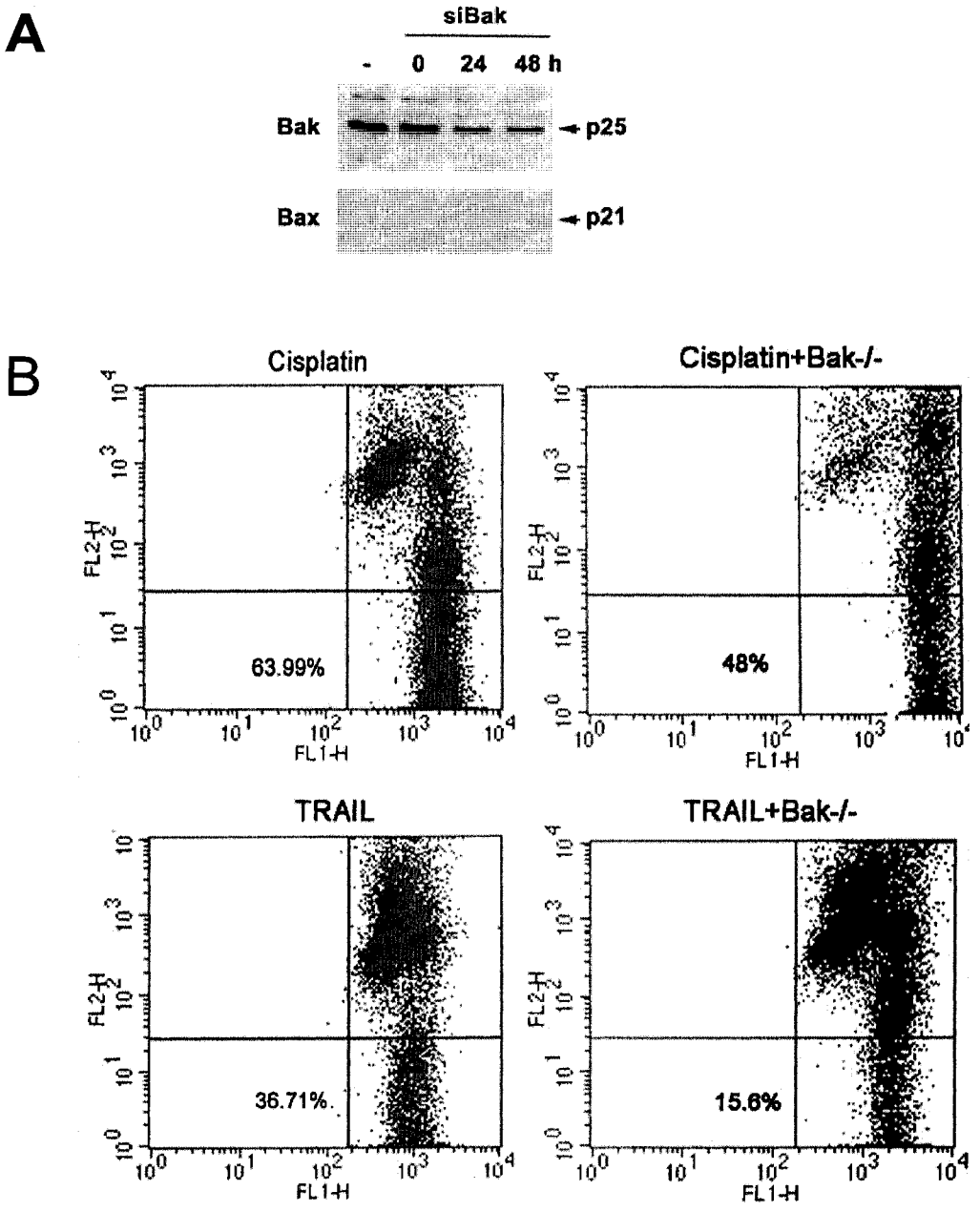

Figure 2.7. Reduced MMP damage of Bak knockdown cells after TRAIL or cisplatin treatment. Transient transfection of Bak siRNA down-regulates expression of Bak from two to three fold in a time-dependent fashion, as shown by Western blotting (A). Changes in MMP mediated by TRAIL or cisplatin are inhibited when cells down-regulated Bak (B).

2.3. Discussion

Apoptosis in cancer cells can be triggered by extracellular stimuli that mediate at least two apoptotic signaling pathways, the so called death receptor-initiated extrinsic and mitochondria-associated intrinsic pathways [7, 26]. Regardless of the entry site of apoptosis, these two pathways cooperatively amplify apoptotic signaling for cell death. Indeed, here we showed that exposure of Jurkat cells to conventional chemotherapy drugs, such as cisplatin and etoposide, caused cleavage of both caspase-8 and caspase-9. When cells were exposed to TRAIL in a time-dependent manner, caspase-8 was cleaved earlier than any other caspases, including caspase-9 [27]. However, cisplatin cleaved all caspases at a similar time of just over 6 hours. In order to address the issue of which caspase is an initiator responsible for chemotherapy-induced apoptosis, we used specific caspase inhibitors for each caspase in the TRAIL-resistant clones. As shown in this study, pretreatment of caspase-9 inhibitor, but not caspase-8 inhibitor, inhibited cisplatin-induced caspase cleavage and apoptosis. Similarly, apoptosis induced by cisplatin or etoposide was not influenced by the absence of caspase-8 or FADD, which are a necessity for TRAIL-induced apoptosis in Jurkat cells. These results were consistent with the observation that the caspase-8 inhibitor failed to inhibit chemotherapy-induced apoptosis in wild-type Jurkat cells.

Bcl-2 and Bcl-xL are known as inhibitory proteins of mitochondria-mediated apoptosis. In the present study, we showed that exogenous Bcl-2 or Bcl-xL over-expression can diminish TRAIL or cisplatin-induced caspase-9 cleavage and apoptotic cell death. Cisplatin treatment increased changes in MMP in Jurkat cells, whereas Bcl-2 or Bcl-xL over-expression alleviated changes in MMP. Jurkat cells used in our study do

not express the Bax protein, but the Bax homologue, Bak, was expressed [28]. It has been reported that Bax and Bak double deficient Jurkat cells were resistant to apoptosis induced by either TRAIL or other chemotherapeutic drugs [9, 29]. We have previously shown that chemotherapy profoundly up-regulates Bak expression in glioma cells [7]. In this study, our data indicated that down-regulation of Bak inhibits both cisplatin and TRAIL-induced MMP changes. Together, these imply that Bcl-2 or Bcl-xL are both potential counterparts for Bak-mediated mitochondrial apoptosis in Jurkat cells. In conclusion, the pro-apoptotic activity of chemotherapeutic drugs, such as cisplatin and etoposide was independent of membrane-bound death receptors, but depended on Bcl-2 family expression.

In the TRAIL-induced apoptosis pathway, either loss of crucial apoptotic factors, such as FADD or caspase-8, at the DISC level, or down-regulation of Bak in the the mitochondrial level, causes cells to become resistant to TRAIL killing. Moreover, over-expression of anti-apoptotic factors at the mitochondria level, such as Bcl-2 and Bcl-X_L, causes cells to become resistant to TRAIL-induced apoptosis.

2.4. References

1. Takeda, K., et al., *Critical role for tumor necrosis factor-related apoptosis-inducing ligand in immune surveillance against tumor development.* J Exp Med, 2002. **195**(2): p. 161-9.
2. Cretney, E., et al., *Increased susceptibility to tumor initiation and metastasis in TNF-related apoptosis-inducing ligand-deficient mice.* J Immunol, 2002. **168**(3): p. 1356-61.
3. Pan, G., et al., *An antagonist decoy receptor and a death domain-containing receptor for TRAIL.* Science, 1997. **277**(5327): p. 815-8.
4. Gura, T., *How TRAIL kills cancer cells, but not normal cells.* Science, 1997. **277**(5327): p. 768.
5. Hao, C., et al., *TRAIL inhibits tumor growth but is nontoxic to human hepatocytes in chimeric mice.* Cancer Res, 2004. **64**(23): p. 8502-6.
6. Hao, C., et al., *Induction and intracellular regulation of tumor necrosis factor-related apoptosis-inducing ligand (TRAIL) mediated apotosis in human malignant glioma cells.* Cancer Res, 2001. **61**(3): p. 1162-70.
7. Song, J.H., et al., *TRAIL triggers apoptosis in human malignant glioma cells through extrinsic and intrinsic pathways.* Brain Pathol, 2003. **13**(4): p. 539-53.
8. Hersey, P. and X.D. Zhang, *How melanoma cells evade trail-induced apoptosis.* Nat Rev Cancer, 2001. **1**(2): p. 142-50.
9. LeBlanc, H., et al., *Tumor-cell resistance to death receptor--induced apoptosis through mutational inactivation of the proapoptotic Bcl-2 homolog Bax.* Nat Med, 2002. **8**(3): p. 274-81.
10. Shankar, S., X. Chen, and R.K. Srivastava, *Effects of sequential treatments with chemotherapeutic drugs followed by TRAIL on prostate cancer in vitro and in vivo.* Prostate, 2005. **62**(2): p. 165-86.
11. Ray, S. and A. Almasan, *Apoptosis induction in prostate cancer cells and xenografts by combined treatment with Apo2 ligand/tumor necrosis factor-related apoptosis-inducing ligand and CPT-11.* Cancer Res, 2003. **63**(15): p. 4713-23.
12. Park, S.J., et al., *Taxol induces caspase-10-dependent apoptosis.* J Biol Chem, 2004. **279**(49): p. 51057-67.
13. Ferreira, C.G., et al., *Chemotherapy triggers apoptosis in a caspase-8-dependent and mitochondria-controlled manner in the non-small cell lung cancer cell line NCI-H460.* Cancer Res, 2000. **60**(24): p. 7133-41.
14. Glaser, T. and M. Weller, *Caspase-dependent chemotherapy-induced death of glioma cells requires mitochondrial cytochrome c release.* Biochem Biophys Res Commun, 2001. **281**(2): p. 322-7.
15. Glaser, T., et al., *Death ligand/receptor-independent caspase activation mediates drug-induced cytotoxic cell death in human malignant glioma cells.* Oncogene, 1999. **18**(36): p. 5044-53.
16. Fridman, J.S. and S.W. Lowe, *Control of apoptosis by p53.* Oncogene, 2003. **22**(56): p. 9030-40.
17. Nguyen, J.T. and J.A. Wells, *Direct activation of the apoptosis machinery as a mechanism to target cancer cells.* Proc Natl Acad Sci U S A, 2003. **100**(13): p. 7533-8.

18. Slee, E.A., et al., *Ordering the cytochrome c-initiated caspase cascade: hierarchical activation of caspases-2, -3, -6, -7, -8, and -10 in a caspase-9-dependent manner.* J Cell Biol, 1999. **144**(2): p. 281-92.
19. Zamzami, N. and G. Kroemer, *The mitochondrion in apoptosis: how Pandora's box opens.* Nat Rev Mol Cell Biol, 2001. **2**(1): p. 67-71.
20. Connolly, D.T., et al., *Determination of the number of endothelial cells in culture using an acid phosphatase assay.* Anal Biochem, 1986. **152**(1): p. 136-40.
21. Song, J.H., et al., *Cisplatin down-regulation of cellular Fas-associated death domain-like interleukin-1beta-converting enzyme-like inhibitory proteins to restore tumor necrosis factor-related apoptosis-inducing ligand-induced apoptosis in human melanoma cells.* Clin Cancer Res, 2003. **9**(11): p. 4255-66.
22. Wang, P., et al., *Role of death receptor and mitochondrial pathways in conventional chemotherapy drug induction of apoptosis.* Cell Signal, 2006. **18**(9): p. 1528-35.
23. Yang, T.T., P. Sinai, and S.R. Kain, *An acid phosphatase assay for quantifying the growth of adherent and nonadherent cells.* Anal Biochem, 1996. **241**(1): p. 103-8.
24. Xiao, C., et al., *Tumor necrosis factor-related apoptosis-inducing ligand-induced death-inducing signaling complex and its modulation by c-FLIP and PED/PEA-15 in glioma cells.* J Biol Chem, 2002. **277**(28): p. 25020-5.
25. Chatterjee, D., et al., *Induction of apoptosis in 9-nitrocamptothecin-treated DU145 human prostate carcinoma cells correlates with de novo synthesis of CD95 and CD95 ligand and down-regulation of c-FLIP(short).* Cancer Res, 2001. **61**(19): p. 7148-54.
26. Igney, F.H. and P.H. Krammer, *Death and anti-death: tumour resistance to apoptosis.* Nat Rev Cancer, 2002. **2**(4): p. 277-88.
27. Song, J.H., et al., *TRAIL triggers apoptosis in malignant glioma cells through extrinsic and intrinsic pathways.* Brain Pathol, 2003. **13**(4): p. 539-553.
28. Han, J., et al., *Differential involvement of Bax and Bak in TRAIL-mediated apoptosis of leukemic T cells.* Leukemia, 2004. **18**(10): p. 1671-80.
29. Wei, M.C., et al., *Proapoptotic BAX and BAK: a requisite gateway to mitochondrial dysfunction and death.* Science, 2001. **292**(5517): p. 727-30.

Chapter 3: Inhibition of RIP and c-FLIP enhances TRAIL-induced apoptosis in pancreatic cancer cells

A portion of this chapter is published as: ***Wang, Peng****, et al., Inhibition of RIP and c-FLIP enhances TRAIL-induced apoptosis in pancreatic cancer cells. Cell Signal, 2007.* ***19****(11): p. 2237-46 (Appendix 2). c-FLIP part work was done by Jing Zhang.*

3.0 Introduction

Pancreatic cancer is the fourth leading cause of cancer death in the United States [2]. The high mortality rate of pancreatic cancers is due in part to their resistance to chemotherapy and radiation [3]. Therefore, there is a need for the development of new therapies. Tumor necrosis factor-related apoptosis-inducing ligand (TRAIL) is normally expressed by natural killer cells in immune surveillance against tumorigenesis and a natural cancer killer [4]. There are several lines of evidence to support the therapeutic utility of TRAIL in human pancreatic cancers: i) pancreatic cancers express TRAIL death receptors, DR4 and DR5 [5]; ii) recombinant TRAIL can induce apoptosis in pancreatic cancer cells [6]; injection of an adenoviral vector expressing TRAIL in pancreatic cancer xenografts suppresses the xenograft growth [7]; and iv) systemic injection of TRAIL inhibits the growth of patients' pancreatic cancer xenografts [8]. These studies, however, have also shown that many pancreatic cancers [6, 8, 9] are resistant to TRAIL treatment and that combination therapies are required to overcome TRAIL resistance [10, 11].

TRAIL-induced apoptosis occurs through its binding to death receptor DR4 and DR5, recruitment of intracellular Fas-associated death domain (FADD) and caspase-8 to the receptors, leading to assembly of the death-inducing signaling complex (DISC) [12]. In the DISC, caspase-8 is cleaved and initiates an apoptotic cascade through the cleavage of caspase-3. Unfortunately, pancreatic cancers express the X-linked inhibitor of apoptosis protein (XIAP) [13-15] that interacts with caspase-3 and inhibits its cleavage [16]. To bypass this, caspase-8 can cleave Bcl-2 inhibitory BH3-domain protein (Bid), which in turn interacts with Bax and Bak to induce a change in the mitochondrial membrane potential and release the second mitochondrial-derived activator of caspase

(Smac) [17]. Smac interacts with XIAP and thus releases its inhibition of caspase-3 cleavage [18]. Bid also induces mitochondrial release of Cytochrome c [19], leading to caspase-9 cleavage of caspase-3, promoting TRAIL-induced apoptosis [20]. The mitochondrial pathway is therefore required for TRAIL-induced apoptosis. Bcl-2 and Bcl-xL interact with Bax and Bak and protect the mitochondrial membrane potential [21]. Correspondingly, the high expression levels of Bcl-2 and Bcl-xL also contribute to TRAIL resistance in pancreatic cancer cells [11, 22].

The nuclear factor-κB (NF-κB) is constitutively activated in the majority of pancreatic cancers [23] and it may contribute to the cancer resistance to TRAIL, perhaps through the up-regulation of Bcl-xL and XIAP [24]. On the other hand, TRAIL treatment leads to the activation of NF-κB in pancreatic cancer cells [24, 25]. TRAIL-induced NF-κB activation requires DR4/DR5-mediated recruitment of receptor-interacting protein (RIP) to the DISC [26]. RIP in turn recruits the inhibitor of κB (IκB) kinases (IKK) to the DISC, leading to the phosphorylation of IκB and subsequent activation of NF-κB [27, 28]. Inhibition of IκB and the NF-κB p65 subunit eliminates TRAIL resistance in pancreatic cancer cells [24, 25]. Here, we further show that selective knockdown of RIP reduces TRAIL resistance in pancreatic cancer cells. This study suggests that targeting of the inhibitory proteins in the DISC can eliminate TRAIL resistance in pancreatic cancer cells.

We have shown that cellular Fas-associated death domain-like interleukin-1β-converting enzyme-inhibitory protein (c-FLIP) is recruited to the DISC in TRAIL-resistant glioma and melanoma cells [29, 30]. The c-FLIP protein contains death effector domains through which it interacts with caspase-8, inhibiting caspase-8 cleavage in the

DISC [31]. Here we show that selective knockdown of c-FLIP with RNA interfering (RNAi) eliminates its inhibition of caspase-8 cleavage and thus enhances TRAIL-induced apoptosis in pancreatic cancer cells.

3.1. Materials and methods

3.1.1. Materials and antibodies

Recombinant soluble human TRAIL (amino acids 114–281) was purchased from PeproTech, Inc. (Rocky Hill, USA). The tetrapeptide caspase inhibitor carbobenzyloxy-Val-Ala-Asp(OMe)fluoromethyl ketone (z-VAD-fmk) (R&D Systems, Minneapolis, USA) was prepared as a 20 mM stock in DMSO and stored at -20°C in aliquots until use. Cisplatin, camptothecin (Sigma-Aldrich Canada Ltd., Oakville, Ontario, Canada), and Celecoxib (LKT laboratories, INC) were prepared as stock solution in DMSO. The mouse monoclonal antibodies included anti-FADD (Transduction Laboratories, Lexington, USA), anti-caspase-8 (MBL, Nagoya, Japan), anti-RIP (BD PharMingen, San Diego, CA), anti-c-FLIP (Alexis Biochemicals, San Diego, CA), and anti-DFF45 (StressGen Biotechnologies Inc., Victoria, British Columbia, Canada). Rabbit polyclonal anti-caspase-3 was purchased from StressGen, and anti-DR4 and anti-DR5 were obtained from BD Biosciences (San Diego, USA). Horseradish peroxidase-conjugated goat anti-mouse and goat anti-rabbit antibodies were from Jackson IR Labs (West Grove, PA). All of the other chemicals used were of analytical grade and purchased from Sigma-Aldrich, unless otherwise indicated.

3.1.2. Cell cultures, cell viability and apoptosis assay

Six human pancreatic cancer cell lines were obtained from the American Type Culture Collection (Rockville, MD); PANC-1 and PACA-2 were cultured in DMEM (Invitrogen, Carlsbad, CA); ASPC-1 and BXPC-3 in RPMI1640 medium (Invitrogen); CAPAN-1 in IMDM medium (Invitrogen); and CAPAN-2 in McCoy 5α medium (Invitrogen). Medium was supplemented with 10% fetal bovine serum and 1% antibiotics (Invitrogen). For the cell viability assay, cells were plated in a 96-well plate ($1x10^4$ cells per well), cultured overnight, and treated or untreated with different agents. After incubation for the times indicated in the Results, cells were washed and cell death was determined by an acid phosphatase assay. In brief, 100 μL buffer containing 0.2 M sodium acetate (pH 5.5), 0.2 % (v/v) Triton X-100 and 20 mM *p*-nitrophenyl phosphate (Sigma 104 phosphatase substrate) were added to each well. The plates were incubated at 37 °C for 2 h and the reaction was stopped by the addition of 10 μL 1 M NaOH to each well and the color developed was measured at 405 nm by a microplate reader (Bio-Rad). Data was expressed as mean ± SD.

3.1.3. Flow cytometry for sub-G_1 apoptotic cells and mitochondrial membrane potential

Apoptotic sub-G_1 cells were detected by flow cytometric analysis of the cell cycle [32]. In brief, cells were fixed in 70% ethanol at 4°C. The DNA of the fixed cells was stained using a propidium iodide-RNase solution (PBS containing 20 μg/mL propidium iodide, 200 μg/mL DNase-free RNase A, and 0.1% Triton X-100) for 30 min at 20 °C in the dark. The cell cycle status of the cells was analyzed with a flow cytometer using Cell Quest™ software (Becton Dickinson) and ModFit LT software (Verity Software House Inc.). Mitochondrial membrane potential was monitored by the indicator dye 5,5',6,6'-

tetrachloro-1,1',3,3'-tetraethylbenzimidazolcarbocyanine iodide (JC-1) using Mīt-E-Psi™ Apoptosis and Mitochondria Permeability Detection Kit (Biomol International, Plymouth Meeting, PA). In brief, the cells (2-3x10^6 cells/mL), treated or untreated, were suspended in the JC-1 solution and incubated for 15 min at 37 °C. The cells were then quantified for J-aggregate fluorescence intensity using a Becton Dickinson FACScan™ (Mountain View, CA). In normal healthy cells, JC-1 accumulated in the mitochondria, resulting in red fluorescence whereas the apoptotic cells appeared green due to the increased mitochondrial membrane permeability. Data analysis was processed using Cell Quest™ software (Becton Dickinson).

3.1.4. SDS-PAGE and Western blot

Cells in culture were harvested and lysed in 20 mM Tris-HCl (pH 7.4) containing 150 mM NaCl, 2 mM EDTA, 10% glycerol, 1% Triton X-100, 1 mM phenylmethylsulfonyl fluoride and a protease inhibitor cocktail (Sigma). The lysed cells were centrifuged at 20 000 *g* for 15 min. The supernatant was collected and protein concentrations were determined by the Bradford protein assay following the manufacturer's protocol (Bio-Rad). Equal amounts of protein were separated through SDS-PAGE gels and transferred onto nitrocellulose membranes (Bio-Rad). The membranes were incubated overnight at 4°C first with the primary antibody and then for 1 hour with the horseradish peroxidase-conjugated-secondary antibody. The membranes were developed by chemiluminescence (Amersham Biosciences, Piscataway, USA).

3.1.5. c-FLIP cDNA transfection

The pEF FLAG-c-FLIP$_L$ and pcDNA-FLAG-c-FLIP$_S$ (kind gifts from Dr. Peter H. Krammer, German Cancer Research Center, Heidelberg, Germany) were transfected in cells using the LipofectAMINE 2000 following the manufacturer's protocol (Invitrogen). The transfected cells were grown for 24 h before being subjected to the cell death assay and Western blot analysis.

3.1.6. RIP and c-FLIP shRNA construct and transfection

RNA interference (RNAi) is a recently developed method of gene silencing that introduces double stranded RNA (dsRNA) into cells, resulting in post-transcriptional gene silencing. The small interfering RNA (siRNA) is a 21-23 nucleotide (nt) double stranded RNA with 2 nt overhangs at each 3' ends [33]. Upon transfection into mammalian cells, they are incorporated into an RNA-induced silencing complex (RISC), a complex that cleaves mRNA complementary to the siRNA, leading to silencing of that gene (Fig 3.1) [33-36].

For a vector-based RNAi, a short hairpin double-stranded RNA (shRNA) was cloned into the BamHI-XhoI site of pRNAT-U6.1/neo-cGFP vector (GenScript Corporation, Piscataway, NJ). The shRNA specific sequence against c-FLIP was: 5'-*GATCCC*GTGTCGGGGACTTGGCTGAACT***TTGATATCCG***AGTTCAGCCAAGTCC CCGACATTTTTTCCAA*CTCGAG*-3'; the RIP shRNA sequence was 5'-*GGATCCC*GTACCACTAGTCTGACGGATAA***TTGATATCCG***TTATCCGTCAGACT AGTGGTATTTTTTCCAA*CTCGAG*-3'. The underlined, bold and italic letters denote the hairpin loop, terminal signal and target sites of the restriction enzymes, BamHI and XhoI, respectively (Fig 3.2). The empty vector and the vectors containing RIP and c-

FLIP shRNA were transfected into cells by LipofectAMINE 2000 (Invitrogen).

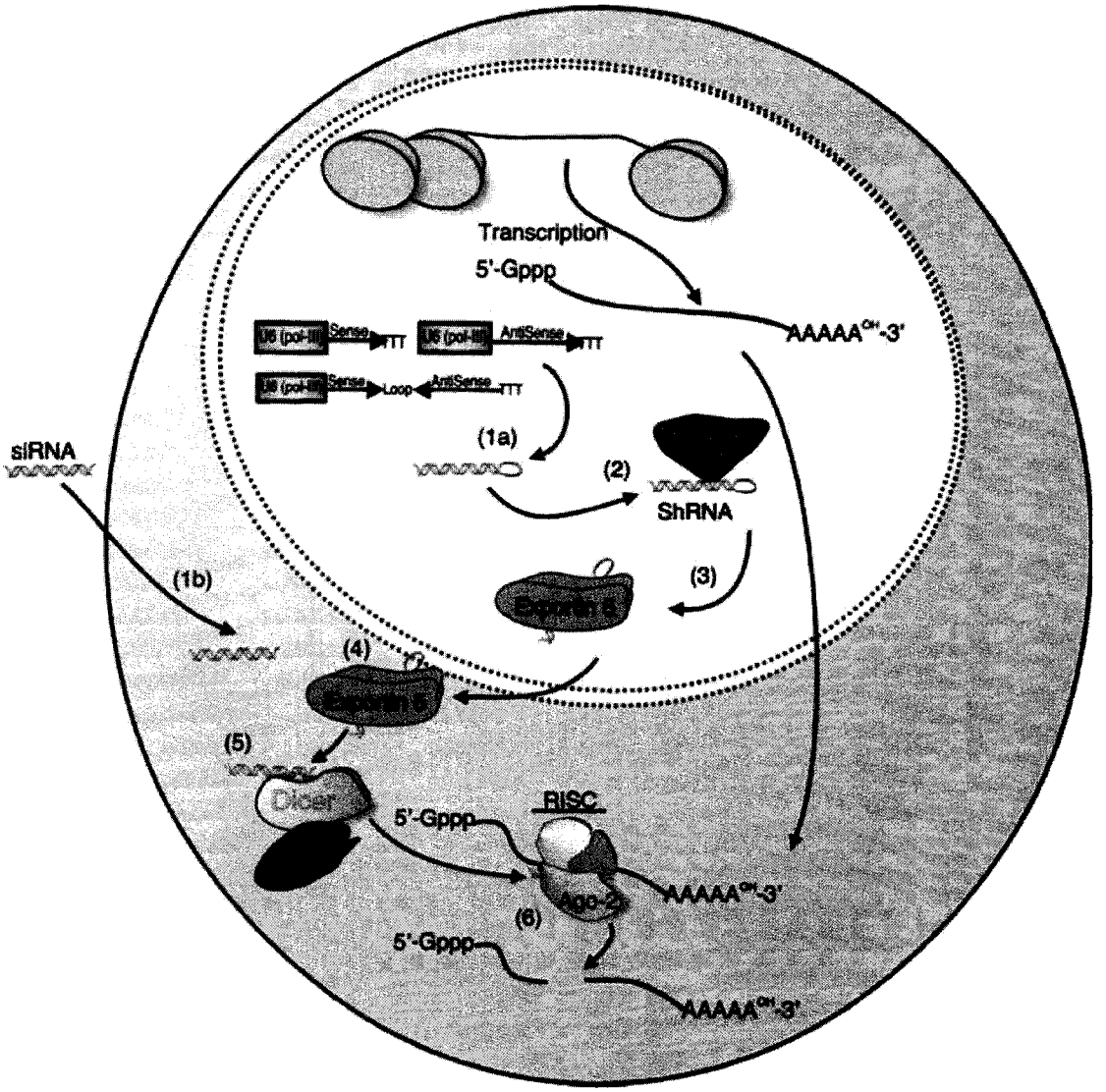

Figure 3.1 Model of shRNA gene silencing mechanism. shRNAs are transfected into cells where they are processed, exported out of the nucleus, and assembled into an RNA-induced silencing complex (RISC). In the RISC, siRNAs are unwound by the helicase activity of the complex and target complimentary mRNA, through base pairing, for cleavage and degradation by the RISC complex. (Reproduced from siRNA-mediated transcriptional gene silencing: the potential mechanism and a possible role in the histone code. Adapted from [1])

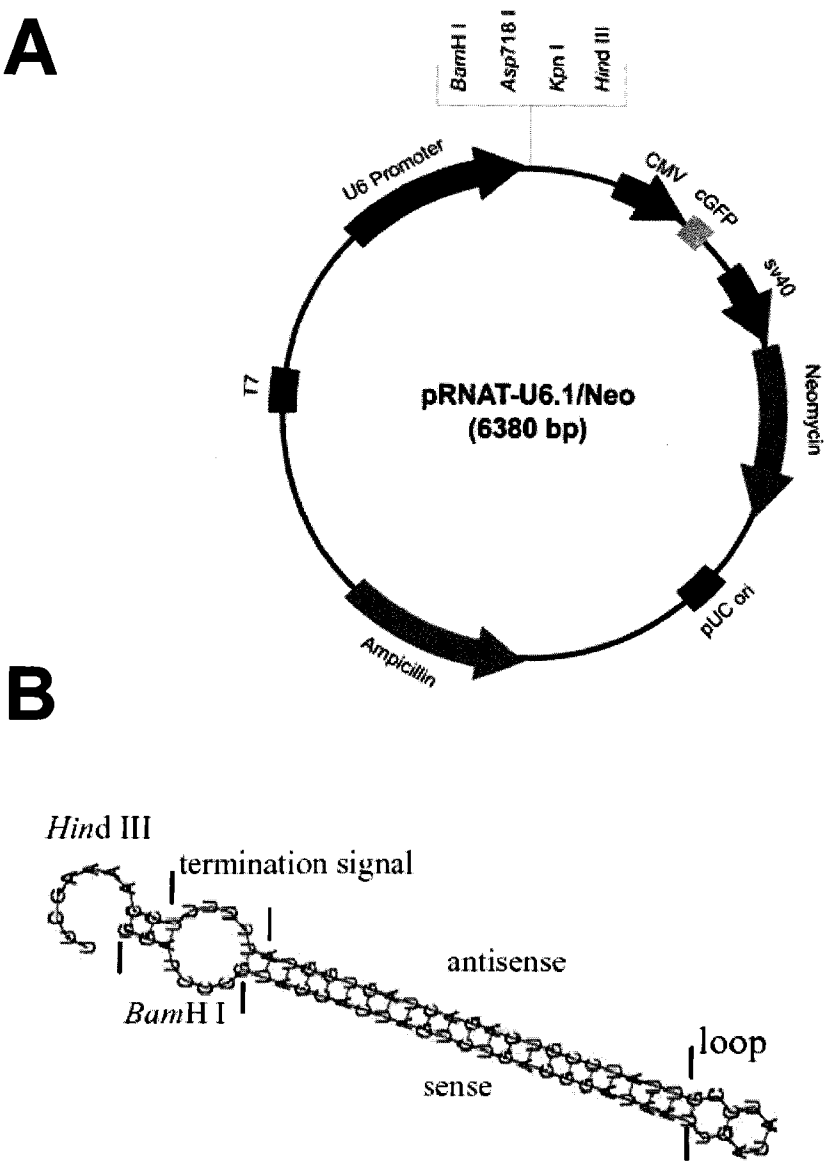

Figure 3.2 Map of plasmid pRNAT-U6.1/Neo and encoded shRNA. A. pRNAT-U6.1/Neo is a GenScript siRNA expression vector which is designed for mammalian transfection It uses the U6 promoter for siRNA expression. (Reproduced from http://www.genscript.com/cgi-bin/products/marker.cgi?code=SD1211) B. The insert, encoding a short hairpin targeting c-FLIP and RIP, was inserted in pRNAT-U6.1/Neo vector.

3.2 Results

3.2.1. The inhibition of caspase-8 cleavage contributes to TRAIL resistance

The autoproteolytic cleavage of caspase-8 in the DISC is the most upstream event in TRAIL-induced apoptosis [37]. To examine if caspase-8 inhibition plays a role in TRAIL-resistance in pancreatic cancer cells, we examined the caspase-8-initiated caspase cascade in TRAIL-sensitive and resistant pancreatic cancer cells. Pancreatic cancer cell lines PANC-1, ASPC-1, BXPC-3, PACA-2, CAPAN-1 and CAPAN-2 were treated with a series of dilutions of TRAIL for 24 h and examined for cell viability by the acid phosphatase assay [32]. The results showed that BXPC-3 and PACA-2 were sensitive, whereas PANC-1, ASPC-1, CAPAN-1 and CAPAN-2 were resistant (Fig. 3.3.A). Cell lines were then treated with 300 ng/mL of TRAIL and examined by Western blot for cleavage of caspase-8. Caspase-8 exists in two isoforms (p53, p55) [38] and is cleaved in the DISC through two consecutive steps [39]: the first step generates large (p43 and p42) and small (p12) subunits and the second step produces a prodomain and p18 and p10 active subunits. A Western blot with anti-caspase-8 antibody detected p43, p42 and p18 cleavage products in TRAIL-sensitive BXPC-3 and PACA-2, but not in TRAIL-resistant PANC-1 and ASPC-1 cell lines (Fig. 3.3.B). The results indicate that caspase-8 cleavage is inhibited in TRAIL-resistant pancreatic cancer cells.

The mitochondrial pathway is involved in TRAIL-induced apoptosis [11, 22] and caspase-9 is the apoptosis-initiating caspase of this pathway [21]. The cleavage of caspase-9 was examined to determine if the mitochondrial pathway is activated in the pancreatic cancer cell lines. Western blots detected cleavage products of caspase-9 in

TRAIL-sensitive but not resistant pancreatic cancer cell lines (Fig. 3.3.B). Both caspase-8 and caspase-9 can cleave caspase-3, which in turn cleaves DNA fragmentation factor 45 (DFF45) in the execution of apoptotic cell death [40]. We therefore examined the cleavage of caspase-3 and DFF45 and found the cleavage products of caspase-3 (p24, p17) and DFF45 (p25, p17, p11) in TRAIL-sensitive but not resistant pancreatic cancer cell lines (Fig. 3.3.B). These studies indicate that caspase-8-initiated caspase cascade is activated in TRAIL-sensitive but inhibited in TRAIL-resistant pancreatic cell lines.

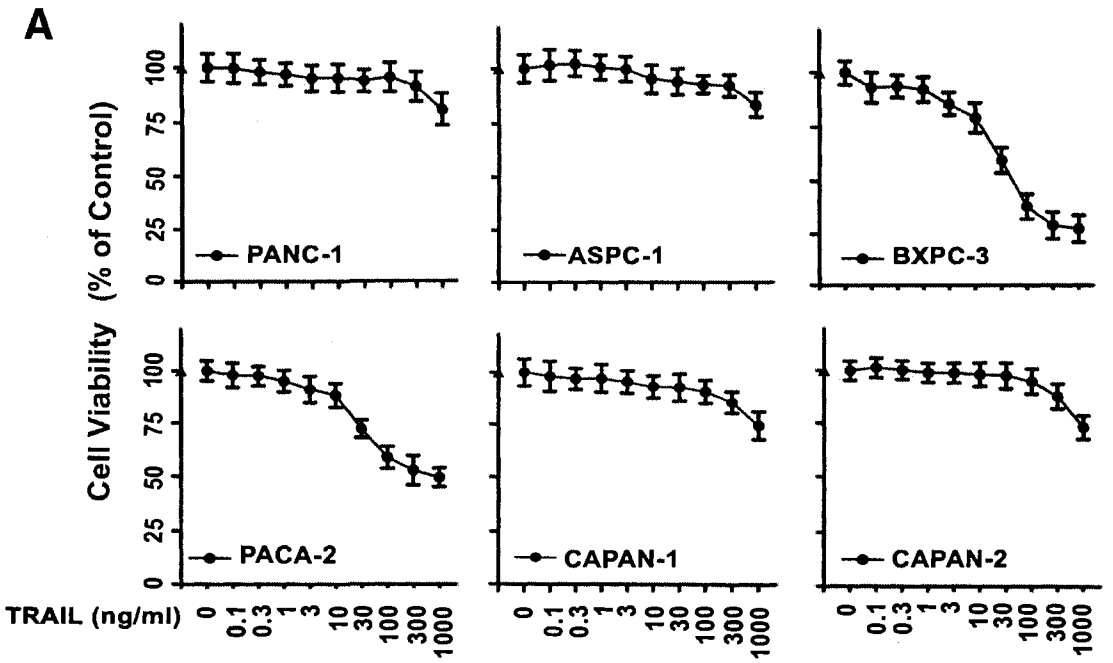

Figure 3.3 Caspase-8-initiated caspase cascade is inhibited in TRAIL-resistant pancreatic cancer cells. (A) Six human pancreatic cancer cell lines were treated with recombinant TRAIL for 24 h in the doses indicated and subjected to cell viability analysis.

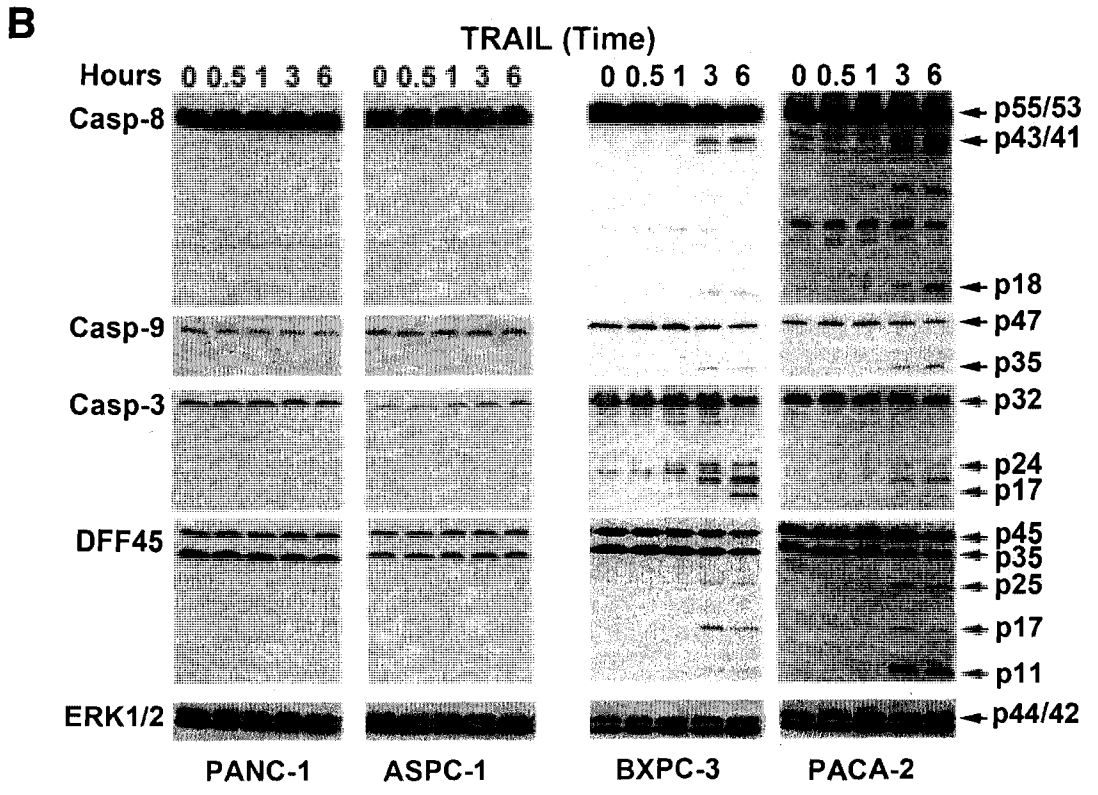

Figure 3.3 (B) Western blot analysis for the cleavage of caspase-8 (Casp-8), caspase-9, caspase-3 and DFF45 of four of the cell lines treated with 300 ng/mL TRAIL for the times indicated. ERK1/2 was the loading control.

3.2.2. Knockdown of c-FLIP and RIP sensitizes the resistant cells to TRAIL

We have shown that c-FLIP is recruited to the DISC where it inhibits caspase-8 cleavage in glioma and melanoma [29, 30]. To examine the role of c-FLIP in TRAIL resistance in pancreatic cancers, we applied RNAi technology and selectively knocked down c-FLIP in TRAIL-resistant pancreatic cancer cells. A double stranded small interfering RNA (siRNA) duplex targeting to the c-FLIP nucleotides 535-555 has been proven to knockdown both c-$FLIP_L$ and c-$FLIP_S$ [41]. We therefore synthesized a short hairpin RNA (shRNA) specific to c-FLIP nucleotides 535-555 and inserted the shRNA in the pRNAt-U6.1 vector. The c-FLIP shRNA vector and its empty vector were transfected into TRAIL-resistant PANC-1 and ASPC-1 for 24 h.

The transfection of the c-FLIP shRNA vector, but not the empty vector, significantly inhibited the expression of c-$FLIP_L$ and c-$FLIP_S$ (Fig. 3.4.A). The c-FLIP shRNA and empty vector transfected cells were treated with 300 ng/ml TRAIL; cell viability analysis showed a significant cell death (Fig. 3.4.B) and Western blots detected caspase-8 cleavage products in the c-FLIP shRNA, but not empty vector transfected cells (Fig. 3.4.C). These results indicate the role of c-FLIP in TRAIL resistance in pancreatic cancer cells.

RIP plays a critical role in the TRAIL-induced activation of NF-κB [37]. Here, we further examined the role of RIP in TRAIL-resistance in pancreatic cancer cells. To this end, we constructed pRNAt-U6.1 vector by inserting shRNA specific to RIP nucleotides 837-857. The transfection of RIP shRNA vector inhibited the expression of RIP protein (Fig. 3.4.A).

The RIP shRNA vector and empty vector transfected cells were treated with 300 ng/mL TRAIL. Cell viability analysis showed a significant cell death; and Western blot detected caspase-8 cleavage (Fig. 3.4.B,C). This study demonstrates for the first time the role of RIP in TRAIL resistance in pancreatic cancer cells. These data indicate that RIP and c-FLIP play crucial anti-apoptotic roles at the DISC level in the TRAIL-induced apoptosis pathway.

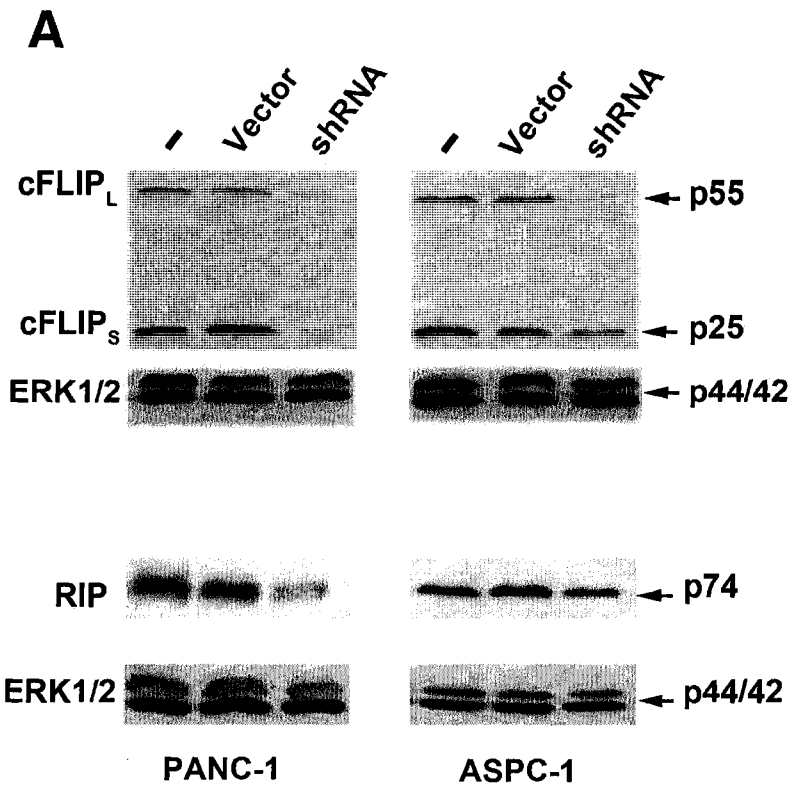

Figure 3.4 Selective knockdown of c-FLIP and RIP sensitizes the resistant cell to TRAIL-induced apoptosis. (A) PANC-1 and ASPC-1 were transfected with the c-FLIP and RIP shRNA expressing and empty vector, respectively, for Western blot analysis of the expression of c-FLIP$_L$ and c-FLIP$_S$ (top two panels) and RIP (the bottom two panels) with ERK1/2 as the loading control.

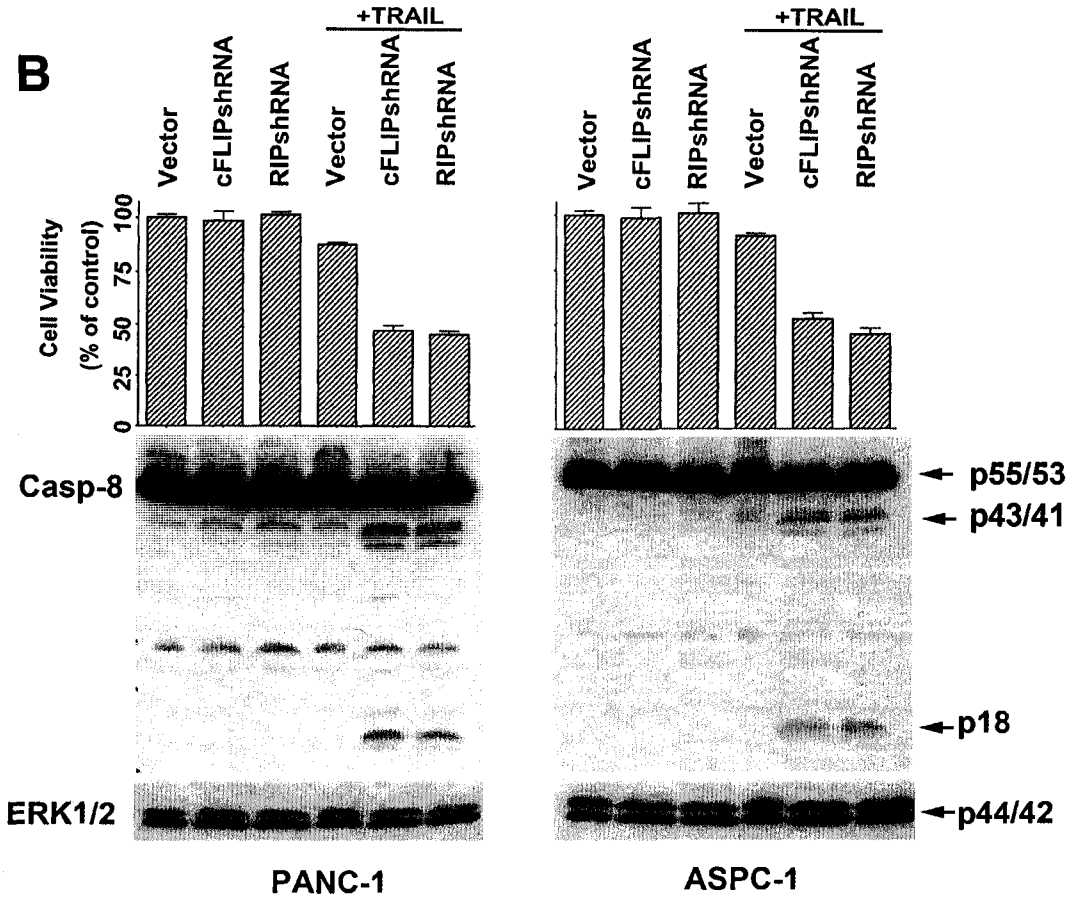

Figure 3.4 (B) The transfected cell lines were treated with 300 ng/mL TRAIL or left untreated either for 24 h for cell viability assay (top panel) or for 3 h for Western blot analysis of caspase-8 cleavage (bottom panel).

3.2.3. Caspase-8 cleaves RIP in TRAIL-induced apoptosis

To examine the molecular mechanisms that control c-FLIP and RIP-mediated inhibition of caspase-8 cleavage in TRAIL resistant cells, we compared the protein expression levels of c-FLIP, RIP and other DISC proteins, such as DR4, DR5, FADD and caspase-8, in TRAIL-sensitive and -resistant pancreatic cancer cells. Western blot analysis showed that the protein expression levels of DR4, DR5, FADD and caspase-8 were relatively consistent through all the cell lines and did not correlate to TRAIL sensitivity (Fig. 3.5.A). In contrast, the expression of c-FLIP proteins was lower in TRAIL-sensitive than TRAIL-resistant cell lines (Fig. 3.5.A). The c-FLIP protein exists in two forms: the long form c-$FLIP_L$ and the short form c-$FLIP_S$ [31]. Both c-$FLIP_L$ and c-$FLIP_S$ were expressed at significantly lower levels in sensitive cells than in the resistant cells, except for the PANC-1 cell line in which c-$FLIP_L$ was lower but c-$FLIP_S$ was higher (Fig. 3.5.A). This analysis suggests the higher levels of c-$FLIP_L$ and c-$FLIP_S$ contribute to the inhibition of caspase-8 in TRAIL-resistant pancreatic cancer cells.

In contrast to c-FLIP, RIP expression was consistent and had no correlation to TRAIL sensitivity of these pancreatic cancer cell lines (Fig. 3.5.A). However, selective knockdown of RIP in TRAIL-resistant cell lines sensitized the cells to TRAIL-induced apoptosis through activation of caspase-8 (Fig. 3.4.). Caspase-8 has been reported to cleave RIP in TNF-induced apoptosis [42]. To examine this in TRAIL signaling, TRAIL-sensitive and resistant pancreatic cancer cell lines were treated with 300 ng/ml of TRAIL for 6 h. Western blots detected the cleavage of RIP from the full length (74 kDa) to cleavage product (42 kDa) in TRAIL-sensitive but not resistant cell lines (Fig. 3.5.B).

Treatment with either caspase-8 inhibitor, z-IETD-fmk, or pan-caspases inhibitor, z-VAD-fmk, eliminated TRAIL-induced cleavage of RIP in TRAIL-sensitive cell lines (Fig. 3.5.C). Taken together, these results suggest that the c-FLIP is insufficient for inhibition of caspase-8 in TRAIL-sensitive cells, leading to the caspase-8 activation and cleavage of RIP in TRAIL-induced apoptosis.

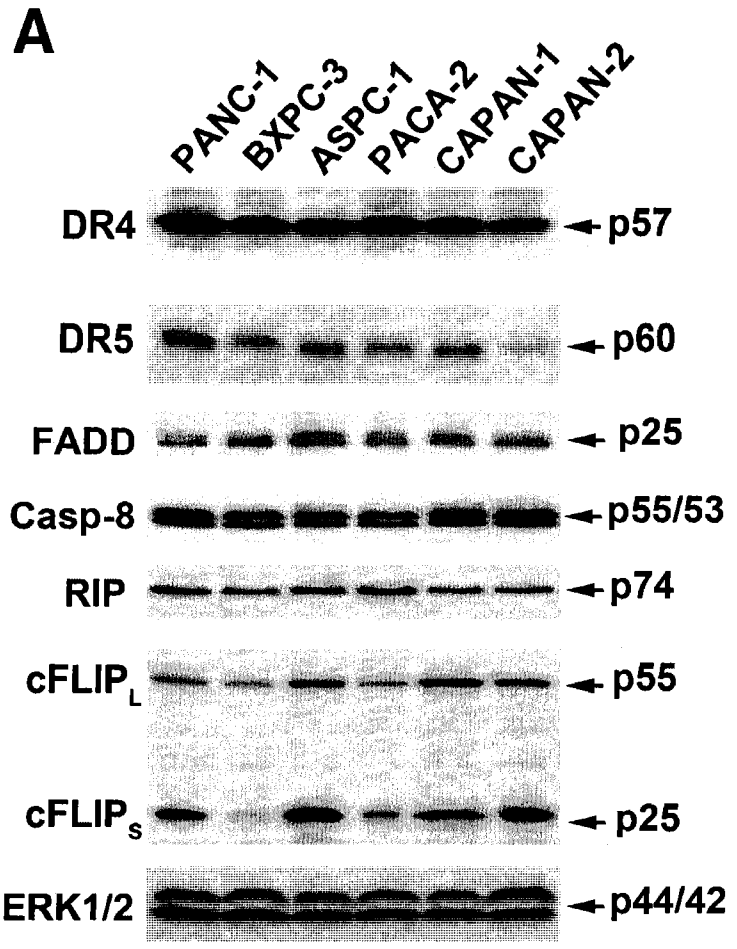

Figure 3.5 Caspase-8 cleaves RIP in TRAIL-sensitive but not resistant pancreatic cancer cells. (A) Six pancreatic cell lines were examined by Western blot for the expression of the DISC proteins.

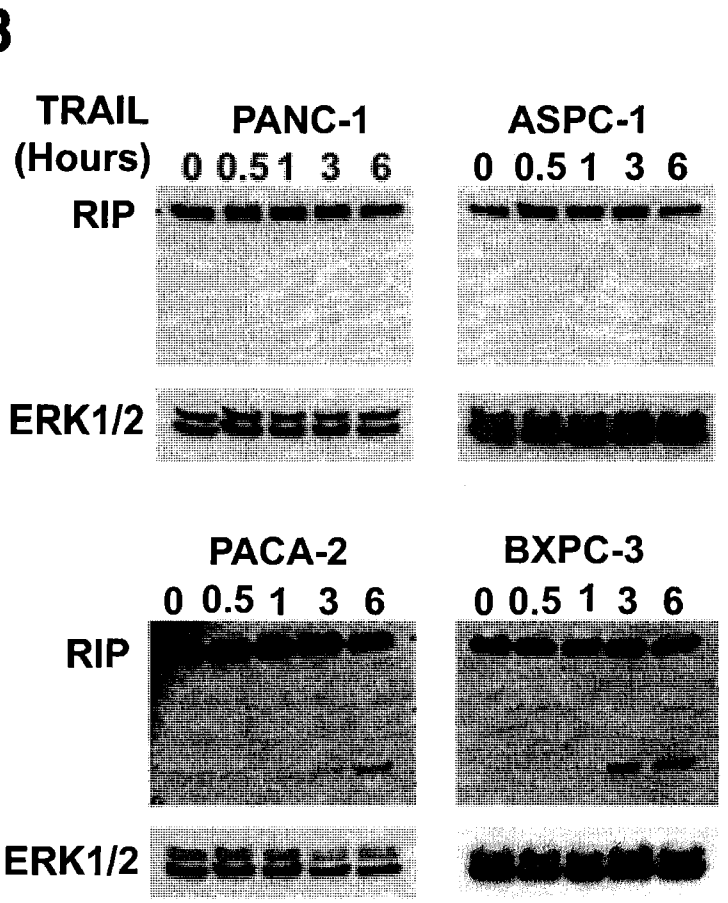

Figure 3.5 (B) TRAIL-resistant PANC-1 and ASPC-1 and TRAIL-sensitive PACA-2 and BXPC-3 lines were treated with 300 ng/ml of TRAIL for the time indicated on the top of panels and then subjected to Western blot detection of p42 RIP cleavage product.

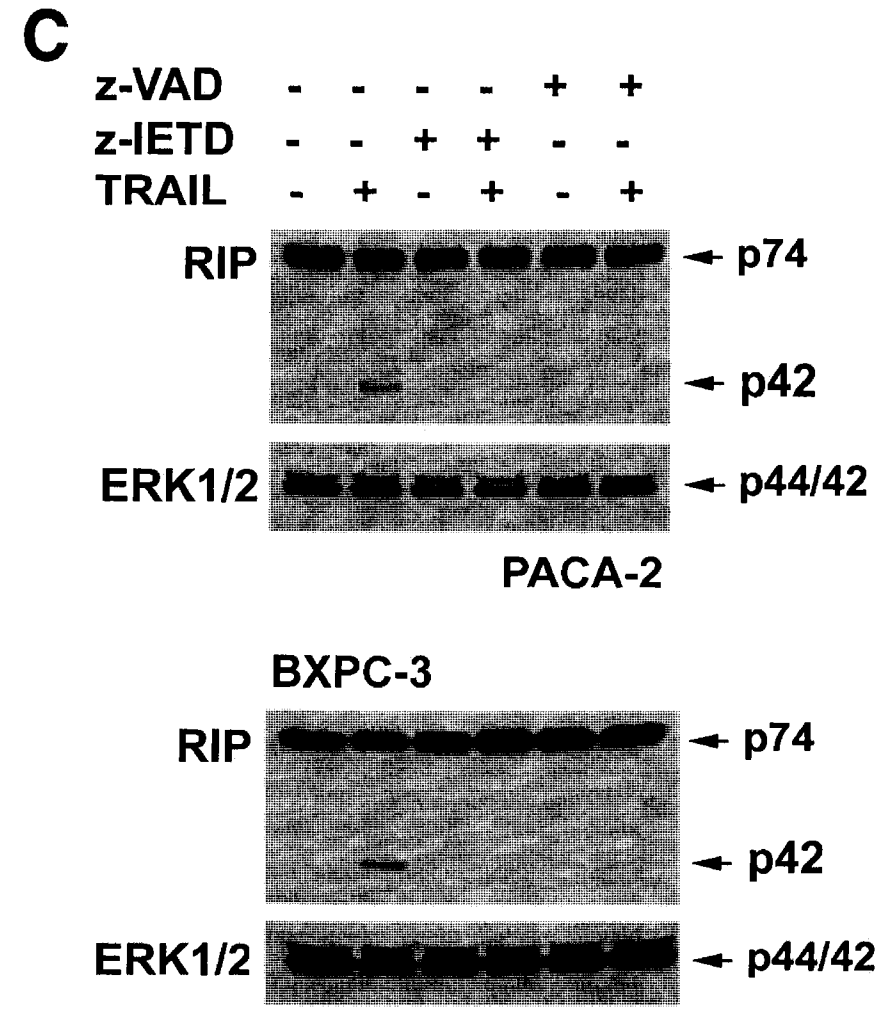

Figure 3.5 (C) TRAIL-induced cleavage of RIP in PACA-2 and BXPC-3 cell lines was inhibited by the presence of z-VAD and z-IETD. ERK1/2 was used as a loading control.

3.2.4. Knockdown of c-FLIP and RIP facilitates TRAIL-induced mitochondrial activation

TRAIL-induced apoptosis requires the activation of the mitochondrial pathway in pancreatic cancer cells [11, 22] in that caspase-8 cleaves Bid, which in turn interacts with Bax and Bak and induces the mitochondrial membrane potential change [21]. To examine this in c-FLIP and RIP knockdown cells, we examined the mitochondrial potential by flow cytometry using the Mīt-E-Psi™ Apoptosis and Mitochondria Permeability Detection Kit. TRAIL-resistant PANC-1 cell line was transfected with the c-FLIP or RIP shRNA pRNAt-U6.1 vector, respectively and then treated with 300 ng/ml TRAIL for 16 h. Flow cytometry showed a significant increase in the cells with the loss of the mitochondrial membrane potential in the cultures transfected with c-FLIP shRNA (from 1.12% to 52.4%) and the RIP shRNA (from 1.25% to 48.04%) (Fig. 3.6.A).

To further confirm apoptotic cell death, the c-FLIP and RIP shRNA vector transfected PANC-1 cells were examined by flow cytometry for cell cycle and subG1 apoptotic cells. The transfection of c-FLIP shRNA and RIP vector showed no effect on the percentage of subG1 cells and cell cycle status of PANC-1 cells. TRAIL treatment, however, led to a dramatic increase of subG1 cells in the c-FLIP shRNA (from 0.52% to 46.06%) and the RIP shRNA transfected PANC-1 cells (from 1.23% to 40.22%) (Fig. 3.6.B). The presence of pan-caspase inhibitor z-VAD-fmk reduced the subG1 cells from 46.06% to 10.83% and from 40.22% to 7.26%, respectively in the c-FLIP shRNA and RIP shRNA transfected cells (Fig. 3.6.B). Taken together, these studies suggest the involvement of the mitochondrial pathway in TRAIL-induced apoptosis in TRAIL-resistant pancreatic cancer cells once the c-FLIP and RIP inhibition of caspase-8 cleavage

is released in the resistant pancreatic cancer cells.

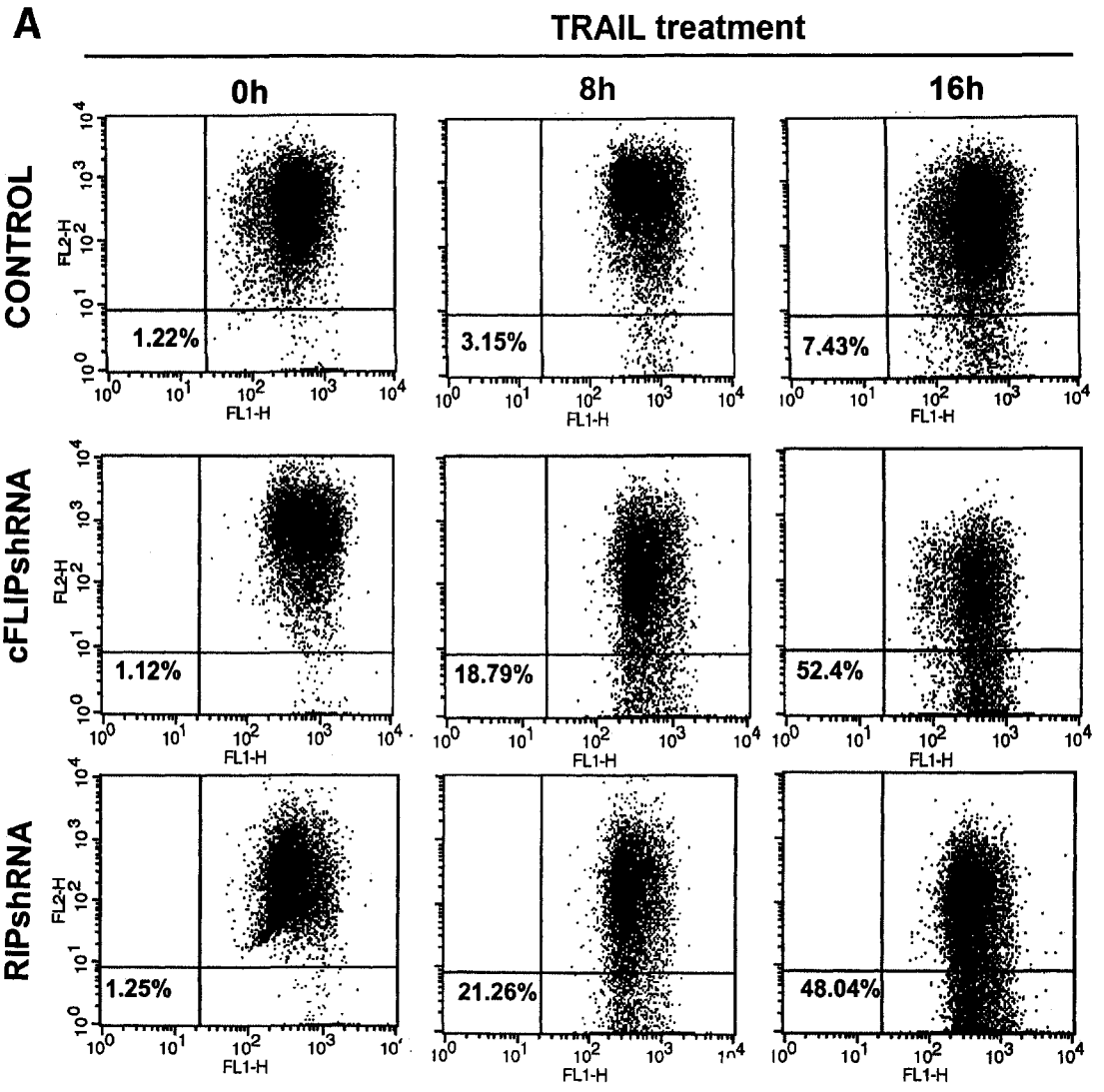

Figure 3.6 TRAIL activates the mitochondrial pathway in c-FLIP and RIP knockdown cells. (A) TRAIL-resistant PANC-1 cell line was transfected with the empty vector (control), c-FLIP shRNA and RIP siRNA and examined by flow cytometry for the mitochondrial membrane potential change. The right upper labels the negative cells and the lower quadrant indicates the positive cells.

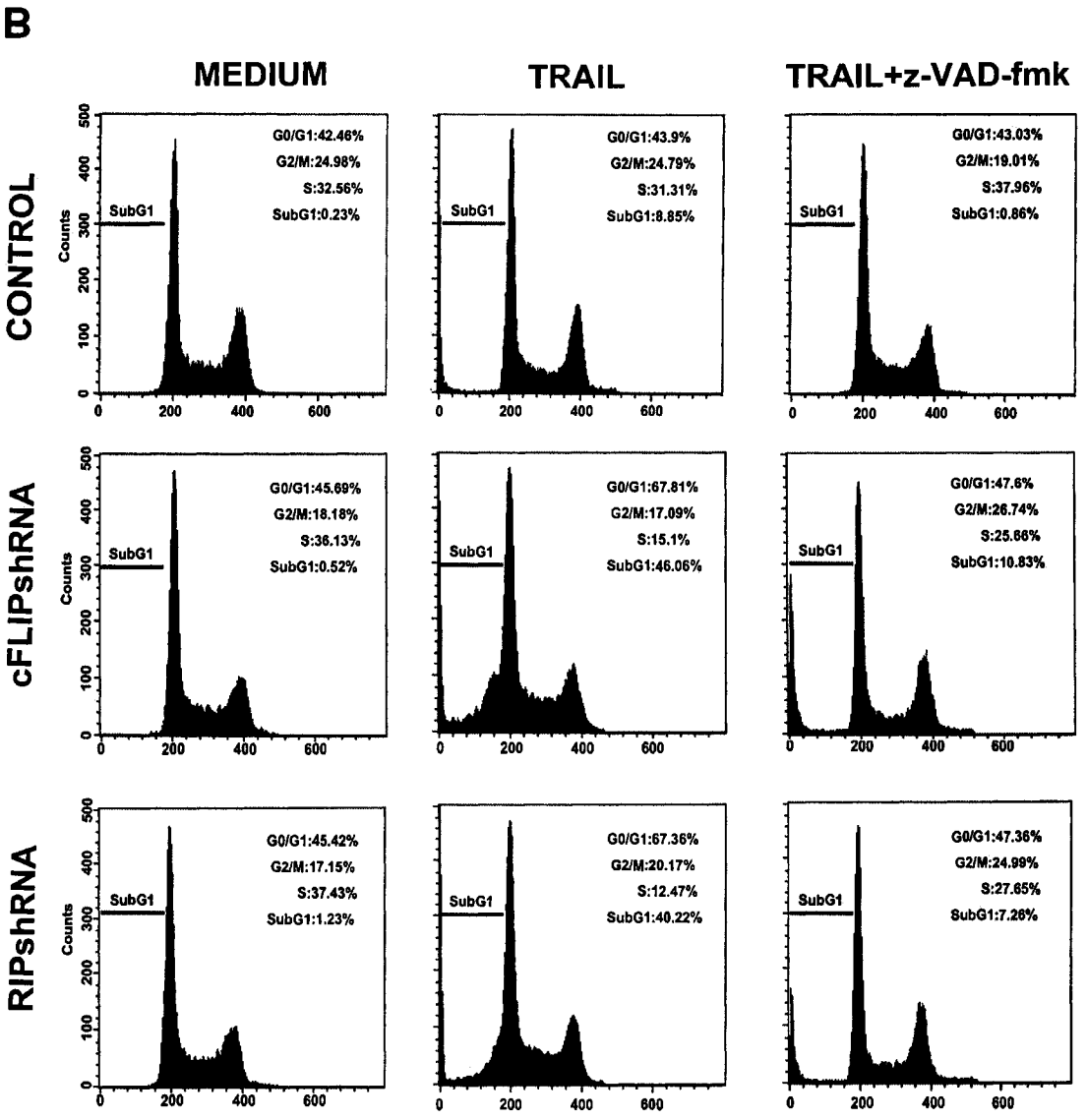

Figure 3.6 (B) The transfected cells were examined for subG1 apoptotic cells by flow cytometry analysis of cell cycle. SubG1 cells are presented as the percentage of the total cells. Similarly, the cells in G0/G1, G2/M and S phase are shown as the percentage of the total cells

3.2.5. Over-expression of c-FLIP$_L$ or c-FLIP$_S$ or both results in TRAIL resistance

To further define the role of c-FLIP$_L$ and c-FLIP$_S$ in TRAIL-resistance, we over-expressed c-FLIP$_L$ or c-FLIP$_S$ or both in the TRAIL-sensitive PACA-2 cell line that normally has lower levels of the c-FLIP proteins (Fig. 3.5.A). The PACA-2 cell line was transfected with pEF FLAG-c-FLIP$_L$ or pcDNA-FLAG-c-FLIP$_S$ or both and the FLAG-c-FLIP$_L$ and FLAG-c-FLIP$_S$ were detected by Western blots with higher molecular weights than the endogenous c-FLIP$_L$ and c-FLIP$_S$ protein (Fig. 3.7.A). The pEF FLAG-c-FLIP$_L$ transfected PACA-2 cells were treated with 300 ng/mL TRAIL and Western blot analysis showed that the cleavage of caspase-8 was inhibited as compared with non-transfected cells (Fig. 3.7.B). When the PACA-2 cell line was transfected with FLAG-c-FLIP$_L$ vector, FLAG-c-FLIP$_S$ vector or both, the transfectants were then treated with 300 ng/mL TRAIL. Western blotting showed the inhibition of caspase-8 cleavage in the transfected cells (Fig. 3.7.C), while flow cytometric analysis of the cell cycle revealed a significant decrease in subG1 apoptotic cells (Fig. 3.7.D). The mitochondrial membrane potential assay showed inhibition of the potential change in the transfected cells as compared with non-transfected cells (Fig. 3.7.E). These studies indicate that c-FLIP inhibits the caspase-8-initiated apoptotic cascades in pancreatic cancer cells.

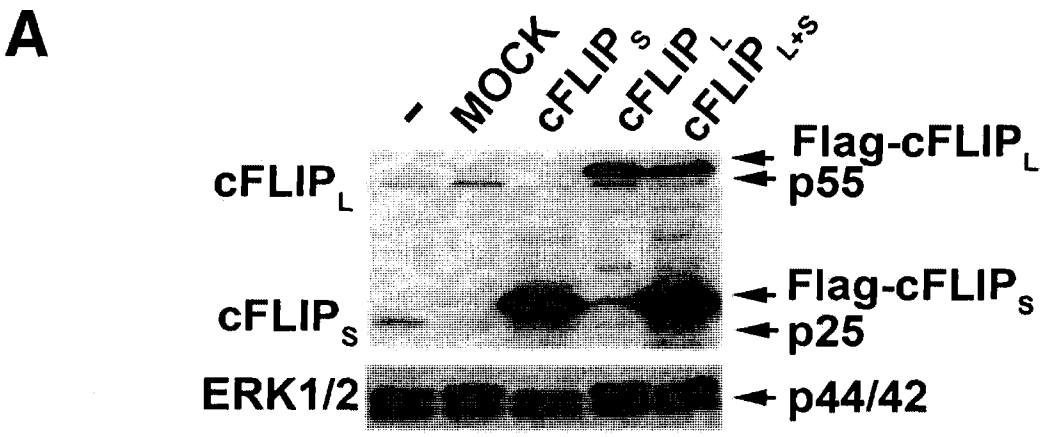

Figure 3.7 Over-expression of c-FLIP$_L$, c-FLIP$_S$ or both inhibits TRAIL-induced apoptosis. (A) TRAIL-sensitive PANC-2 cell line was transfected with the FLAG-c-FLIP$_L$ cDNA, FLAG-c-FLIP$_S$ cDNA or both with non-transfected cells (-) and empty vector (MOCK) transfected cells as controls. After 24 h of incubation, the transfectants were examined by Western blots for the expression of the transfected proteins. The endogenous c-FLIP$_L$ and c-FLIP$_S$ were labeled by arrows and molecular weights (p55, p25).

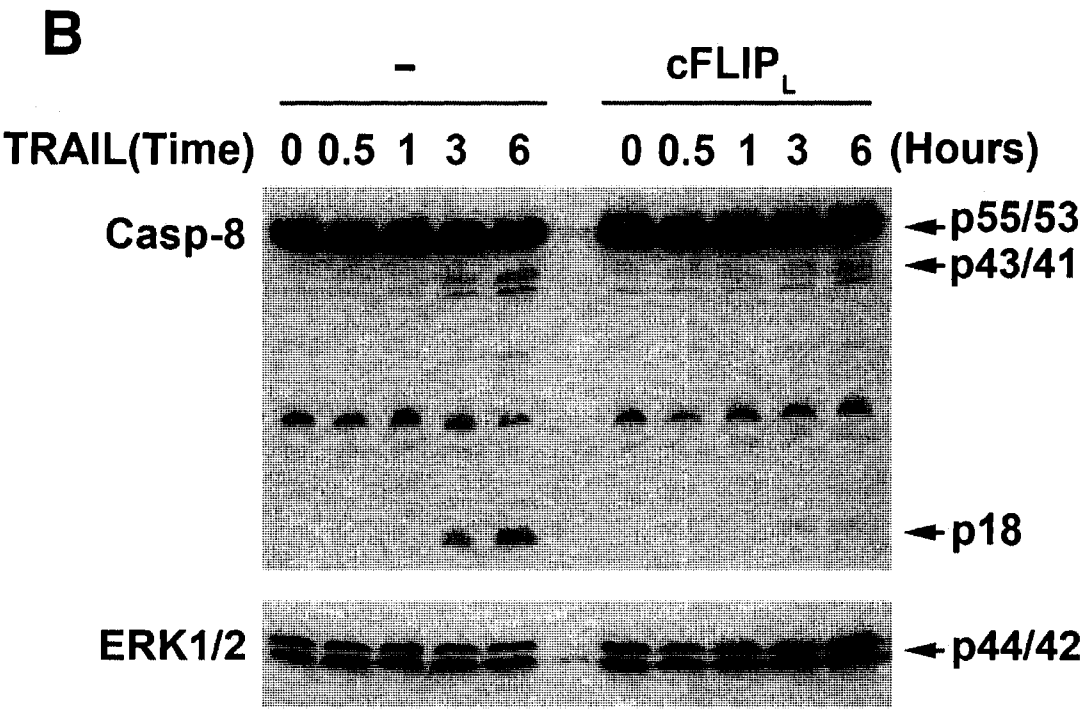

Figure 3.7 (B) Western blot examination of caspase-8 cleavage in non-transfected and FLAG-c-FLIP$_L$ cDNA transfected PANC-2 cells treated with 300 ng/mL TRAIL for the times indicated.

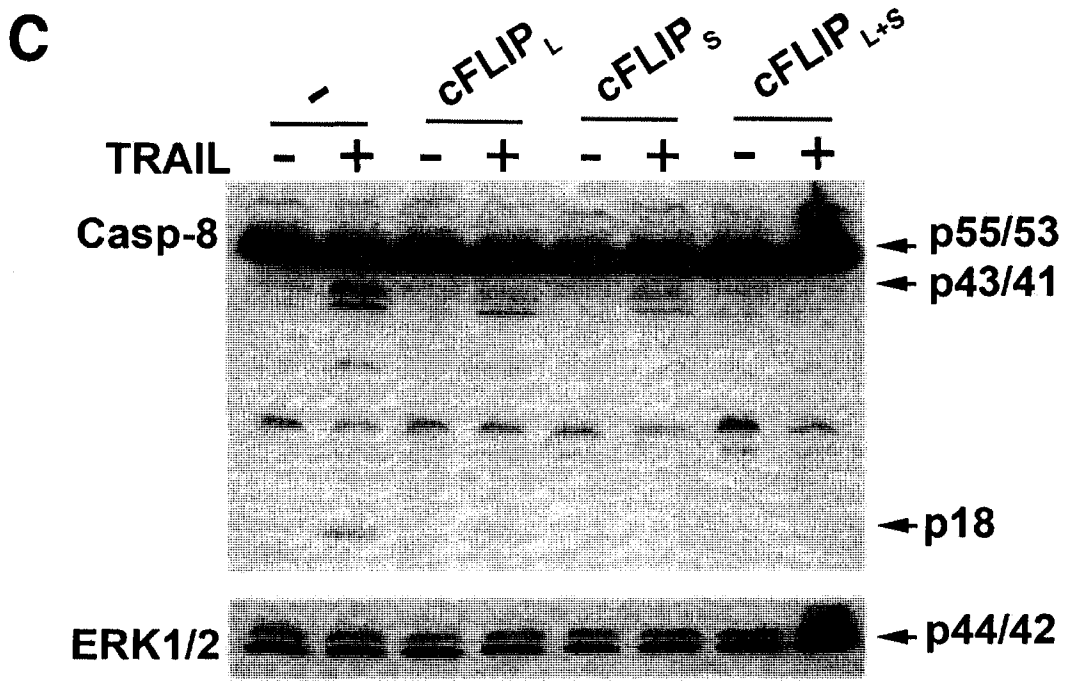

Figure 3.7 (C) Western blot examination of caspase-8 cleavage in non-transfected, and FLAG-c-FLIP$_L$ cDNA and FLAG-c-FLIP$_S$ cDNA transfected PANC-2 cells treated with 300 ng/mL TRAIL for 3 h.

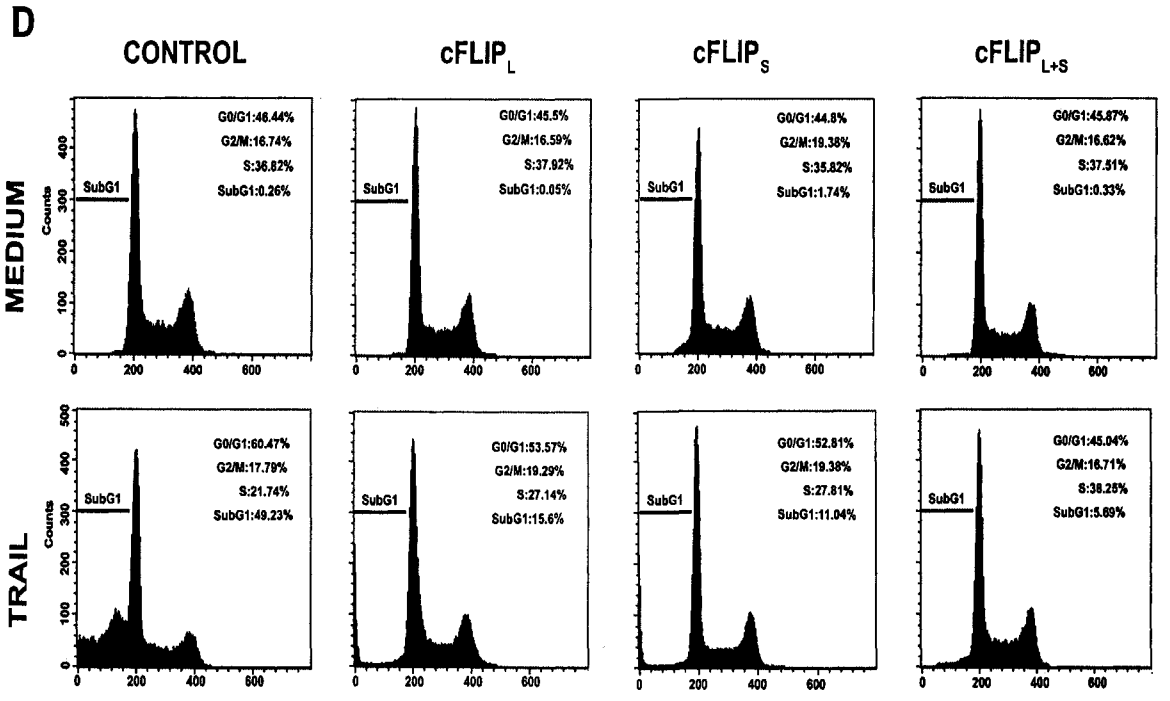

Figure 3.7 (D) Flow cytrometry analysis for subG1 cells and cell cycle of transfected and non-transfected (Control) cells treated with 300 ng/mL TRAIL for 16 h.

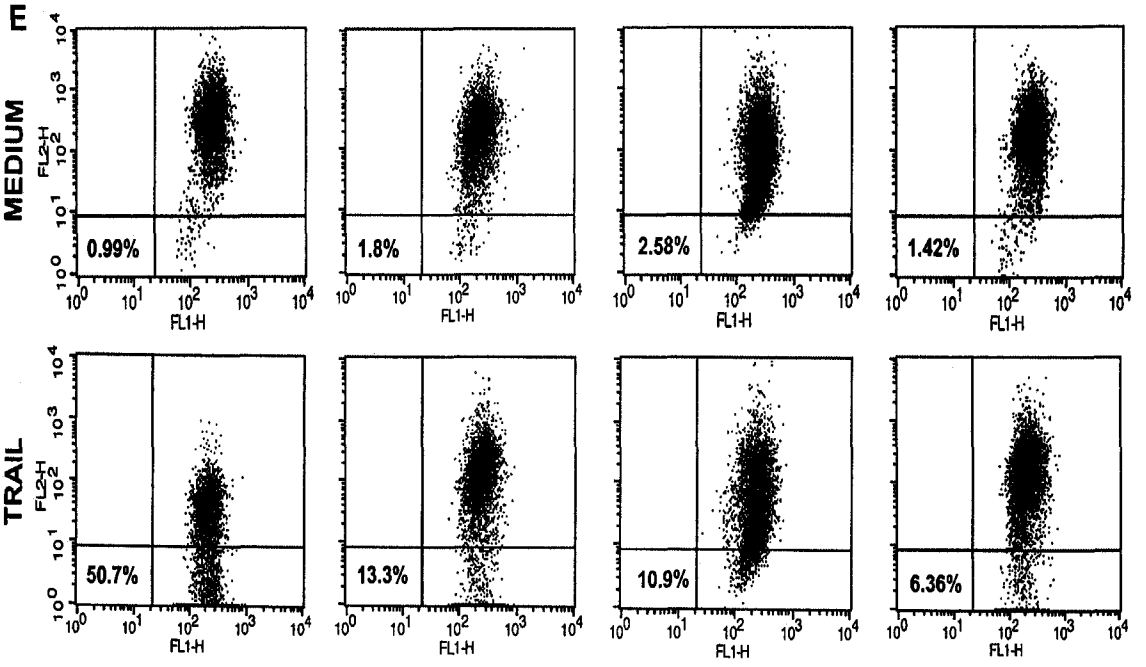

Figure 3.7 (E) Flow cytometry analysis for mitochondrial membrane potential changes of transfected and non-transfected (Control) cells treated with 300 ng/mL TRAIL for 16 h.

3.3. Discussion

TRAIL has recently emerged as a novel cancer therapeutic agent because it selectively induces apoptotic cell death in human cancer over normal human cells. TRAIL-induced apoptosis occurs through the extrinsic DR4/DR5-mediated caspase-8 caspase cascade and the caspase-8-initiated Bid-induced mitochondrial intrinsic pathways [37]. Several groups have shown that TRAIL-induced extrinsic and intrinsic apoptotic pathways do exist in human pancreatic cancer cell lines [7, 10] and patients' tumors [8]. However, these studies have further shown that these apoptotic pathways are inhibited in the majority of the human cancer cell lines [6, 10] and tumors [8]. Bcl-xL is highly expressed in pancreatic cancers [43] and inhibits the mitochondrial pathway [22], thus contributing to TRAIL resistance in pancreatic cancers. In this study, we show that the c-FLIP inhibition of caspase-8 prevents the TRAIL-induced caspase-8-initiated extrinsic caspase cascade and intrinsic mitochondrial pathway in human pancreatic cancer cells.

Although c-FLIP is constitutively expressed in normal cells, it is highly expressed in human cancers and thus is implicated in tumorigenesis [31]. The *c-FLIP* gene is expressed in two forms of protein: c-$FLIP_S$ which has two death effector domains and c-$FLIP_L$ which contains two death effector domains and a caspase-8-like domain that lack caspase-8 catalytic activity [31]. Through the interaction of the death effector domains, FADD recruits c-$FLIP_L$ and c-$FLIP_S$ and caspase-8 to the DISC, where c-$FLIP_L$ and c-$FLIP_S$ interact with caspase-8 and inhibit its cleavage in human glioma and melanoma cells [29, 30]. Here, we show that both c-$FLIP_L$ and c-$FLIP_S$ are highly expressed in TRAIL-resistant as compared with TRAIL-sensitive pancreatic cancer cells. Transfection

of c-FLIP$_L$ and c-FLIP$_S$ in the TRAIL-sensitive cells results in TRAIL resistance, whereas shRNA knockdown of c-FLIP$_L$ and c-FLIP$_S$ eliminates TRAIL resistance. This study is in keeping with a study of non-small cell lung carcinoma cells that found that selective knockdown of c-FLIP$_L$ sensitizes the resistant lung cancer cells to TRAIL [44]. Moreover, this study shows that inhibition of c-FLIP$_L$ and c-FLIP$_S$ facilitates TRAIL-induced caspase-8 cleavage and mitochondrial activation in TRAIL-resistant pancreatic cancer cells. This result indicates that the c-FLIP inhibition of caspase-8 cleavage is the most upstream event in TRAIL resistance in human pancreatic cancer cells.

The high activity of NF-κB in pancreatic cancers has been implicated in pancreatic cancer progression and resistance to therapies and is one of the clinical hallmarks for poor prognosis [23]. Recent studies have shown that NF-κB may contribute to TRAIL resistance through the up-regulation of Bcl-xL [11] and XIAP [13-15] and c-FLIP [45]. Recent studies have further shown that TRAIL activates NF-κB in pancreatic cancer cells [24, 25]. TRAIL-induced activation of NF-κB requires the recruitment of RIP and IKK to the DISC, leading to the phosphorylation of I-κB and activation of NF-κB [27, 28]. Inhibition of either I-κB [15, 25], NF-κB p65 subunit [24] or RIP, as demonstrated in this study, eliminates TRAIL resistance in pancreatic cancer cells. These studies indicate that targeting of the proteins in the NF-κB pathway may provide a therapeutic approach that can overcome TRAIL resistance in pancreatic cancer cells.

3.4. References

1. Morris, K.V., *siRNA-mediated transcriptional gene silencing: the potential mechanism and a possible role in the histone code.* Cell Mol Life Sci, 2005. **62**(24): p. 3057-66.
2. Jemal, A., et al., *Cancer statistics, 2005.* CA Cancer J Clin, 2005. **55**(1): p. 10-30.
3. Mulcahy, M.F., A.O. Wahl, and W. Small, Jr., *The current status of combined radiotherapy and chemotherapy for locally advanced or resected pancreas cancer.* J Natl Compr Canc Netw, 2005. **3**(5): p. 637-42.
4. Smyth, M.J., et al., *Nature's TRAIL--on a path to cancer immunotherapy.* Immunity, 2003. **18**(1): p. 1-6.
5. Ozawa, F., et al., *Effects and expression of TRAIL and its apoptosis-promoting receptors in human pancreatic cancer.* Cancer Lett, 2001. **163**(1): p. 71-81.
6. Matsuzaki, H., et al., *Combination of tumor necrosis factor-related apoptosis-inducing ligand (TRAIL) and actinomycin D induces apoptosis even in TRAIL-resistant human pancreatic cancer cells.* Clin Cancer Res, 2001. **7**(2): p. 407-14.
7. Jacob, D., et al., *Suppressing orthotopic pancreatic tumor growth with a fiber-modified adenovector expressing the TRAIL gene from the human telomerase reverse transcriptase promoter.* Clin Cancer Res, 2004. **10**(10): p. 3535-41.
8. Hylander, B.L., et al., *The anti-tumor effect of Apo2L/TRAIL on patient pancreatic adenocarcinomas grown as xenografts in SCID mice.* J Transl Med, 2005. **3**(1): p. 22.
9. Ibrahim, S.M., et al., *Pancreatic adenocarcinoma cell lines show variable susceptibility to TRAIL-mediated cell death.* Pancreas, 2001. **23**(1): p. 72-9.
10. Jacob, D., et al., *Suppression of pancreatic tumor growth in the liver by systemic administration of the TRAIL gene driven by the hTERT promoter.* Cancer Gene Ther, 2005. **12**(2): p. 109-15.
11. Bai, J., et al., *Predominant Bcl-XL knockdown disables antiapoptotic mechanisms: tumor necrosis factor-related apoptosis-inducing ligand-based triple chemotherapy overcomes chemoresistance in pancreatic cancer cells in vitro.* Cancer Res, 2005. **65**(6): p. 2344-52.
12. Ashkenazi, A. and V.M. Dixit, *Death receptors: signaling and modulation.* Science, 1998. **281**(5381): p. 1305-8.
13. Trauzold, A., et al., *Multiple and synergistic deregulations of apoptosis-controlling genes in pancreatic carcinoma cells.* Br J Cancer, 2003. **89**(9): p. 1714-21.
14. Vogler, M., et al., *Regulation of TRAIL-induced apoptosis by XIAP in pancreatic carcinoma cells.* Oncogene, 2007. **26**(2): p. 248-57.
15. Braeuer, S.J., et al., *Constitutively activated nuclear factor-kappaB, but not induced NF-kappaB, leads to TRAIL resistance by up-regulation of X-linked inhibitor of apoptosis protein in human cancer cells.* Mol Cancer Res, 2006. **4**(10): p. 715-28.
16. Deng, Y., Y. Lin, and X. Wu, *TRAIL-induced apoptosis requires Bax-dependent mitochondrial release of Smac/DIABLO.* Genes Dev, 2002. **16**(1): p. 33-45.

17. Du, C., et al., *Smac, a mitochondrial protein that promotes cytochrome c-dependent caspase activation by eliminating IAP inhibition.* Cell, 2000. **102**(1): p. 33-42.
18. Li, L., et al., *A small molecule Smac mimic potentiates TRAIL- and TNFalpha-mediated cell death.* Science, 2004. **305**(5689): p. 1471-4.
19. Luo, X., et al., *Bid, a Bcl2 interacting protein, mediates cytochrome c release from mitochondria in response to activation of cell surface death receptors.* Cell, 1998. **94**(4): p. 481-90.
20. Li, P., et al., *Cytochrome c and dATP-dependent formation of Apaf-1/caspase-9 complex initiates an apoptotic protease cascade.* Cell, 1997. **91**(4): p. 479-89.
21. Desagher, S. and J.C. Martinou, *Mitochondria as the central control point of apoptosis.* Trends Cell Biol, 2000. **10**(9): p. 369-77.
22. Hinz, S., et al., *Bcl-XL protects pancreatic adenocarcinoma cells against CD95- and TRAIL-receptor-mediated apoptosis.* Oncogene, 2000. **19**(48): p. 5477-86.
23. Slee, E.A., et al., *Ordering the cytochrome c-initiated caspase cascade: hierarchical activation of caspases-2, -3, -6, -7, -8, and -10 in a caspase-9-dependent manner.* J Cell Biol, 1999. **144**(2): p. 281-92.
24. Khanbolooki, S., et al., *Nuclear factor-kappaB maintains TRAIL resistance in human pancreatic cancer cells.* Mol Cancer Ther, 2006. **5**(9): p. 2251-60.
25. Trauzold, A., et al., *CD95 and TRAIL receptor-mediated activation of protein kinase C and NF-kappaB contributes to apoptosis resistance in ductal pancreatic adenocarcinoma cells.* Oncogene, 2001. **20**(31): p. 4258-69.
26. Chaudhary, P.M., et al., *Death receptor 5, a new member of the TNFR family, and DR4 induce FADD-dependent apoptosis and activate the NF-kappaB pathway.* Immunity, 1997. **7**(6): p. 821-30.
27. Lin, Y., et al., *The death domain kinase RIP is essential for TRAIL (Apo2L)-induced activation of IkappaB kinase and c-Jun N-terminal kinase.* Mol Cell Biol, 2000. **20**(18): p. 6638-45.
28. Harper, N., et al., *Modulation of tumor necrosis factor apoptosis-inducing ligand-induced NF-kappa B activation by inhibition of apical caspases.* J Biol Chem, 2001. **276**(37): p. 34743-52.
29. Xiao, C., et al., *Tumor necrosis factor-related apoptosis-inducing ligand-induced death-inducing signaling complex and its modulation by c-FLIP and PED/PEA-15 in glioma cells.* J Biol Chem, 2002. **277**(28): p. 25020-5.
30. Xiao, C., et al., *Inhibition of CaMKII-mediated c-FLIP expression sensitizes malignant melanoma cells to TRAIL-induced apoptosis.* Exp Cell Res, 2005. **304**(1): p. 244-55.
31. Irmler, M., et al., *Inhibition of death receptor signals by cellular FLIP.* Nature, 1997. **388**(6638): p. 190-5.
32. Song, J.H., et al., *Interferon gamma induces neurite outgrowth by up-regulation of p35 neuron-specific cyclin-dependent kinase 5 activator via activation of ERK1/2 pathway.* J Biol Chem, 2005. **280**(13): p. 12896-901.
33. Elbashir, S.M., et al., *Functional anatomy of siRNAs for mediating efficient RNAi in Drosophila melanogaster embryo lysate.* Embo J, 2001. **20**(23): p. 6877-88.
34. Zamore, P.D., et al., *RNAi: double-stranded RNA directs the ATP-dependent cleavage of mRNA at 21 to 23 nucleotide intervals.* Cell, 2000. **101**(1): p. 25-33.

35. Elbashir, S.M., et al., *Duplexes of 21-nucleotide RNAs mediate RNA interference in cultured mammalian cells.* Nature, 2001. **411**(6836): p. 494-8.
36. Elbashir, S.M., W. Lendeckel, and T. Tuschl, *RNA interference is mediated by 21- and 22-nucleotide RNAs.* Genes Dev, 2001. **15**(2): p. 188-200.
37. Hao, C., et al., *Modulation of TRAIL signaling complex.* Vitam Horm, 2004. **67**: p. 81-99.
38. Scaffidi, C., et al., *FLICE is predominantly expressed as two functionally active isoforms, caspase-8/a and caspase-8/b.* J Biol Chem, 1997. **272**(43): p. 26953-8.
39. Medema, J.P., et al., *FLICE is activated by association with the CD95 death-inducing signaling complex (DISC).* Embo J, 1997. **16**(10): p. 2794-804.
40. Liu, X., et al., *DFF, a heterodimeric protein that functions downstream of caspase-3 to trigger DNA fragmentation during apoptosis.* Cell, 1997. **89**(2): p. 175-84.
41. Song, J.H., et al., *Human astrocytes are resistant to Fas ligand and tumor necrosis factor-related apoptosis-induced apoptosis.* J Neurosci, 2006. **26**(12): p. 1-10.
42. Lin, Y., et al., *Cleavage of the death domain kinase RIP by caspase-8 prompts TNF-induced apoptosis.* Genes Dev, 1999. **13**(19): p. 2514-26.
43. Evans, J.D., et al., *Detailed tissue expression of bcl-2, bax, bak and bcl-x in the normal human pancreas and in chronic pancreatitis, ampullary and pancreatic ductal adenocarcinomas.* Pancreatology, 2001. **1**(3): p. 254-62.
44. Sharp, D.A., D.A. Lawrence, and A. Ashkenazi, *Selective Knockdown of the Long Variant of Cellular FLICE Inhibitory Protein Augments Death Receptor-mediated Caspase-8 Activation and Apoptosis.* J Biol Chem, 2005. **280**(19): p. 19401-9.
45. Ravi, R., et al., *Regulation of death receptor expression and TRAIL/Apo2L-induced apoptosis by NF-kappaB.* Nat Cell Biol, 2001. **3**(4): p. 409-16.

Chapter 4:

Targeted Quantitative Mass Spectrometric Identification of Proteins Differentially Expressed between Bax Positive and Bax Deficient Colorectal Cancer Clones

A version of this chapter will be submitted for publication to Journal of Proteome Research

4.0 Introduction

Bax was identified in 1993 as a Bcl-2-interacting protein that promoted apoptosis [1]. As a multi-domain protein, Bax contains three homologous domains (BH1, BH2, and BH3) and consists of a bundle of α-helices. These enable its localization and pore-formation on the membranes of organelles, such as the mitochondrion and endoplasmic reticulum [2-4]. Bax can form homo-dimers with itself or hetero-dimers with other Bcl-2 family proteins through the interaction of the BH3 domain [1, 5]. As a pro-apoptotic protein, Bax plays a crucial role in regulating cell survival and death. Based on data provided by gene ablation studies in mice, Bax deficient mice have been shown to have a developmental neuronal cell death defect [6]. Elevated Bax protein levels have also been found in neurons that undergo cell death during brain ischemia or after excitotoxic lesion with quinolinic acid [7, 8]. In the area of cancer treatment, cells from Bax deficient mice are resistant to various stimuli that kill cells via the mitochondria-dependent pathway, such as X-ray irradiation, DNA damage drugs, and agents inducing ER stress [9]. From a clinical perspective, marked elevations of Bax have been found in astrocytes from patients with HIV-induced encephalitis and in myocardiocytes from patients with myocardial infarctions [10, 11]. Moreover, patients with rhabdomyosarcoma with Bax expressing tumors were reported to have a longer overall survival [12]. During the conventional treatment of chronic lymphocytic leukemia, patients with higher Bax expression have shown better response [13]. High levels of Bax are also predictive of response in patients with chronic myeloid leukemia to imatinib treatment [14]. Consequently, Bax has emerged as a crucial prognosis biomarker and drug discovery target for the treatment of various diseases. However, the mechanisms by which Bax

regulates cell death, the pathways of Bax activation and suppression, and the interactions between Bax and other proteins remain largely unknown.

Up to now, Bax was reported to usually localize in the cytosol and mitochondrion, but translocates to the mitochondrion under most apoptotic stimuli [9, 15]. In mitochondria, Bax regulates mitochondrial membrane potential (MMP) changes and promotes release of apoptogenic proteins, including Cytochrome c, Smac, and Apoptosis inducing factor (AIF), under apoptotic stimuli [16, 17]. However, the mechanism by which Bax regulates MMP changes is still controversial. It has been reported that Bax regulates MMP changes by forming a mitochondrial permeability transition (MPT) pore consisting of voltage-dependent anion channels (VDAC), adenine nucleotide translocase (ANT), and cyclophilin-D (CyP-D) [18, 19]. But the process by which Bax induces MMP changes has also been reported to be independent of the formation of MPT pores [20] and neither VDAC nor ANT are involved in this process [21-23]. An alternative model indicates that Bax along with lipid conspirators can release these apoptotic proteins from mitochondria without MPT pore formation or permanent disruption in the mitochondrial membrane [22, 24]. Moreover, Bax over-expression results in apoptosis in the absence of any stimuli, suggesting that Bax is sequestered by other proteins in the cytosol under normal conditions [25]. However, the binding partners of Bax in the cytosol are still unclear and other proteins that interact with or regulate Bax activation are still highly controversial. In order to gain insight into the relative protein profile differences between Bax positive and deficient clones, a quantitative mass spectrometric approach was used to identify and quantify proteins of interest.

Selective isotopic labeling protocols have been developed for identification and quantification in mass spectrometry experiments. Introduction of an isotopically enriched tag allows discrimination and relative quantification between two samples during an MS survey scan or an MS/MS fragmentation spectrum. Peaks from the same peptide appear in the same MS or MS/MS spectrum, but are separated by the mass difference of the isotope tags and have intensities related to their abundance. Previous work in our laboratory has shown the potential of dimethylation after guanidination (2-MEGA) protocol as a method to determine differentially expressed proteins from complex biological samples [26, 27]. In addition to determining proteins that interact with Bax, we wanted to evaluate the error rate and quantification accuracy of the 2-MEGA protocol. In order to increase confidence in the quantification results, the samples were analyzed twice. Initially, the Bax deficient clone served as the internal reference and was used to interrogate the wild type clone; in the second experiment the wild type clone was the internal reference and was compared against the Bax deficient clone. The internal reference was labeled using the light isotopic reagent, while the sample was labeled with the heavy isotopic reagent. When the same peptide was identified in both experiments, it was expected that the ratio between the heavy and light labeled peaks would be significantly greater than one in one system and significantly less than one in the complementary system. This two-sided study design has the potential to minimize errors from chemical noise which artificially increases the signal from one observed peak. If a quick comparison of the ratios reveals the same skewed value from both experiments, there is an overlapping peak and that candidate can be removed.

For this study, liquid chromatography matrix-assisted laser desorption ionization mass spectrometry (LC-MALDI MS) was used as an alternative to liquid chromatography electrospray ionization mass spectrometry (LC-ESI MS). By fractionating onto a MALDI plate, the data analysis and sample acquisition steps are decoupled. After a series of MS survey scans is performed, data analysis is used to identify peptides with matching characteristics, such as m/z ratio, chromatographic behavior, and relative expression level. After comparing neighboring fractions, MS/MS analysis was performed on selected peaks at a later time. Selection of reproducible candidates based on chromatographic conditions and confirmation of differential expression prior to MS/MS analysis may facilitate selection of lower abundance peaks in MS spectra. Other previous reports have shown the benefits of using LC-MALDI MS for "directed" quantitative analysis [28].

Taken together, we chose the Bax+/- and Bax-/- HCT 116 clones as the research model and used targeted-quantitative mass spectrometry to examine the differentially expressed protein profile between the two clones. By analyzing this profile, we drew a cellular signaling map for Bax interactions with other proteins to provide clues to the molecular basis by which Bax regulates apoptosis and a powerful reference list of Bax-interacting proteins for the further research.

4.1. Materials and methods

4.1.1. Materials and antibodies

Recombinant soluble human TRAIL (amino acids 114–281) was purchased from PeproTech, Inc. (Rocky Hill, USA). The mouse antibodies used included: anti-caspase-8 (MBL, Nagoya, Japan), anti-VDAC-1, anti-VDAC-2, anti-HSP70, anti-HSP90β (Santa Cruz Biotechnology), anti-MRP1 (StessGen), and anti-cytochrome c (BD Bioscience). The rabbit antibodies used included anti-caspase-9 (Cell Signal), anti-caspase-3, anti-HSP90α (StressGen), anti-MIF, and anti-14-3-3 theta (Santa Cruz Biotechnology). The goat antibodies included anti-HSP60 (StessGen), anti-peroxiredoxin, and anti-LRP130 (Santa Cruz Biotechnology). Horseradish peroxidase conjugated goat anti-mouse, donkey anti-goat, and goat anti-rabbit antibodies were from Jackson IR Labs (West Grove, USA). LC-MS grade water, acetonitrile, and methanol were purchased from Fisher Scientific. LC-MS grade trifluoroacetic acid was purchased from Fluka. Isotopically enriched formaldehyde ($^{13}CD_2O$) was purchased from Cambridge Isotope Laboratories (Andover, MA). Sequencing grade modified trypsin was purchased from Promega (Madison, WI). MG132 was purchased from Calbiochem (Darmstadt, German). All other chemicals used were of analytical grade and purchased from Sigma-Aldrich, unless otherwise indicated.

4.1.2. Cell cultures, cell viability and apoptosis assay

The human HCT116 Bax+/- and Bax-/- clones were cultured in McCoy 5α medium (Invitrogen) supplemented with 10% FBS, and 1% antibiotics. For cell viability assay, the HCT116 Bax+/- and Bax-/- cells were collected by centrifugation (300 *g* for 5 min) and the pellet was resuspended in culture medium. The monolayered cells ($2x10^4$ cells/100 μL) were replanted in each well of 96-well plate and cultured overnight and then treated with different doses of TRAIL. After incubation, cells were washed once

with 100 μL PBS. Cell death was determined by an acid phosphatase assay. Briefly, 100 μL buffer containing 0.2 M sodium acetate (pH 5.5), 0.2 % (v/v) Triton X-100 and 20 mM *p*-nitrophenyl phosphate were added to each well. The plates were placed in a water-jacketed incubator at 37 °C for 2 h. The reaction was stopped by the addition of 10 μL 1M NaOH to each well and the color developed was measured at 405 nm, using a microplate reader (Bio-Rad).

4.1.3. Western blot analysis

Cells in culture were harvested and lysed in 20 mM Tris-HCl (pH 7.4) containing 150 mM NaCl, 2 mM EDTA, 10% glycerol, 1% Triton X-100, 1 mM phenylmethylsulfonyl fluoride, and protease inhibitor cocktail (Sigma). The lysed cells were centrifuged at 20 000 *g* for 15 min and the supernatant was collected. Protein concentrations in the supernatant were determined by the BCA assay following the manufacturer's protocol (Bio-Rad). Equal amounts of protein were separated on SDS-PAGE gels, transferred onto Immunoblot membranes (Bio-Rad) and detected with enhanced chemiluminescence (ECL) reagents (Amersham Biosciences, Piscataway, USA).

4.1.4. Targeted LC-MALDI-MSMS analysis with 2-MEGA labeling

4.1.4.1. Cell Lysis and Protein Digestion

Cells were lysed using a French press at 35 000 psi with two passes into PBS. Proteins were precipitated by adding four parts acetone (v/v) and chilled overnight at -80

°C. Samples were centrifuged at 3 900 *g* for 60 minutes at 4°C. The supernatant was removed and discarded. Protein pellets (~7 mg) were solubilized using 1% SDS before dilution to 0.1% SDS. Ammonium bicarbonate was added to a final concentration of 100 mM, followed by addition of dithiothreitol and iodoacetamide to reduce and carbamidomethylate cysteines and digestion by trypsin in a 1:30 (w/w) ratio.

4.1.4.2. Desalting

Samples were desalted and quantitated using reversed-phase liquid chromatography using 0.1% TFA and 4% acetonitrile in water as solvent A and 0.1% TFA in acetonitrile as solvent B. The following gradient program was used (time in mins., % B): 0.00, 0%; 5.00, 0%; 5.01, 90%; 10.00, 90%; 15.00, 0%; 25.00, 0 % B. The flow rate used was 1.0 mL/min using a 4.6 mm i.d. x 50 mm C_{18} 3μm particle size column (Varian). Samples were quantitated by using their absorbance at 280 nm.

4.1.4.3. 2-MEGA Isotopic Labelling

Peptides were labeled using the 2-MEGA labeling method [26, 27]. In brief, samples were adjusted to pH 11 using 2M NaOH and 6M O-methylisourea was added. Samples were heated to 65 °C for 25 minutes to guanidinate the lysines. The pH of the solution was adjusted with 10% TFA to approximately pH 7. Formaldehyde (4%, v/v) and sodium cyanoborohydride (1M) were added to dimethylate the N-termini. Light chain labeling was performed using a 4% formaldehyde solution prepared by dilution of 37% formaldehyde. Heavy chain labeling was performed using a 4% formaldehyde solution prepared from $^{13}CD_2O$. Samples were then desalted and quantitated as described

previously. Post-quantitation, heavy chain labeled Bax +/- was mixed with light chain labeled Bax -/- (A_HB_L) in a 1:1 ratio based on the total peptide content by weight. Similarly, light chain labeled Bax +/- was mixed with heavy chain labeled Bax -/- (A_LB_H).

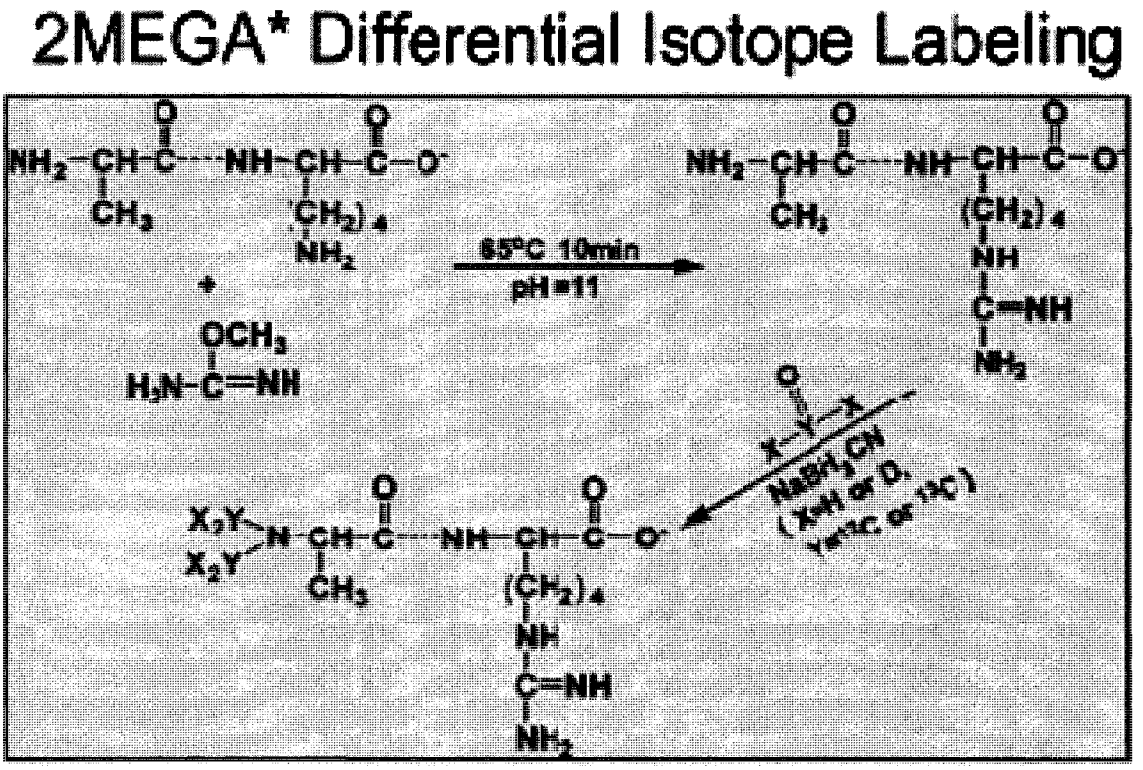

Fig 4.1 The guanidination reaction selectively modifies the lysines. The N-terminus of the resulting peptide is isotopically labeled with either d(0),^{12}C-formaldehyde (+28 Da) or d(2),^{13}C-formaldehyde (+34 Da). (Reproduced from Chengjie Ji, Journal of Proteome Research 2005, 4, 2099-2108

4.1.4.4. Strong Cation Exchange Chromatography

Labelled peptide mixtures were separated by strong cation exchange chromatography using 50 mM KH_2PO_4 (pH 2.8) as solvent A and 1M KCl in 50mM KH_2PO_4 (pH 2.8) as solvent B. The following gradient program was used (time in mins., % B): 0, 0%; 7, 0%; 8, 3%; 36, 14%; 44, 20 %; 49, 30%; 53, 50%; 58, 50 %; 60, 0%; 70, 0%. Fractions were collected for one minute from 17 to 71 minutes, then desalted and quantitated using the previously described method. Fractions were pooled together to form ~10 μg samples.

4.1.4.5. Online LC-MALDI MS

Fractions were separated and analyzed by LC-MALDI MS using a homemade LC-MALDI interface. Approximately 10 μg was separated on a 1.0 mm i.d. x 150 mm C_8 column and directly spotted online to a homemade 400-well MALDI plate. 0.1% TFA with 4% ACN in water was used as solvent A and 0.1% TFA in ACN was used as solvent B. The following gradient program was used (time in mins., % B): 0, 0%; 19, 0 %; 20, 5%; 145, 30%; 156, 40%; 175, 45%; 180, 0%; 185, 0%. 20 s fractions were collected from 40 to 174 minutes. MALDI wells were spotted with 0.6 μL of 0.6 μg/μL 2,5-dihydroxybenzoic acid solution in 50:50 methanol/water and allowed to dry. In using similar chromatographic behavior and mass-to-charge ratio as parameters to identify reproducibly differentially expressed peptides, consistent experimental conditions were necessary. HPLC mobile phases were prepared in large-scale batches and stored at 4 °C over the duration of the study period. Corresponding pooled SCX fractions were run on

the LC-MALDI on consecutive days in order to account for variations in the mobile phase over time.

4.1.4.6. MS Analysis and Targeted MS/MS Analysis

MS spectra were taken with an Applied Biosystems/MDS Sciex QSTAR XL. MS spectra were analyzed to determine peaks with a minimum signal-to-noise ratio of eight using ProTSData software. Peaks were further classified as pairs if a second peak was found with a mass difference of 6.032 ± 0.10 Da, corresponding to the difference in mass of the light and heavy chain labeling. Pairs with a relative difference greater than 1.50 or less than 0.67 were placed into a 'pairs reference list'. Unpaired peaks with a signal-to-noise ratio greater than 15 were placed into a 'peaks reference list'. As different pooled fractions were run, the reference lists were matched against one another to identify peaks found under similar chromatographic conditions (±3 min in RPLC retention time, ±2 SCX fractions, and ±0.2 Da in m/z ratio). If a pair was found in both reference lists within the reference criteria it was selected for targeted MS/MS analysis. The analysis of the unpaired peaks was performed in the same way, requiring the same chromatographic conditions and the presence of an unpaired peak with mass difference ± (6.023 ± 0.2 Da) in the complementary system.

4.1.4.7. MASCOT Database Search and Data Analysis

Candidate pairs and peaks were run using automated MS/MS via an inclusion list. Spectral data were searched using MASCOT with the following parameters: taxonomy: *Homo sapiens* (human); enzyme: trypsin; missed cleavages: 2; fixed modifications:

guanidination (K) and carbamidomethylation (C); MS tolerance: 0.2 Da; MS/MS tolerance: 0.1 Da. Additional parameters included a modified ESI-QUAD-TOF ion fragmentation series that permitted a-type ions. Data were searched twice; first selecting the light isotope modification (+C_2H_4, +28.0313 Da, N-term) and then selecting the heavy isotope modification (+$^{13}C_2D_4$, +34.0631 Da, N-term) to identify peaks with either labeling chain.

Peptide and protein identification data was extracted from the MASCOT files using homemade software (ProteinExtractor). Relative ratios for the identified peptide pairs were taken from the ProTSData output. In cases where the peptide eluted over multiple reversed-phase fractions, the fraction containing the highest intensity of the peptide peak was used. When a peak identified did not have a pair, its relative ratio was taken as its signal-to-noise ratio divided by eight (the maximum signal-to-noise ratio possible for the unobserved peak).

4.1.4.8. Protein-Protein Interaction Networks Analysis Using Human Interactome Map (HiMAP) and Metacore

HiMAP and Metacore were used to map the differentially expressed proteins into biological networks. Differentially expressed proteins were converted into appropriate gene symbols and uploaded into both HiMAP and Metacore for analysis. The protein-protein interaction analysis was based on literature-confirmed interactions from the Human Protein Reference Database, yeast-two-hybrid-defined interactions, and predicted interactions generated by a Bayesian Analysis. For network analysis, two algorithms were used: 1) the sparse interaction algorithm to map direct protein-protein interactions

among differentially expressed proteins; 2) the bridge interaction algorithm to map shortest path for interaction.

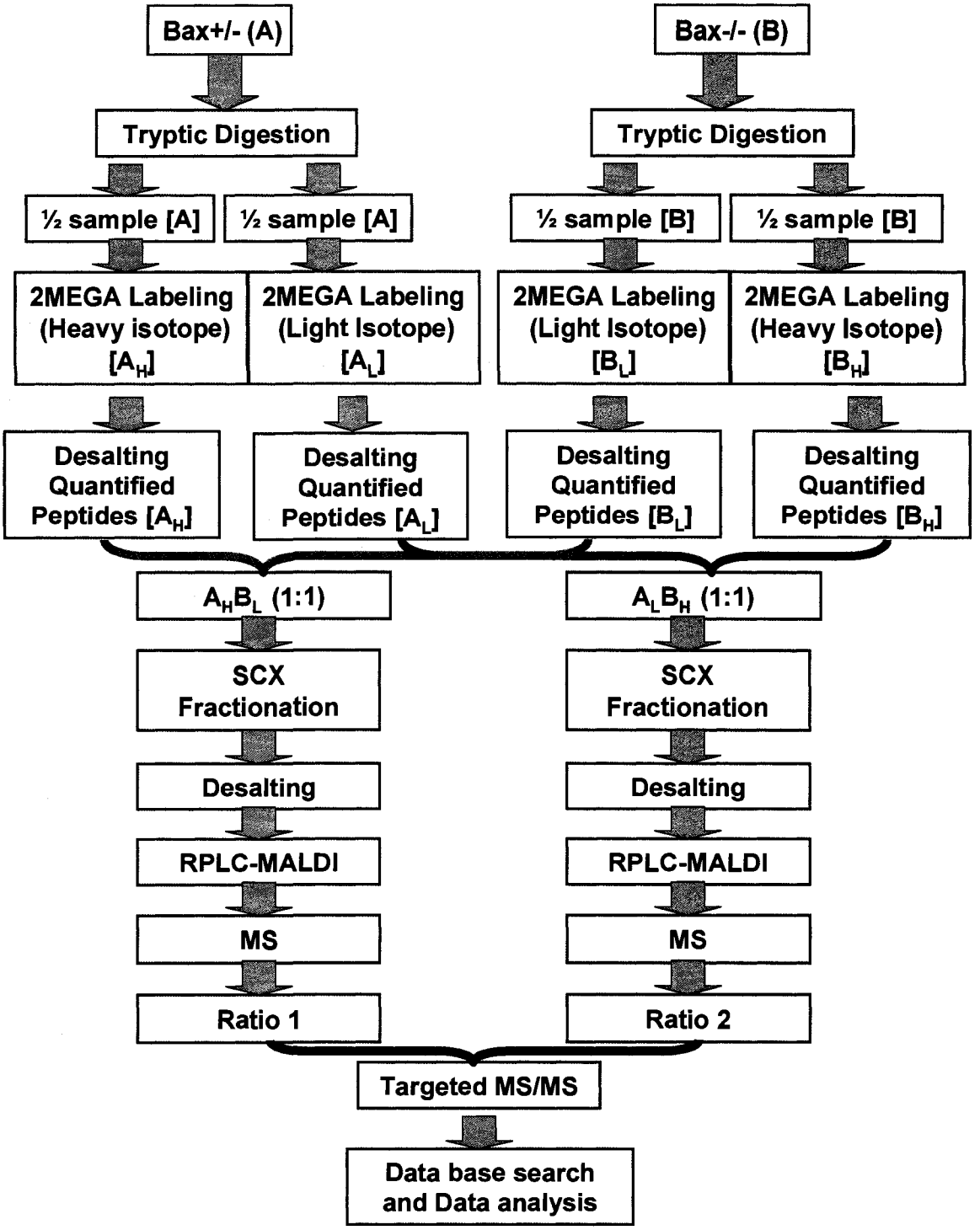
Bax+/- (A)
Bax-/- (B)
Tryptic Digestion
Tryptic Digestion
½ sample [A]
½ sample [A]
½ sample [B]
½ sample [B]
2MEGA Labeling (Heavy isotope) [A_H]
2MEGA Labeling (Light Isotope) [A_L]
2MEGA Labeling (Light Isotope) [B_L]
2MEGA Labeling (Heavy Isotope) [B_H]
Desalting Quantified Peptides [A_H]
Desalting Quantified Peptides [A_L]
Desalting Quantified Peptides [B_L]
Desalting Quantified Peptides [B_H]
A_HB_L (1:1)
A_LB_H (1:1)
SCX Fractionation
SCX Fractionation
Desalting
Desalting
RPLC-MALDI
RPLC-MALDI
MS
MS
Ratio 1
Ratio 2
Targeted MS/MS
Data base search and Data analysis

Figure 4.2. **Workflow of the 2-mega labeling quantitative mass spectrometry analysis.**
HCT116 Bax+/- (A) and Bax-/- (B) were separately lysed, digested with modified trypsin, and chemically labeled with heavy chain (H) and light chain (L) isotopic labels. After desalting all four samples, A_HB_L and A_LB_H were mixed in a 1:1 ratio followed by SCX separation. Pooled SCX fractions were analyzed with LC-MALDI MS and peaks were analyzed to determine matching results based on three parameters (m/z ratio, SCX retention time, RPLC retention time) to determine the MS/MS identification target lists. Automated MS/MS analyses were run on the candidates, followed by a MASCOT database search to identify differentially expressed proteins

4.2 Results

4.2.1. Bax plays a crucial role in TRAIL-induced apoptosis pathway.

The Bax-regulated mitochondria associated apoptotic pathway is involved in multi-stimuli induced cell death including traditional chemotherapeutic drugs, radiation, and death ligands. Here, we use TRAIL-induced apoptosis as an example. HCT116 colon cancer cell line and its Bax-/- clone were treated with TRAIL in a dose dependent manner with cell viability studies demonstrating that TRAIL killed the HCT116 cell line but not the Bax deficient clone (Fig 4.3.A). Contrast microscope images show that TRAIL induced a great portion of the apoptotic bodies formation in the wild type (Wt) HCT116 clone but not in the Bax-/- clone (Fig 4.3.B). Western blots show cleavage of caspase-8 and its downstream targets caspase-9 and caspase-3 in the Wt HCT116 cell line. In contrast, only cleavage of caspase-8, but not caspase-9 and caspase-3, was detected in the Bax-/- clone (Fig 4.3.C). This result demonstrates that TRAIL-induced apoptosis is inhibited in the Bax-/- cells and that Bax plays a crucial role in the TRAIL-induced apoptosis pathway. Furthermore, Bax-regulation of apoptosis occurs downstream of caspase-8 at the mitochondrial level. Here, using the TRAIL-induced apoptosis model, we show that Bax is the crucial regulator in the mitochondria-associated apoptosis pathway. Moreover, to further explore the Bax-mediated apoptosis signal network by using targeted MS/MS analyses; we first validated the targeted MS/MS method through standard analysis.

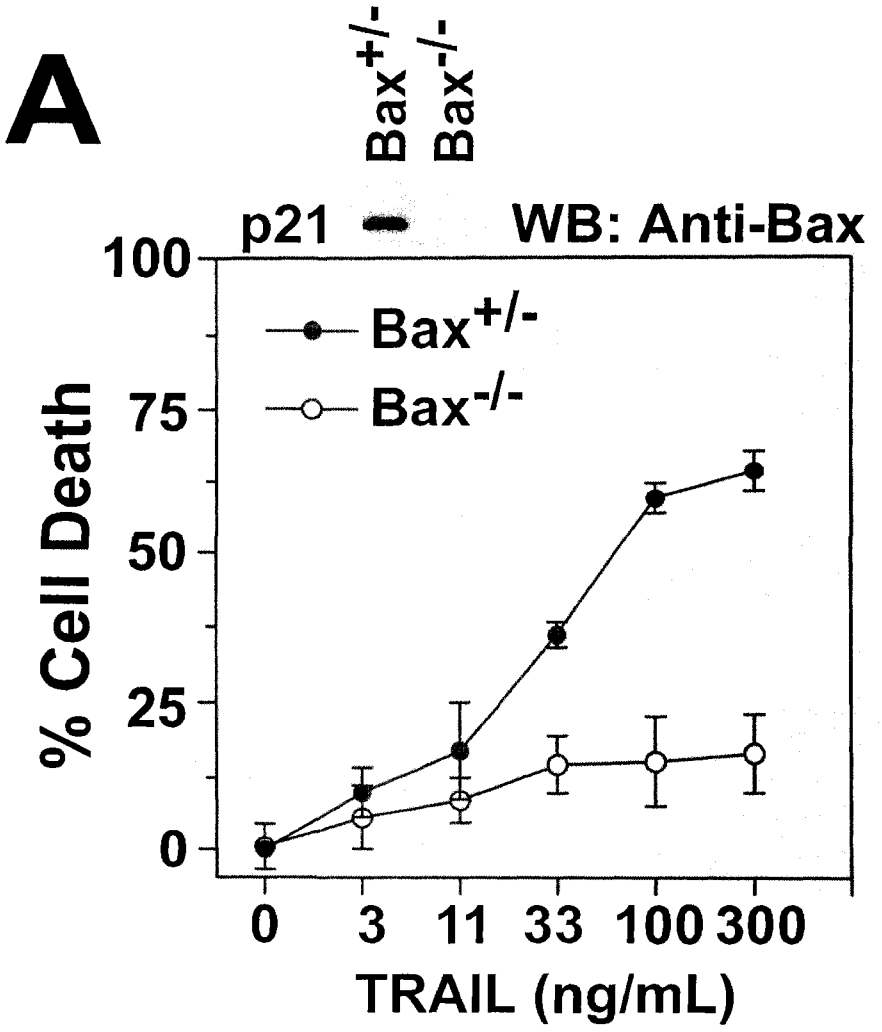

Fig 4.3 TRAIL-induced apoptosis in Bax+/- and Bax-/- cells. (A) Bax plays a crucial role in the TRAIL-induced apoptosis pathway. HCT 116 Bax+/- and Bax-/- cells were analyzed via Western blotting for Bax expression levels, and treated with recombinant TRAIL for 24 h in the doses indicated and subjected to cell viability analysis.

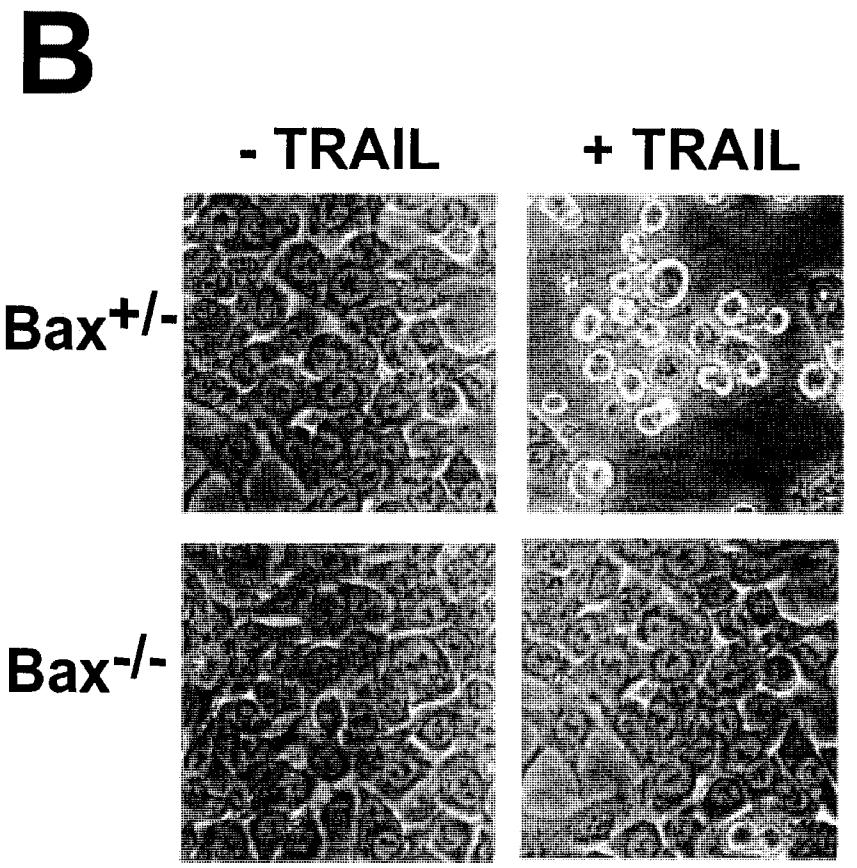

Fig 4.3 (B) Bax+/- and Bax-/- HCT 116 clones were treated with 100 ng/mL TRAIL for 4 hours for microsope imaging and the detection of apoptotic bodies.

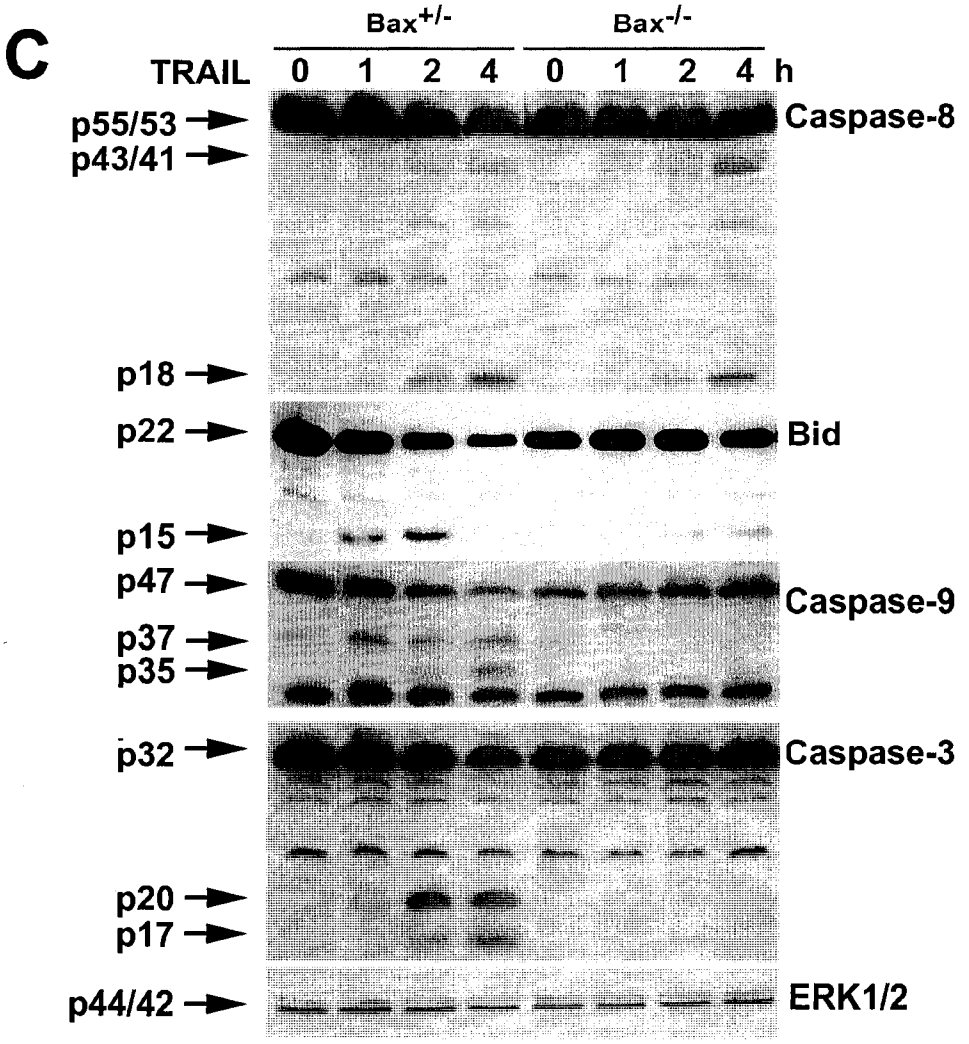

Fig 4.3 (C) Bax+/- and Bax-/- clones were treated with 100 ng/mL TRAIL for the times as indicated for Western blot analysis of the cleavage of caspase-8, caspase-9, Bid, and Caspase-3 with ERK1/2 as the loading control.

4.2.2. Method Validation of Quantitative MS Analysis using 2-MEGA

To qualify the 2-MEGA labeling for quantification, a 1:1 mixture of cytochrome c and myoglobin was used as a test system to evaluate the confidence intervals for this study. The protein solution was digested with trypsin and half of the sample was labeled with the light chain modification and the other half with the heavy chain modification. The samples were desalted, quantified, and mixed in a light:heavy ratio of 2:1 and 1:2 to determine the experimental values. There are totally 20 peptides (12 from cytochrome c, and 8 from myoglobin) were identified. Ratios of 2.00 and 0.51 were observed in the two systems with an average coefficient of variation (CV) of 0.25. Based on the above results of the determined CV, the threshold for differential expression in our quantification experiment system was set at 1.50-fold, which represents two standard deviations and 95% confidence in differential expression, assuming normality with the random error.

4.2.3. Quantitative Mass Spectrometry Analysis using 2-MEGA

HCT116 colon cancer cells and the Bax-/- cells were completely lysed by passage through a French press at high pressure and proteins were extracted by precipitating pellets with acetone, before re-solubilization with SDS. Samples were carbamidomethylated, digested with trypsin, and then simultaneously quantified and desalted. Both Bax+/- and Bax -/- digests were divided into halves and labeled using the 2-MEGA protocol. Reaction with O-methylisourea at alkaline pH converted the ε–amino side-chain of lysines into guanidino functionalities, introducing a +42.0218 Da modification. Subsequent dimethylation of the N-terminus of the peptides produced a +28.0313 Da modification with regular formaldehyde (CH_2O) and a +34.0631 Da

modification when isotopically enriched formaldehyde ($^{13}CD_2O$) was used. If the same peptide was present in both samples, it would be identified in the MS scan as a pair of peaks with a mass difference of 6.032 Da. If the peptide was only present in one of the two samples, a single, unpaired peak would be observed. Identification of the peptide using MS/MS determined which modification was present on its N-terminus and therefore which sample it was originally from. All of the labeled digests were quantified and desalted to facilitate accurate 1:1 mixing. The Bax +/- heavy chain samples were mixed with the Bax -/- light chain samples and *vice versa*. Peptide mixtures were separated by SCX chromatography, desalted, quantified, and pooled. Pooled fractions were separated onto a homemade 400 well MALDI plate using an online LC-MALDI interface, followed by an MS survey scan [29].

4.2.4. MS and MS/MS Analysis

Pairs with relative ratios greater than 1.50 or less than 0.67 were selected for inclusion onto a reference list. Peaks with S/N ratio greater than 15 were also placed onto an inclusion list for comparison against other peaks from the corresponding system. As pooled fractions were run, the reference lists for the pairs were compared against one another to determine differentially expressed peptides in both labeling systems. The conditions for a "matched" peptide pair were based on typically observed limits for reproducibility in our laboratory (±3 mins in RPLC retention time, ± 2 SCX fractions, and ±0.2 Da in mass). Identified pairs were then analyzed by MALDI MS/MS. The peak reference lists were analyzed in a similar fashion using the same chromatographic retention conditions, but with the requirement that the mass-to-charge ratio of the second

peak was ± (6.023 ± 0.100) Da. Since a heavy chain labeled peptide found in one system would be found as a light-chain labeled peptide in the complementary system, this m/z restriction was used to increase confidence in the peak matches. The peaks were analyzed automatically by MALDI MS/MS via use of an inclusion list. Identified peptides from MASCOT were combined with quantification data from ProTSData to determine quantification values. From the list of identified peptides, the minimal list of protein accounting for all of the identified peptides was generated. Ratios for identified peaks were calculated by dividing the peak's signal-to-noise ratio by eight, the maximum height possible for the absent paired peak.

4.2.5. Quantitation and Identification Analysis

Overlaid MS spectra identified as HELQANCYEEVK from cofilin-1 in the A_LB_H and A_HB_L systems are shown in Fig 4.4.A. The figure shows the relative ratio observed in the A_HB_L system (Light/Heavy = 2.65) and the corresponding change in the complementary A_LB_H system (Light/Heavy = 0.48). In both cases, the Bax -/- clone (the "B" portion of the systems) shows relative over-expression by approximately 2.4-fold in both systems. The MS/MS spectra for identification of heavy-chain labeled HELQANCYEEVK are shown in Fig 4.4.B. Moreover, overlaid MS spectra identified as ISSIQSIVPALEIANAHR from HSP60 are shown in Fig 4.4.C and 4.4.D. Consistent ratios between the A_HB_L system (0.23) and A_LB_H system (2.33) were observed which indicated the down-regulation of HSP60 in the Bax-/- clone.

The figure highlights the advantages of using MALDI instead of electrospray in the study design. While peptide ISSIQSIVPALEIANAHR was found in the same SCX

fraction, it was found in two slightly different reversed-phase fractions; conversely, the peptide, HELQANCYEEVK, while present in the same reversed-phase fraction, was found in neighboring SCX fractions. Overlaying the MS survey scans for these identified peaks shows the expected reversed ratios between the light and heavy isotope labeled samples in the complementary systems. By fractioning onto MALDI plates, samples are "stored" on plates while the data analysis can be performed to find peptides that may vary slightly in their m/z ratio or chromatographic behavior, but are similar enough to be considered matches. In contrast, samples run with electrospray ionization are consumed during analysis, so identifying candidates subject to the same parameters would require re-running the same sample several times.

Since the mass-to-charge ratio difference and chromatographic behaviors of matched pairs were sufficiently stringent conditions, peptide pairs were considered identified if any of the four constituent peaks were identified. Approximately 69% (123 out of 179) of peptides identified from the pairs data were identified by at least two MS/MS scans scoring above the identity threshold. While most pairs showed qualitatively correct ratios (increasing in one system and decreasing in the complement), four pairs were found with the same direction in both systems. Two of the pairs were found to be overlapping with other peaks and were discarded after manual data analysis. There was no clear rationale for why the other two pairs were incorrect and are likely due to random error or chemical noise. When comparing across both runs, 84% of the peptide pairs (150 out of 179) had relative errors of less than 50%, with the average relative error for all pairs peptides being 28%.

Similarly to the pairs, the single peaks were considered positively identified if either matched peak was found to score above identity. After manual data checking, twelve peptides scoring above the identity threshold from the peaks data were found to be from misidentified pairs and were discarded. This is likely due to an error with the software used to determine the peaks and pairs which occasionally included observed peaks as both a pair and an unpaired peak. Of the remaining positively identified 133 peptides, 85 (64%) were identified in only one system with 48 (36%) positively identified in both systems. While the majority of the peak values are within a 50% relative error of each other (94 out of 133; 71%), the average relative error is larger than with the pairs (38% vs. 28%). There is also a larger percentage of peptides with a relative error greater than 50% in the peaks versus the pairs (29% vs. 17%). A total of 312 unique peptides were identified from the pairs and peaks data to generate a list of 199 unique differentially labeled proteins categorized by various protein functions. (Supplementary Table 1).

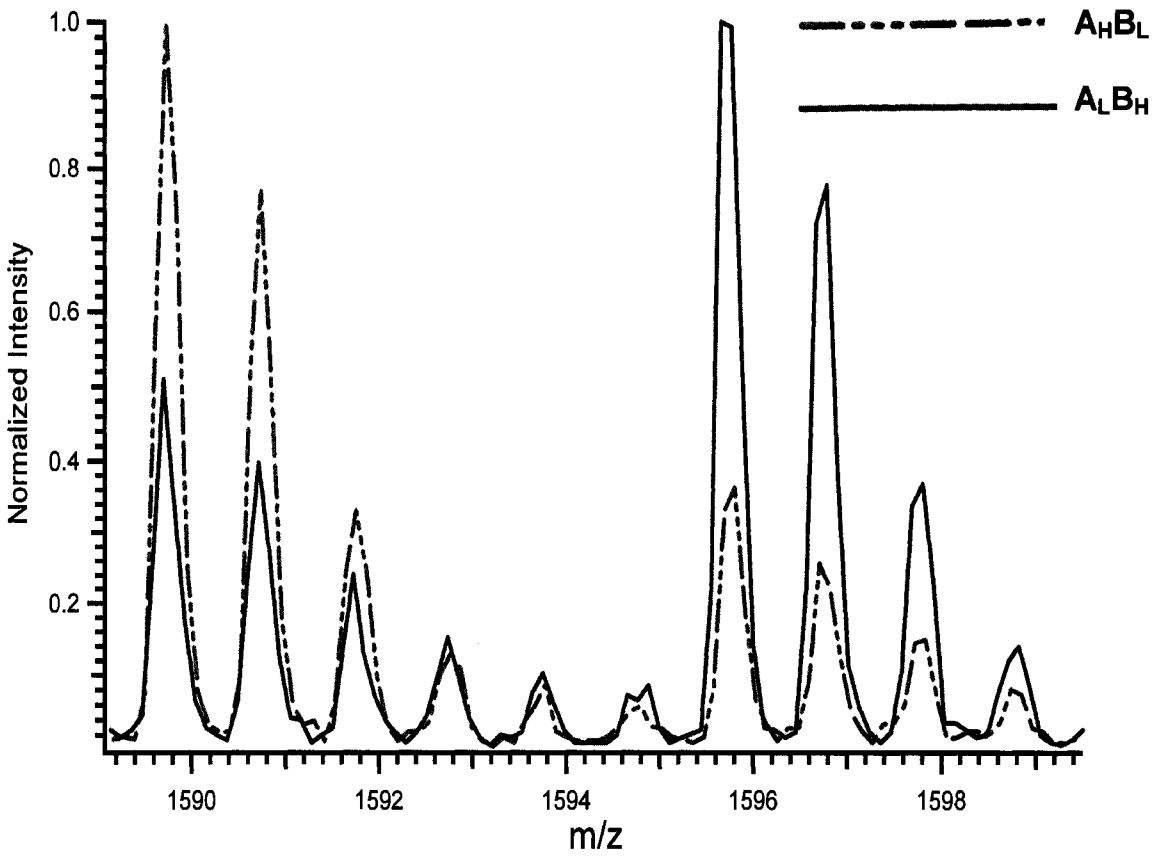

Fig 4.4 (A) Overlaid MS spectra of light chain (1589.7 Da) and heavy chain (1595.7 Da) HELQANCYEEVK from cofilin 1. The paired peaks show the expected 6.023 Da mass difference from the light and heavy chain peaks. Consistent ratios between the A_HB_L and A_LB_H systems (A_HB_L: 2.65 and A_LB_H 0.48) were found, indicating the up-regulation of cofilin 1 in the Bax -/- clone.

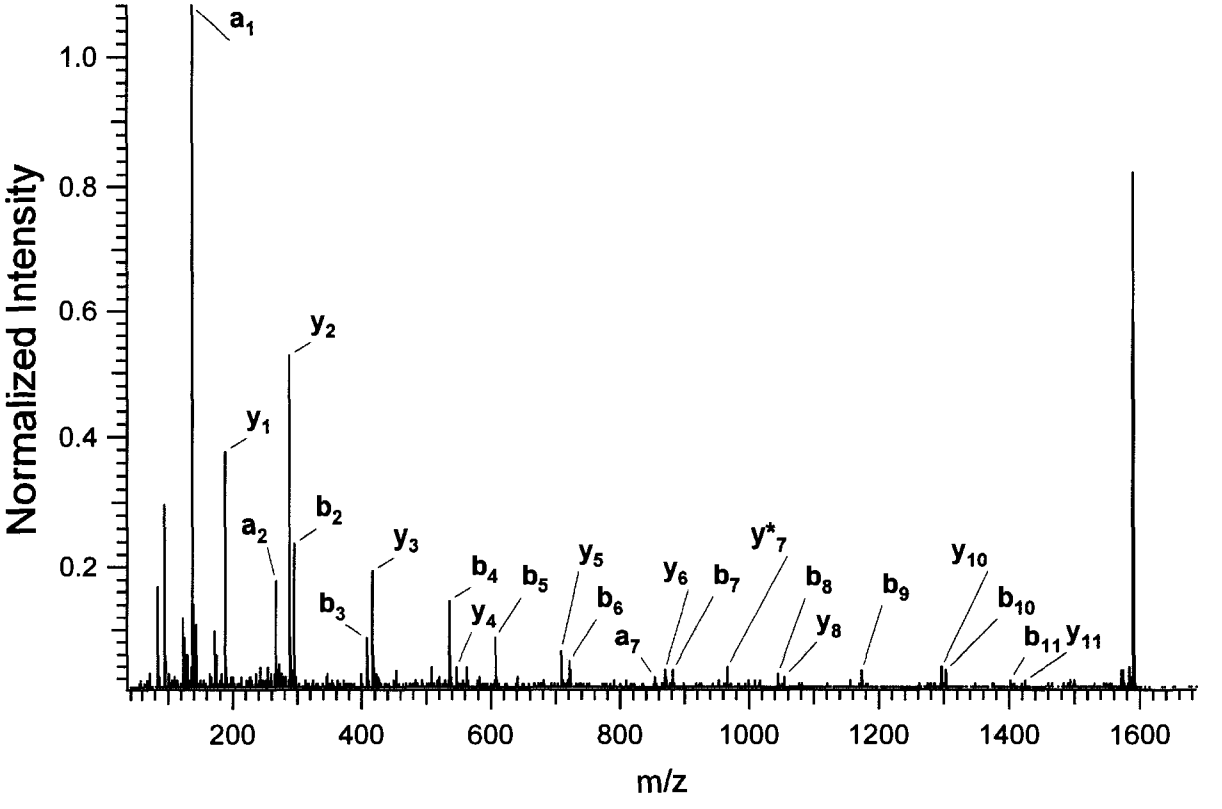

Fig 4.4 (B) (B) MS/MS spectra of heavy chain HELQANCYEEVK is shown.

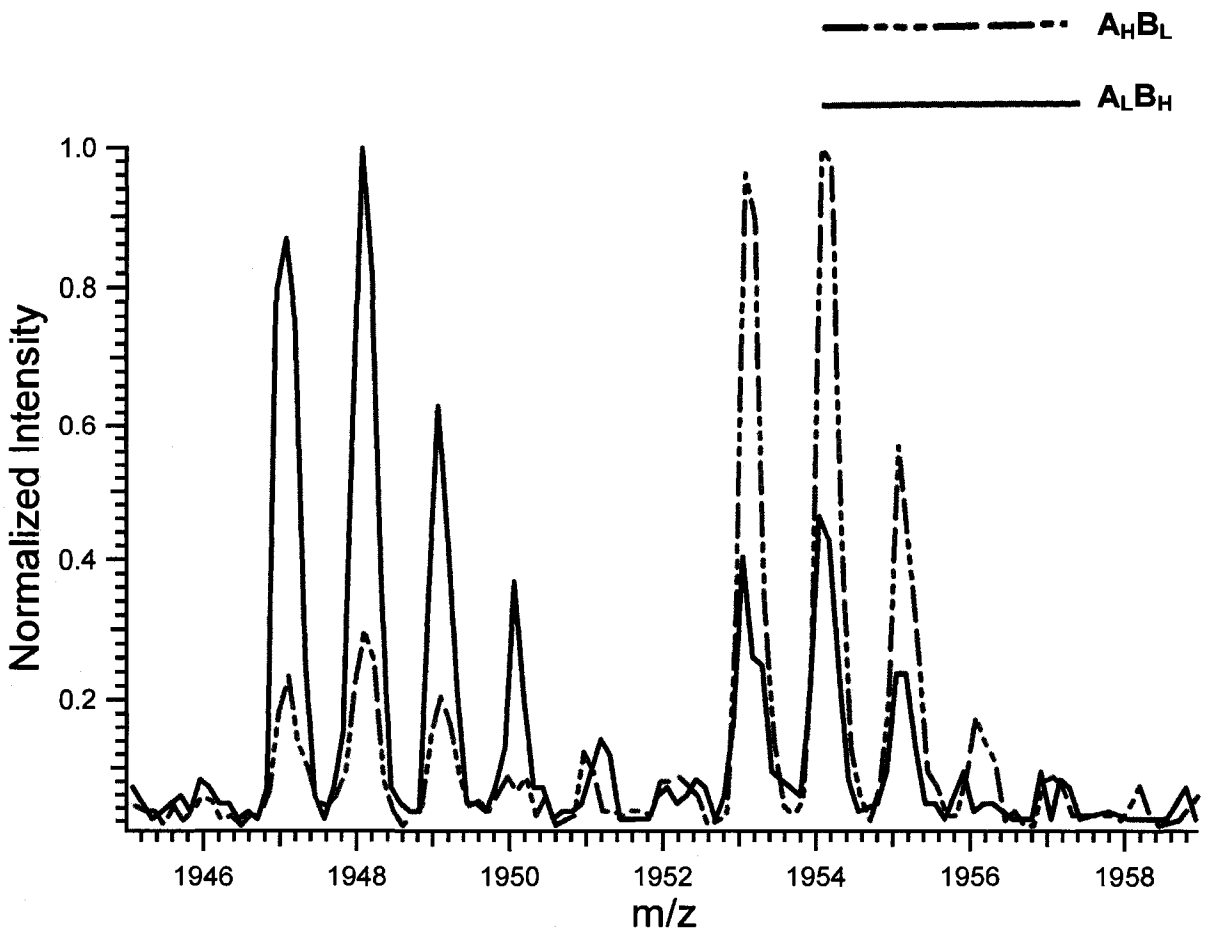

Fig 4.4 (C) Overlaid MS spectra of light chain (1947.1 Da) and heavy chain (1953.1 Da) from HSP60 with the characteristic 6.023 Da difference. Consistent ratios between the A_HB_L system (0.23) and A_LB_H system (2.33) were found, indicating down-regulation of HSP60 in the Bax -/- clone.

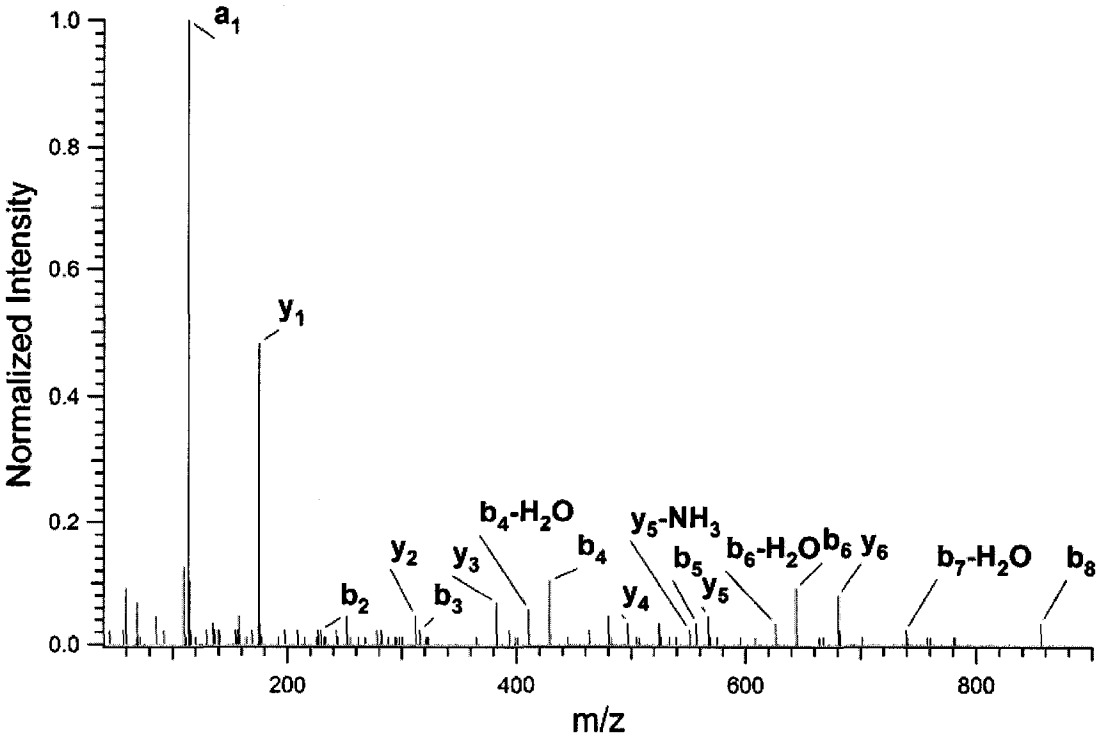

Fig 4.4 (D) MS/MS spectrum of the heavy chain ISSIQSIVPALEIANAHR from HSP60 is shown.

4.2.6. Analysis of interaction network of proteins differentially expressed between WT and Bax-/- HCT 116 clones using HiMAP

To explore possible interactions among differentially expressed proteins identified by 2-MEGA labeling and the targeted MS approach, these 199 proteins were analyzed by searching literature and the Swiss-Prot database for various protein functions and protein-protein interactions. Among these proteins, 57 differentially expressed proteins involved in the processes of apoptosis, cell cycle regulation, DNA repair, stress regulation, detoxification, drug resistance, protein modification, and cellular signaling were selected to be analyzed with HiMAP and Metacore [30] (Table 1). Thirty of these proteins were connected using the sparse interaction algorithm, which connects proteins based on direct known or predicted interactions (Fig 4.5.A). Using the bridge path algorithm, which allows intermediary proteins to map short paths of interaction, 46 of the 57 differentially expressed proteins of these proteins were brought together in the network (Fig 4.5.B). Among these proteins, four groups of valuable proteins, including MPT channel proteins, heat shock proteins, Bax-regulator proteins, and oxidative stress triggered proteins, were found differentially expressed between Bax+/- and Bax-/- clones (Table 2). These data indicate that Bax functions not only as an apoptotic signal executor by modulating the damage of mitochondria membrane potential, but also as a regulator for different cellular networks which affect the expression level of other proteins.

Table1

	Protein Name	Swiss-Prot Name	Swiss-Prot ID	Peptide Sequence	Subcellular Location	Function	Ratio1	Ratio2	Regulation
1	Voltage-dependent anion-selective channel protein 2	VDAC2	P45880	GFGFGLVK	Mitochondrion outer membrane	Voltage-gated anion channel porin activity	5.52	2.56	Down
2	Voltage-dependent anion-selective channel protein 1	VDAC1	P21796	VTQSNFAVGYK	Mitochondrion outer membrane	Apoptogenic cytochrome c release channel	2.26	1.90	Down
				FGIAAK			1.85	2.20	
				GYGFGLIK			2.04	3.36	
3	Cytochrome c.	CYC	P99999	TGPNLHGLFGR	Mitochondrion matrix	DNA fragmentation during apoptosis	5.59	1.67	Down
4	Ubiquinol-cytochrome c reductase complex	UCRQ	O14949	AYPHVFTK	Mitochondrion inner membrane	Ubiquinol-cytochrome-c reductase activity	3.22	3.84	Down
5	14-3-3 protein theta	1433T	P27348	VFYLK	Cytoplasm	Protein binding	9.48	1.66	Down
				DSTLIMQLLR			4.54	6.71	
6	Leucine-rich PPR motif-containing protein 130	LPPRC	P42704	AFAETHIK	Mitochondrion, nucleus, nucleoplasm	Single-stranded DNA binding	1.75	1.98	Down
7	Galectin-1	LEG1	P09382	LPDGYEFK	Cytoplasm	Positively regulation of I-kB kinase/NF-kB cascade	0.21	0.22	Uncertain
				SFVLNLGK			4.72	2.19	
8	Cofilin-1	COF1	P23528	HELQANCYEEVK	Nucleus, cytoplasm	Protein binding, anti-apoptosis	0.38	0.48	Up
9	DNA-dependent protein kinase catalytic subunit	PRKDC	P78527	EHPFLVK	Nucleus	Protein binding; protein kinase activity	4.76	4.02	Down
				HGDLPDIQIK			1.94	2.62	
10	RNA-binding protein FUS	FUS	P35637	AAIDWFDGK	Nucleus	Protein binding;RNA binding	3.51	1.73	Down

11	FACT complex subunit SPT16	SPT16	Q9Y5b9	VQFHLK	Nucleus	Positive transcription elongation factor	5.87	6.80	Down
12	ATP-dependent DNAhelicase II 80 kDa subunit	KU86	P13010	LFQCLLHR	Nucleus	Double-strand break repair	3.37	6.66	Down
				ANPQVGVAFPHIK			2.07	2.84	
13	ATP-dependent DNA helicase II70 kDa subunit	KU70	P12956	ILELDQFK	Nucleus	Double-strand break repair	2.83	2.54	Down
				SDSFENPVLQQHFR			3.34	2.80	
14	APendonuclease 1	APEX1	P27695	EAAGEGPALYEDPPDQK		Repair DNA oxidative damage	0.32	0.49	Up
15	60 kDa heat shock protein	CH60	P10809	ISSIQSIVPALEIANAHR	Mitochondrion matrix	Regulation of apoptosis	4.35	2.33	Down
16	T-complex protein 1 subunit theta	TCPQ	P50990	FAEAFEAIPR	Cytoplasm	ATPase activity	1.74	1.84	Down
17	T-complex protein 1 subunit epsilon	TCPE	P48643	SLHDALCVIR	Cytoplasm	Protein binding	6.94	6.29	Down
18	T-complex protein 1 subunit alpha	TCPA	P17987	SLHDALCVVK	Cytoplasm	Unfolded protein binding	6.79	6.29	Down
				IHPTSVISGYR			3.72	2.04	
19	T-complex protein 1 subunit eta	TCPH	Q99832	LLDVVHPAAK	Cytoplasm	Regulation of progression through cell cycle	1.59	1.71	Down
				YNFFTGCPK			2.24	2.38	
20	T-complex protein 1 subunit delta	TCPD	P50991	AYILNLVK	Cytoplasm, melanosome	Regulation of progression through cell cycle	6.30	3.21	Down
21	Heat shock protein HSP 90-beta	HS90B	P08238	ALLFIPR	Cytoplasm	Nitric-oxide synthase regulator activity	16.67	17.88	Down
				APFDLFENK			1.81	1.64	
				FYEAFSK			2.71	1.73	
				EQVANSAFVER			2.42	4.06	
22	Heat shock protein HSP 90-alpha	HS90A	P07900	YESLTDPSK	Cytoplasm, melanosome	Protein homodimerization	0.49	0.61	Uncertain
				ELHINLIPNK			3.74	1.61	
				FENLCK			0.61	0.55	

				HIYYITGETK			9.50	5.69	
				ALLFVPR			4.17	11.45	
				APFDLFENR			1.72	1.58	
				VILHLK			1.50	1.59	
				LGIHEDSQNR			10.60	3.09	
				NPDDITNEEYGEFYK			1.97	2.86	
23	Heat shock protein 90 kDa beta member 1	ENPL	P14625	EFGTNIK	ER lumen, melanosome	Anti-apoptosis	0.51	0.59	Uncertain
				YLNFVK			1.50	2.64	
				SILFVPTSAPR			3.22	2.15	
24	Heat shock 70 kDa protein 8	HSP7C	P11142	FEELNADLFR	Cytoplasm, Melanosome	Protein folding;response to unfolded protein	3.20	2.75	Uncertain
				NQTAEKEEFEHQQK			2.35	3.39	
				IINEPTAAAIAYGLDK			2.19	2.59	
				TVTNAVVTVPAYFNDSQR			2.24	1.99	
				EIAEAYLGK			0.26	0.16	
				EEFEHQQK			0.35	0.40	
25	Heat shock 70 kDa protein 1	HSP71	P08107	DAGVIAGLNVLR	ER, mitochondrion, nucleus	Anti-apoptosis	5.97	4.90	Down
				LVNHFVEEFK			5.26	2.76	
26	Hsc70-interacting protein	F10A1	P50502	AIDLFTDAIK	Cytoplasm	Protein binding, bridging	2.10	3.57	Down
27	Heat shock 70 kDaprotein 5	GRP78	P11021	ELEEIVQPIISK	ER lumen, melanosome	Anti-apoptosis;negative regulation of caspase activity	1.52	1.59	Uncertain
				IQQLVK			0.30	0.60	
				VTHAVVTVPAYFNDAQR			2.54	4.78	
28	Heat shock protein 75 kDa (TNFR-associated protein 1)	TRAP1	Q12931	GVVDSEDIPLNLSR	Mitochondrion	Tumor necrosis factor receptor binding	2.55	2.61	Down
29	Annexin-1	ANXA1	P04083	SEDFGVNEDLADSDAR	Cornified envelope; cytoplasm	Anti-apoptosis	0.62	0.57	Uncertain
				NALLSLAK			1.71	1.56	
				VLDLELK			2.00	1.71	
30	Annexin-3	ANXA3	P12429	SEIDLLDIR	Cytoplasm	Signal transduction	3.38	4.43	Down

31	Annexin-5	ANXA5	P08758	SEIDLFNIR	Cytoplasm	Anti-apoptosis	2.93	2.93	Down
32	Peroxiredoxin-1	PRDX1	Q06830	LVQAFQFTDK	Cytoplasm, melanosome	Eliminating peroxides generated during metabolism.	3.41	3.97	Down
33	Peroxiredoxin-5	PRDX5	P30044	VNLAELFK	Mitochondrion, cytoplasm, peroxisome	Peroxidase activity, response to oxidative stress	9.45	2.76	Down
34	Peroxiredoxin-6	PRDX6	P30041	LPFPIIDDR	Cytoplasm, lysosome, cytoplasmic vesicle	Antioxidant activity;response to oxidative stress	1.73	2.35	Uncertain
				DINAYNCEEPTEK			0.35	0.52	
35	Multidrug resistance-associated protein 1	MRP1	P33527	DKVLAIR	Membrane; multi-pass membrane protein	Response to drug;transport	0.47	0.40	Up
36	Phosphoglycerate kinase 1	PGK1	P00558	LGDVYVNDAFGTAHR	Cytoplasm	phosphoglycerate kinase activity; ATP binding	2.63	5.52	Down
37	Ubiquitin-conjugating enzyme E2 L3	UB2L3	P68036	IYHPNIDEK	Ubiquitin ligase complex	Enzyme binding;ubiquitin-protein ligase activity	2.06	3.30	Down
38	Ubiquitin.	UBIQ	P62988	MQIFVK	Cytoplasm, nucleus	Protein binding; transcription regulator activity	3.45	4.44	Uncertain
				ESTLHLVLR			7.49	5.57	
				EGIPPDQQR			0.49	0.45	
39	Proteasome subunit alpha type 1	PSA1	P25786	FVFDRPLPVSR	Cytoplasm, nucleus	RNA binding	8.71	5.80	Down
40	Proteasome subunit alpha type 6	PSA6	P60900	LLDSSTVTHLFK	Cytoplasm, nucleus	Endopeptidase activity; protein binding; RNA binding	3.06	4.13	Down
41	Tumor necrosis factor type 1 receptor-associated protein 2	PSMD2	Q13200	LAQGLTHLGK	Proteasome regulatory particle	Protein binding	2.14	2.21	Down
42	26S proteasome non-ATPase regulatory subunit 11	PSD11	O00231	EASIDILHSIVK	Proteasome complex	Protein binding	2.95	4.76	Down

43	Peptidyl-prolyl cis-trans isomerase A	PPIA	P62937	FEDENFILK	Cytoplasm	Unfolded protein binding;virion binding	3.86	3.22	Down
44	Protein KIAA1045.	K1045	Q9uPv7	MGVLMSK		Protein binding	5.55	4.84	Down
45	Zinc finger protein 335.	ZN335	Q9h4z2	RAHAGPGAFK	Nucleus (Probable)	Transcriptional regulation	2.33	2.44	Down
46	Peptidyl-prolyl cis-trans isomerase B precursor	PPIB	P23284	VIFGLFGK	ER lumen, melanosome	Peptidyl-prolyl cis-trans isomerase activity	17.29	7.69	Down
47	Macrophage migration inhibitory factor	MIF	P14174	LLCGLLAER	Extracellular region	Cell proliferation;negative regulation of apoptosis	2.52	1.81	Down
48	Pyruvate kinase isozymes M1/M2	KPYM	P14618	SVETLK	Cytosol	Protein binding;pyruvate kinase activity	0.60	0.59	Uncertain
				GIFPVLCK			3.56	1.61	
				LNFSHGTHEYHAETIK			7.11	2.75	
				LDIDSPPITAR			3.53	2.56	
49	C-mycpromoter-binding protein (MBP-1)	ENOA (ENO1)	P06733	IGAEVYHNLK	Cytoplasm, cell membrane	Phosphopyruvate hydratase activity	0.60	0.64	Up
				LNVTEQEK			0.64	0.47	
				YISPDQLADLYK			0.13	0.38	
50	Protein S100-A6	S10A6	P06703	LQDAEIAR	Cytoplasm; nuclear envelope; ruffle	Calcium ion binding	0.58	0.64	Up
51	Beta-actin	ACTB	P60709	LDLAGR	Cytoplasm	protein binding;structural constituent of cytoskeleton	0.41	0.28	Uncertain
				GYSFTTTAER			0.15	0.17	
				AVFPSIVGRPR			73.13	86.88	
				EITALAPSTMK			2.17	2.05	
				SYELPDGQVITIGNER			6.68	7.90	
52	C-myc purine-binding transcription factor PUF	NDKB	P22392	GLVGEIIK	Cytoplasm, nucleus	Protein binding;transcription factor activity	1.88	2.00	Uncertain
				SCAHDWVYE			0.47	0.48	

53	p21 Ras GTPase-activating protein-associated p62	SAM68	Q07666	FNFVGK	Nucleus, membrane	Cell cycle arrest	1.97	1.71	Down
54	Glyceraldehyde-3-phosphate dehydrogenase	G3P	P04406	YDNSLK	Cytoplasm		0.59	0.55	Up
				YDDIK			0.48	0.52	
55	High mobility group protein B1	HMGB1	P09429	IKGEHPGLSIGDVAK	Nucleus	Anti-apoptosis	7.76	4.75	Down
56	Protein SET	SET	Q01105	EFHLNESGDPSSK	Cytoplasm, cytosol, ER, nucleus, nucleoplasm	DNA replication	2.03	1.69	Down
57	Exportin-1	XPO1	O14980	AVGHPFVIQLGR	Cytoplasm, nucleus, nucleoplasm, nucleolus	Protein binding	3.52	2.42	Down
	Ratio=Bax+/- ÷ Bax-/-								
	Up=Up-regulation								
	Down=Down-regulation								

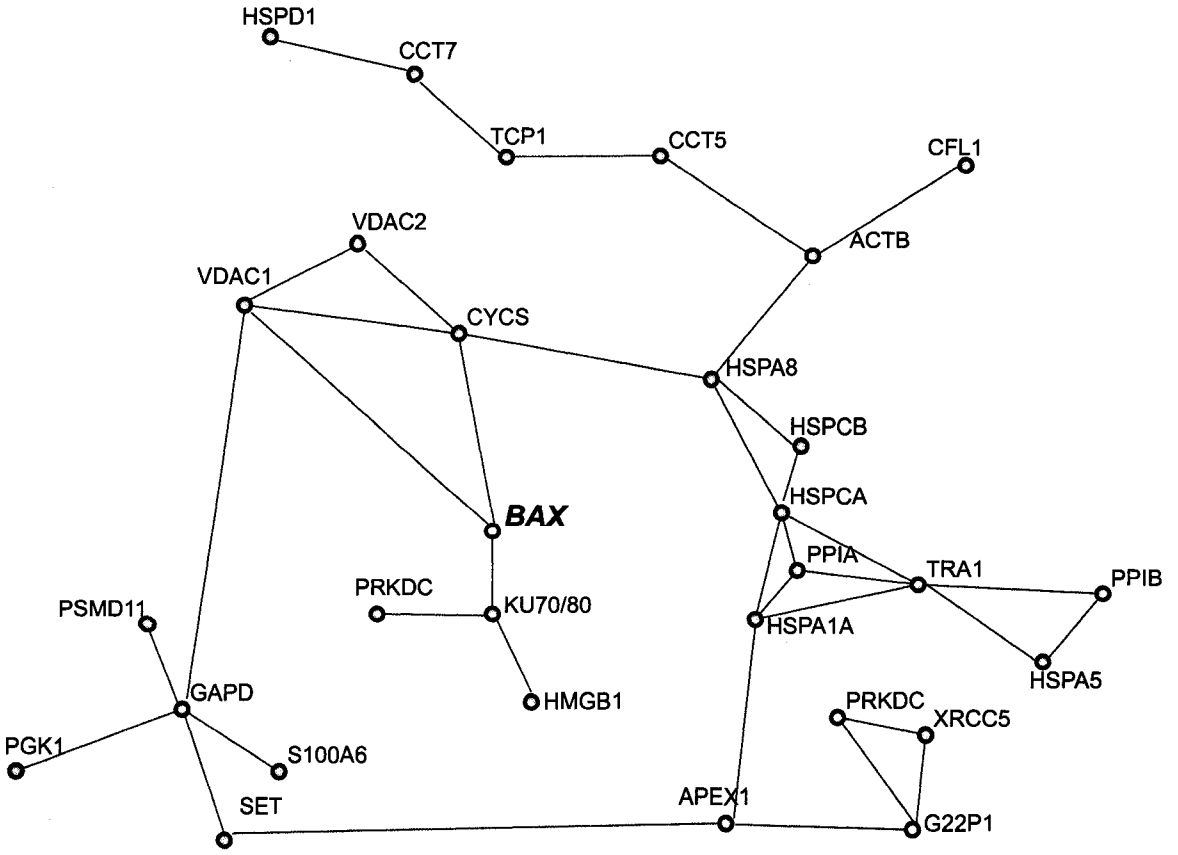

Fig 4.5 Biological network analysis of differentially expressed proteins between Bax+/- and Bax-/- HCT116 clones using the HiMAP mapping tool. (A) The network was generated using direct connections to map interactions between the 57 apoptosis-related proteins identified from the quantitative MS analysis.

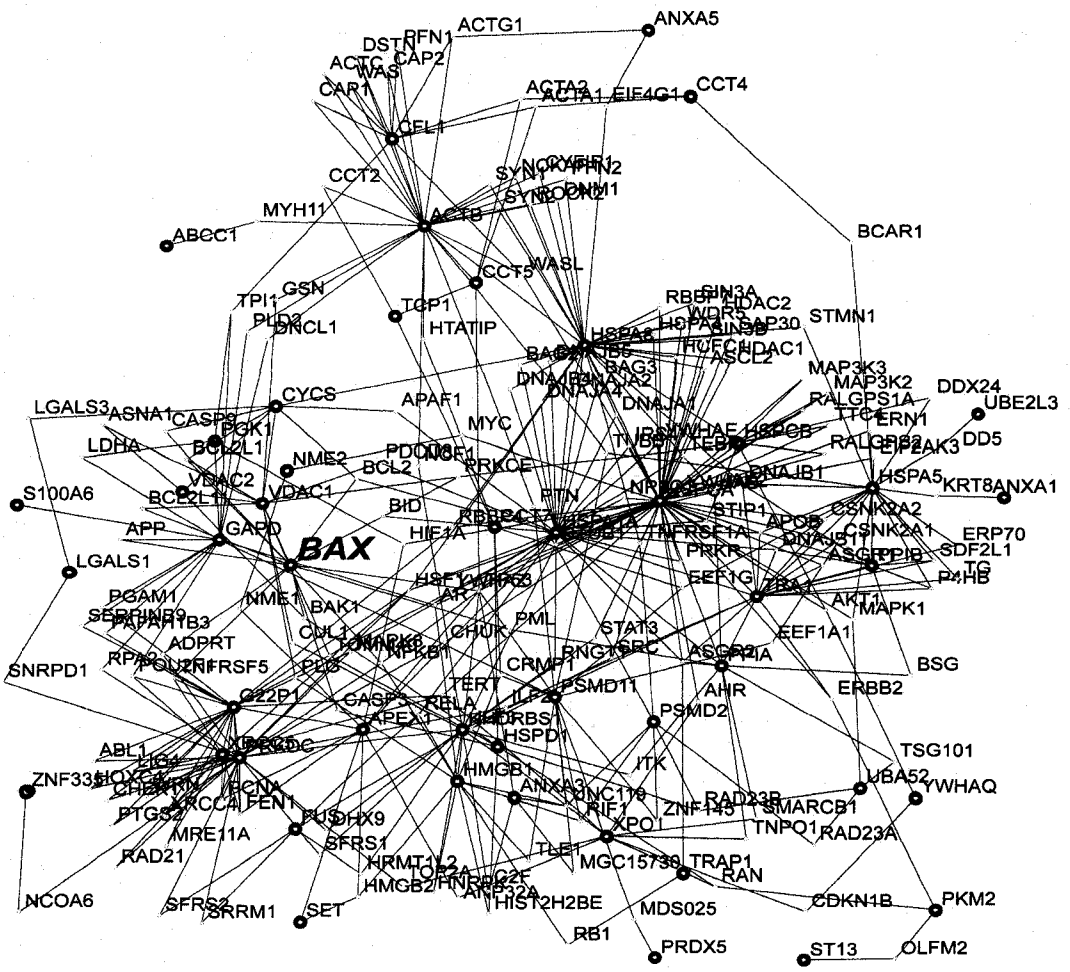

Fig 4.5 (B) The network was generated using the bridge algorithm to map interactions between the 57 apoptotic proteins identified from quantitative MS analysis. Large red circles denote identified differentially expressed proteins, whereas small yellow circles denote bridged proteins. Gene names are given in Supplementary Table 1.

Table 2

Group		Protein Name	Swiss-Prot Name	Swiss-Prot ID	Function	Ratio	Regulation
MPT Channel proteins							
	1	Voltage-dependent anion-selective channel protein 2	VDAC2	P45880	Voltage-gated anion channel porin activity	4.04	Down
	2	Voltage-dependent anion-selective channel protein 1	VDAC1	P21796	Apoptogenic cytochrome c release channel	2.27	Down
	3	Cytochrome c.	CYC	P99999	DNA fragmentation during apoptosis	3.63	Down
Bax-regulator proteins							
	4	14-3-3 protein theta	1433T	P27348	Protein binding	5.60	Down
	5	ATP-dependent DNAhelicase II 80 kDa subunit	KU86	P13010	Double-strand break repair	3.73	Down
	6	ATP-dependent DNA helicase II70 kDa subunit	KU70	P12956	Double-strand break repair	2.88	Down
	7	DNA-dependent protein kinase catalytic subunit	PRKDC	P78527	Protein binding; protein kinase activity	3.34	Down
	8	Macrophage migration inhibitory factor	MIF	P14174	Cell proliferation;negative regulation of apoptosis	2.16	Down
HSP family members							
	9	60 kDa heat shock protein	CH60	P10809	Regulation of apoptosis	3.34	Down
	10	Heat shock protein HSP 90-beta	HS90B	P08238	Nitric-oxide synthase regulator activity	6.11	Down
	11	Heat shock protein HSP 90-alpha	HS90A	P07900	Protein homodimerization		Uncertain
	12	Heat shock protein 90 kDa beta member 1	ENPL	P14625	Anti-apoptosis		Uncertain
	13	Heat shock 70 kDa protein 8	HSP7C	P11142	Protein folding;response to unfolded protein		Uncertain
	14	Heat shock 70 kDa protein 1	HSP71	P08107	Anti-apoptosis	4.72	Down
	15	Hsc70-interacting protein	F10A1	P50502	Protein binding, bridging	2.83	Down
	16	Heat shock 70 kDaprotein 5	GRP78	P11021	Anti-apoptosis;negative regulation of caspase activity		Uncertain
	17	TNFR-associated protein 1	TRAP1	Q12931	Tumor necrosis factor receptor binding	2.58	Down

	18	T-complex protein 1 subunit theta	TCPQ	P50990	ATPase activity	1.79	Down
	19	T-complex protein 1 subunit epsilon	TCPE	P48643	Protein binding	6.62	Down
	20	T-complex protein 1 subunit alpha	TCPA	P17987	Unfolded protein binding	4.71	Down
	21	T-complex protein 1 subunit eta	TCPH	Q99832	Regulation of progression through cell cycle	1.98	Down
	22	T-complex protein 1 subunit delta	TCPD	P50991	Regulation of progression through cell cycle	4.75	Down
Oxidative stress triggered proteins							
	23	Annexin-1	ANXA1	P04083	Anti-apoptosis		Uncertain
	24	Annexin-3	ANXA3	P12429	Signal transduction	3.90	Down
	25	Annexin-5	ANXA5	P08758	Anti-apoptosis	2.93	Down
	26	Peroxiredoxin-1	PRDX1	Q06830	Eliminating peroxides generated during metabolism.	3.69	Down
	27	Peroxiredoxin-5	PRDX5	P30044	Peroxidase activity, response to oxidative stress	6.10	Down
	28	Peroxiredoxin-6	PRDX6	P30041	Antioxidant activity;response to oxidative stress		Uncertain
	29	C-mycpromoter-binding protein (MBP-1)	ENOA (ENO1)	P06733	Phosphopyruvate hydratase activity	0.48	Up
	30	Protein S100-A6	S10A6	P06703	Calcium ion binding	0.61	Up
	31	Pyruvate kinase isozymes M1/M2	KPYM	P14618	Protein binding;pyruvate kinase activity		Uncertain
Ratio=Bax+/- ÷ Bax-/-		**Up=Up-regulation**	**Down=Down-regulation**				

4.2.7. Validation of selected differentially expressed proteins by Western blot analysis

Eight of the proteins differentially expressed in the current study were subjected to biological validation by Western blot analysis: VDAC1, VDAC2, 14-3-3 theta, macrophage migration inhibitory factor (MIF), HSP70, HSP90β, HSP60, and leucine-rich PPR motif-containing protein (LRP130). Since the major function of Bax is involved in apoptotic cell death, most of these proteins were selected because of their involvement in apoptotic signaling pathways. HSP90β was selected because several peptides were found with contradictory expression levels. VDAC1, VDAC2, 14-3-3 theta, MIF, HSP70, HSP60, and LRP130 were found to be down-regulated, which is qualitatively consistent with the mass spectrometric data. HSP90β was found to be down-regulated in the Bax-/- clone (Fig 4.6A).

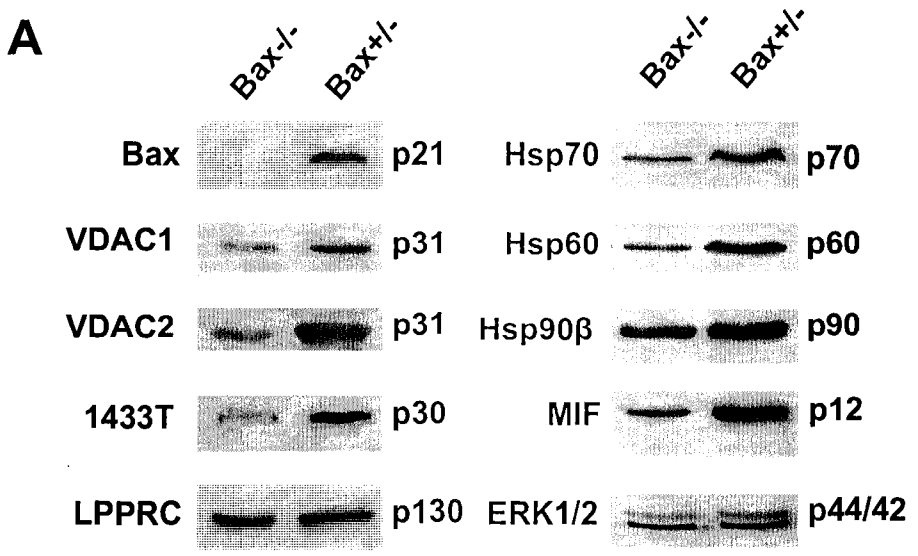

Fig 4.6 (A) Validation of selected differentially expressed proteins between Bax+/- and Bax-/- clones by Western blot analysis. Bax+/- and Bax-/- HCT116 clones were examined by Western blotting for the expression of VDAC-1, VDAC-2, 14-3-3 theta, MIF, HSP60, HSP70, HSP90β, and LRP130 with ERK1/2 as the loading control.

4.2.8. Proteasome inhibition effects on expression levels of selected differentially expressed proteins

Since the down-regulation of protein expression level primarily comes from the degradation of the targeted protein by the ubiquitin proteasome system, Bax-/- cells were treated with a low dose of proteasome inhibitor, MG132, in the time courses, followed by Western blot analysis of the eight validated down-regulated proteins. The expression level of VDAC-2, 14-3-3 theta, MIF, and HSP70 were found to be restored after MG132 treatment (Fig 4B) while no significant expression level changes in the other four proteins were observed.

Proteins were down-regulated, either because of the decrease of the target gene expression, or because these proteins are degraded at the protein level by the proteasome system. Since Bax is not a transcription factor, the degradation of these identified proteins in the Bax-/- clone may be the major cause for the down-regulation. To confirm this phenomenon, we used a proteasome inhibitor to treat the Bax-/- cells. Once the proteasome system was inhibited, certain crucial down-regulated proteins, including VDAC-2, 14-3-3 theta, HSP70, and MIF, were observed to be up-regulated. These data indicate that Bax interacts with these proteins and affects the stability of these proteins, and once Bax was knocked off, these proteins were degraded by proteasome system.

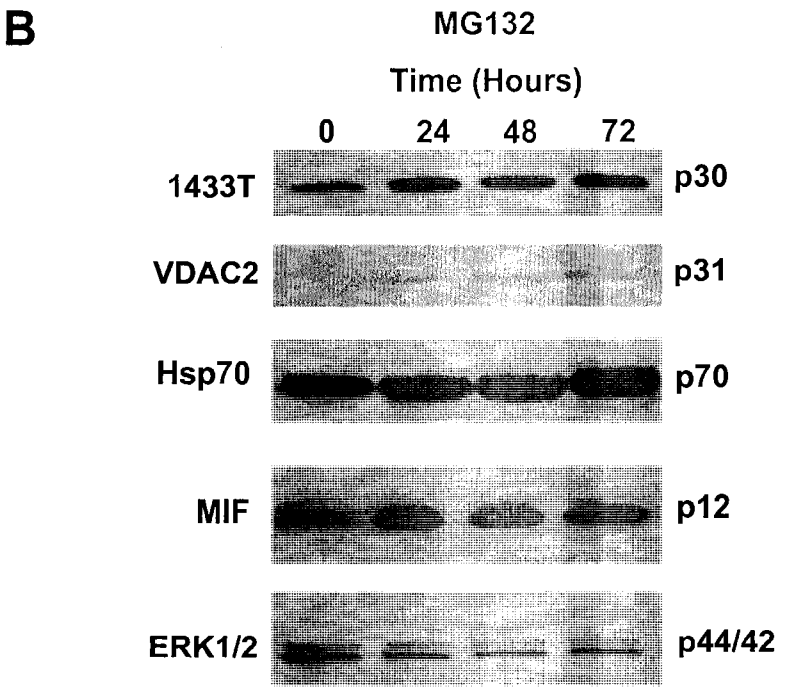

Fig 4.6 (B) The expression of VDAC-2, 14-3-3 theta, MIF, HSP70 were detected in the Bax-/- HCT116 clone treated with 0.1 μM MG132 for the indicated time with ERK1/2 as the loading control.

4.3. Discussion

Bax plays a crucial role in multiple processes, including cell cycle regulation, stress regulation, detoxification, and especially apoptosis. In previous reports, Bax-/- cells are resistant to multiple stimuli-induced apoptosis, including radiation, and DNA damage drugs. In our research, even though Bak and other apoptotic factors remain, the Bax-/- clone is still completely resistant to TRAIL-induced apoptosis. These reports and data indicate that Bax not only works as an apoptotic executor but also regulates different cellular processes by interacting with other proteins. To further investigate these interactions, we used a targeted-quantitative MS method to identify the differentially expressed protein profile between Bax+/- and Bax-/- clones.

4..3.1. Study Design Rationale

With the vast majority of proteins remaining generally unchanged, a targeted mass spectrometric approach was desired to selectively analyze only differentially expressed proteins. The two-sided study design was chosen to minimize quantification inaccuracies resulting from spectral sampling during MS analysis (random error) and potentially identify low abundance peptides. Due to the overall complexity of most biological samples, even simple shotgun proteomics identification experiments can have a significant degree of variability in terms of the peptides and proteins identified. Although this study design effectively doubles the instrument time used, the increased reliability in the identification and quantification data determines genuine changes in the Bax+/- and Bax-/- proteome profiles by applying stringent conditions for both identification and quantification. The 2-MEGA protocol was selected since it: 1) is a

global mass-tagging strategy for quantification by MS; 2) uses MS-based quantification that allows candidate selection prior to sequencing; and 3) is readily amenable with LC-MALDI for cross-system comparison. Fig 4.4. shows the advantage of using the two-sided experimental design to confirm quantification values. Although the candidate peaks were selected using data analysis software, overlaying MS spectra from complementary systems allows facile manual confirmation of differential expression in peptide pairs. This provides a simple check to determine that the peptides have similar retention behavior and that the quantification accuracy has not been compromised by neighboring peaks.

4.3.2. Kinetic Isotope Effect and LC-MALDI Fractionation

Reliable quantification from MS scans is complicated by differing elution profiles arising from the kinetic isotope effect and the online fractionation process of LC-MALDI. Even in cases where the kinetic isotope effect is small, high abundance peptides will elute over multiple consecutive fractions. For pairs and peaks eluting over multiple fractions (SCX, RPLC, or both), the pair or peak with the highest intensity in the MS survey scans was selected as the ratio for that peptide. It was found that there was no advantage between using the aforementioned method versus weighting the ratios with the observed intensities over multiple fractions. Since the kinetic isotope effect from the dimethylation is between 1 and 3 seconds and the peak width for most peptides in RPLC is ~15 seconds, the overall elution profiles are quite similar. Any variation from the kinetic isotope effect is effectively reduced by the fractionation process in LC-MALDI which averages peptide elution over 20 seconds.

4.3.3. Accuracy of Pairs versus Peaks

It was found that the quantification values of peaks between the systems were likely to be less consistent than the pairs values. Quantification with a single peak is equivalent to quantfication using its absolute intensity, since the signal-to-noise ratio of the unobserved pair is conservatively assumed to be a fixed value of eight. Since absolute signal reproducibility in the MS of complex mixtures is low, comparison across two different sample spots in two different systems may lead to large differences in calculated expression. Despite these confounding factors, 39 out of 39 peaks with a relative error greater than 50% had an observed differential expression level of at least three fold in one system and often had at least a two fold change in expression level in both systems. As such, there is still a high degree of confidence in the general expression trend observed, but exact confidence intervals in the peaks data are difficult to estimate.

4.3.4. Reproducibility

Quantification reproducibility, measured as the relative error for matched pairs/peaks across both systems, was found to deteriorate under certain conditions. First, in cases where one peak is significantly higher than the other, quantification values were skewed towards higher values. Since the peak selection algorithm calculates the baseline using a rolling average of data points, a relatively high abundance peak artificially increases the calculated baseline at the nearby corresponding pair, ultimately reducing the signal-to-noise ratio of the lower intensity peak. The overall qualitative nature of the data from both the pairs and peaks quantification data are generally internally consistent, with only two cases where the ratios in both experimental systems were contradictory after

manual data analysis. With improvements in peak picking software, the manual data analysis step could be minimized. In both the pairs and peaks data, greater than threefold relative changes in expression levels can be difficult to quantify exactly, but are simple to identify with a high degree of discrimination.

Overall, the data present a consistent profile of the differentially expressed proteins between the Bax+/- and Bax-/- clones. The confirmation of eight candidates by Western blot analysis increases confidence in the quantification results. Seven of the proteins (VDAC1, VDAC2, 14-3-3 theta, MIF, HSP70, HSP60, and LRP130) which were predicted to be down-regulated were clearly observed to be down-regulated in the Western blots. HSP90β was believed to be down-regulated in the Bax-/- clone from the mass spectrometry results, and was shown to be down-regulated via the Western blot results. The contradictory values for HSP90β arise from sequence similarity between various proteins in the heat shock family. Since most of the peptide ratios were down-regulated, especially those unique to HSP90β, the predicted down-regulation is considered consistent with the Western blot result.

4.3.5. Bioinformatic analysis of expressed proteins differently between Wt and Bax-/- HCT116 clones

The 199 identified differentially expressed proteins were categorized by known functions, such as apoptosis, cell cycle regulation, DNA repair, and stress regulation by searching previous reports and literature from Pub-Medline and the ExPASY Proteomics Server. Of the 56 classified proteins (Table 2), 47 were connected using HiMAP and Metacore; some of the key groups are highlighted (Fig 4.7).

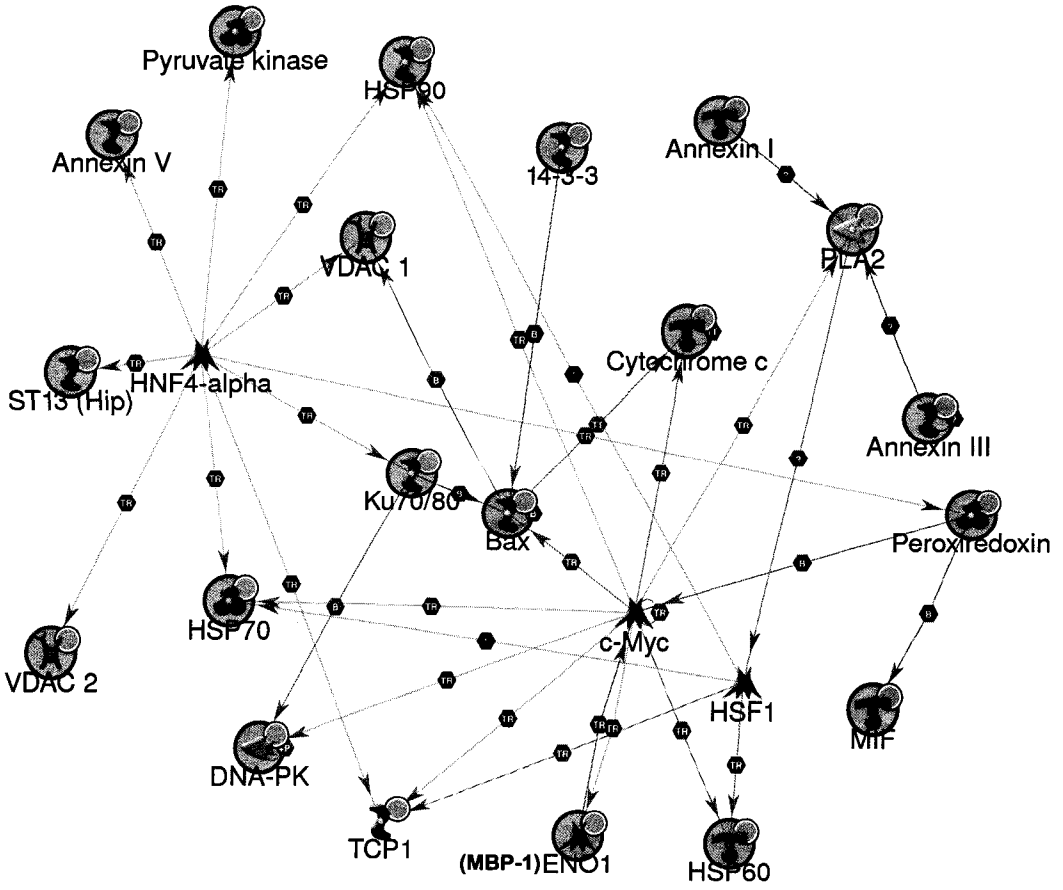

Fig 4.7 Bioinformatic analysis of four key groups of proteins expressed differentially between Bax+/- and Bax-/- clones. Four crucial groups of differentially expressed proteins were analyzed by using a shortest pathway algorithm with the Metacore program.

4.3.5.1. VDAC1, VDAC2, Glyceraldehyde-3-phosphate dehydrogenase (GADPH), and cytochrome c

Bax has been reported to be required for the release of apoptotic factors, such as cytochrome c, from mitochondria by changing MMP in response to various stimuli. However, it remains largely unclear how Bax promotes mitochondrial membrane permeabilization. The most widely accepted possibility is that Bax interacts with VDAC1/ANT and cyclophilin-D to form an MPT, through which cytochrome c, Smac, apoptosis-inducing factor (AIF), and DIABLO are released to the cytosol to activate downstream caspase-dependent and caspase-independent cell death pathways [31, 32]. There are also other reports indicating that VDAC is not indispensable for Bax-driven cell death [21]. An alternative possibility is that the translocation of Bax to mitochondria induces a non-specific lipid pore which is associated with mitochondrial membrane fission and fusion [33-35]. It was found that MPT channel proteins, including VDAC1 and VDAC2, and an MPT-associated apoptotic factor, cytochrome c, were down-regulated more than 2-fold in the Bax deficient clone. Since proteasome inhibitor restores the decreased VDAC2 level in the Bax deficient clone, Bax knock off may affect the stability of VDAC2 by proteasome system (Fig 4.6B). These data indicate that Bax deficient cells become resistant to most apoptotic stimuli, not only because of the loss of Bax, but also due to down-regulation of MPT channel proteins that control their apoptotic potential. Moreover, once GADPH [36], a VDAC1 interacting partner, was up-regulated in the Bax-deficient clone, its interacting proteins, including phosphoglycerate kinase 1 (predicted interaction), Protein SET [37], and 26S protcasome non-ATPase regulatory

subunit 11 (yeast two-hybrid dataset) were down-regulated by negative feedback regulation (Fig 4.5.A).

4.3.5.2. DNA-PK complex, MIF, and 14-3-3θ

It was also determined that KU70, KU86, and PRKDC were found to be down-regulated more than 2.5-fold in the Bax deficient clone. These three proteins have been reported to form the DNA-dependent protein kinase complex (DNA-PK) which could associate with and promote KU70 to move into the nucleus, releasing Bax to be activated in the cytosol under various apoptotic stimuli [38-43] (Fig 4.5A). Once the DNA-PK complex is down-regulated in the Bax deficient clone, its DNA-binding regulatory component, high mobility group protein B1 (HMGB1), was also down-regulated (Fig 4.5A) [44]. As the Bax regulator, the down-regulation of these proteins may come from the negative feedback in the Bax deficient clone.

MIF, a pro-inflammatory cytokine, has been reported to inhibit apoptosis by inhibiting MMP changes [45]. Here, we found that MIF was down-regulated more than 2-fold in the Bax deficient clone. Another Bax-regulator, 14-3-3θ, previously reported to directly bind to Bax [46, 47], has also been identified as a down-regulated protein in the Bax deficient clone. Although 14-3-3ε, 14-3-3ζ, and 14-3-3σ have also been reported to directly bind to Bax, they were not identified in the study [48]. Both MIF and 14-3-3θ have been reported to interact with Bax to inhibit Bax-driven cell death. Proteasome inhibitor restored the MIF and 14-3-3θ expression level in the Bax deficient clone (Fig 4.5B), which indicates that as a downstream molecule of MIF and 14-3-3θ, Bax can regulate the stability of these up-stream regulators via the proteasome system (Fig 4.6B).

Once Bax was knocked out, these proteins were down-regulated by the increased level of degradation.

4.3.5.3. HSP60, T-complex protein-1(TCP-1), HSP70, HSP90α, HSP90β, and C-myc promoter-binding protein (MBP-1, ENO1)

HSP60 has anti- as well as pro-apoptotic roles. Hsp60 has been found to inhibit cell death by sequestering Bax, thereby preventing its translocation to the mitochondrial membrane [49]. Conversely, HSP60 has been reported to drive the maturation of caspase-3 in mitochondria and thus promotes apoptosis [50]. TCP-1, containing the chaperone of the HSP60, may be specifically adapted to folding actin and tubulins [51]. TCP-1 and HSP60 were identified to be both down-regulated in the Bax deficient clone. Five of the seven TCP-1 subunits (α, β, δ, ε, η, α, and θ) were identified to be down-regulated in the Bax deficient clone. These data suggest that TCP-1 may interact with Bax with its shared chaperonin with HSP60 and the interaction of Bax with TCP-1 affects the stability of this protein. Similarly to HSP60, other heat shock protein family members, including HSP70, its interaction protein HSP70 interaction protein (Hip), HSP90α, and HSP90β, were found to be differentially expressed in the Bax deficient clone. Although there are some controversial data in peptide level quantification (Table 1), Western blotting results clearly indicate the down-regulation of HSP70 and HSP90β in the Bax deficient clone (Fig 4.6A). Both HSP70 and HSP90 are mostly anti-apoptotic by inhibiting the translocation of Bax and the downstream apoptosome complex formation [52, 53]. Even though these three heat shock proteins, including HSP60, HSP70, and HSP90, are closely involved in regulation of the mitochondria-associated apoptotic pathway, there is no

evidence of their direct interaction with Bax. Proteasome inhibitor restored the HSP70 level in the Bax deficient clone which indicates that the down-regulation of HSP70 may come from the increased degradation level of HSP70 in the Bax deficient clone. Moreover, based on the Metacore analysis, the down-regulation of HSP60, HSP90 or even HSP70 may come from the decreased transcription of these HSPs caused by the inhibition of c-Myc function in the Bax deficient clone (Fig 4.7) [54]. Although the down-regulation of c-Myc was not directly observed in our study, the MBP-1 (ENO1) which is the crucial repressor of c-Myc promoter [55], was found up-regulated more than two fold in the Bax deficient clone (Fig 4.7). These data indicate that Bax knock off up-regulates the MBP-1, which in turn represses the transcriptions of HSPs regulated by c-Myc. MBP-1 was also reported to induce apoptosis by activating caspase-3, caspase-9 and PARP cleavage. It was found to interact with Bcl-2 family proteins since exogenous expression of Bcl-2 blocked MBP-1 mediated apoptosis [56] and expressing MBP-1 reduced the expression of Bcl-xL [57]. It suggests that increased MBP-1 expression may be needed to block free Bcl-xL, once the ratio of Bcl-xL/Bax was in balance in the Bax deficient clone.

4.3.5.4. Peroxiredoxins, Pyruvate kinase, S100A6, and Annexins

Peroxiredoxins (Prx) are a family of multifunctional antioxidant peroxidases that have various functions, including cellular protection against oxidative stress, modulation of intracellular signaling cascades, and regulation of cell proliferation. In the current study, two members of the peroxiredoxin family, peroxiredoxin-1 and -5, were found down-regulated in the Bax deficient clone. Peroxiredoxins function as antioxidant

enzymes, especially Prx 1 which interacts with the oncogene products, c-Abl and c-Myc, to regulate cell proliferation and anti-apoptosis [58]. Their down-regulation may come from the down-regulation of pyruvate kinase in the Bax deficient clone, since microarray data have shown that the inhibition of pyruvate kinase gene expression led to decreased expression of downstream peroxiredoxin genes (Fig 4.7) [59]. Moreover, reactive oxygen species (ROS) production was greatly decreased in the Bax deficient clone and thus, oxidative stress triggered proteins, including peroxiredoxins, were down-regulated.

Three members of the annexin superfamily were found differentially expressed in the Bax deficient clone, including Annexin-1, -3, and -5. By binding calcium or phospholipids, these proteins regulate cell proliferation and death signals [60]. Over-expression of Annexin-1 promotes apoptosis by inducing the dephosphorylation of BAD, which allows BAD to translocate to the mitochondria. Moreover, Bcl-2 inhibits the translocation of Annexin-1 to the nucleus during apoptosis [61]. Two of three identified peptides from Annexin-1 were found down-regulated in the Bax deficent clone. Based on the Metacore analysis, the down-regulation of the Annexin-1 may also come from the inhibition of c-Myc function in the Bax deficient clone (Fig 4.7). The down-regulation of these annexins further decreases the apoptotic cell death potential in the HCT116 Bax-/- cells.

Another stress response protein, S100A6, was found up-regulated in the Bax deficient clone. S100A6, a member of the S100 family of proteins, was reported to express in several types of cancers, including colorectal carcinoma [62]. It likely acts as the linker between Ca^{2+} and ROS signaling pathways and was reported to be dramatically decreased during TRAIL-induced apoptosis [63]. Although there is no evidence of a

direct interaction of S100A6 with Bax, S100A4, another member of the S100 family sharing sequence similarity with S100A6, was found to down-regulate Bax expression in VWR cells [64]. Meanwhile, it was reported that S100A6 exerts its physiological function by interacting with GADPH in a calcium-dependent manner [65] and thus, increased S100A6 may come from the increased GADPH in the Bax-/- clone (Fig 4.5.A). By increasing S100A6, the Bax deficient clone becomes more difficult to kill by various apoptotic stimuli.

In summary, using targeted quantitative MS proteomic analysis, we identified a total of 199 proteins expressed differentially between the wild type and Bax deficient HCT116 clone, including proteins involved in apoptosis, DNA repair, stress-induced proteins, cell cycle regulation proteins, cytoskeletal rearrangements, and signal transduction molecules. Within these proteins, four groups of proteins are highlighted here because of their important roles in the Bax-modulated apoptosis pathway. First, MPT channel proteins, including VDAC-1, VDAC-2, and cytochrome c, are significantly down-regulated in the Bax deficient clone, which may result from instability and/or degradation after losing their binding partner or regulator Bax. Second, Bax-regulator proteins, such as KU70, KU80, PRKDC, 14-3-3 theta, and MIF, which directly or indirectly interact with Bax to modulate Bax-mediated apoptosis, may be down-regulated after downstream target protein Bax was knocked out via negative feedback regulation. The third group of proteins is the heat shock protein family members, including HSP60, HSP70, TCP-1, HSP90α, and HSP90β. These proteins play both pro- and anti-apoptosis roles. In the Bax deficient cells, the down-regulation of these HSPs may be due to the inhibition of c-Myc-regulated transcription via the up-regulation of the c-Myc repressor,

MBP-1. Once Bax was knocked out, these proteins involved in protein folding, sorting, and degradation, are also down-regulated. Some cell skeletal and structural proteins are also correspondingly down-regulated by the decrease of these HSPs. The fourth group was the oxidative stress-triggered proteins, Peroxiredoxins, Pyruvate kinase, S100A6, and Annexins. The down-regulation of Peroxiredoxins may be due to the decrease of pyruate kinase in the Bax deficient clone. The down-regulation of the Annexins may also come from the inhibition of c-Myc function in the Bax deficient clone. S100A6 was identified as being up-regulated in the Bax deficient clone which may come from the decrease of Bax-regulated protease activity.

Bax plays a central role in various stimuli-induced apoptosis pathways. Even though Bak and other apoptotic executors remain in the Bax deficient clone, it is not clear why the Bax deficient clone is resistant to most apoptosis stimuli, including DNA-damage drugs and death ligands. By using targeted quantitative MS analysis, we provide a differentially expressed protein profile between wild type and Bax deficient clones. These data indicate that Bax functions, not only as an apoptotic signal executor by modulating the damage of mitochondria membrane potential, but also as a regulator for the expression level of other proteins. By modulation of some crucial proteins, the Bax deficient clone further lost its apoptotic potential. Using the novel targeted quantitative mass spectrometry analysis greatly decreases the percentage of false information, since we used an internal reference (A_LB_H vs A_HB_L) to identify and analyze only differentially expressed proteins. Our findings through the quantitative MS analysis enabled us to draw a detailed protein profile map with the Bax as the central protein. The expression of most

of these proteins has not been reported to be related to Bax and thus novel targets for the further study of Bax-modulated cell signals have been provided.

1. Oltvai, Z.N., C.L. Milliman, and S.J. Korsmeyer, *Bcl-2 heterodimerizes in vivo with a conserved homolog, Bax, that accelerates programmed cell death.* Cell, 1993. **74**(4): p. 609-19.
2. Akao, Y., et al., *Multiple subcellular localization of bcl-2: detection in nuclear outer membrane, endoplasmic reticulum membrane, and mitochondrial membranes.* Cancer Res, 1994. **54**(9): p. 2468-71.
3. Krajewski, S., et al., *Investigation of the subcellular distribution of the bcl-2 oncoprotein: residence in the nuclear envelope, endoplasmic reticulum, and outer mitochondrial membranes.* Cancer Res, 1993. **53**(19): p. 4701-14.
4. Suzuki, M., R.J. Youle, and N. Tjandra, *Structure of Bax: coregulation of dimer formation and intracellular localization.* Cell, 2000. **103**(4): p. 645-54.
5. Yang, E., et al., *Bad, a heterodimeric partner for Bcl-XL and Bcl-2, displaces Bax and promotes cell death.* Cell, 1995. **80**(2): p. 285-91.
6. Deckwerth, T.L., et al., *BAX is required for neuronal death after trophic factor deprivation and during development.* Neuron, 1996. **17**(3): p. 401-11.
7. Krajewski, S., et al., *Upregulation of bax protein levels in neurons following cerebral ischemia.* J Neurosci, 1995. **15**(10): p. 6364-76.
8. Hughes, P.E., et al., *Excitotoxic lesion of rat brain with quinolinic acid induces expression of p53 messenger RNA and protein and p53-inducible genes Bax and Gadd-45 in brain areas showing DNA fragmentation.* Neuroscience, 1996. **74**(4): p. 1143-60.
9. Wei, M.C., et al., *Proapoptotic BAX and BAK: a requisite gateway to mitochondrial dysfunction and death.* Science, 2001. **292**(5517): p. 727-30.
10. Krajewski, S., et al., *Expression of pro- and anti-apoptosis gene products in brains from paediatric patients with HIV-1 encephalitis.* Neuropathol Appl Neurobiol, 1997. **23**(3): p. 242-53.
11. Misao, J., et al., *Expression of bcl-2 protein, an inhibitor of apoptosis, and Bax, an accelerator of apoptosis, in ventricular myocytes of human hearts with myocardial infarction.* Circulation, 1996. **94**(7): p. 1506-12.
12. Armistead, P.M., et al., *Expression of receptor tyrosine kinases and apoptotic molecules in rhabdomyosarcoma: correlation with overall survival in 105 patients.* Cancer, 2007. **110**(10): p. 2293-303.
13. Saxena, A., et al., *Mcl-1 and Bcl-2/Bax ratio are associated with treatment response but not with Rai stage in B-cell chronic lymphocytic leukemia.* Am J Hematol, 2004. **75**(1): p. 22-33.
14. Lange, T., et al., *High levels of BAX, low levels of MRP-1, and high platelets are independent predictors of response to imatinib in myeloid blast crisis of CML.* Blood, 2003. **101**(6): p. 2152-5.
15. Wolter, K.G., et al., *Movement of Bax from the cytosol to mitochondria during apoptosis.* J Cell Biol, 1997. **139**(5): p. 1281-92.
16. Eskes, R., et al., *Bid induces the oligomerization and insertion of Bax into the outer mitochondrial membrane.* Mol Cell Biol, 2000. **20**(3): p. 929-35.
17. von Ahsen, O., et al., *Preservation of mitochondrial structure and function after Bid- or Bax-mediated cytochrome c release.* J Cell Biol, 2000. **150**(5): p. 1027-36.
18. Crompton, M., *Bax, Bid and the permeabilization of the mitochondrial outer membrane in apoptosis.* Curr Opin Cell Biol, 2000. **12**(4): p. 414-9.

19. Pastorino, J.G., et al., *The overexpression of Bax produces cell death upon induction of the mitochondrial permeability transition.* J Biol Chem, 1998. **273**(13): p. 7770-5.
20. Eskes, R., et al., *Bax-induced cytochrome C release from mitochondria is independent of the permeability transition pore but highly dependent on Mg2+ ions.* J Cell Biol, 1998. **143**(1): p. 217-24.
21. Baines, C.P., et al., *Voltage-dependent anion channels are dispensable for mitochondrial-dependent cell death.* Nat Cell Biol, 2007. **9**(5): p. 550-5.
22. Kuwana, T., et al., *Bid, Bax, and lipids cooperate to form supramolecular openings in the outer mitochondrial membrane.* Cell, 2002. **111**(3): p. 331-42.
23. Antonsson, B., et al., *Bax is present as a high molecular weight oligomer/complex in the mitochondrial membrane of apoptotic cells.* J Biol Chem, 2001. **276**(15): p. 11615-23.
24. Arnoult, D., et al., *Mitochondrial release of apoptosis-inducing factor occurs downstream of cytochrome c release in response to several proapoptotic stimuli.* J Cell Biol, 2002. **159**(6): p. 923-9.
25. Jurgensmeier, J.M., et al., *Bax directly induces release of cytochrome c from isolated mitochondria.* Proc Natl Acad Sci U S A, 1998. **95**(9): p. 4997-5002.
26. Ji, C., N. Guo, and L. Li, *Differential dimethyl labeling of N-termini of peptides after guanidination for proteome analysis.* J Proteome Res, 2005. **4**(6): p. 2099-108.
27. Ji, C., et al., *Identification and quantification of differentially expressed proteins in E-cadherin deficient SCC9 cells and SCC9 transfectants expressing E-cadherin by dimethyl isotope labeling, LC-MALDI MS and MS/MS.* J Proteome Res, 2005. **4**(4): p. 1419-26.
28. Pan, S., et al., *High throughput proteome screening for biomarker detection.* Mol Cell Proteomics, 2005. **4**(2): p. 182-90.
29. Young, J.B. and L. Li, *An impulse-driven liquid-droplet deposition interface for combining LC with MALDI MS and MS/MS.* J Am Soc Mass Spectrom, 2006. **17**(3): p. 325-34.
30. Rhodes, D.R., et al., *Probabilistic model of the human protein-protein interaction network.* Nat Biotechnol, 2005. **23**(8): p. 951-9.
31. Henry-Mowatt, J., et al., *Role of mitochondrial membrane permeabilization in apoptosis and cancer.* Oncogene, 2004. **23**(16): p. 2850-60.
32. Sharpe, J.C., D. Arnoult, and R.J. Youle, *Control of mitochondrial permeability by Bcl-2 family members.* Biochim Biophys Acta, 2004. **1644**(2-3): p. 107-13.
33. Frank, S., et al., *The role of dynamin-related protein 1, a mediator of mitochondrial fission, in apoptosis.* Dev Cell, 2001. **1**(4): p. 515-25.
34. Fransson, A., A. Ruusala, and P. Aspenstrom, *Atypical Rho GTPases have roles in mitochondrial homeostasis and apoptosis.* J Biol Chem, 2003. **278**(8): p. 6495-502.
35. Karbowski, M., et al., *Spatial and temporal association of Bax with mitochondrial fission sites, Drp1, and Mfn2 during apoptosis.* J Cell Biol, 2002. **159**(6): p. 931-8.
36. Tarze, A., et al., *GAPDH, a novel regulator of the pro-apoptotic mitochondrial membrane permeabilization.* Oncogene, 2007. **26**(18): p. 2606-20.

37. Carujo, S., et al., *Glyceraldehyde 3-phosphate dehydrogenase is a SET-binding protein and regulates cyclin B-cdk1 activity.* Oncogene, 2006. **25**(29): p. 4033-42.
38. Sawada, M., P. Hayes, and S. Matsuyama, *Cytoprotective membrane-permeable peptides designed from the Bax-binding domain of Ku70.* Nat Cell Biol, 2003. **5**(4): p. 352-7.
39. Sawada, M., et al., *Ku70 suppresses the apoptotic translocation of Bax to mitochondria.* Nat Cell Biol, 2003. 5(4): p. 320-9.
40. Yoo, C.B. and P.A. Jones, *Epigenetic therapy of cancer: past, present and future.* Nat Rev Drug Discov, 2006. **5**(1): p. 37-50.
41. Mazumder, S., et al., *Interaction of a Cyclin E Fragment with Ku70 Regulates Bax-mediated Apoptosis.* Molecular and cellular biology, 2007.
42. Sawada, M., et al., *Ku70 suppresses the apoptotic translocation of Bax to mitochondria.* Nature cell biology., 2003. 5(4): p. 320-329.
43. Subramanian, C., et al., *Ku70 acetylation mediates neuroblastoma cell death induced by histone deacetylase inhibitors.* Proc Natl Acad Sci U S A, 2005. **102**(13): p. 4842-7.
44. Yumoto, Y., et al., *High mobility group proteins 1 and 2 can function as DNA-binding regulatory components for DNA-dependent protein kinase in vitro.* J Biochem (Tokyo), 1998. **124**(3): p. 519-27.
45. Baumann, R., et al., *Macrophage migration inhibitory factor delays apoptosis in neutrophils by inhibiting the mitochondria-dependent death pathway.* Faseb J, 2003. **17**(15): p. 2221-30.
46. Nomura, M., et al., *14-3-3 Interacts directly with and negatively regulates pro-apoptotic Bax.* J Biol Chem, 2003. **278**(3): p. 2058-65.
47. Porter, G.W., F.R. Khuri, and H. Fu, *Dynamic 14-3-3/client protein interactions integrate survival and apoptotic pathways.* Seminars in cancer biology., 2006. **16**(3): p. 193-192.
48. Samuel, T., et al., *The G2/M regulator 14-3-3sigma prevents apoptosis through sequestration of Bax.* J Biol Chem, 2001. **276**(48): p. 45201-6.
49. Kirchhoff, S.R., S. Gupta, and A.A. Knowlton, *Cytosolic heat shock protein 60, apoptosis, and myocardial injury.* Circulation, 2002. **105**(24): p. 2899-904.
50. Samali, A., et al., *Presence of a pre-apoptotic complex of pro-caspase-3, Hsp60 and Hsp10 in the mitochondrial fraction of jurkat cells.* Embo J, 1999. **18**(8): p. 2040-8.
51. Leroux, M.R. and E.P. Candido, *Subunit characterization of the Caenorhabditis elegans chaperonin containing TCP-1 and expression pattern of the gene encoding CCT-1.* Biochem Biophys Res Commun, 1997. **241**(3): p. 687-92.
52. Gotoh, T., et al., *hsp70-DnaJ chaperone pair prevents nitric oxide- and CHOP-induced apoptosis by inhibiting translocation of Bax to mitochondria.* Cell Death Differ, 2004. **11**(4): p. 390-402.
53. Pandey, P., et al., *Negative regulation of cytochrome c-mediated oligomerization of Apaf-1 and activation of procaspase-9 by heat shock protein 90.* Embo J, 2000. **19**(16): p. 4310-22.
54. Calderwood, S.K., et al., *Heat shock proteins in cancer: chaperones of tumorigenesis.* Trends Biochem Sci, 2006. **31**(3): p. 164-72.

55. Perconti, G., et al., *The kelch protein NS1-BP interacts with alpha-enolase/MBP-1 and is involved in c-Myc gene transcriptional control.* Biochim Biophys Acta, 2007. **1773**(12): p. 1774-85.
56. Ray, R.B., *Induction of cell death in murine fibroblasts by a c-myc promoter binding protein.* Cell Growth Differ, 1995. **6**(9): p. 1089-96.
57. Ghosh, A.K., et al., *MBP-1 mediated apoptosis involves cytochrome c release from mitochondria.* Oncogene, 2002. **21**(18): p. 2775-84.
58. Immenschuh, S. and E. Baumgart-Vogt, *Peroxiredoxins, oxidative stress, and cell proliferation.* Antioxid Redox Signal, 2005. **7**(5-6): p. 768-77.
59. Aisaki, K., et al., *Glycolytic inhibition by mutation of pyruvate kinase gene increases oxidative stress and causes apoptosis of a pyruvate kinase deficient cell line.* Exp Hematol, 2007. **35**(8): p. 1190-200.
60. Buckingham, J.C., et al., *Annexin 1, glucocorticoids, and the neuroendocrine-immune interface.* Ann N Y Acad Sci, 2006. **1088**: p. 396-409.
61. Lim, L.H. and S. Pervaiz, *Annexin 1: the new face of an old molecule.* Faseb J, 2007. **21**(4): p. 968-75.
62. Komatsu, K., et al., *Increased expression of S100A6 (Calcyclin), a calcium-binding protein of the S100 family, in human colorectal adenocarcinomas.* Clin Cancer Res, 2000. **6**(1): p. 172-7.
63. Leong, S., R.I. Christopherson, and R.C. Baxter, *Profiling of apoptotic changes in human breast cancer cells using SELDI-TOF mass spectrometry.* Cell Physiol Biochem, 2007. **20**(5): p. 579-90.
64. Schmidt-Hansen, B., et al., *Functional significance of metastasis-inducing S100A4(Mts1) in tumor-stroma interplay.* J Biol Chem, 2004. **279**(23): p. 24498-504.
65. Filipek, A., et al., *Characterization of the cell-cycle-regulated protein calcyclin from Ehrlich ascites tumor cells. Identification of two binding proteins obtained by Ca2(+)-dependent affinity chromatography.* Eur J Biochem, 1991. **195**(3): p. 795-800.
66. Alessi, D.R., et al., *PD 098059 is a specific inhibitor of the activation of mitogen-activated protein kinase kinase in vitro and in vivo.* J Biol Chem, 1995. **270**(46): p. 27489-94.

Supplementary Table

Proteins Involved in Apoptosis						
#	Protein name	Swiss-Prot Name	Peptide Sequence	Go Function	Regulation	HiMap ID
1	Voltage-dependent anion-selective channel protein 2	VDAC2	GFGFGLVK	Anion transport	Down	VDAC2
2	Voltage-dependent anion-selective channel protein 1	VDAC1	VTQSNFAVGYK	Anion transport;apoptotic program	Down	VDAC1
			FGIAAK			
			GYGFGLIK			
3	Cytochrome c	CYC	TGPNLHGLFGR	Caspase activation	Down	CYCS
4	Ubiquinol-cytochrome c reductase complex ubiquinone-binding proteinQP-C	UCRQ	AYPHVFTK	Electron transport	Down	HSPC051
5	14-3-3 protein theta	1433T	VFYLK	Intracellular signaling cascade	Down	YWHAQ
			DSTLIMQLLR			
6	Leucine-rich PPR motif-containing protein	LPPRC	AFAETHIK	Mitochondrion transport along microtubule	Down	LRPPRC
7	Galectin-1	LEG1	LPDGYEFK	Regulation of apoptosis	Uncertain	LGALS1
			SFVLNLGK			
8	Cofilin-1	COF1	HELQANCYEEVK	Anti-apoptosis	Up	CFL1
Replication AND Repair						

9	DNA-dependent protein kinase catalytic subunit	PRKDC	EHPFLVK	Protein modification process	Down	PRKDC
			HGDLPDIQIK			
10	RNA-binding protein FUS	FUS	AAIDWFDGK		Down	FUS
11	FACT complex subunit SPT16	SPT16	VQFHLK	Transcription from RNA polymerase II promoter	Down	KIAA1045
12	ATP-dependent DNA helicase 2 subunit 2	KU86	LFQCLLHR	DNA recombination	Down	XRCC5
			ANPQVGVAFPHIK			
13	ATP-dependent DNA helicase 2 subunit 1	KU70	ILELDQFK	Positive regulation of transcription	Down	G22P1
			SDSFENPVLQQHFR			
14	DNA-(apurinic or apyrimidinic site) lyase	APEX1	EAAGEGPALYEDPPDQK		Up	APEX1
Stress-related proteins and chaperones						
15	60 kDa heat shock protein	CH60	ISSIQSIVPALEIANAHR	Protein folding	Down	HSPD1
16	T-complex protein 1 subunit theta	TCPQ	FAEAFEAIPR		Down	CCT8
17	T-complex protein 1 subunit epsilon	TCPE	SLHDALCVIR		Down	CCT5
18	T-complex protein 1 subunit alpha	TCPA	SLHDALCVVK	Tubulin folding	Down	TCP1
			IHPTSVISGYR			
19	T-complex protein 1 subunit eta	TCPH	LLDVVHPAAK	Regulation of progression through cell cycle	Down	CCT7
			YNFFTGCPK			

20	T-complex protein 1 subunit delta	TCPD	AYILNLVK	Regulation of progression through cell cycle	Down	CCT4
21	Heat shock protein HSP 90-beta	HS90B	ALLFIPR	Response to unfolded protein	Uncertain	HSPCB
			APFDLFENK			
			FYEAFSK			
			EQVANSAFVER			
22	Heat shock protein HSP 90-alpha	HS90A	YESLTDPSK	Mitochondrial transport	Uncertain	HSPCA
			ELHINLIPNK			
			FENLCK			
			HIYYITGETK			
			ALLFVPR			
			APFDLFENR			
			VILHLK			
			LGIHEDSQNR			
			NPDDITNEEYGEFYK			
23	Heat shock protein 90 kDa beta member 1	ENPL	EFGTNIK	Anti-apoptosis	Uncertain	TRA1
			YLNFVK			
			SILFVPTSAPR			
24	Heat shock 70 kDa protein 8	HSP7C	FEELNADLFR	Response to unfolded protein	Uncertain	HSPA8
			NQTAEKEEFEHQQK			
			IINEPTAAAIAYGLDK			
			TVTNAVVTVPAYFNDSQR			
			EIAEAYLGK			
			EEFEHQQK			
25	Heat shock 70 kDa protein 1	HSP71	DAGVIAGLNVLR	Anti-apoptosis	Down	HSPA1A

			LVNHFVEEFK			
26	Hsc70-interacting protein (Hip)	F10A1	AIDLFTDAIK	Protein folding	Down	ST13
27	Heat shock 70 kDaprotein 5	GRP78	ELEEIVQPIISK	Negative regulation of caspase activity	Uncertain	HSPA5
			IQQLVK			
			VTHAVVTVPAYFNDAQR			
28	TNFR1-associated protein	TRAP1	GVVDSEDIPLNLSR		Down	TRAP1
Detoxification and Drug resistance						
29	Peroxiredoxin-6	PRDX6	LPFPIIDDR	Response to oxidative stress		PRDX6
			DINAYNCEEPTEK			
30	Annexin A1	ANXA1	SEDFGVNEDLADSDAR	Anti-apoptosis	Uncertain	ANXA1
			NALLSLAK			
			VLDLELK			
31	Annexin A5	ANXA5	SEIDLFNIR	Anti-apoptosis;signal transduction	Down	ANXA5
32	Peroxiredoxin-1	PRDX1	LVQAFQFTDK	Cell proliferation;skeletal development	Down	PRDX1
33	Peroxiredoxin-5	PRDX5	VNLAELFK	Response to oxidative stress	Down	PRDX5
34	Multidrug resistance-associated protein 1	MRP1	DKVLAIR	Response to drug;transport	Up	ABCC1
35	Phosphoglycerate kinase 1	PGK1	LGDVYVNDAFGTAHR	Phosphorylation	Down	PGK1

Folding, Sorting and degradation						
36	Ubiquitin-conjugating enzyme E2 L3	UB2L3	IYHPNIDEK	Protein modification process	Down	UBE2L3
37	Ubiquitin	UBIQ	MQIFVK	Axon guidance;cell cycle	Uncertain	UBA52
			ESTLHLVLR			
			EGIPPDQQR			
38	Proteasome subunit alpha type 1	PSA1	FVFDRPLPVSR		Down	PSMA1
39	Proteasome subunit alpha type 6	PSA6	LLDSSTVTHLFK	Ubiquitin-dependent protein catabolic process	Down	PSMA6
40	26S proteasome non-ATPase regulatory subunit 2	PSMD2	LAQGLTHLGK		Down	PSMD2
41	26S proteasome non-ATPase regulatory subunit 11	PSD11	EASIDILHSIVK		Down	PSMD11
42	Peptidyl-prolyl cis-trans isomerase A	PPIA	FEDENFILK	Protein folding	Down	PPIA
43	Protein KIAA1045	K1045	MGVLMSK		Down	KIAA1045
44	Zinc finger protein 335	ZN335	RAHAGPGAFK	Involved in transcriptional regulation	Down	ZNF335
45	Peptidyl-prolyl cis-trans isomerase B precursor	PPIB	VIFGLFGK		Down	PPIB
DNA, RNA processing Proteins						
46	Nucleoside diphosphate kinase B	NDKB	GLVGEIIK	Cell adhesion;negative	Uncertain	NME2

				regulation of apoptosis		
			SCAHDWVYE			
47	Src-associated in mitosis 68kDa protein	SAM68	FNFVGK	Cell cycle arrest;cell proliferation	Down	KHDRBS1
48	Interleukin enhancer-binding factor 3	ILF3	LAAFGQLHK	M phase;negative regulation of transcription	Down	ILF3
49	Nascent polypeptide-associated complex subunit alpha	NACA	IEDLSQQAQLAAAEK	Translation	Up	NACA
50	Eukaryotic translation initiation factor 3 subunit 9	IF39	FAVLHGEAPR	Translational initiation	Down	EIF3S9
			GTYLATFHQR			
51	DNA replication licensing factor MCM2	MCM2	QLHLNQLIR	Cell cycle;DNA replication	Down	MCM2
52	Poly [ADP-ribose] polymerase 14	PAR14	QLQLSPR		Down	PARP14
53	Exportin-1	XPO1	AVGHPFVIQLGR		Down	XPO1
54	Eukaryotic initiation factor 4A-I	IF4A1	ATQALVLAPTR		Up	EIF4A1
55	High mobility group protein HMG-I/HMG-Y	HMGA1	KQPPVSPGTALVGSQK			HMGA1
56	Prohibitin-2	PHB2	ESVFTVEGGHR	Negative regulation of transcription	Down	PHB2
			IVQAEGEAEAAK			
57	Heterogeneous nuclear ribonucleoprotein A1	ROA1	IFVGGIK	Nuclear import	Down	HNRPA1
58	Heterogeneous nuclear ribonucleoprotein U	HNRPU	DLPEHAVLK	RNA processing	Down	HNRPU

			LLEQYKEESK			
59	Heterogeneous nuclear ribonucleoprotein K	HNRPK	LFQECCPHSTDR	RNA processing;signal transduction	Down	HNRPK
60	Heterogeneous nuclear ribonucleoprotein A0	ROA0	LFVGGLK	mRNA processing	Down	HNRPA0
61	Heterogeneous nuclear ribonucleoproteins C1/C2	HNRPC	SDVEAIFSK	Nuclear mRNA splicing, via spliceosome	Uncertain	HNRPC
			VDSLLENLEK			
			IVGCSVHK			
			QKVDSLLENLEK			
62	Transcription elongation factor B polypeptide 1	ELOC	EIPSHVLSK	Regulation of transcription	Down	TCEB1
63	Splicing factor, proline- and glutamine-rich	SFPQ	FATHAAALSVR	mRNA processing;RNA splicing	Down	SFPQ
64	Splicing factor, arginine/serine-rich 3	SFRS3	AFGYYGPLR			SFRS3
65	Splicing factor, arginine/serine-rich 7	SFRS7	AFSYYGPLR	mRNA processing;RNA splicing	Down	SFRS7
66	Aspartyl-tRNA synthetase	SYDC	VFSIGPVFR	Protein complex assembly	Down	DARS
			LQSGICHLFR			
67	High mobility group protein B1	HMGB1	IKGEHPGLSIGDVAK	Anti-apoptosis	Down	HMGB1
68	Non-POU domain-containing octamer-binding protein	NONO	FACHSASLTVR	mRNA processing;RNA splicing	Down	NONO
69	rRNA 2'-O-methyltransferase fibrillarin	FBRL	IVALNAHTFLR	rRNA processing	Down	FBL

Cell cycle regulation and cell proliferation						
70	Alpha-actinin-4	ACTN4	ALDFIASK	Positive regulation of cell motility	Uncertain	ACTN4
			VQQLVPK			
71	Protein S100-A6	S10A6	LQDAEIAR	Axonogenesis	Up	S100A6
72	ETS homologous factor	EHF	DILLNPDK		Down	EHF
73	Proliferating cell nuclear antigen	PCNA	YLNFFTK	Cell proliferation	Down	PCNA
74	NHP2-like protein 1	NH2L1	AYPLADAHLTK	Regulation of progression through cell cycle	Down	NHP2L1
75	Neuroepithelial cell-transforming gene 1 protein	ARHG8	GDHRSPASAQK	Regulation of cell growth	Down	NET1
76	Rootletin	CROCC	LALLEEAR	Centrosome organization and biogenesis	Down	CROCC
77	Inosine-5'-monophosphate dehydrogenase 2	IMDH2	REDLVVAPAGITLK	Regulation of cell growth	Down	IMPDH2
78	Nuclear migration protein nudC	NUDC	VVTVHLEK	Cell proliferation	Down	NUDC
79	Proliferation-associated protein 2G4	PA2G4	AFFSEVER	Cell cycle arrest;cell proliferation	Down	PA2G4
80	MBP-1	ENOA	IGAEVYHNLK	Negative regulation of cell growth	Up	ENO3
			LNVTEQEK			
			YISPDQLADLYK			

81	Structural maintenance of chromosomes protein 5	SMC5	VNAVIAPK		Up	SMC5L1
82	Enhancer of rudimentary homolog	ERH	ADTQTYQPYNK	Pyrimidine nucleoside metabolic process	Up	ERH
83	GTP-binding nuclear protein Ran	RAN	FNVWDTAGQEK	Androgen receptor signaling pathway	Down	RAN
			SIVFHR			
84	Dolichyl-diphosphooligosaccharide--protein glycosyltransferase 67 kDasubunit precursor	RIB1	LAHLGVQVK	Protein amino acid N-linked glycosylation	Uncertain	RPN1
			IILPEGAK			
Cell structure, Motility and Signal Transduction						
85	Calmodulin-like protein 3	CALL3	EAFSLFDK		Down	CALML3
86	Nephrocystin-1	NPHP1	DAKGNEGLVPR	Cell-cell adhesion;excretion	Down	NPHP1
87	Protein Wnt-4 precursor	WNT4	RVGSSRALVPR	Cell-cell signaling	Down	WNT4
88	Dapper homolog 1	DACT1	ASHNLK		Down	DACT1
89	Myosin light polypeptide 6	MYL6	HVLVTLGEK	Muscle filament sliding	Down	MYL6
			EAFQLFDR			
90	Chloride intracellular channel protein 1	CLIC1	LHIVQVVCK	Chloride transport;signal transduction	Down	CLIC1
91	Nesprin-2	SYNE2	QILRLLR		Down	SYNE2
92	Histone H1.2	H12	ASGPPVSELITK		Up	HIST1H1C

93	Histone H4.	H4	ISGLIYEETR	Phosphoinositide-mediated signaling	Down	H4/O
94	Lamin-B1.	LMNB1	LAVYIDKVR		Down	LMNB1
95	Keratin, type I cytoskeletal 18	K1C18	LEAEIATYR	Anatomical structure morphogenesis	Down	KRT18
96	Macrophage migration inhibitory factor	MIF	LLCGLLAER	Cell proliferation	Down	MIF
97	Septin-11.	SEPT11	VNIIPIIAK	Protein heterooligomerization	Down	SEPT11
98	Tubulin beta chain	TBB5	ISVYYNEATGGK	Natural killer cell mediated cytotoxicity	Down	TUBB
99	Lamin-B2.	LMNB2	DLESLFHR			LMNB2
100	Ezrin	EZRI	QLFDQVVK	Actin filament bundle formation	Down	VIL2
			IGFPWSEIR			
			APDFVFYAPR			
			LFFLQVK			
			QYFHQLEK			
101	Myosin-9	MYH9	LDPHLVLDQLR	Regulation of cell shape	Down	MYH9
102	Tubulin alpha-3C/D chain	TBA3C	FDLMYAK	Microtubule-based process	Down	TUBA2
			QLFHPEQLITGK			
			DVNAAIATIK			
103	Keratin, type I cytoskeletal 19	K1C19	FETEQALR	Sarcomere organization	Uncertain	KRT19
			SLLEGQEDHYNNLSASK			

			ILGATIENSR			
			EELAYLK			
			LASYLDK			
			LASYLDKVR			
			LEQEIATYR			
104	Protein disulfide-isomerase precursor	PDIA1	ENLLDFIK	Peptidyl-proline hydroxylation	Uncertain	P4HB
			NNFEGEVTK			
			ILEFFGLK			
105	Actin, cytoplasmic 1	ACTB	LDLAGR	Cell motility	Uncertain	ACTB
			GYSFTTTAER			
			AVFPSIVGRPR			
			EITALAPSTMK			
			SYELPDGQVITIGNER			
106	Keratin, type II cytoskeletal 8	K2C8	EYQELMNVK	Cytoskeleton organization and biogenesis	Uncertain	KRT8
			FASFIDK			
			YEDEINKR			
			LEGLTDEINFLR			
			FASFIDKVR			
			YEELQSLAGK			
			QLYEEEIR			
107	Histone H1.1	H11	ALAAAGYDVEK	Spermatogenesis	Uncertain	HIST1H1A
			SGVSLAALKK			
108	Histone H2B type 1-C/E/F/G/I	H2B1C	QVHPDTGISSK	Nucleosome assembly	Uncertain	HIST1H2BC
			LLLPGELAK			

109	Histone H2A type 1-D	H2A1D	NDEELNK	Nucleosome assembly	Uncertain	HIST1H2AD
			HLQLAIR			
110	Protein SET	SET	EFHLNESGDPSSK	Negative regulation of histone acetylation	Down	SET
Proteins Invovled in Metabolic and biosynthetic processes						
111	Coproporphyrinogen III oxidase	HEM6	EAEILEVLR	Heme biosynthetic process	Down	CPOX
112	Threonyl-tRNA synthetase	SYTC	LADFGVLHR		Down	TARS
113	ATP synthase subunit beta	ATPB	VVDLLAPYAK		Down	ATP5B
			IGLFGGAGVGK			
114	Elongation factor Tu	EFTU	FNLILR	Translational elongation	Down	TUFM
			EHLLLAR			
115	Lactase-phlorizin hydrolase precursor	LPH	LLKALK		Up	LCT
116	ADP/ATP translocase 2	ADT2	LLLQVQHASK	Transport	Down	SLC25A5
			QIFLGGVDKR			
117	Beta-1,3-galactosyltransferase 1	B3GT1	EFDAR	Protein amino acid glycosylation	Down	B3GALT1
118	Fatty acid synthase (EC 2.3.1.85)	FAS	HGLYLPTR	Fatty acid metabolic process	Down	FASN
			FDASFFGVHPK			

119	Chondromodulin-1 precursor	LECT1	DNSFLSSK	Proteoglycan metabolic process	Down	LECT1
120	Annexin A3	ANXA3	SEIDLLDIR	Signal transduction	Down	ANXA3
121	Polyadenylate-binding protein 3	PABP3	FSPAGPILSIR	mRNA metabolic process	Down	PABPC3
			IVATKPLYVALAQR			
122	Glucose-6-phosphate isomerase	G6PI	AVLHVALR	Carbohydrate metabolic process	Down	GPI
123	Trifunctional enzyme subunit beta	ECHB	AALTGLLHR	Fatty acid beta-oxidation	Down	HADHB
124	Transketolase (EC 2.2.1.1)	TKT	NSTFSEIFK		Down	TKT
125	Glutathione S-transferase P	GSTP1	ASCLYGQLPK	Anti-apoptosis	Down	GSTP1
			HFVALSTNTTK		Down	
126	Phosphoglycerate mutase 1	PGAM1	HYGGLTGLNK	Glycolysis	Down	PGAM1
127	Phosphoserine aminotransferase	SERC	FGTINIVHPK	Pyridoxine biosynthetic process	Down	PSAT1
128	Phosphoglycerate mutase 2	PGAM2	VLIAAHGNSLR	Striated muscle contraction	Down	PGAM2
129	Probable glycosyltransferase GLT28D1	GT281	FSAFLDK		Down	GLT28D1
130	Heparan sulfate glucosamine 3-O-sulfotransferase 3B1	OST3B	EVVRRLR	heparan sulfate proteoglycan biosynthesis	Down	HS3ST3B1
131	Trifunctional purine biosynthetic protein adenosine-3	PUR2	AIAFLQQPR		Down	GART
			IYSHSLLPVLR			

132	Rab GDP dissociation inhibitor beta	GDIB	VICILSHPIK	Signal transduction	Down	GDI2
133	Neutral alpha-glucosidase AB precursor	GANAB	GLLEFEHQR		Down	GANAB
			FRIDELEPR			
134	Aspartate aminotransferase	AATC	HIYLLPSGR	Aspartate catabolic process	Down	GOT1
135	Rho GDP-dissociation inhibitor 1	GDIR	YIQHTYR	Anti-apoptosis	Down	ARHGDIA
136	Leukotriene A-4 hydrolase	LKHA4	APLPLGHIK	Inflammatory response	Down	LTA4H
137	Creatine kinase B-type	KCRB	DLFDPIIEDR		Down	CKB
138	Citrate synthase	CISY	VVPGYGHAVLR	Carbohydrate metabolic process	Down	CS
139	Aldehyde dehydrogenase 1A3	AL1A3	LLHQLADLVER	Lipid metabolic process	Down	ALDH1A3
140	Elongation factor 1-alpha 1	EF1A1	EVSTYIK	Translational elongation	Uncertain	EEF1A1
			STTTGHLIYK			
			YEEIVK			
			LPLQDVYK			
			EHALLAYTLGVK	Translational elongation		
141	Elongation factor 2	EF2	FYAFGR		Down	EEF2
			VFSGLVSTGLK			
			FSVSPVVR			
			EDLYLKPIQR			
142	Triosephosphate isomerase	TPIS	IAVAAQNCYK		Uncertain	TPI1
			HVFGESDELIGQK			

			FFVGGNWK			
143	L-lactate dehydrogenase A chain	LDHA	VTLTSEEEAR		Uncertain	LDHA
			ISGFPK			
			SADTLWGIQK			
			FIIPNVVK			
			DQLIYNLLK			
144	Pyruvate kinase isozymes M1/M2	KPYM	SVETLK	Glycolysis		PKM2
			GIFPVLCK			
			LNFSHGTHEYHAETIK			
			LDIDSPPITAR			
145	L-lactate dehydrogenase B chain	LDHB	SADTLWDIQK		Uncertain	LDHB
			LSGLPK			
			LKDDEVAQLK			
146	Fructose-bisphosphate aldolase A	ALDOA	VLAAVYK	Striated muscle contraction	Uncertain	ALDOA
			ADDGRPFPQVIK			
147	Glyceraldehyde-3-phosphate dehydrogenase	G3P	YDNSLK	glycolysis	Up	GAPDH
			YDDIK			
148	ATP synthase gamma chain	ATPG	HLLIGVSSDR		Down	ATP5C1
Ribosomal proteins						
149	40S ribosomal protein S4, Y isoform 2.	RS4Y2	YALTGDEVK		Up	RPS4Y2
150	40S ribosomal protein S9.	RS9	LFEGNALLR	Translation	Down	RPS9
			QVVNIPSFIVR			

151	40S ribosomal protein S20.	RS20	LIDLHSPSEIVK	Translation	Down	RPS20
152	40S ribosomal protein S28.	RS28	EGDVLTLLESER	Translation	Down	RPS28
153	40S ribosomal protein S3.	RS3	FVADGIFK	Translation	Down	RPS3
			HVLLR			
154	40S ribosomal protein S25.	RS25	AALQELLSK	Translation	Down	RPS25
155	40S ribosomal protein S16.	RS16	LLEPVLLLGK	Translation	Down	RPS16
156	40S ribosomal protein S3a.	RS3A	ACQSIYPLHDVFVR	Induction of apoptosis;translational initiation	Down	RPS3A
157	40S ribosomal protein S7.	RS7	HVVFIAQR	Translation	Down	RPS7
158	40S ribosomal protein S4, X isoform	RS4X	LSNIFVIGK	Cell proliferation	Down	RPS4X
			HPGSFDVVHVK			
159	40S ribosomal protein S29	RS29	DIGFIK	Translation	Down	RPS29
160	40S ribosomal protein S18	RS18	IPDWFLNR	Translation	Down	RPS18
			FQHILR			
161	40S ribosomal protein S2	RS2	SPYQEFTDHLVK	Translation	Down	RPS2
162	40S ribosomal protein S23	RS23	GHAVGDIPGVR	Translation	Down	RPS23
163	40S ribosomal protein S14	RS14	IEDVTPIPSDSTR	Negative regulation of transcription		RPS14
			ELGITALHIK			

164	40S ribosomal protein S30	RS30	FVNVVPTFGK	Translation	Down	FAU
165	60S ribosomal protein L11	RL11	YDGIILPGK	Protein targeting;translation	Up	RPL11
166	60S ribosomal protein L7	RL7	AGNFYVPAEPK	Translation	Up	RPL7
			TTHFVEGGDAGNR			
167	60S ribosomal protein L5	RL5	QFSQYIK	Translation		RPL5
168	60S ribosomal protein L26	RL26	HFNAPSHIR	Translation	Down	RPL26
169	60S ribosomal protein L18	RL18	ILTFDQLALDSPK	Translation	Down	RPL18
170	60S ribosomal protein L34	RL34	AFLIEEQK	Translation		RPL34
171	60S acidic ribosomal protein P0	RLA0	IIQLLDDYPK	Translation	Down	RPLP0
172	60S ribosomal protein L3	RL3	IGQGYLIK	Translation	Down	RPL3
173	60S ribosomal protein L24	RL24	VFQFLNAK	Translation		RPL24
174	60S ribosomal protein L13a	RL13A	LAHEVGWK		Down	RPL13A
			YLAFLR			
175	60S ribosomal protein L30	RL30	YVLGYK	Translation	Down	RPL30
176	60S ribosomal protein L35a	RL35A	AIFAGYK		Down	RPL35A
177	60S ribosomal protein L6	RL6	YYPTEDVPR	Regulation of transcription	Down	RPL6
			HLTDAYFK			
178	60S ribosomal protein L31	RL31	EYTINIHK	Translation	Down	RPL31

			IHGVGFK			
179	60S ribosomal protein L12	RL12	IGPLGLSPK			RPL12
180	60S ribosomal protein L13	RL13	LILFPR	Translation	Down	RPL13
181	60S ribosomal protein L7a	RL7A	TNYNDRYDEIR	Translation	Down	RPL7A
182	60S ribosomal protein L15	RL15	YIQELWR	Translation	Down	RPL15
183	60S ribosomal protein L14	RL14	VAYVSFGPHAGK	Translation	Down	RPL14
184	60S ribosomal protein L10	RL10	GAFGKPQGTVAR		Down	RPL10
185	Ribosomal protein L22-like 1	RL22L	TGNLGNVVHIER		Down	RPL22L1
Others						
186	Putative GTP-binding protein 9	GTPB9	IGIVGLPNVGK		Down	PTD004
187	ATP-binding cassette sub-family A member 7	ABCA7	IWFNNK		Down	ABCA7
188	Apolipoprotein B-100 precursor	APOB	QHLFVK	Circulation;lipid transport;signal transduction	Up	APOB
189	Putative adenylate kinase-like protein C9orf98	CI098	DAEEQVK		Up	C9ORF98
190	Suppressor of T-cell receptor signaling 1	STS1	MDVVFGK		Up	KIAA1959
191	Kinesin-like protein KIF21A	KI21A	DHYIK		Down	KIF21A

192	4F2 cell-surface antigen heavy chain	4F2	GLVLGPIHK	Cell growth;tryptophan transport	Down	SLC3A2
193	Vacuolar ATP synthase catalytic subunit A	VATA	HFTEFVPLR	Transport	Down	ATP6V1A
194	Transmembrane protein 33	TMM33	LPHFQLSR		Down	TMEM33
195	Tetratricopeptide repeat protein 26	TTC26	AFDVLER		Down	TTC26
196	Platelet-activating factor acetylhydrolase IB subunit gamma	PA1B3	ALHSLLLR	Lipid metabolic process	Down	PAFAH1B3
197	Mucolipin-2.	MCLN2	LGLQILK		Down	MCOLN2
198	Spermatid perinuclear RNA-binding protein	STRBP	LHVAVK		Down	STRBP
199	Cylicin-1	CYLC1	NDEESTDADSEPKGDSKK	Spermatogenesis	Down	CYLC1
	Down= Down-regulation					
	Up=Up-regulation					

Chapter 5: Discussion and Future Directions

Cancer is a group of widespread diseases which are characterized by unlimited growth of immature cells. In Canada, 38% of women and 44% of men will develop cancer during their lifetime with 24% of women and 29% men ultimately dying from cancer (based on the most recent statistics from the national cancer institute of Canada). Put another way, one out of every four Canadians will die from cancer.

Traditional treatment methods for cancer include radiation therapy, local surgery, chemotherapy, and immune therapy. Radiation and local surgery are suitable for targeted local treatment or as one part of a general combination treatment for the cancer patients who have an early stage of cancer. But since cancer cells always grow in an uncontrolled way, chemotherapy will need to be used to control advanced-stage cancers or types of cancers that are not suitable for local treatment methods. Using these general treatments, we aim to kill cancer cells to slow or even stop them from growing or spreading.

As a powerful treatment affecting the whole body, chemotherapy drugs are an effective way to kill the cells that are rapidly dividing. Since chemotherapy drugs can not differentiate between the cancer cells and rapidly proliferating cells, healthy cells with a high proliferation rate, including blood cells, hair follicle cells, bone marrow cells, and cells from the mouth, stomach and bowel mucous membrane, are also damaged when patients receive chemotherapy. Once these cells are damaged, some side-effects, such as hair loss, anemia, fatigue, and nausea often occur. Moreover, since most chemotherapy drugs are metabolized through the liver, hepatotoxicity becomes another major side-effect of the chemotherapy. Altogether, cancer patients undergoing chemotherapy may die because of these life-threatening side-effects, such as liver failure resulting from hepatotoxicity, serious infection resulting from the decrease of white blood cells, and

intra bleeding from low blood platelet counts. These side-effects have driven most cancer researchers to find a global therapy agent targeting only cancer cells but with no or limited side-effects on healthy cells. To this end, the property of selectively killing tumor cells has made TRAIL one of the most promising novel biotherapeutic agents for cancer therapy. Based on the early results from clinical trials of TRAIL agents, no major dose-limiting toxicity was reported, but no major clinical responses were observed either. It suggests that the major goal of TRAIL research will focus on increasing our understanding of the biological mechanisms underling tumor resistance.

The efficacy of treatment with traditional chemotherapeutic drugs, such as cisplatin or TRAIL, is due to their ability to induce tumor cell apoptosis. However the molecular mechanism underlying chemotherapy-induced and TRAIL-induced apoptosis is often debated because of the inconsistent reports of their apoptotic signaling pathway. So, in this research project, we initially used a leukemia research model to differentiate the chemotherapy-induced apoptosis pathway from the TRAIL-induced apoptosis pathway. To show that conventional chemotherapy drugs can trigger the caspase cascade, including caspase-8, -9, -3 and DNA fragmentation factor, Jurkat T leukemia cells were treated with cisplatin or etoposide in a dose-dependent and a time-dependent manner. Cisplatin and etoposide both induced apoptosis in wild-type Jurkat T leukemia cells. On the other hand, when pretreated with the pan-caspase inhibitor z-VAD-fmk, apoptosis did not occur, indicating that these chemotherapy drugs mediated caspase-dependent apoptosis. However, the chemotherapy drug induction of apoptosis was not inhibited by treatment with z-IETD-fmk, a caspase-8 inhibitor. There was no difference in cell death between wild-type and caspase-8 or FADD-deficient Jurkat cells after treatment with

either chemotherapy drug. In addition, cisplatin-induced apoptosis was abrogated by the over-expression of either Bcl-2 or Bcl-xL or by the down-regulation of Bak, which diminished changes in the mitochondrial membrane potential and decreased the amount of cytochrome c released from mitochondria. These results indicate that conventional chemotherapy drug-triggered apoptosis is indispensable, and its pathway is independent of the death receptor.

In contrast, caspase-8 or FADD-deficient Jurkat cells are completely resistant to TRAIL-induced apoptosis, which is also abrogated by over-expression of either either Bcl-2 or Bcl-xL or down-regulation of Bak. These data indicate that both the death receptor-initiated extrinsic pathway and mitochondria-associated intrinsic pathway are crucial for TRAIL-induced apoptosis. This kind of apoptosis is initiated from the death receptor level. After addressing the different apoptosis pathways induced by traditional chemotherapy drugs and TRAIL, the second challenge becomes how to develop TRAIL as a new cancer treatment, since most cancer cells are resistant to TRAIL-killing.

Based on the research data presented, the majority of TRAIL resistance comes from two levels: the DISC level and the mitochondrial level. At the DISC level, there are two major mechanisms involved in TRAIL-resistance. The first is loss of crucial apoptotic factors, including death receptor [1], FADD and caspase-8. Once cells lose these crucial apoptotic factors, they become completely resistant to TRAIL-induced apoptosis because of the blockage of the transmission of the death signal to the downstream molecules.

The second resistance mechanism is the over-expression of anti-apoptotic factors, including RIP and c-FLIP. By using pancreatic cancer as the research model, we found

that the majority of human pancreatic cancers are unfortunately resistant to TRAIL treatment. Here, we show that the inhibition of caspase-8 cleavage is the most upstream event in TRAIL resistance in pancreatic cancers. TRAIL treatment led to the cleavage of caspase-8 and downstream caspase-9, caspase-3, and DNA fragmentation factor 45 (DFF45) in TRAIL-sensitive pancreatic cancer cell lines (BXPC-3, PACA-2). This caspase-8-initiated caspase cascade, however, was inhibited in TRAIL-resistant pancreatic cancer cell lines (PANC-1, ASPC-1, CAPAN-1, CAPAN-2). The long and short forms of c-FLIP (c-$FLIP_L$, c-$FLIP_S$) were highly expressed in the TRAIL-resistant cells as compared to the sensitive cells. Knockdown of c-$FLIP_L$, and c-$FLIP_S$ by shRNA rendered the resistant cells sensitive to TRAIL-induced apoptosis through the cleavage of caspase-8 and activation of the mitochondrial pathway. RIP has been reported in TRAIL-induced activation of NF-κB and it is shown here that knockdown of RIP sensitizes resistant cells to TRAIL-induced apoptosis. These results indicate the role of c-FLIP and RIP in caspase-8 inhibition in the mediation of TRAIL resistance in the DISC level. Moreover, once the up-stream DISC inhibition was released by down-regulation of RIP or c-FLIP, TRAIL-induced mitochondria-associated intrinsic pathway was also activated.

Both c-$FLIP_L$ and c-$FLIP_S$ have been reported to be recruited to the TRAIL-DISC in various cancer models including glioma cells [2], NSCLC [3], melanoma cells [4], and pancreatic cancer cells (In this research, data was not shown). c-$FLIP_S$ was shown to block caspase-8 activation in the DISC by its competitive interaction with FADD and caspase-8 , which in turn blocks the second step of caspase-8 activation. However, the role of c-$FLIP_L$ in the DISC is controversial since it is reported to help and block the

caspase-8 activation in different cancer models. In our pancreatic research model, we found that over-expression c-$FLIP_L$ clearly inhibited TRAIL-induced caspase-8 activation in the sensitive cells. This result is also in line with the finding that shRNA-mediated down-regulation of c-FLIP sensitized TRAIL-resistant pancreatic cancer cell lines to TRAIL-induced apoptosis. Moreover, c-FLIP deficient mice show the same phenotype as caspase-8- and FADD-deficient mice [5-8]. These reports strengthen our finding that both c-$FLIP_S$ and c-$FLIP_L$ are crucial anti-apoptotic factors at the DISC level.

In contrast to c-FLIP, similar levels of RIP expression were found in both the TRAIL-resistant and TRAIL-sensitive pancreatic cancer cell lines in this research. Moreover, in the fibrosarcoma cell model, RIP was not found in the TRAIL-DISC but was found in the later formed, complex II, in which DR5 was absent [9]. These data make the anti-apoptotic role of RIP in the TRAIL-induced apoptosis pathway more controversial. In this research, RIP was found to be recruited to the TRAIL-resistant DISC and was cleaved in TRAIL-sensitive pancreatic cancer cell lines upon TRAIL stimulation. The cleavage of RIP is completely inhibited by general caspase inhibitor or caspase-8 inhibitor, indicating that caspase-8 cleaves RIP in TRAIL-induced apoptosis. Moreover, down-regulating RIP with shRNA sensitized TRAIL-resistant pancreatic cancer cells. This clearly indicates the crucial anti-apoptotic role of RIP in TRAIL-induced apoptosis pathway.

But how RIP mediates the TRAIL-resistance in the pancreatic cancer model still needs to be further clarified. In most reports, RIP-inhibition of caspase-8 activation may come from the RIP-mediated NF-κB activation. The findings of high activity of NF-κB and that TRAIL activates NF-κB in pancreatic cancer cell lines is consistent with

pancreatic cancer progression and resistance to therapies and strengthens the aforementioned theory. Recently, RIP was reported to mediate the DISC assembly in non-rafts in TRAIL resistant NSCLC cells to activate the NF-κB and inhibit apoptosis [10]. Whether or not this resistance mechanism accuractely matches the pancreatic cancer model still needs to be further explored.

At the mitochondrial level, we found that the TRAIL resistance comes from either over-expression of anti-apoptotic factors, including Bcl-2 and Bcl-xL, or down-regulation of pro-apoptotic proteins that include Bax and Bak. In the leukemia model, over-expression of Bcl-2 or Bcl-xL blocks TRAIL-induced MMP changes and thus inhibits the activation of caspase-3. Down-regulating Bak with Bak siRNA decreases TRAIL-induced MMP changes and blocks apoptosis. In the colorectal cancer model, there is no difference in upstream caspase-8 activation between Bax positive and Bax deficient cells. However, Bax deficiency completely blocks the TRAIL-induced caspape-9 and caspase-3 activation and then inhibits TRAIL-induced apoptosis.

As mentioned in the introduction, there are two models, the direct and indirect activation models, involved in the activation of such pro-apoptotic factors as Bax and Bak in the TRAIL-induced mitochondria-associated intrinsic pathway. Based on our data in the Jurkat cell line, the indirect activation model seems more convincing since either over-expression of Bcl-2 and Bcl-xL or down-regulating Bak blocks TRAIL-induced apoptosis. In the pancreatic research model, it is also reported that the high expression level of Bcl-xL contributes to the TRAIL-resistance of the pancreatic cancer cells [11, 12]. These data indicate that the relative ratio of anti-apoptotic factors to pro-apoptotic factors is the key regulatory factor at the mitochondrial level that decides the fate of cancer cells

upon TRAIL treatment.

Besides Bak, the other pro-apoptotic factor at the mitochondrial level, Bax, also plays a crucial role in the TRAIL-induced apoptosis. In this research using the colorectal cancer model, we found that Bax deficiency has no effects in TRAIL-induced caspase-8 activation, indicating again that the caspase-8 activation is the upstream event of the mitochondria-associated apoptotic pathway. To our surprise, even though there is still Bak expression, Bax deficient cells are completely resistant to TRAIL-induced apoptosis. TRAIL failed to induce any mitochondria downstream caspase-9 and caspase-3 activation in Bax deficient cells. These findings indicate that, Bax not only works as a pro-apoptotic factor, but also regulates the apoptosis process in other ways. To further explore the mechanisms underlying the Bax-mediated apoptosis, we decided to compare the protein expression profile differences between Bax positive and Bax negative cells using large scale quantitative mass spectrometry.

In recent years, quantitative MS techniques [13, 14] have emerged as a powerful tool to efficiently identify differentially expressed proteins across different biological samples [15, 16]. From among the several quantitative MS strategies that have been developed recently, 2-MEGA labeling with targeted LC-MALDI-MS/MS was chosen in this research for two reasons. Using 2-MEGA labeling, we are able to perform large scale sample analysis and by using targeted LC-MALDI-MS/MS analysis, the selective analysis of low abundance proteins is available. With this new and powerful technique, 56 differentially expressed proteins involved in the apoptosis-related process, including DNA repair, stress-induced process, cell cycle regulation, cytoskeletal rearrangements, and signal transduction, were identified.

Within these proteins, four groups of proteins are highlighted here because of their important roles in the Bax-modulated apoptosis pathway. The first group, the MPT channel proteins that includes VDAC-1, VDAC-2, and cytochrome c, are significantly down-regulated in the Bax deficient clone. Based on previous reports, this down-regulation may result from instability and/or degradation after losing their binding partner or regulator Bax. The second group is comprised of the Bax-regulatory proteins, including KU70, KU80, PRKDC, 14-3-3θ, and MIF, which have been reported to interact directly or indirectly with Bax to modulate Bax-mediated apoptosis. Their down-regulation may come from the negative feedback regulation after the downstream target protein Bax was knocked out. The third group of proteins is the heat shock protein family members, including HSP60, HSP70, TCP-1, HSP90α, and HSP90β. These proteins play both pro- and anti-apoptosic roles. In the Bax deficient cells, the down-regulation of these HSPs may be due to the inhibition of c-Myc-regulated transcription via the up-regulation of the c-Myc repressor, MBP-1. Once Bax was knocked out, these proteins involved in protein folding, sorting, and degradation are also down-regulated. Some cell skeletal and structure proteins are also correspondingly down-regulated by the decrease of these HSPs. It has been reported by several groups that Bax plays a central role in orchestrating c-Myc-induced apoptosis since ablation of Bax genes renders many types of cells resistant to c-Myc-dependent apoptosis [17, 18]. However it is still unclear how Bax deficiency blocks c-Myc-dependent apoptosis. Here, our data indicate that knocking out the Bax up-regulates MBP-1, which in turn represses the c-Myc function.

The fourth major group of identified proteins is oxidative stress triggered proteins:

peroxiredoxins, pyruvate kinase, S100A6, and annexins. The down-regulation of peroxiredoxins may be due to the decrease of pyruate kinase in the Bax deficient clone. The down-regulation of the annexins may also come from the inhibition of c-Myc function in the Bax deficient clone. S100A6 proteins were identified as being up-regulated in the Bax deficient clone which may come from the decrease of Bax-regulated protease activity.

Using bioinformatic tools to map the protein-protein interactions among these four groups of proteins, we were able to draw a protein profile map with Bax as the centrol protein. It explains why the Bax deficient clone is completely resistant to most apoptotic stimuli, including DNA-damage drugs and death ligands, even though Bak and other apoptotic executors remain in the Bax deficient clone. These data indicate that Bax functions, not only as an apoptotic signal executor by modulating the damage of mitochondria membrane potential, but also as a regulator for the expression level of other proteins. By modulation of some crucial proteins, the Bax deficient clone further lost its apoptotic potential.

In summary, a large body of research evidence has now been gathered on the underlining resistance mechanisms of cancer cells to TRAIL-induced apoptosis. Given the results presented above, TRAIL-resistance focuses at two levels: the DISC level and the mitochondrial level. At the DISC level, either loss of crucial molecules, including DRs, FADD, and caspase-8, or over-expression of the anti-apoptotic factors, including RIP and c-FLIP, blocks TRAIL-induced apoptosis. At the mitochondrial level, either over-expression of anti-apoptotic factors, including Bcl-2 and Bcl-xL, or down-regulation of pro-apoptotic factors, including Bax and Bak, is involved.

These findings clarify the TRAIL-induced apoptosis signal transduction pathway and indicate the crucial TRAIL-killing regulators. Mediating these factors may enable us to develop new TRAIL-based therapeutic strategies since the efficacy of TRAIL-alone therapy will be limited by the fact that most tumors are TRAIL-resistant. It has been reported that combination treatment of TRAIL with some chemotherapy drugs enhances TRAIL killing in many tumors. For example, the first line drug of treatment of pancreatic cancers, gemcitabine is able to sensitize TRAIL-induced killing of pancreatic cancer cells by down-regulating Bcl-xL. In our research, we found that the chemotherapeutic agents, camptothecin, celecoxib, and cisplatin, can overcome TRAIL resistance in pancreatic cancer cells by inhibiting c-FLIP expression and releasing its inhibition of caspase-8 activation [19].

Looking to the future, the molecular events regulating these pro- or anti-apoptotic factors leading to TRAIL-resistance are still not fully characterized. A detailed picture for TRAIL-resistance is beginning to emerge based on this thesis work that has laid a foundation for following separate, but highly linked, future investigations.

First, at the DISC level, we have demonstrated that RIP and c-FLIP are two crucial anti-apoptotic factors. However, after decades of research on TRAIL, the protein components of TRAIL-DISC are still unclear. Are there any other apoptosis-regulators recruited to TRAIL-DISC? How do they regulate the TRAIL-sensitivity of the cancer cells? Future studies in which TRAIL-sensitive and TRAIL-resistant DISC are purified, followed by LC-ESI-MS/MS analysis should serve as a valuable tool to address and answer these questions. By comparing the different TRAIL-DISC components purified from TRAIL-sensitive and TRAIL-resistant cancer cells, other apoptosis-regulators at the

DISC level may be addressed.

Second, another question that remains for c-FLIP and RIP at the DISC level is how they are regulated at the DISC. It has been reported that c-FLIP is ubiquitinated and phosphorylated in the DISC [20, 21], and RIP is ubiquitinated in the TRAIL-DISC [22]. How do these post-translation modifications regulate RIP and c-FLIP function at the DISC? What molecules at the TRAIL-DISC regulate these post-translation modifications of RIP or c-FLIP?

Third, the investigations reported in this thesis clearly demonstrate that Bax not only functions as a pro-apoptotic factor but also regulates the expression and the stability of other proteins. What remain somewhat unclear are the Bax binding partners at the mitochondrial level upon TRAIL treatment. By using a specific purification technique ,such as tandem affinity purification combined with LC-ESI-MS/MS analysis, we may be able to purify and further identify the Bax binding partner in both TRAIL-sensitive and TRAIL-resistant cancer cells.

Taken together, while much remains to be discovered regarding TRAIL-induced apoptosis signaling pathway, the data contained within this thesis address several facets of TRAIL-resistance mechanisms. These findings advance our understanding of the TRAIL signaling network at the molecular level, provide the basis to interfere with the TRAIL-induced apoptosis pathway to overcome TRAIL resistance, and thus assist the future development of TRAIL-based tumor therapy.

1. Song, J.H., et al., *Interferon gamma induces neurite outgrowth by up-regulation of p35 neuron-specific cyclin-dependent kinase 5 activator via activation of ERK1/2 pathway.* J Biol Chem, 2005. **280**(13): p. 12896-901.
2. Song, J.H., et al., *TRAIL triggers apoptosis in malignant glioma cells through extrinsic and intrinsic pathways.* Brain Pathol, 2003. **13**(4): p. 539-553.
3. Song, J.H., et al., *siRNA targeting c-FLIP sensitizes non-small cell lung carcinoma cells to TRAIL-induced apoptosis.* AACR 94th Annual Meeting, Orlando, Florida, March 27-31, 2004, 2004.
4. Xiao, C., et al., *Inhibition of CaMKII-mediated c-FLIP expression sensitizes malignant melanoma cells to TRAIL-induced apoptosis.* Exp Cell Res, 2005. **304**(1): p. 244-55.
5. Ye, J., et al., *Regulation of the NF-kappaB activation pathway by isolated domains of FIP3/IKKgamma, a component of the IkappaB-alpha kinase complex.* J Biol Chem, 2000. **275**(13): p. 9882-9.
6. Yeh, J.H., et al., *Mitogen-activated protein kinase kinase antagonized fas-associated death domain protein-mediated apoptosis by induced FLICE-inhibitory protein expression.* J Exp Med, 1998. **188**(10): p. 1795-802.
7. Yeh, W.C., et al., *Requirement for Casper (c-FLIP) in regulation of death receptor-induced apoptosis and embryonic development.* Immunity, 2000. **12**(6): p. 633-42.
8. Yeh, W.C., et al., *FADD: essential for embryo development and signaling from some, but not all, inducers of apoptosis.* Science, 1998. **279**(5358): p. 1954-8.
9. Varfolomeev, E., et al., *Molecular determinants of kinase pathway activation by Apo2 ligand/tumor necrosis factor-related apoptosis-inducing ligand.* J Biol Chem, 2005. **280**(49): p. 40599-608.
10. Song, J.H., et al., *Lipid rafts and nonrafts mediate tumor necrosis factor related apoptosis-inducing ligand induced apoptotic and nonapoptotic signals in non small cell lung carcinoma cells.* Cancer Res, 2007. **67**(14): p. 6946-55.
11. Evans, J.D., et al., *Detailed tissue expression of bcl-2, bax, bak and bcl-x in the normal human pancreas and in chronic pancreatitis, ampullary and pancreatic ductal adenocarcinomas.* Pancreatology, 2001. **1**(3): p. 254-62.
12. Bai, J., et al., *Predominant Bcl-XL knockdown disables antiapoptotic mechanisms: tumor necrosis factor-related apoptosis-inducing ligand-based triple chemotherapy overcomes chemoresistance in pancreatic cancer cells in vitro.* Cancer Res, 2005. **65**(6): p. 2344-52.
13. Flory, M.R., et al., *Advances in quantitative proteomics using stable isotope tags.* Trends Biotechnol, 2002. **20**(12 Suppl): p. S23-9.
14. Goshe, M.B. and R.D. Smith, *Stable isotope-coded proteomic mass spectrometry.* Curr Opin Biotechnol, 2003. **14**(1): p. 101-9.
15. Steen, H. and M. Mann, *The ABC's (and XYZ's) of peptide sequencing.* Nat Rev

Mol Cell Biol, 2004. **5**(9): p. 699-711.
16. Shevchenko, A., et al., *Linking genome and proteome by mass spectrometry: large-scale identification of yeast proteins from two dimensional gels.* Proc Natl Acad Sci U S A, 1996. **93**(25): p. 14440-5.
17. Dansen, T.B., et al., *Specific requirement for Bax, not Bak, in Myc-induced apoptosis and tumor suppression in vivo.* J Biol Chem, 2006. **281**(16): p. 10890-5.
18. Jamerson, M.H., et al., *Bax regulates c-Myc-induced mammary tumour apoptosis but not proliferation in MMTV-c-myc transgenic mice.* Br J Cancer, 2004. **91**(7): p. 1372-9.
19. Wang, P., et al., *Inhibition of RIP and c-FLIP enhances TRAIL-induced apoptosis in pancreatic cancer cells.* Cell Signal, 2007. **19**(11): p. 2237-46.
20. Kim, Y., et al., *An inducible pathway for degradation of FLIP protein sensitizes tumor cells to TRAIL-induced apoptosis.* J Biol Chem, 2002. **277**(25): p. 22320-9.
21. Poukkula, M., et al., *Rapid turnover of c-FLIPshort is determined by its unique C-terminal tail.* J Biol Chem, 2005. **280**(29): p. 27345-55.
22. Lee, T.H., et al., *The kinase activity of Rip1 is not required for tumor necrosis factor-alpha-induced IkappaB kinase or p38 MAP kinase activation or for the ubiquitination of Rip1 by Traf2.* J Biol Chem, 2004. **279**(32): p. 33185-91.
23. Alessi, D.R., et al., *PD 098059 is a specific inhibitor of the activation of mitogen-activated protein kinase kinase in vitro and in vivo.* J Biol Chem, 1995. **270**(46): p. 27489-94.